Echocardiography in the CCU

Eyal Herzog
Edgar Argulian
Editors

Z.F

Springer

Echocardiography in the CCU

Eyal Herzog · Edgar Argulian
Editors

Echocardiography in the CCU

Springer

Editors
Eyal Herzog
Mount Sinai St Luke's Hospital
New York, NY
USA

Edgar Argulian
Mount Sinai St Luke's Hospital
New York, NY
USA

ISBN 978-3-319-90277-7 ISBN 978-3-319-90278-4 (eBook)
https://doi.org/10.1007/978-3-319-90278-4

Library of Congress Control Number: 2018943696

Printed on acid-free paper

This Springer imprint is published by the registered company Springer International Publishing AG part of Springer Nature.
The registered company address is: Gewerbestrasse 11, 6330 Cham, Switzerland

To our families, patients, technicians, colleagues, and trainees who have continuously supported us and taught us so much over the years.

Preface

The field of critical care cardiology has evolved considerably over the past few decades. Cardiac units in the 1970s and the 1980s were practically coronary care units typically populated by patients with acute and often uncomplicated myocardial infarction or unstable angina. Contemporary cardiac care units (CCU) are cardiac intensive care units (CICU) where the focus is management of patients with multisystem diseases, advanced hemodynamic compromise, complex ventricular arrhythmias, and established or incipient multiorgan failure.

Development of echocardiography paralleled the progress made in acute cardiovascular care. The initial use of echocardiography was to detect pericardial effusion and cardiac tumors. However, the current applications of various echocardiographic modalities include an extended list of pathological and therapeutic indications. Currently, echocardiography is fundamental to the management of patients with acute cardiovascular diseases. Timely performed echocardiography can lead to a change in therapy in majority of patients with an acute cardiovascular condition.

In this book, we discuss the essential role of various echocardiographic modalities in the modern acute cardiovascular care by highlighting the applications of echocardiography in the most common clinical scenarios.

As an example, in the section of echocardiography in acute chest pain syndromes we outline the use of echocardiography in acute coronary syndromes, mechanical complications of myocardial infarction, and in acute aortic syndromes. We provide a novel pathway for the use of echo in patients with acute chest pain. In the section of echocardiography in dyspnea we outline structured and comprehensive echocardiographic evaluation of patients with suspected cardiac acute and subacute dyspnea in the acute care settings.

It is our hope that this book will serve as a teaching tool to help save the lives of patients with heart disease in the CCU.

New York, NY, USA — Eyal Herzog
New York, NY, USA — Edgar Argulian

Acknowledgments

We would like to acknowledge the extraordinary work of Candice Francis from our office at Mount Sinai St. Luke's Hospital in New York; she is our right hand in assisting our trainees and patients in the hospital and is also the editing coordinator of this book. We would also like to acknowledge Danny Pudpud, who is the Manager of our Echo Lab and the person responsible for most of the images in this book.

Contents

Part I Syndrome-Based Echocardiography in the CCU

1 Echocardiographic Assessment of Acute Chest Pain in the CCU . . . 3
Eyal Herzog, Jagat Narula, and Edgar Argulian

2 Echocardiographic Assessment of Acute Dyspnea in the CCU 27
Edgar Argulian, Jagat Narula, and Eyal Herzog

3 The Arrhythmia Patient in the CCU – Impact of Echocardiography 45
Alan Sugrue, Subir Bhatia, Vaibhav Vaidya, and Sam Asirvatham

4 Echocardiography in Patients with Syncope 67
Karthik Seetharam, Brandon W. Calenda, and Farooq A. Chaudhry

5 Echocardiography in Cardiac Arrest and Resuscitation. 77
Soheila Talebi, Edgar Argulian, and Eyal Herzog

6 Echocardiography in a Patient with a New Murmur 93
Julie Friedman and Muhamed Saric

7 Echocardiography in Acute Neurologic Syndrome 113
Gregory Katz and Muhamed Saric

Part II Application of Echocardiography in the CCU

8 Hemodynamic Assessment in the CCU by Echocardiography. 135
Yuvrajsinh J. Parmar, Craig Basman, and Itzhak Kronzon

9 Cardiac Point of Care Ultrasound in the CCU 149
Allison Selby, Eyal Herzog, and Edgar Argulian

10 Non-cardiac Point of Care Ultrasound in the CCU. 165
Nick Pakzad, Ismini Kourouni, Joseph P. Mathew, and Gopal Narayanswami

11 Contrast Echocardiography in the Cardiac Care Unit 215
Eyal Herzog, Seyed Hamed Hosseini Dehkordi, and Edgar Argulian

12 Use of Echocardiography in Patients with Intracardiac Devices 227
Edward Chu, Karthik Seetharam, Brandon W. Calenda, and Farooq A. Chaudhry

13 Echocardiography in Structural Cardiac Interventions 245
Gnalini Sathananthan, Gila Perk, and Amir Ahmadi

Index 263

Part I
Syndrome-Based Echocardiography in the CCU

Chapter 1
Echocardiographic Assessment of Acute Chest Pain in the CCU

Eyal Herzog, Jagat Narula, and Edgar Argulian

Abstract The field of critical care cardiology has evolved considerably over the past few decades. Cardiac units in the 1970s and the 1980s were practically coronary care units, where the units most frequently were populated by patients with acute and often uncomplicated myocardial infarction or unstable angina. Detection and rapid treatment of arrhythmias were the primary goals of therapy. Contemporary cardiac care units (CCU) have transformed into Cardiac intensive care units (CICU) where the focus has since shifted towards the management of patients with multisystem diseases, advanced hemodynamics compromise, complex ventricular arrhythmias, and established or incipient multi-organ failure. The two most common clinical scenarios leading to acute chest pain syndrome in CCU patients are acute coronary syndrome and acute aortic syndrome.

Keywords Chest pain · Aortic dissection · Acute coronary syndrome · Myocardial infarction

Introduction

The field of critical care cardiology has evolved considerably over the past few decades. Cardiac units in the 1970s and the 1980s were practically coronary care units, where the units most frequently were populated by patients with acute and often uncomplicated myocardial infarction or unstable angina. Detection and rapid treatment of arrhythmias were the primary goals of therapy. Contemporary cardiac care units (CCU) have transformed into cardiac intensive care units (CICU) where the focus has since shifted towards the management of patients with multisystem diseases, advanced hemodynamics compromise, complex ventricular arrhythmias, and established or incipient multi-organ failure. In addition, at many institutions,

E. Herzog (✉) · J. Narula · E. Argulian
Mount Sinai St. Luke's Hospital, New York, NY, USA
e-mail: Eyal.Herzog@mountsinai.org; jagat.narula@mountsinai.org; Edgar.Argulian@mountsinai.org

E. Herzog, E. Argulian (eds.), *Echocardiography in the CCU*,
https://doi.org/10.1007/978-3-319-90278-4_1

CCUs manage an increasing number of patients undergoing advanced therapies such as therapeutic hypothermia, transcatheter valve procedures, or ventricular assist device therapies.

Advances in echocardiography paralleled the progress made in critical care cardiology. The initial use of echocardiography was to detect pericardial effusion and cardiac tumors. However, the current applications of various forms of echocardiography include an extended list of pathological and therapeutic indications. Currently, echocardiography is fundamental to the management of patients with acute cardiovascular diseases. It has been shown that timely performed echocardiography can lead to a change in therapy in up to 80% of patients with an acute cardiovascular condition [1].

Different ultrasound modalities, from basic point-of-care ultrasound to advanced echocardiographic imaging, can be used for evaluation of patients with an acute cardiovascular condition (Table 1.1). Transthoracic echocardiography (TTE) is usually the frontline imaging modality. Transesophageal echocardiography (TEE) commonly follows a nondiagnostic TTE. However, in certain clinical scenarios, such as acute aortic syndrome, acute valvular regurgitation, acute prosthetic value dysfunction, atrial fibrillation or atrial flutter, and stroke, TEE could be performed first. Contrast echocardiography allows improved visualization of the endocardium and it has become an integral part of echocardiography in the modern critical care units. Pocket-sized imaging devices are occasionally used as a fast initial screening in an emergency setting, as well as an extension of physical examination in the intensive care units [1].

The two most common clinical scenarios leading to acute chest pain syndrome are acute coronary syndrome and acute aortic syndrome.

Table 1.1 Ultrasound modalities in evaluation of patients with suspected cardiac causes of acute cardiovascular conditions

Point-of-care cardiac ultrasound
Comprehensive transthoracic echocardiogram
Limited/focused transthoracic echocardiogram (intracardiac device positioning, etc.)
Transesophageal echocardiogram
Contrast echocardiography
Stress echocardiogram including dobutamine echocardiography
Speckle-tracking echocardiography for assessment of myocardial mechanics
3D echocardiography
Lung ultrasound
Vascular ultrasound for intravenous access

Echocardiography in Acute Coronary Syndrome

The last few decades have witnessed remarkable progress in the understanding of the pathophysiology of acute coronary syndrome (ACS). ACS incorporates a spectrum of clinical entities, ranging from unstable angina and non-ST-elevation ACS to ST-elevation myocardial infarction. Developments in the field of echocardiography have paralleled the progress made in ACS.

Assessment of Regional Systolic Function in Acute Coronary Syndrome

Occlusion of an epicardial coronary artery at the time of acute coronary syndrome leads to a loss of contractile function in the myocardial segments subtended by that vessel. The magnitude and duration of wall motion abnormalities depend on the severity, extent, and duration of the coronary occlusion.

In unstable angina (UA) or in non-ST-elevation ACS, left and right ventricular wall motion may be normal unless TTE is performed during an episode of chest pain.

ST-elevation myocardial infarction (STEMI) often results from an acute occlusion of a major coronary vessel. If the total cessation of coronary flow lasts for more than 3–6 h, myocardial necrosis will occur and the myocardium in the affected segments will be replaced with a fibrous tissue over the subsequent weeks [2].

The magnitude of regional contractile loss in acute coronary syndrome is usually assessed semiquantitatively. It is usually interpreted clinically as follows [2]:

1. Interpretation of wall motion abnormalities as seen in Table 1.2
2. Extent and location of affected segments
3. Suspected coronary artery distribution (left anterior descending artery vs. right coronary artery vs. left circumflex artery)

Table 1.2 Left ventricular wall motion scoring

	Score
Normal or hyperkinetic	1
Hypokinetic (reduced thickening)	2
Akinetic (absent or negligible thickening)	3
Dyskinetic (systolic thinning or stretching, aneurysmal)	4
Wall motion score index = Sum of individual segment scores/number of evaluated segments	

Assessment of Global Systolic Function in Acute Coronary Syndrome

Global left ventricular systolic function in acute coronary syndrome is assessed by both wall motion scoring and left ventricular ejection fraction.

Wall Motion Scoring

Wall motion scoring analysis assigns a numeric value to the degree of contractile dysfunction in each segment. The scoring criteria endorsed by American Society of echocardiography (ASE) are seen in Table 1.2.

Once all segments are assigned individual scores, a total score is calculated as a sum of individual scores. A wall motion score index (WMSI) is then calculated as a ratio between the total score over the number of evaluated segments. The WMSI is a dimensionless index. A 17-segment model is commonly used to allow for standardized communication within echocardiography and with other imaging modalities [3]. For a fully visualized normal ventricle the total score is 17 (all segments have normal contractility). However, ASE does not recommend to score the true apical segment of the 17 segments. Since all 17 segments are evaluated, the wall score index of a normal heart is 17/17 = 1. For abnormal ventricles, the higher the WMSI, the more significant the wall motion abnormality.

Figures 1.1 and 1.2 depict echocardiographic views of the left ventricle, demonstrating the left ventricular wall segments and their typical corresponding coronary distributions [4]. The utilization of image-enhancing agents (echocardiographic contrast microbubbles) has improved the detection of wall motion abnormalities, and therefore the confidence in delineation of the affected segments.

Assessment of Left Ventricular Ejection Fraction

Left ventricular ejection fraction (LVEF) has been consistently shown to be one of the most powerful predictors of mortality and morbidity in patients with heart disease [5]. LVEF is the single most powerful predictor of mortality and the risk for developing life-threatening ventricular arrhythmias after myocardial infarction [6]. Furthermore, once the acute coronary syndrome resolves, the residual LVEF is important for treatment options as LVEF cutoff values are built into recommendations for both medical and implantable device therapies. By definition, LVEF is the percentage of the end-diastolic volume that is ejected with each systole as the stroke volume. Thus, to calculate the LVEF one needs to estimate the end-systolic and end-diastolic volumes of the left ventricle.

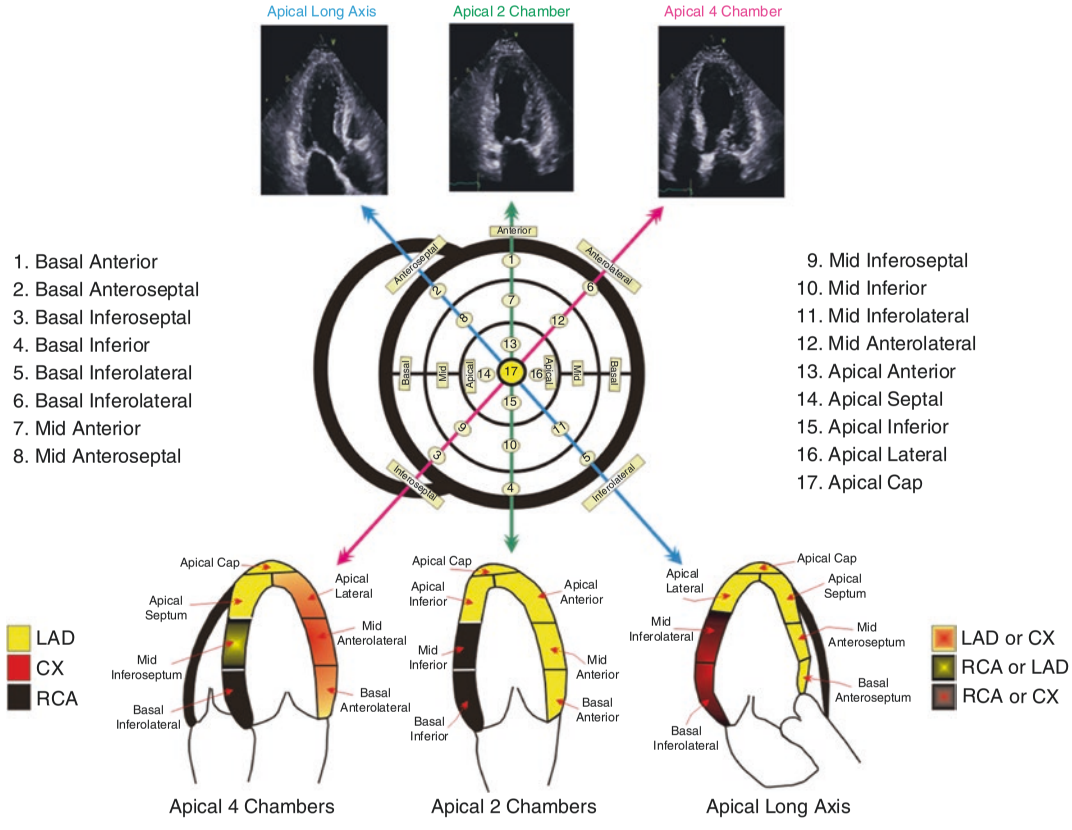

Fig. 1.1 Apical four-chamber (A4C), apical two-chamber (A2C), and apical long-axis (ALX) views in relation to the bull's-eye display of the LV segments (center). Top panels show echocardiographic images and bottom panels depict the LV wall segments visualized in each view

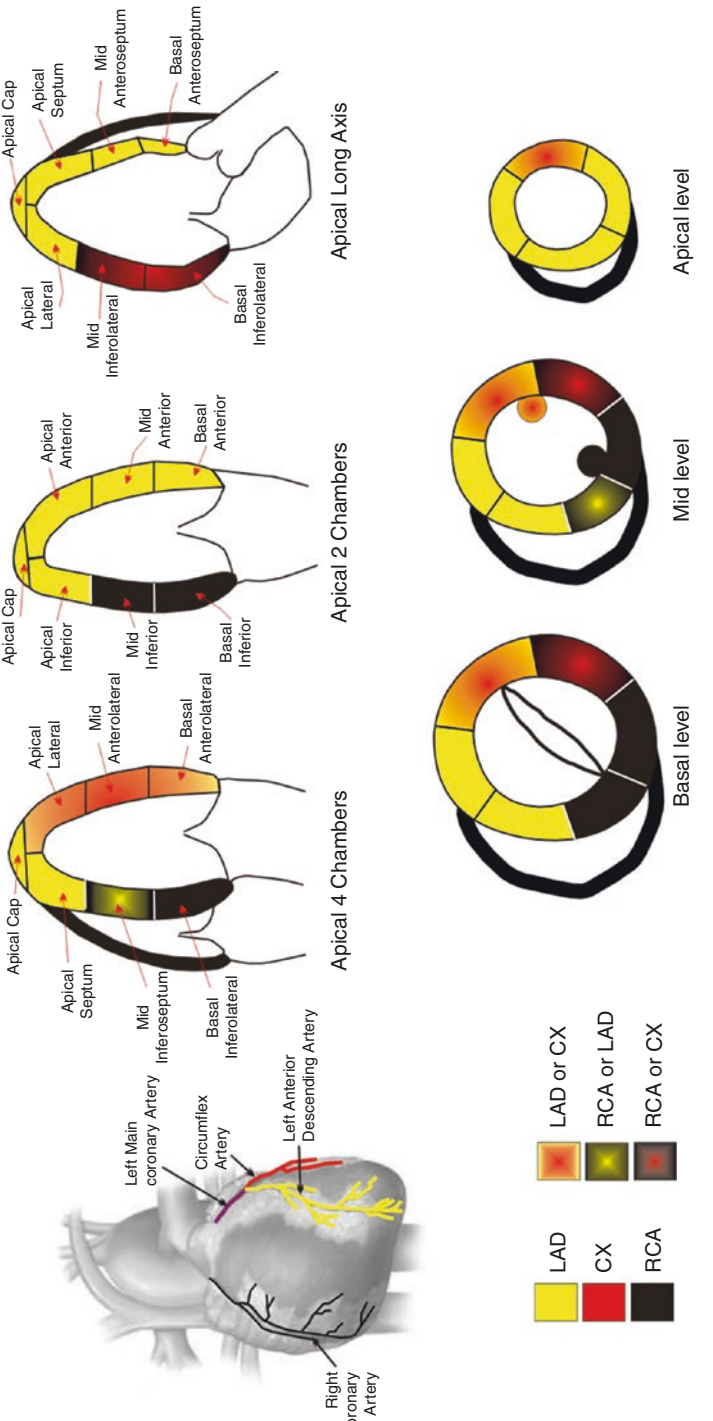

Fig. 1.2 Distributions of the right coronary artery (RCA), left anterior descending artery (LAD), and circumflex coronary artery (CX)

The Ischemic Cascade

The ischemic cascade refers to a sequence of events that occur in the myocardium after the onset of ischemia [7]. Myocardial perfusion is determined by coronary blood flow and myocardial oxygen consumption. Any imbalance in this supply and demand relationship results in myocardial ischemia. The mechanical, electrographic, and clinical events that follow the development of ischemia were formally described in 1985 by Hauser et al. [8], and were later termed the "ischemic cascade" [9]. Classically the observable changes occur sequentially (Fig. 1.3) starting with perfusion abnormalities leading to abnormalities in wall function, then ischemic electrocardiogram (ECG) changes, and finally angina. Echocardiography has the ability to detect these pathophysiologic changes in the myocardium at the early stages and therefore is more sensitive than history, physical examination, and ECG for identification of myocardial ischemia.

Echocardiography for the diagnosis of suspected acute ischemia is most helpful in subjects with a high clinical index of suspicion but with nondiagnostic ECG because it allows real-time assessment of myocardial function.

Of note, troponin elevation with chest pain may not be related to an acute coronary syndrome, but rather be secondary to other cardiovascular pathologies such as valvular disease (e.g., severe aortic stenosis or regurgitation) which can induce ischemia by causing LV wall stress; acute heart failure due to systolic and/or diastolic dysfunction; or acute pulmonary embolism with right ventricular strain. Echocardiography is a valuable tool to detect and quantify these abnormalities, regardless of whether the patient is having an acute coronary syndrome.

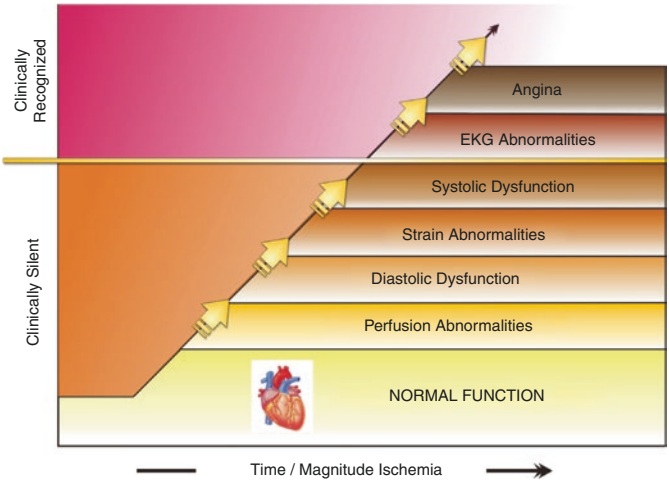

Fig. 1.3 The ischemic cascade. Myocardial dysfunction occurs in a predictable sequence that is detectable prior to clinical symptoms

Pathway for the Use of Echocardiography in Patients with Cardiac Chest Pain (Fig. 1.4)

In the United States it is estimated that about eight million people present each year to the emergency departments with complaints of acute chest pain. If the chest pain is clearly not of a cardiac origin, the patients should be treated accordingly and transthoracic echocardiography (TTE) is seldom needed. If the cause of chest pain appears to be of a cardiovascular etiology then the initial evaluation should include history, physical examination, 12-lead ECG, chest X-ray (CXR), and laboratory tests including cardiac biomarkers (CPK and troponin).

As outlined earlier, ACS incorporates a spectrum of clinical entities ranging from unstable angina and non-STE ACS to STEMI.

The AHA/ACC guidelines in 2014 combined the term unstable angina and the non-STEMI to one group defined as non-STE ACS [10]. The European Society of Cardiology (ESC) guidelines in 2015 still recommend keeping both entities separate [11]. Out of all patients presenting with chest pain only the minority actually have ACS. Among ACS patients, most patients have non-STE ACS.

TTE is an integral part of the management of patients with ACS as seen in Fig. 1.4.

In patients with STEMI, it is now well accepted that patients should preferably be referred to a site that can perform primary percutaneous coronary intervention (PCI). TTE should not be done immediately as it may delay the transfer to the cardiac catheterization laboratory for PCI. TTE should be performed *only after* the intervention is completed.

Patients with non-STE ACS should be treated per current guidelines [10, 11] and *TTE should be performed as soon as possible* to exclude any structural heart disease.

Currently, the use of contrast echo is a standard of care for patients in whom two of more consecutive left ventricle (LV) segments are not well visualized, or when there is a need to rule out an apical thrombus.

For patients whose chest pain is of a cardiovascular etiology but not due to ACS, TTE should be performed *immediately* if the symptoms persist and the patient has active ongoing chest pain.

If the symptoms of chest pain had subsided we recommend to continue the serial evaluation for ACS [10, 11] and perform *TTE as needed*.

If TTE shows an evidence of new wall motion abnormalities, a diagnosis of coronary artery disease is likely. Similarly, contrast echocardiography is necessary when the endocardial definition is poor.

For patients in whom a diagnosis of ACS is ruled out, and they do not have evidence of new wall motion abnormalities, other cardiac etiologies should be considered. These include acute aortic syndrome, acute pericardial disease, pulmonary embolism, aortic stenosis, or hypertrophic cardiomyopathy.

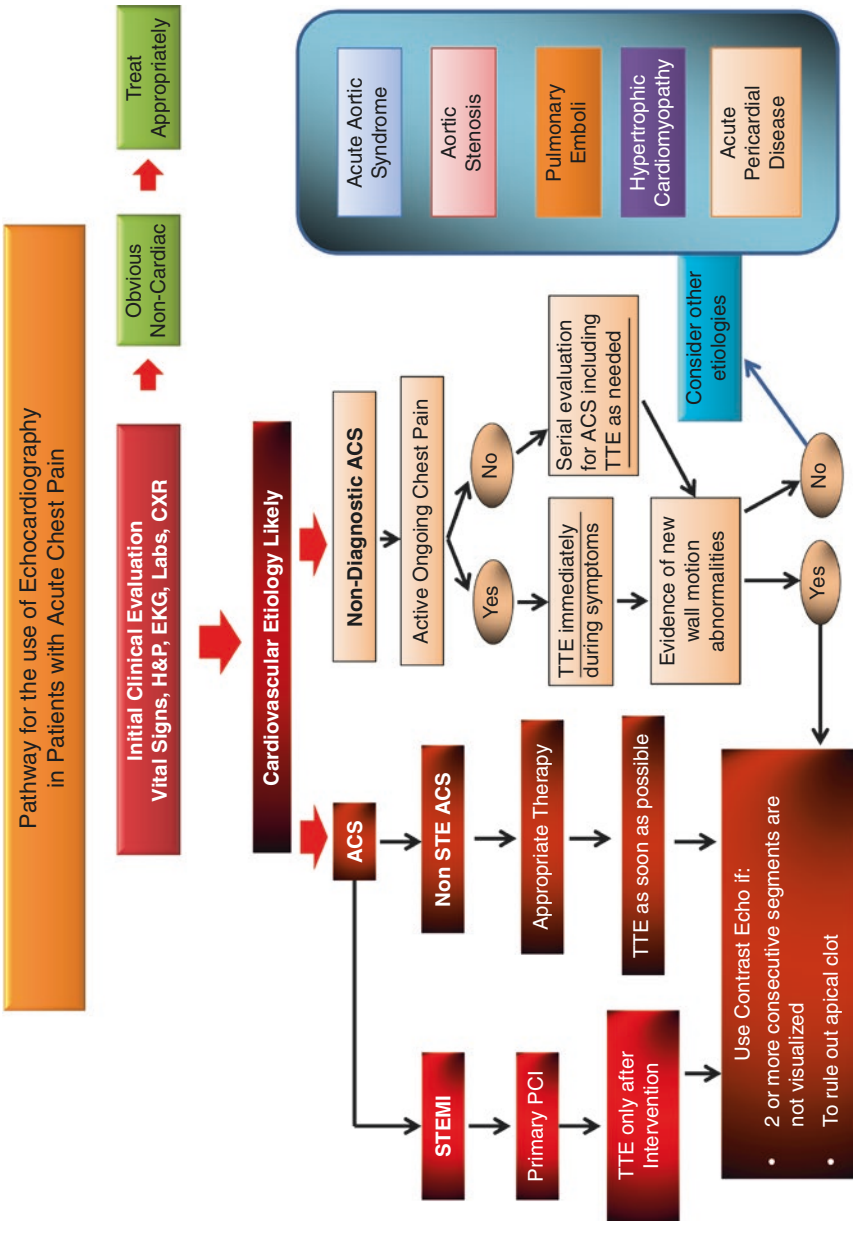

Fig. 1.4 Pathway for the use of echocardiography in patients with acute chest pain

Echocardiography in the Diagnosis and Management of Mechanical Complications of Myocardial Infarction

Mechanical complications of acute myocardial infarction (AMI) result in some of the deadliest cardiovascular outcomes. It is difficult to assess the true incidence of these complications as both clinical and autopsy series differ considerably. It is important to realize that these catastrophic events can occur within minutes to hours after the inciting event, or even days to weeks later. Mechanical complications of acute myocardial infarctions can be divided into two major categories: acute-phase complications and chronic-phase complications. Table 1.3 outlines acute-phase complications and the chronic-phase complications of AMI.

Echocardiography is the key imaging modality in the assessment of these complications.

Left Ventricular Free Wall Rupture

Left ventricular free wall rupture (LVFWR) is an almost universally fatal complication of AMI. Despite advances in the reduction of both mortality and morbidity from AMI, death related to LVFWR remains high.

Myocardial rupture more often involves the left ventricle rather than the right ventricle, and rarely involves the atria [12]. The infarct commonly affects the anterior and lateral walls of the left ventricle near the junction of the infarcted and normal myocardium.

Figure 1.5 demonstrates a TTE of a patient with inferolateral free wall rapture.

Figure 1.6 demonstrates a case of LV free wall rupture causing pericardial tamponade with thrombus formation in the pericardial space.

Ventricular Septal Rupture

The rupture of the interventricular septum is another deadly complication of AMI. Rapid diagnosis, aggressive medical therapy, and prompt surgical intervention are essential to increase the chances of survival.

In the pre-reperfusion era, rupture of the interventricular septum was estimated to occur in 1–2% of patients with acute myocardial infarction and to account for

Table 1.3 Acute-phase vs. chronic-phase complications in acute myocardial infarction

Acute phase	Chronic phase
Left ventricular free wall rupture	True ventricular aneurysm
Ventricular septal rupture	Ventricular pseudoaneurysm
Right ventricular infarction	Left ventricular thrombus
Acute mitral regurgitation	

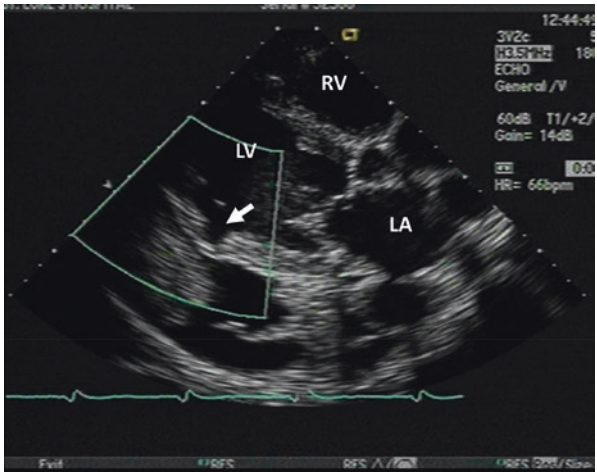

Fig. 1.5 Parasternal long-axis view of a transthoracic echocardiogram demonstrating a inferolateral free wall rupture (*arrow*); *RV* right ventricle, *LV* left ventricle, *LA* left atrium

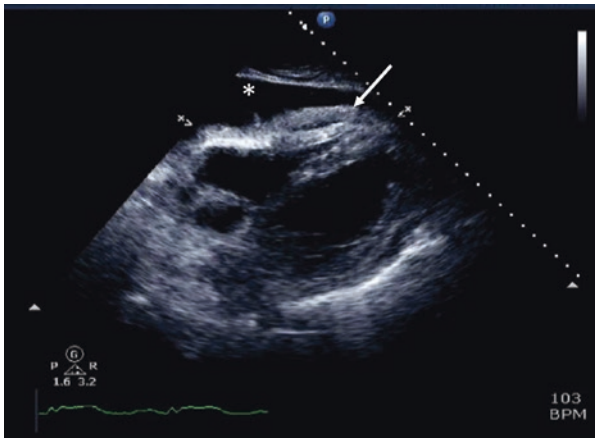

Fig. 1.6 Subcostal view showing pericardial effusion (*asterisk*) with a thrombus in the pericardial space (*arrow*). This was caused by a ventricular free wall rupture after an acute myocardial infarction and the patient developed cardiac tamponade physiology

approximately 5% of deaths in this setting. This complication typically occurs within the first week after infarction, with a mean time from symptom onset of 3–5 days. The classic risk factors for septal rupture in the pre-reperfusion era included hypertension, advanced age, female sex, and absence of a history of myocardial infarction or angina [13]. Prognosis for ventricular septal rupture in the pre-reperfusion era was very poor. With the advent of thrombolysis and percutaneous intervention, incidence and outcomes have changed.

In the current era, early reperfusion therapy may prevent the extensive myocardial necrosis that is associated with ventricular rupture. Patients generally have a mean time of 1 day from infarction to development of a ventricular septal rupture (VSR).

The ventricular septum is a very vascular structure. The rarity of septal rupture and the variable infarct location relate to the fact that the interventricular septum has a dual

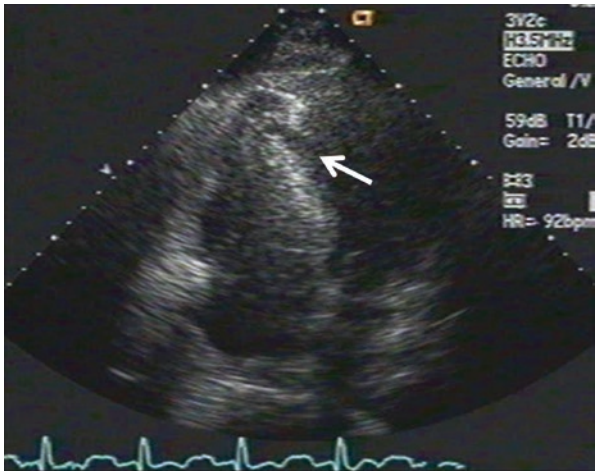

Fig. 1.7 Apical four-chamber view of a transthoracic echocardiogram demonstrating a ventricular septal rupture in the distal portion of the interventricular septum (*arrow*)

blood supply. The anterior two-thirds are supplied by the left anterior descending coronary artery and its branches. The posterior one-third is supplied by branches of the posterior descending artery, which arises from the right coronary or the left circumflex artery, depending on the dominance of the circulation [14]. Similar to the free wall rupture, interventricular septal rupture occurs most frequently with a first myocardial infarction when there is less likely to be collateral blood flow. In this setting, with an abrupt cessation of blood flow in the infarct-related artery, no collateral flow exists to support the infarcted zone, thereby making the septum prone to rupture.

Figure 1.7 demonstrates an apical four-chamber view of a transthoracic echocardiogram demonstrating a ventricular septal rupture in the distal portion of the interventricular septum (arrow).

Figure 1.8 demonstrates a case of apical ventricular septal rupture in a patient with an acute LAD territory MI.

Right Ventricular Infarction

Right ventricular infarction (RVI) complicates up to half of inferior wall left ventricular infarctions [15].

Coronary blood flow to the right ventricle is unique in that it occurs in both systole and diastole. In the majority of patients the right coronary artery (RCA) supplies the right ventricle through the acute marginal branches, as well as the inferior wall and posterior interventricular septum through the posterior descending artery in right dominant systems. Typically, RVI occurs when there is occlusion of the RCA proximal to the acute marginal branches. It can also occur with an occlusion of the left circumflex in patients who have a left dominant system. Although quite rare, occlu-

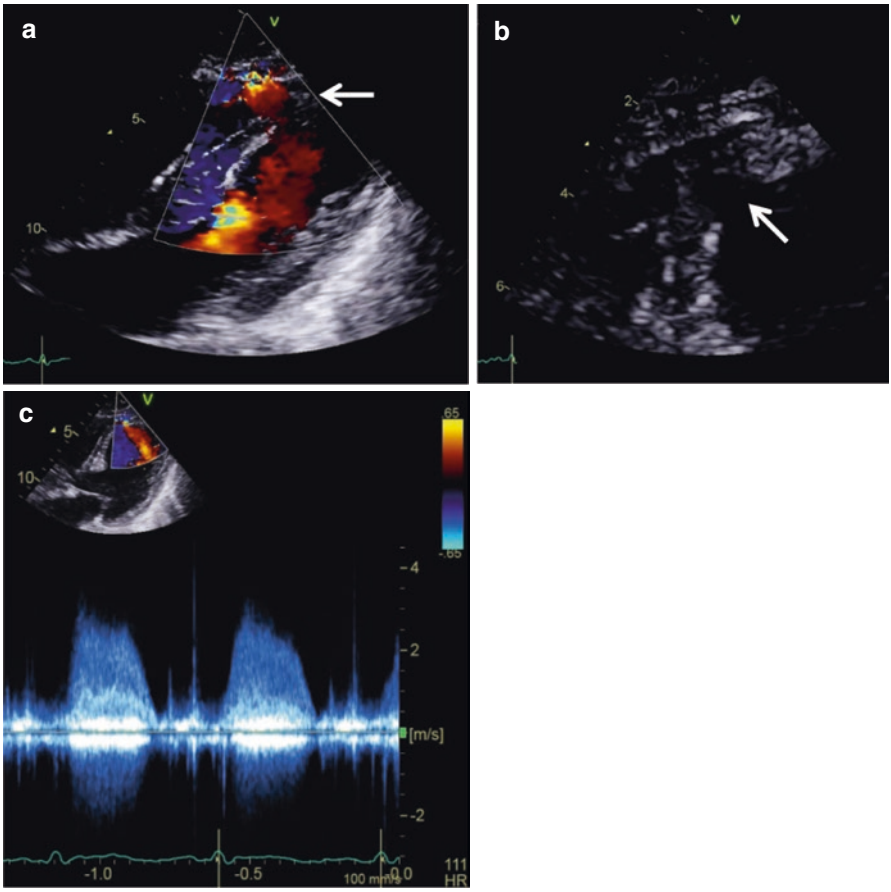

Fig. 1.8 Subcostal view showing apical ventricular septal rupture with flow from the left ventricle to right ventricle: (**a**) color Doppler flow, (**b**) VSR defect seen with 2D imaging, (**c**) continuous-wave Doppler demonstrating gradient across VSR

sion of the left anterior descending artery may result in infarction of the anterior right ventricle [15].

Acute underperfusion of the right ventricular free wall and adjacent interventricular septum leads to a stunned and noncompliant right ventricle. Loss of the right ventricular contractility results in a serious deficit in the left ventricular preload with a resultant drop in cardiac output, thereby causing systemic hypotension.

Acute right ventricular dilatation causes a leftward shift of the interventricular septum, increasing left ventricular end-diastolic pressure with a resultant decrease in left ventricular compliance and cardiac output (Fig. 1.9).

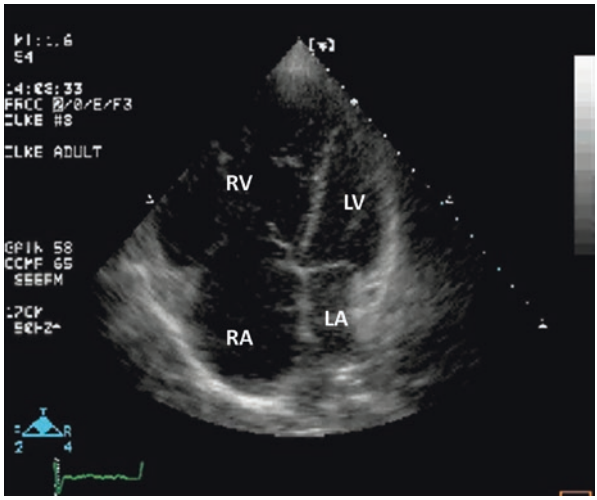

Fig. 1.9 Apical four-chamber view of a transthoracic echocardiogram demonstrating a dilated and severely hypokinetic right ventricle compressing the left ventricle. *RV* right ventricle, *RA* right atrium, *LV* left ventricle, *LA* left atrium

Acute Mitral Regurgitation

Acute mitral regurgitation (MR) is another major fatal mechanical complication of acute myocardial infarction. The three main causes of MR in the setting of an AMI include ischemic papillary muscle dysfunction, papillary muscle or chordal rupture, and left ventricular dilatation [16].

Figure 1.10 demonstrates an apical four-chamber view of a transthoracic echocardiogram showing mitral regurgitation as a result of an inferior wall myocardial infarction.

Figure 1.11 shows a ruptured papillary muscle resulting in severe mitral regurgitation, requiring urgent surgical intervention.

True Ventricular Aneurysm

In contrast to the acute complications of myocardial infarction, the chronic complications of AMI are not immediately life threatening. They have a different presentation and require different treatment. A true left ventricular aneurysm (LVA) is a common chronic complication of AMI that is important to diagnose.

Approximately 70–85% of LVAs are located in the anterior or apical walls, and in most cases are due to complete occlusion of the LAD coronary artery in the absence of collateralization. However, 10–15% of cases involve the inferior and basal walls due to right coronary artery occlusion. A rare finding is a lateral LVA, which is the result of an occluded left circumflex coronary artery.

LVA has been described as a well-delineated and distinct break ("hinge point") in the LV geometry and contour present in both systole and diastole. The pathognomonic feature is a wide mouth that enables communication with the aneurysmal cavity (Figs. 1.12 and 1.13).

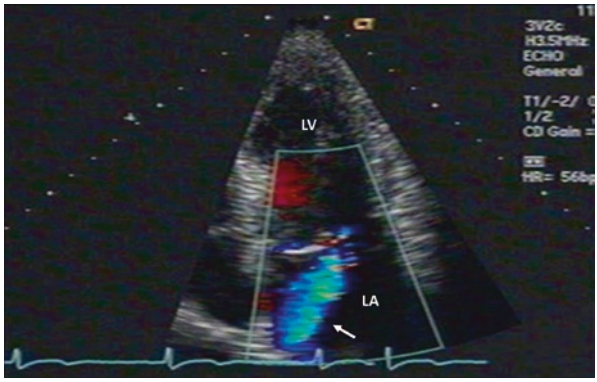

Fig. 1.10 Apical four-chamber view of a transthoracic echocardiogram showing mitral regurgitation as a result of an inferior wall myocardial infarction (arrow)

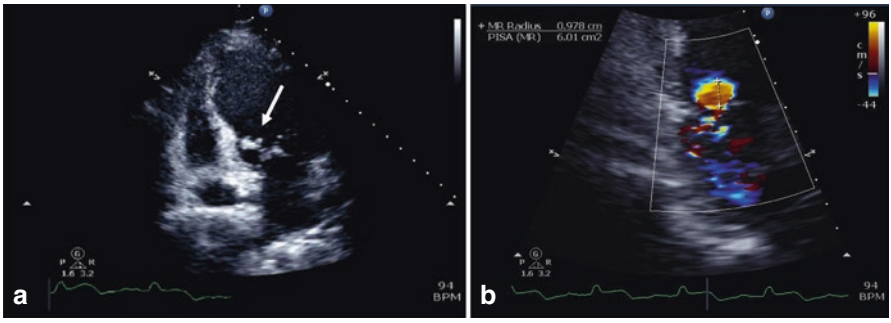

Fig. 1.11 Papillary muscle rupture. (**a**) Apical four-chamber view showing ruptured head of the papillary muscle (arrow). (**b**) Apical three-chamber view with color Doppler demonstrating severe mitral regurgitation with large PISA radius. *PISA* Proximal isovelocity surface area

Although the size of an aneurysm varies widely, most are within 1–8 cm in diameter. The wall of the aneurysm typically consists of a hybrid of necrotic myocardium and white fibrous scar tissue. This wall is extremely thin and delicate and may calcify over an extended period of time. Of note, it is imperative to distinguish between a LVA and a pseudoaneurysm, which is characterized by a narrow neck and has a distinct "shelf-like" opening.

Left Ventricular Pseudoaneurysm

A left ventricular pseudoaneurysm (LVPA) or false aneurysm is a less common form of a ventricular aneurysm and presents in <1% of patients post-myocardial infarction.

An LVPA forms when cardiac rupture is contained by adherent pericardium or scar tissue. Unlike a true aneurysm, a LVPA is devoid of endocardium or myocardium and since these aneurysms are prone to rupture a quick and accurate diagnosis is of extreme importance. Unlike a true LVA whereby the walls consist of dense fibrous

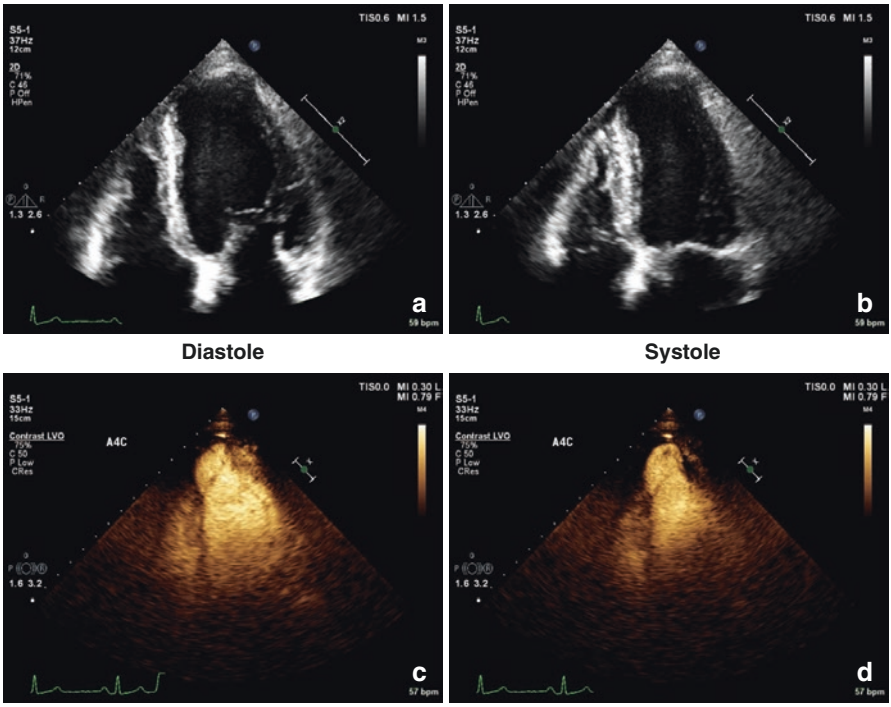

Fig. 1.12 (**a**–**d**) Apical four-chamber view in diastole (**a**) and systole (**b**) and with echo contrast, respectively (**c**, **d**), showing a large apical AMI with a large apical aneurysm with no clot

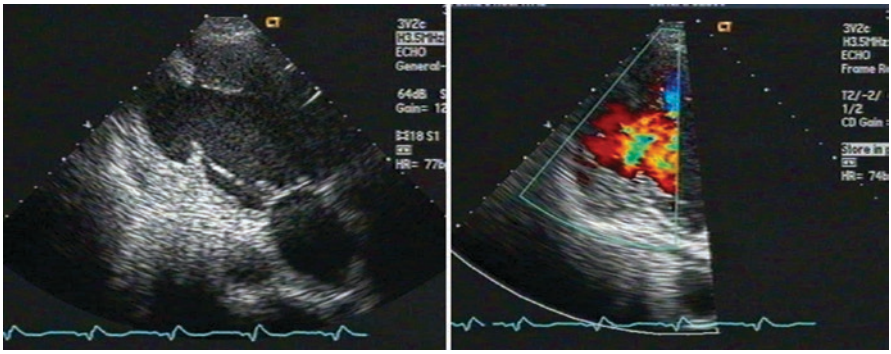

Fig. 1.13 Apical three-chamber view (left) obtained from transthoracic echocardiogram revealing a large left ventricular aneurysm, enhanced with color flow Doppler (right) establishing an area of communication between the normal left ventricle and the aneurysmal portion

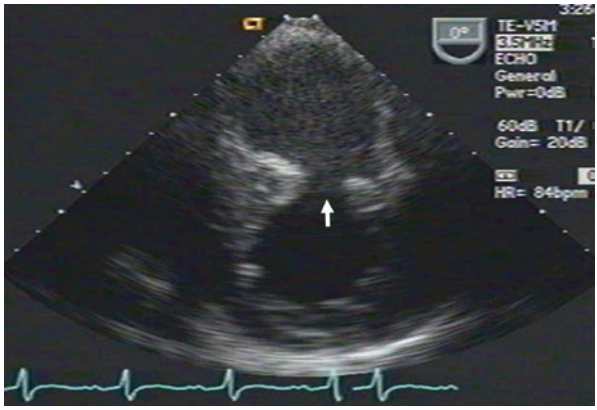

Fig. 1.14 Short-axis view of the left ventricle (lower cavity) during transesophageal echocardiography. Large pseudoaneurysm is seen (higher cavity). Notice the narrow "bottleneck" opening (arrow)

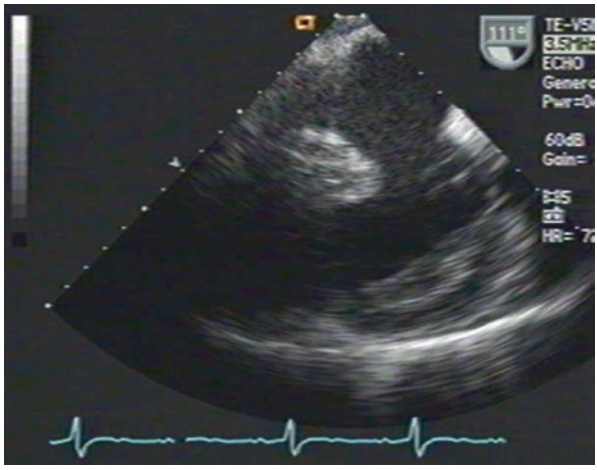

Fig. 1.15 Short-axis view from transesophageal echocardiogram depicting a large pseudoaneurysm (higher cavity). Notice the narrow "shelf-like" opening into the aneurysmal cavity

tissue with excellent tensile strength, the wall of a LVPA is comprised of thrombus and varying portions of the epicardium and parietal pericardium. It is the result of an AMI (typically an inferior or posterolateral wall AMI) with myocardial rupture and hemorrhage into the pericardial space, becoming progressively compressive. Cardiac tamponade occurs, thereby preventing further hemorrhage into the pericardium. Over time, thrombus organizes with overall poor structural integrity, and thus is prone to inevitable rupture, which can be a fatal event [17].

Echocardiography can usually distinguish a pseudoaneurysm from a true aneurysm by the appearance of a connection between the aneurysm and ventricular cavity. LVPA have a narrow neck, typically less than 40% of the maximal aneurysm diameter, which causes an abrupt interruption in the ventricular wall contour (Figs. 1.14 and 1.15). In contrast, true aneurysms are nearly as wide at the neck as they are at the apex.

Left Ventricular Thrombus

A mural LV thrombus is a common sequela of an AMI and most commonly develops in the presence of a large infarction. Thrombi are prone to originate in regions of stasis; they are most commonly noted to occur in the apex but may also occur in lateral and inferior aneurysms. Characteristically, a thrombus has a nonhomogeneous echo density with a margin distinct from the underlying wall, which is akinetic to dyskinetic (Figs. 1.16 and 1.17). A thrombus is more likely to occur following an AMI in the LAD artery distribution (up to 33%) than in regions supplied by the right coronary or circumflex coronary arteries (<1%).

Echocardiography Acute Aortic Syndrome

Acute aortic syndrome (AAS) represents a spectrum of life-threatening conditions with similar clinical presentation and the need for urgent management. It includes classic acute aortic dissection (CAAD), intramural hematoma (IMH), and penetrating aortic ulcer (PAU) [18, 19].

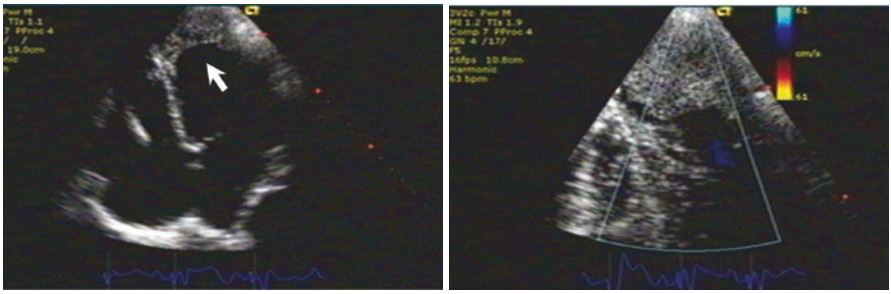

Fig. 1.16 Apical four-chamber views of a transthoracic echocardiogram from a 74-year-old patient 3 months following AMI (top). Notice the large protruding apical thrombus (*arrow*). Color flow imaging (bottom) may be used to demonstrate abnormal flow patterns

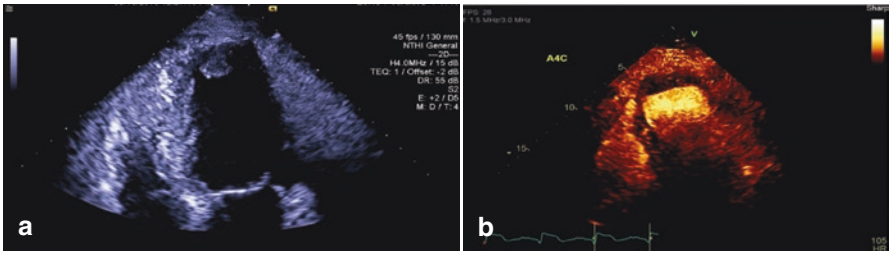

Fig. 1.17 Apical four-chamber view of a transthoracic echocardiogram demonstrating a large left ventricular apical thrombus (**a**). Injection of an echo-contrast agent delineates the linear appearance of this large apical thrombus (**b**)

AAS is characterized by disruption of the media layer of the aorta and typically presents with acute chest pain.

Although the incidence of AAS is lower than that of ACS, AAS carries a higher mortality, and is therefore a critical component of the differential diagnosis of chest pain in the CCU. The International Registry of Acute Aortic Dissection (IRAD) was created in 1996 as a way to combine data acquired from multiple institutions in Europe, North America, and Asia [19]. The 2010 intersocietal guidelines for the diagnosis and management of patients with thoracic aortic disease propose a standard approach to the diagnosis and treatment of AAS [20].

While clinical history and physical exam are important, imaging is essential in the diagnosis of AAS. Transesophageal echocardiography (TEE), computed tomography (CT), and magnetic resonance imaging (MRI) are the preferred imaging modalities and angiography is rarely needed.

AAS is classified based on the location and extent of involvement of the aorta. Two commonly used classifications include the DeBakey and the Stanford systems. The DeBakey system divides aortic dissection into three types based on their anatomical location. Type I originates in the ascending aorta and propagates beyond the aortic arch, type II is limited to the ascending aorta only, and type III is limited to the descending aorta [21]. The Stanford system divides aortic dissections into two types. Type A includes any dissection that involves the ascending aorta, while type B dissections are limited to the descending thoracic aorta [22]. The Stanford classification appears to have wider acceptance and is now used for all three AAS types: CAAD, IMH, and PAU.

Intramural Hematoma

IMH is defined by crescentic or circumferential thickening of the media layer of the aortic wall. IMH is likely due to ruptured vasa vasorum resulting in intramural bleeding but without a detectable intimal tear.

According to the IRAD experience, IMH typically presents with the symptoms of severe chest and back pain, similar to CAAD. However, IMH is less likely to result in severe aortic regurgitation and pulse deficits. IMH is usually unstable and may evolve into CAAD or regresses spontaneously; thus serial imaging is crucial. Stanford type B lesions in the descending aorta are more common than type A lesions in the ascending aorta (65% vs. 35% of all IMH, respectively) [19].

On TEE, IMH is diagnosed if there is regional thickening of the aortic wall >5 mm in a crescentic or circumferential pattern without an intimal flap or tear (Fig. 1.18a–c). Limitations of TEE in diagnosing IMH arise from the TEE's inability to visualize all portions of the aorta including the area around the origin of the brachiocephalic artery and all but the most proximal portions of the abdominal aorta. TEE is very useful in diagnosing complications of IMH, such as pericardial effusion or aortic regurgitation.

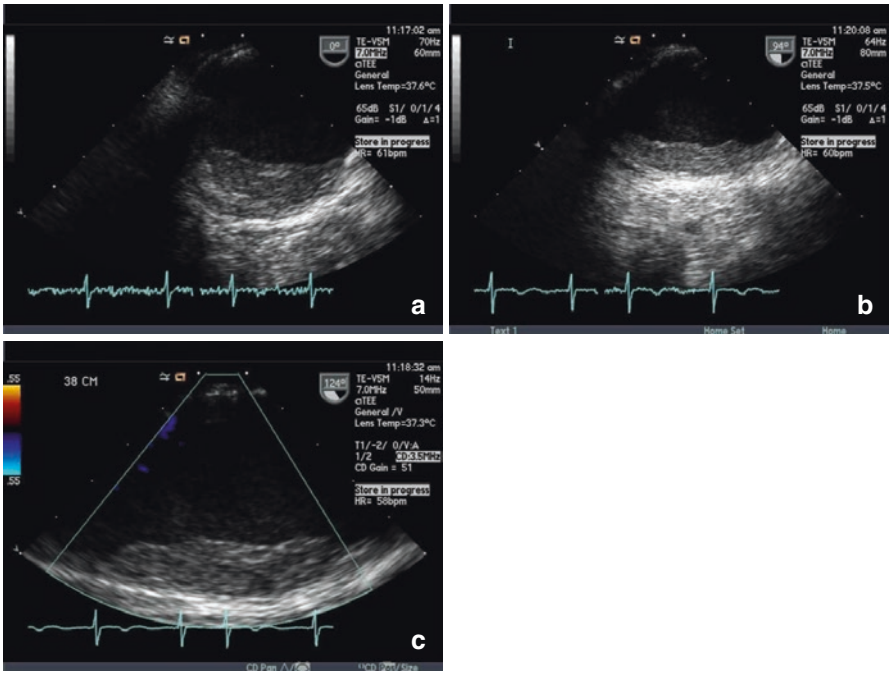

Fig. 1.18 IMH on TEE, showing marked thickening of the aortic wall in a crescentic pattern without an intimal flap or tear, at different TEE angles: (**a**) 0°, (**b**) 94°, (**c**) 124°

Classic Acute Aortic Dissection

CAAD is the most common form of AAS [20]. It occurs in approximately 66–75% of all AAS. The overall incidence of CAAD is low, and is estimated at 0.5–4.0 cases per 100,000 per year, and is thought to affect men more than women in a 2:1 ratio.

CAAD is characterized by an intimal tear, which leads to abnormal blood flow from the aortic lumen into the media. Consequently, there is longitudinal separation of the media layers by blood flow which tears an intimomedial flap from the remainder of the aortic wall. This flap separates the abnormal false lumen from the true aortic lumen. Intimal tears typically occur at the locations within the aorta with the highest shear stress. These are the right side of the ascending aorta immediately distal to the ostium of the right coronary artery (type A dissections) (Fig. 1.19a–c), and immediately distal to the ostium of the subclavian artery adjacent to the insertion of the ligamentum arteriosus (type B dissections).

Complications such as aortic regurgitation and pericardial tamponade can occur, and over time chronic changes such as false lumen thrombosis and aneurysm are common.

The typical symptom of acute aortic dissection is “aortic pain” similar to other forms of AAS. Acute, severe, tearing chest pain is the hallmark symptoms of

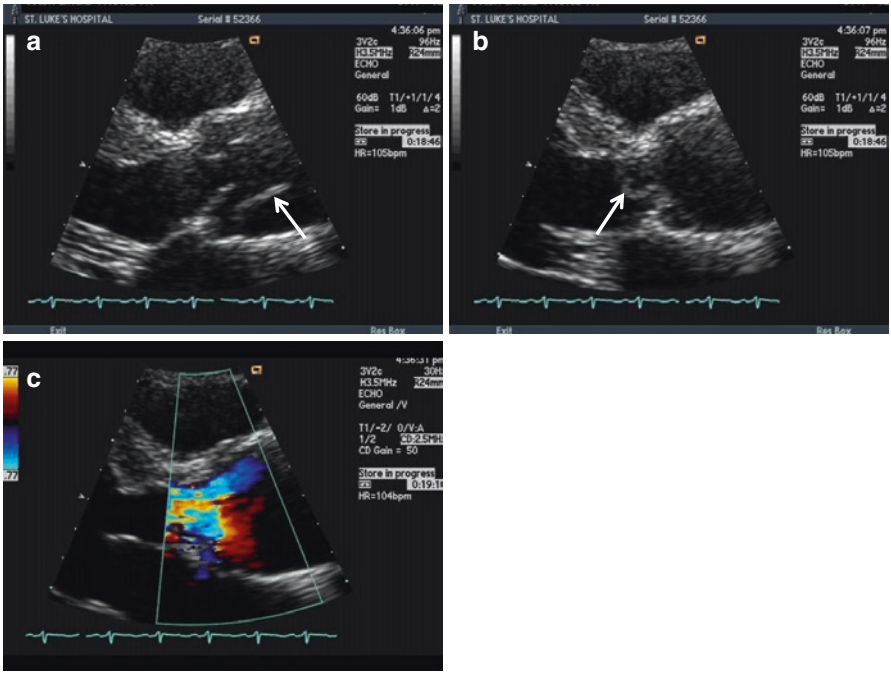

Fig. 1.19 Type A ascending aortic dissection with a distinct dissection flap seen in the ascending aorta (**a** with *arrow*) prolapsing into the aortic valve (**b** with *arrow*) with evidence of severe aortic regurgitation (**c**)

CAAD. Pain limited to the chest is typical of type A CAAD and pain in the back is more often the symptom of type B CAAD.

TEE is useful in the diagnosis of CAAD especially when a CT with contrast cannot be performed, such as in hemodynamically unstable patients or in patients who cannot tolerate iodinated intravenous contrast such as those with renal insufficiency or severe allergy. The reported sensitivity of TEE is 98% and specificity is 63–93%. Findings on TEE are a dissection flap separating the true and false lumen as well as the site of intimal tear represented by flow from the true lumen into the false lumen on color Doppler (Fig. 1.20a, b). Spectral Doppler may help corroborate the diagnosis by demonstrating "to and fro" flow into and out of the false lumen.

The true lumen is identified by its expansion with systole and contraction in diastole. The true lumen is often smaller than the false lumen. In early stages, the false lumen may be echo free or may contain spontaneous echo contrast (also known as "smoke") due to stasis of blood flow. In later more chronic stages, the false lumen may be partly or completely obliterated by thrombus formation (Fig. 1.21a–d).

Complications of CAAD may be seen on echocardiography such as aortic regurgitation, pericardial effusion/tamponade, and wall motion abnormalities indicative of ischemia if there is coronary ostial involvement.

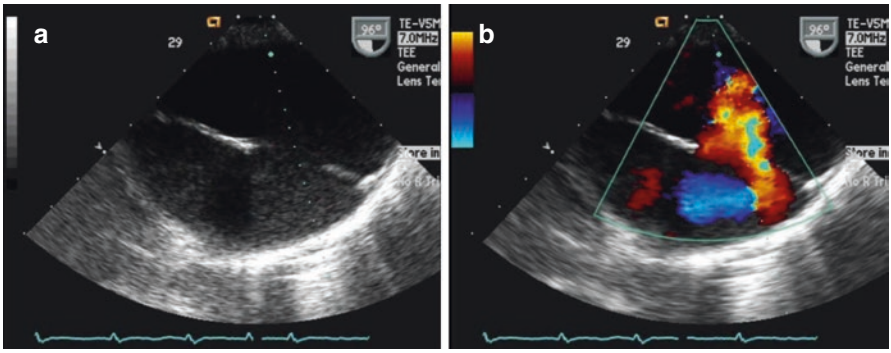

Fig. 1.20 A dissection flap is seen in the descending thoracic aorta separating the true and false lumens; the site of intimal tear is represented by the flow from the true lumen into the false lumen on color Doppler

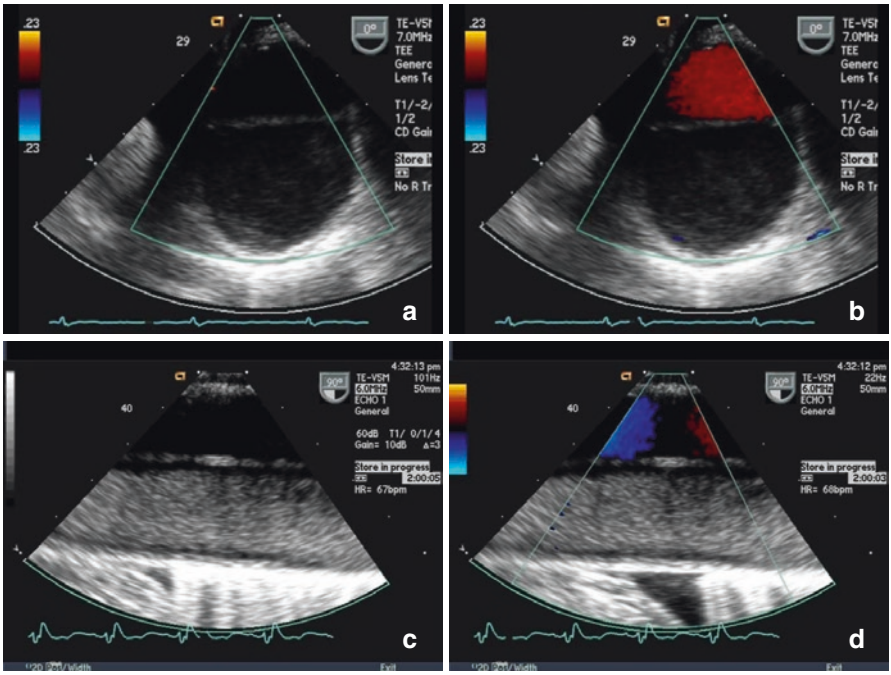

Fig. 1.21 Type B descending aortic dissection with a distinct dissection flap seen in the descending aorta (panel **a**). The true lumen is often smaller than the false lumen. In early stages (panel **b**), the false lumen may be echo free or may contain spontaneous echo contrast (also known as "smoke") due to stasis of blood flow. In later more chronic stages, the false lumen may be partly or completely obliterated by thrombus formation (panels **c**, **d**)

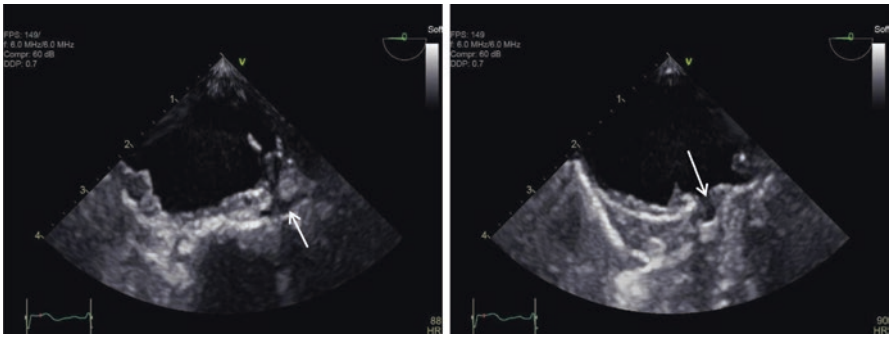

Fig. 1.22 (**a**, **b**): Penetrating aortic ulcer (PAU) develops as an atherosclerotic plaque erodes and penetrates through the elastic lamina into the media layer of the aorta, causing ulceration

It is important not to confuse the intimomedial flap of CAAD with either artifacts or surrounding vascular structures. Linear reverberation artifacts in the ascending aorta should not be mistaken for type A aortic dissection. Typically, reverberation artifacts are located twice as deep as the anterior aortic wall. In addition, a dilated azygos vein adjacent to the descending thoracic aorta may give an illusion of a type B dissection. Color or spectral Doppler imaging in both instances may help distinguish true aortic dissection from its masqueraders.

Penetrating Aortic Ulcer

Penetrating aortic ulcer (PAU) represents the process by which an atherosclerotic plaque erodes and penetrates through the elastic lamina into the media layer of the aorta, causing ulceration (Fig. 1.22a, b). PAU may further erode through the adventitia leading to either focal (pseudoaneurysm) or complete aortic rupture. Thrombus occasionally forms within PAU. In addition, PAU may lead to either IMH or aortic dissection, which is why PAU is characterized as an AAS.

References

1. Lancellotti P, Price S, Edvardsen T, et al. The use of echocardiography in acute cardiovascular care: recommendations of the European Association of Cardiovascular Imaging and the Acute Cardiovascular Care Association. Eur Heart J Cardiovasc Imaging. 2015;16(2):119–46.
2. Panjrath GS, Herzog E, Chaudhry F. Introduction: acute coronary syndrome and echocardiography. In: Herzog E, Chaudhry F, editors. Echocardiography in ACS from prevention to diagnosis and treatment. London: Springer; 2009. p. 1–4.

3. Saric M. Echo assessment of systolic and diastolic function in acute coronary syndrome. In: Herzog E, Chaudhry F, editors. Echocardiography in ACS from prevention to diagnosis and treatment. London: Springer; 2009. p. 37–57.
4. Lang RM, Badano LP, Mor-Avi V, et al. Recommendations for cardiac chamber quantification by echocardiography in adults: an update from the American Society of Echocardiography and the European Association of Cardiovascular Imaging. J Am Soc Echocardiogr. 2015;28: 1–39.
5. Multicenter Postinfarction Research Group. Risk stratification and survival after myocardial infarction. N Engl J Med. 1983;49(6):331–6.
6. Carlson MD, Krishen A. Risk assessment for ventricular arrhythmias after extensive myocardial infarction: what should I do? ACC Curr J Rev. 2003;12(2):90–3.
7. Ansari A, Puthumana J. The "Ischemic Cascade". In: Herzog E, Chaudhry F, editors. Echocardiography in ACS from prevention to diagnosis and treatment. London: Springer; 2009. p. 149–60.
8. Hauser AM, Vellappillil G, Ramos RG, et al. Sequence of mechanical, electrocardiographic and clinical effects of repeated coronary artery occlusion in human beings: echocardiographic observations during coronary angioplasty. J Am Coll Cardiol. 1985;5:193–7.
9. Nesto RW, Kowalchuk MD. The ischemic cascade: temporal sequence of hemodynamic, electrocardiographic and symptomatic expressions of ischemia. Am J Cardiol. 1987;57: 23C–4C.
10. Amsterdam EA, Wenger NK, Brindis RG, et al. AHA/ACC guideline for the management of patients with non-ST-elevation acute coronary syndromes: a report of the American College of Cariology/American Heart Association Task Force on Practice Guideline. J Am Coll Cardiol. 2014;64:e139–228.
11. Roffi M, Patrono C, Collet JP, et al. ESC guidelines for the management of acute coronary syndromes in patients presenting without persistent ST-segment elevation. Eur Heart J. 2016;37:267–315.
12. Becker RC, Gore JM, Lambrew C, et al. for the National Registry of Myocardial Infarction Participants. A composite view of cardiac rupture in the United States National Registry of Myocardial Infarction. J Am Coll Cardiol. 1996;27:1321.
13. Birnbaum Y, Fishbein MC, Blanche C, Siegel RJ. Ventricular septal rupture after acute myocardial infarction. N Engl J Med. 2002;347(18):1426–32.
14. Buda AJ. The role of echocardiography in the evaluation of mechanical complications of acute myocardial infarction. Circulation. 1991;84(3 Suppl):109–21.
15. Kinch JW, Ryan TJ. Right ventricular infarction. N Engl J Med. 1994;34:1211–9.
16. Tcheng JE, Jackman JD, Nelson CL, et al. Outcome of patients sustaining acute ischemic mitral regurgitation during myocardial infarction. Ann Intern Med. 1992;117:18.
17. Frances C, Romero A, Grady D. Left ventricular pseudoaneurysm. J Am Coll Cardiol. 1998;32:557.
18. Vilacosta I, San Roman JA. Acute aortic syndrome. Heart. 2001;85:365–8.
19. Hagan PG, Nienaber CA, Isselbacher EM, et al. The International Registry of Acute Aortic Dissection (IRAD): new insights into an old disease. JAMA. 2000;283:897–903.
20. Hiratzka LF, Bakris GL, Beckman JA, et al. ACCF/AHA/AATS/ACR/ASA/SCA/SCAI/SIR/STS/SVM guidelines for the diagnosis and management of patients with thoracic aortic disease. A report of the American College of Cardiology Foundation/American Heart Association Task Force on Practice Guidelines, American Association for Thoracic Surgery, American College of Radiology, American Stroke Association, Society of Cardiovascular Anesthesiologists, Society for Cardiovascular Angiography and Interventions, Society of Interventional Radiology, Society of Thoracic Surgeons, and Society for Vascular Medicine. J Am Coll Cardiol. 2010;55:e27–e129.
21. Debakey ME, Henly WS, Cooley DA, Morris GC Jr, Crawford ES, Beall AC Jr. Surgical management of dissecting aneurysms of the aorta. J Thorac Cardiovasc Surg. 1965;49:14–49.
22. Daily PO, Trueblood HW, Stinson EB, Wuerflein RD, Shumway NE. Management of acute aortic dissections. Ann Thorac Surg. 1970;10:237–47.

Chapter 2
Echocardiographic Assessment of Acute Dyspnea in the CCU

Edgar Argulian, Jagat Narula, and Eyal Herzog

Abstract Echocardiography is essential in evaluating patients with acute and subacute dyspnea. Depending on the urgency and severity of patient's condition the applications of echocardiography can range from immediate point-of-care ultrasound to assess for gross abnormalities (such as pericardial effusion) to detailed evaluation of underlying structural heart disease. We present a structured approach to evaluation of patients with acute and subacute dyspnea utilizing a wide range of echocardiographic techniques.

Keywords Dyspnea · Heart failure · Pericardial effusion · Pulmonary hypertension

Introduction

Echocardiography is essential in evaluating patients with acute and subacute dyspnea. Depending on the urgency and severity of patient's condition the applications of echocardiography can range from immediate point-of-care ultrasound to assess for gross abnormalities (such as pericardial effusion) to detailed evaluation of underlying structural heart disease. We present a structured approach to evaluation of patients with acute and subacute dyspnea utilizing a wide range of echocardiographic techniques.

A long list of differential diagnoses including cardiac, respiratory, pulmonary, neurologic, and metabolic causes should be considered for nontraumatic shortness of breath in the acute care settings. Some of these causes are obvious upon initial evaluation which includes history, physical examination, electrocardiogram, chest imaging, and laboratory testing but many remain obscure. Echocardiography is an essential tool in evaluating possible cardiac causes of dyspnea due to its portability, time efficiency, and diagnostic accuracy. We advocate for structured and

E. Argulian (✉) · J. Narula · E. Herzog
Mount Sinai St. Luke's Hospital, New York, NY, USA
e-mail: Edgar.Argulian@mountsinai.org; jagat.narula@mountsinai.org; Eyal.Herzog@mountsinai.org

E. Herzog, E. Argulian (eds.), *Echocardiography in the CCU*,
https://doi.org/10.1007/978-3-319-90278-4_2

Table 2.1 Ultrasound modalities in evaluation of patients with suspected cardiac causes of acute and subacute shortness of breath

Point-of-care cardiac ultrasound
Comprehensive transthoracic echocardiogram
Limited/focused transthoracic echocardiogram (intracardiac device positioning, etc.)
Transesophageal echocardiogram
Contrast echocardiography
Stress echocardiogram including dobutamine echocardiography
Speckle-tracking echocardiography for assessment of myocardial mechanics
3D echocardiography
Lung ultrasound
Vascular ultrasound for intravenous access

comprehensive echocardiographic evaluation of patients with suspected cardiac acute and subacute dyspnea in the acute care settings tailored to the urgency of evaluation and specific clinical scenario (Table 2.1 and Fig. 2.1).

Is There a Pericardial Effusion?

Pericardial effusion is present in a substantial proportion of patients (up to 20%) seen in the acute care settings such as emergency department [1]. When evaluating the hemodynamic impact of pericardial effusion one should take into account the acuity of presentation. Acute accumulation of fluid (within minutes to hours) rapidly exceeds the pericardial stretch limit and commonly presents as cardiogenic shock: acute or surgical tamponade requires immediate intervention. Chamber perforation during a percutaneous procedure is a good example of acute tamponade. When pericardial fluid accumulates slowly (within days to weeks) a large amount of fluid can be present without dramatic lowering of the cardiac output [2]. Dyspnea is the cardinal symptom of subacute pericardial tamponade but it is nonspecific. Clinical findings of tamponade include tachycardia, jugular venous distention, pulsus paradoxus, and diminished heart sounds and all lack both sensitivity and specificity [2]. While patients with acute (surgical) tamponade rapidly progress to cardiogenic shock, hypotension is rather uncommon in patients with subacute tamponade who accumulate pericardial effusion within days to weeks. On the contrary, many patients are hypertensive due to high levels of circulating catecholamines in response to hemodynamic stress [3]. Therefore, echocardiography is currently the cornerstone of hemodynamic evaluation of pericardial effusion.

Diagnosis of pericardial effusion can be made with the point-of-care ultrasound with high sensitivity and specificity, even when the examination is done by a noncardiologist [1]. On the other end, diagnosing tamponade physiology requires comprehensive echocardiography using 2D, Doppler, and M-mode examinations [2].

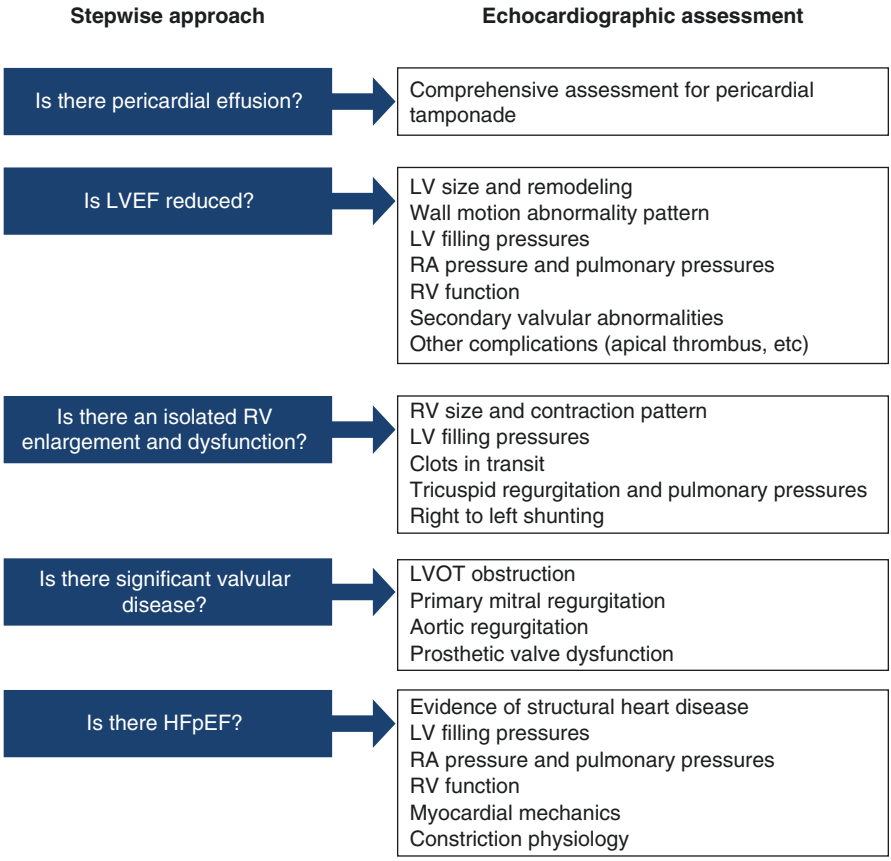

Fig. 2.1 Stepwise approach to echocardiographic assessment of patients with suspected cardiac dyspnea in acute care settings. This approach should be tailored to the urgency of situation and individual patient characteristics

Displaying images for the full respiratory cycle, as opposed to single cardiac cycle, commonly highlight the hemodynamic effects of pericardial effusion.

The size of pericardial effusion seems to be an important but frequently underappreciated part of the echocardiographic assessment. In one study of hospitalized patients with pericardial effusion, the size of the effusion was the only independent predictor of adverse in-hospital outcomes in a multivariate model but not chamber collapse or inferior vena cava plethora [4]. Chamber collapse is a well-recognized phenomenon of pericardial tamponade but it has several pitfalls. Transient buckling of the right atrium is commonly seen in patients with pericardial effusion and it is not specific. A more sustained collapse of the right atrium lasting at least one-third of the cardiac cycle appears to be more specific for cardiac tamponade. Right ventricular early diastolic collapse is a less sensitive finding but has a high specificity. Right ventricular outflow tract should be inspected carefully for the signs of col-

lapse since it is the thinnest area of the right ventricle and M-mode echocardiography should be used for precise timing. Left-sided chamber collapse is much less sensitive but highly specific for tamponade. Importantly, a study by Merce et al. showed that 34% of patients with pericardial effusion but without clinical features of pericardial tamponade had at least one chamber collapse on echocardiography [5]. Therefore, in patients with pericardial effusion who have chamber collapse, one should carefully document respiratory flow variation across valves as a sign of ventricular interdependence and interrogate the inferior vena cava size and collapsibility as a sign of elevated right-sided filling pressures (Fig. 2.2).

The diagnosis of subacute pericardial tamponade requires careful integration of both clinical and imaging data to establish the need for pericardial effusion drainage. We have proposed a score-based approach for evaluating the need for pericar-

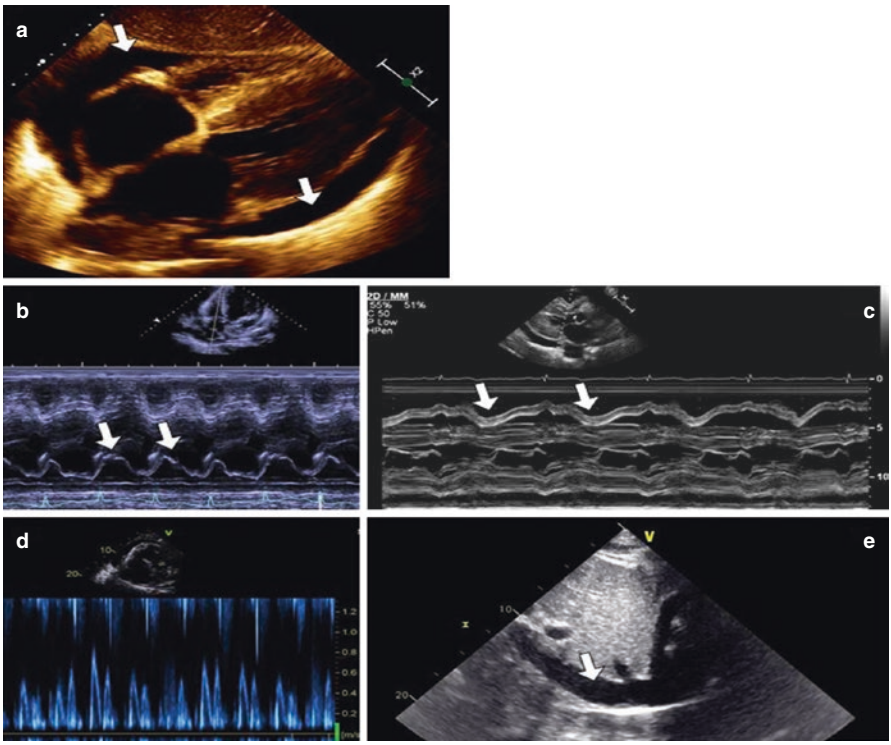

Fig. 2.2 Assessment of pericardial effusion. While circumferential pericardial effusion is commonly easy to recognize by echocardiography (panel **a**, arrows), the assessment of tamponade physiology requires comprehensive echocardiography. M-mode echocardiography allows precise timing of events such as presence and duration of right atrial collapse in apical four-chamber view (panel **b**, arrows) and diastolic right ventricular outflow tract collapse timed against mitral valve opening and closing in modified parasternal long-axis view (panel **c**, arrows). Confirmatory signs include flow variation across the mitral valve (panel **d**) and inferior vena cava engorgement (panel **e**, arrow)

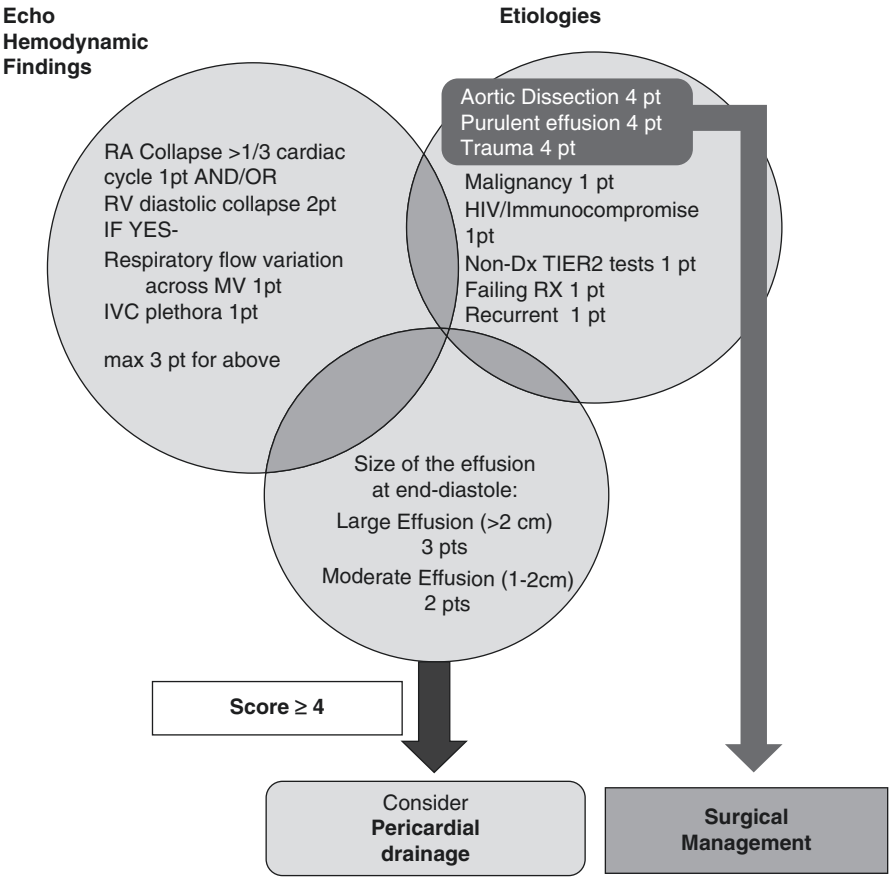

Fig. 2.3 Pericardial effusion scoring index. This index represents a qualitative tool to assist in decision-making for draining pericardial effusion in patients with moderate-to-large pericardial effusion. *Dx* diagnostic, *HIV* human immunodeficiency virus, *RA* right atrium, *RV* right ventricle, *Rx* treatment, *pt* point

dial effusion drainage that integrates three essential categories: etiology of the effusion, effusion size, and hemodynamic data by comprehensive echocardiography (Fig. 2.3) [6]. Similar to our original algorithm, the European Society of Cardiology suggested a stepwise scoring system to guide the decision-making which includes etiology, clinical presentation, and imaging findings [7]. While none of these approaches have rigorous clinical validation they underscore the need for comprehensive evaluation of multiple data points in suspected subacute tamponade before proceeding with pericardiocentesis.

Transesophageal echocardiogram may be required for diagnosing regional pericardial tamponade due to localized effusion or clot causing cardiac chamber compression if transthoracic windows are limited.

Is the Left Ventricular Systolic Function Reduced?

Bedside determination of the left ventricular size and LVEF is the key diagnostic step in evaluating patients with suspected cardiac dyspnea. Several studies have demonstrated feasibility of accurate estimation of the global LV systolic function using point-of-care ultrasound by non-cardiologists [1]. Further characterization of these patients requires comprehensive echocardiography to outline the distribution and pattern of wall motion abnormalities and estimate cardiac filling pressures.

The left ventricular size and global function can be estimated by various echocardiographic techniques with varying degrees of accuracy. Linear measurements (like left ventricular end-diastolic diameter) are quick and easy to perform but assume symmetric left ventricular remodeling and rely on accurate alignment of the measurement angle [8]. Unenhanced 2D biplane planimetry requires operator experience and has several important limitations (geometric assumption, orthogonal orientation of the planes, apical foreshortening, and accurate endocardial border definition); it significantly underestimates left ventricular volumes compared to cardiac magnetic resonance. Use of 3D echocardiography may allow for more accurate volume and LVEF estimation but this technique depends on acoustic windows and operator experience. More importantly, contrast echocardiography has been shown to increase the percentage of interpretable studies, which is especially relevant to acute care settings [9]. Also, it improves the accuracy of left ventricular volume estimation and left ventricular functional assessment. The use of contrast echocardiography results in marked reduction in the interreader variability in the settings of 2D and possibly 3D echocardiography. In one multicenter study, the mean percentage of interreader variability for LVEF estimation was reduced from 14.3% for unenhanced 2D echocardiography to 8.0% for contrast-enhanced 2D echocardiography, a similar level as for cardiac magnetic resonance [10]. Finally, contrast enhancement helps to identify other high-risk findings such as a localized myocardial perfusion abnormality, apical thrombus, left ventricular aneurysm, and pseudoaneurysm (Fig. 2.4). While interpreting the echocardiogram one should recognize that the measures of left ventricular size and performance can be affected by the use of vasoactive and inotropic agents [9].

Shortness of breath can be the sole manifestation of acute coronary syndrome. The specific pattern of wall motion abnormalities in this group of patients commonly suggests the presence of coronary artery disease. In patients with stress-induced cardiomyopathy echocardiographic findings are usually suggestive but not pathognomonic for diagnosis. In addition to the typical variant (apical ballooning), other less common variants have been widely described and can be recognized by echocardiographic abnormalities not fitting into a common coronary artery distribution [9]. Speckle-tracking echocardiography can be used to quantify the degree of longitudinal systolic dysfunction and delineate the extent of myocardial involvement (Fig. 2.5).

Right ventricular dilation and dysfunction have important prognostic significance in patients with left ventricular systolic dysfunction, including patients con-

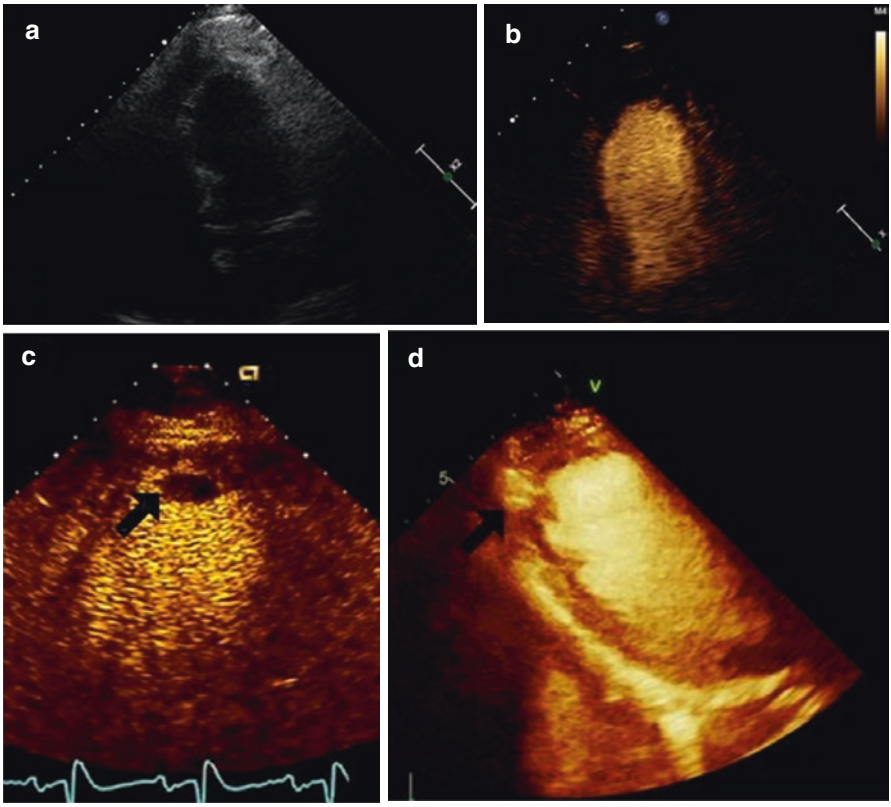

Fig. 2.4 Advantages of contrast echocardiography. Suboptimal echocardiographic image quality is not uncommon in acute care settings making assessment of left ventricular size and function difficult (panel **a**). Use of echocardiographic echocardiography greatly increases the percentage of interpretable studies (panel **b**). Contrast echocardiography also facilitates the recognition of high-risk findings such as left ventricular apical thrombus (panel **c**, arrow) and left ventricular pseudoaneurysm (panel **d**, arrow)

sidered for advanced heart failure therapies. Right ventricular functional assessment is commonly performed using M-mode and tissue Doppler interrogation of the tricuspid annulus as well as fractional area change using 2D echocardiography. Longitudinal strain of the right ventricular free wall obtained using speckle-tracking echocardiography and right ventricular ejection fraction obtained using 3D echocardiography are promising new techniques that require further clinical validation [8].

Secondary valvular abnormalities such as secondary mitral regurgitation and tricuspid regurgitation due to right ventricular dilation are commonly seen in patients with systolic left ventricular failure and should be routinely quantified during comprehensive echocardiography. Secondary valvular abnormalities are dynamic in nature and their severity changes with loading conditions and in response to the therapy.

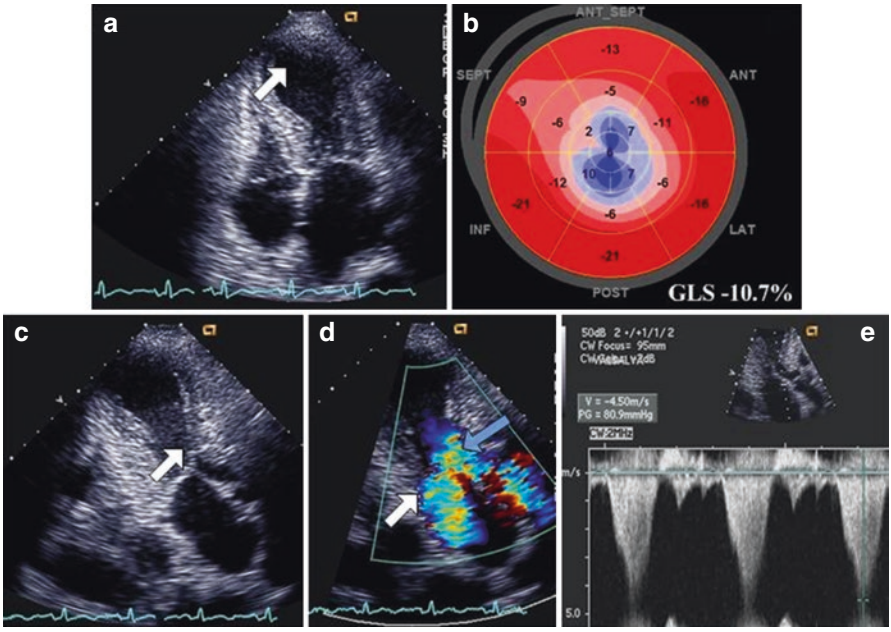

Fig. 2.5 Echocardiographic findings in stress-induced cardiomyopathy. A large area of apical akinesis is seen on the end-systolic frame (panel **a**, arrow). Speckle-tracking echocardiography demonstrates reduction in the global longitudinal strain due to markedly decreased strain values in the apical and mid-ventricular segments (panel **b**). Further interrogation reveals systolic anterior motion of the mitral valve with mitral-septal contact in mid-systole (panel **c**). Color Doppler demonstrates characteristic V sign (panel **d**) due to turbulence in the left ventricular outflow tract (blue arrow) and posteriorly directed secondary mitral regurgitation (white arrow). Spectral Doppler interrogation reveals high left ventricular outflow gradient (panel **e**)

Hemodynamic assessment is the routine part of echocardiographic evaluation in patients with reduced left ventricular ejection fraction since routine invasive assessment is not justified. Decreased cardiac output is commonly reflected by low left ventricular outflow tract velocity time integral (<15 cm). Increased left ventricular filling pressures are suggested by high *E*-wave velocity, short *E*-wave deceleration time (<150 ms), pseudonormal or restrictive mitral inflow pattern, high *E*/*e′* ratio, diastolic-predominant pulmonary venous flow, increased tricuspid regurgitant velocity (>3.2 m/s), and increased end-diastolic pulmonary regurgitation velocity (Fig. 2.6). Elevated right atrial pressure in non-ventilated patients is suggested by engorged inferior vena cava with decreased respiratory collapsibility. On the other hand, in patients with left ventricular systolic dysfunction who have impaired relaxation mitral inflow pattern, low *E*-wave velocity (<50 cm/s) and systolic-predominant pulmonary venous flow left ventricular filling pressures are likely not elevated.

Transthoracic lung ultrasound can be performed bedside to evaluate pleural effusions in patients with suspected heart failure. Also, multiple sonographic B-lines ("comets") are consistent with interstitial pulmonary edema [9].

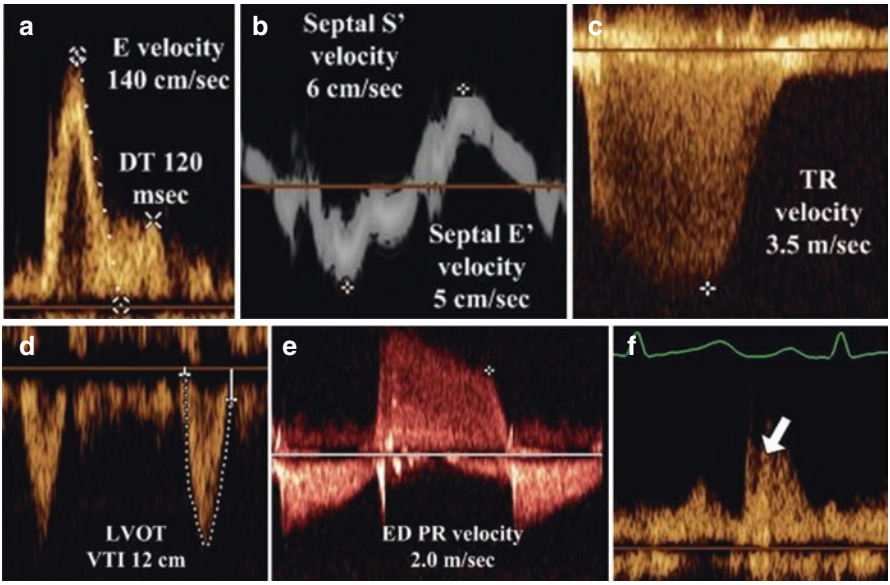

Fig. 2.6 Hemodynamic assessment in patients with shortness of breath and reduced left ventricular ejection fraction. Increased *E* velocity, high *E*/*A* ratio, and short *E*-wave deceleration time are seen (panel **a**). These findings coupled with low tissue Doppler *e′* velocity (panel **b**) and increased *E*/*e′* ratio suggest increased left ventricular filling pressures. This is further confirmed by high tricuspid regurgitant velocity (panel **c**), high end-diastolic pulmonary regurgitant velocity (panel **e**), and D-predominant pulmonary venous flow (panel **f**). Low left ventricular outflow tract velocity time integral (panel **d**) and low tissue Doppler S velocity (panel **b**) are consistent with reduced left ventricular systolic performance

Is There an Isolated Right Ventricular Dysfunction?

Right ventricular enlargement and hypokinesis with preserved LVEF in patients who presents with acute/subacute shortness of breath suggest pulmonary embolism. Right ventricular enlargement can be quickly assessed bedside by comparing right ventricular and left ventricular diameters or end-diastolic areas in the apical four-chamber view. In short-axis views, D-shaped deformation of the interventricular septum and paradoxical septal motion can be observed with significant pulmonary embolism. Rarely, thrombi can be seen trapped in the right atrium, right ventricle, or the pulmonary artery. Right ventricular motion can demonstrate free wall hypokinesis with relative apical sparing (McConnell's sign) but this is not a specific finding [9]. In hemodynamically stable patients suspected of having pulmonary embolism normal transthoracic echocardiogram does not exclude pulmonary embolism but evidence of right ventricular strain puts patients into a high-risk group. On the other hand, in hemodynamically unstable patients normal right ventricular size and function make massive pulmonary embolism highly unlikely.

Hemodynamic assessment of patients with suspected pulmonary hypertension and right ventricular failure includes interrogation of mitral inflow and estimation of pulmonary artery systolic pressure. In patients with pulmonary embolism and other causes of pulmonary hypertension not related to left ventricular failure the mitral inflow pattern commonly demonstrates low *E*-wave velocity and *E*/*A* ratio reversal due to "underfilled" left ventricle but the examination can be limited due to tachycardia-induced E- and *A*-wave fusion or atrial fibrillation. Estimation of the pulmonary artery systolic pressure is based on the tricuspid regurgitant velocity and inferior vena cava-based assessment of the right atrial pressure. In general, pulmonary artery systolic pressure is estimated at a mild-to-moderate range (40–50 mmHg) in patients with significant pulmonary embolism but it can be higher in patients with preexisting pulmonary hypertension.

The accuracy of echocardiography-based estimation of the pulmonary artery systolic pressure has been debated but it is generally reliable with experienced readers. The following caveats highlight the difficulties of reliable estimation of the pulmonary pressures: (1) incomplete tricuspid regurgitation signal, especially in patients with lung disease; (2) failure to obtain the highest tricuspid regurgitation velocity from an off-angle view; (3) presence of severe tricuspid regurgitation; and (4) inaccurate estimation of right atrial pressure. It has been suggested that the echocardiographic estimation is less accurate in patients with right-heart disease but one study reported a high correlation between echocardiography and invasive assessment with experienced readers (the area under the curve for classifying pulmonary hypertension was 0.97) [11]. In that study, only 61% of tricuspid regurgitant jets were deemed interpretable.

Assessment of right atrial pressure by 2D echocardiography using inferior vena cava diameter and collapsibility is currently recommended by the guidelines but the accuracy of this approach is modest (Table 2.2). In one study, the ratio of short and long diameters of the inferior vena cava in cross section obtained by 3D echocardiography has a high diagnostic accuracy reaching area under the curve of 0.98 ($P < 0.01$) to detect central venous pressure ≥10 mmHg (Fig. 2.7) [12]. Also, estimations of the right atrial pressure were more accurately reclassified using the 3D-derived cross-sectional morphology of the inferior vena cava rather than traditional 2D grading (net reclassification improvement, 0.38, $p < 0.01$).

Table 2.2 Estimating right atrial pressure based on the inferior vena cava size (1–2 cm from right atrial junction) and collapsibility

Inferior vena cava size and collapsibility	Estimate of right atrial pressure
Dilated (>2.1 cm) and little collapsibility (<50%)	Elevated (10–20 mmHg)
Normal (< 2.1 cm) but little collapsibility (<50%)	Intermediate (5–10 mmHg)
Dilated (>2.1 cm) but collapsible (>50%)	
Normal (<2.1 cm) and collapsible (>50%)	Normal/low (0–5 mmHg)

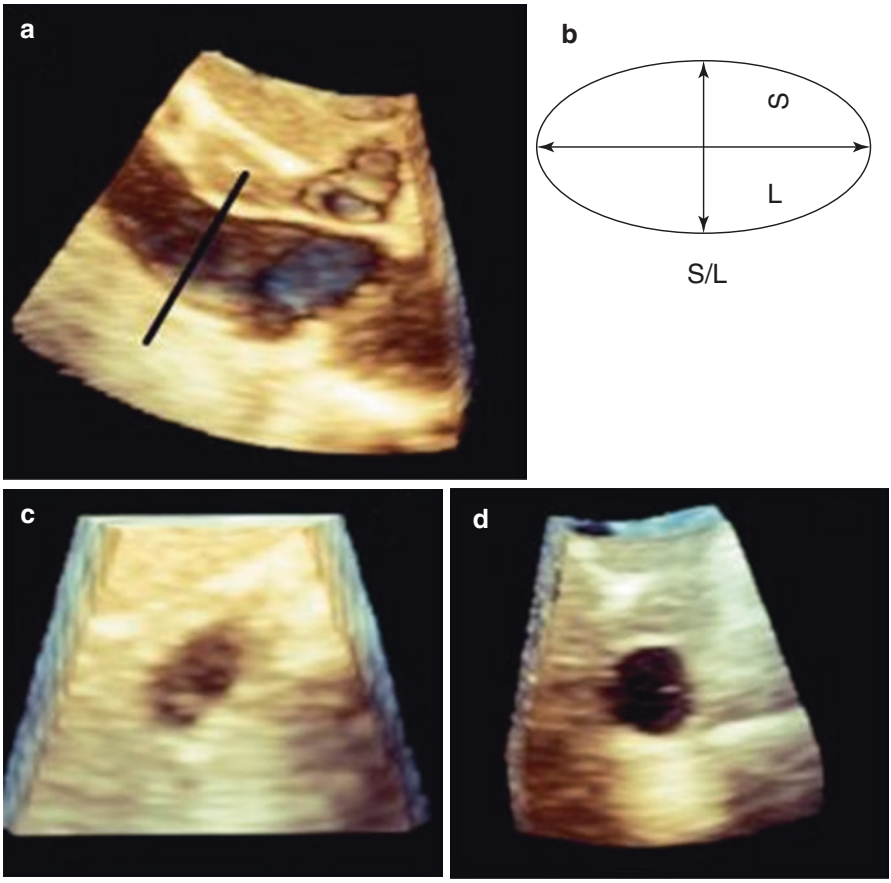

Fig. 2.7 Estimation of the right atrial pressure using cross-sectional imaging of the inferior vena cava. A cross-sectional cut of the inferior vena cava is rendered using 3D echocardiography dataset obtained from the subcostal view (panel **a**). The ratio of the short (S) to long (L) diameter can then be determined (panel **b**). Patients with normal right atrial pressure (<10 mmHg) typically have an ovoid shape of the inferior vena cava (S/L < 0.69) (panel **c**) while patients with elevated right atrial pressure have a round shape (panel **d**)

Are There Any Significant Valvular Abnormalities?

Primary valvular abnormalities can cause acute/subacute shortness of breath and may require urgent lifesaving intervention; therefore, prompt recognition of significant valvular disease is imperative when dealing with patients in acute settings. Echocardiography constitutes the cornerstone of the initial evaluation since history and physical examination findings can be nonspecific and unimpressive.

Valvular diseases causing flow obstruction include dynamic LVOT obstruction by systolic anterior motion of the mitral valve, high-grade aortic stenosis, and mitral stenosis. Dynamic LVOT obstruction is commonly believed to be associated with

hypertrophic cardiomyopathy and significant left ventricular hypertrophy with small cavity size; acute severe resting LVOT obstruction in these patients is a life-threatening condition commonly precipitated by volume depletion [9]. It can also be seen acutely in patients after valve surgery, with acute myocardial infarction and stress-induced cardiomyopathy. On 2D echocardiographic imaging, the systolic anterior motion of the mitral valve with mitral septal contact is seen (Fig. 2.5, panel **c**). Color Doppler imaging demonstrates turbulence in LVOT, commonly with a posteriorly directed jet of secondary mitral regurgitation ("V sign," Fig. 2.5, panel **d**). Spectral Doppler recording identifies the late-peaking envelope of dynamic obstruction (Fig. 2.5, panel **e**).

High-grade aortic stenosis and mitral stenosis are typically long-standing chronic conditions with the rare exception of rapidly growing cardiac masses causing obstruction (like large vegetations). At the same time, compensatory mechanisms that develop in these patients can rapidly fail in the settings of relatively minor hemodynamic insults (infection, pregnancy, arrhythmia, etc.) resulting in acute decompensation. For example, atrial fibrillation can cause acute pulmonary edema in patients with long-standing compensated high-grade mitral stenosis. Therefore, immediate recognition of the underlying valvular abnormality is essential in managing these patients. On the contrary, acute left-sided regurgitant lesions develop in patients without compensatory mechanisms (normal left ventricular and left atrial size and compliance) and typically precipitate immediate and severe clinical decompensation.

Acute primary mitral regurgitation can result from papillary muscle rupture, flail leaflet from spontaneous chordal rupture, and leaflet destruction and perforation due to infective endocarditis. Physical examination is notoriously nonspecific in these patients: the murmur can be soft and unimpressive due to rapid equilibration of left ventricular and atrial pressures. Transthoracic echocardiography typically reveals normal left ventricular size, hyperdynamic left ventricular function, and high *E*-wave velocities. The structural mitral valve pathology can be obvious (like large vegetation) or less impressive (non-midline flail segments) (Fig. 2.8). Truncated, triangular shape of mitral regurgitation on spectral Doppler recording can be seen. Systolic flow reversal in pulmonary veins can also be seen. The jet of mitral regurgitation can be highly eccentric and not readily appreciated on technically difficult transthoracic imaging; therefore, transesophageal echocardiography should be used with a high index of suspicion and inconclusive transthoracic echocardiogram. Transesophageal echocardiogram easily delineates the cause and extent of mitral valve pathology, especially with the use of 3D echocardiography. The estimation of the regurgitation severity should focus on quantitative (PISA, EROA) rather than qualitative measures (color Doppler area) and can be aided by 3D-guided planimetry of the vena contracta area.

Acute aortic regurgitation can result from aortic dissection, infective endocarditis, and traumatic or spontaneous flail aortic leaflet. Transthoracic echocardiog-

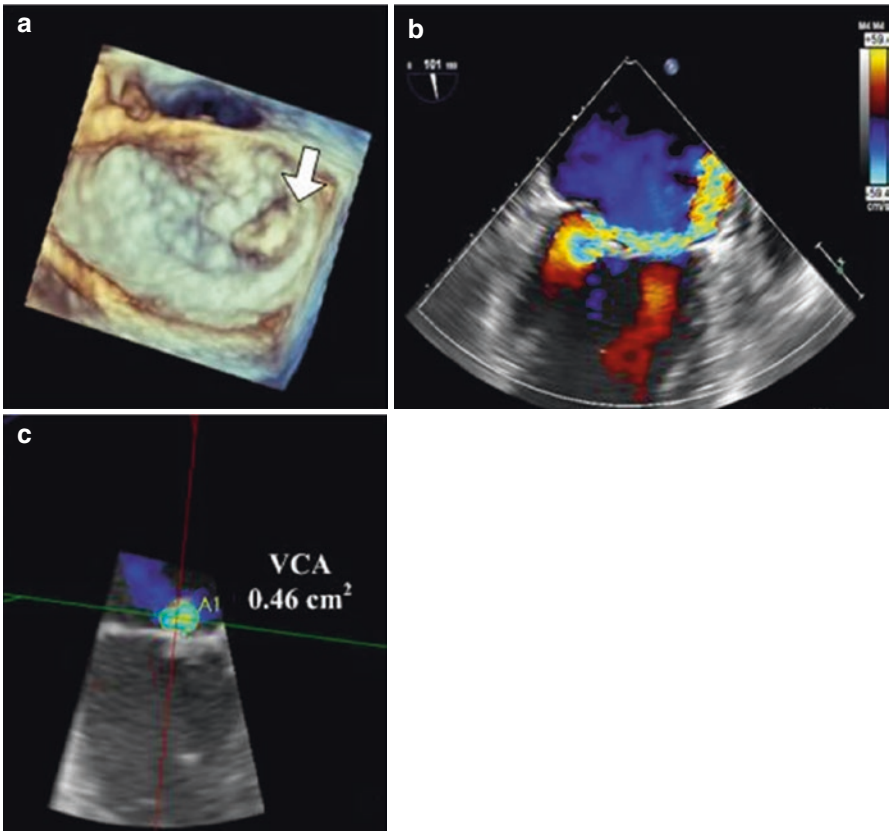

Fig. 2.8 Echocardiographic evaluation of mitral regurgitation. Transesophageal 3D echocardiography with en face view of the mitral valve reveals isolated flail of P3 segment of the posterior leaflet (panel **a**). A highly eccentric jet of mitral regurgitation is seen by color Doppler (panel **b**). 3D-guided 2D planimetry demonstrates rounded vena contracta with area of 0.46 cm^2 consistent with severe mitral regurgitation

raphy can identify the structural valve problem and demonstrate the jet of aortic regurgitation. Hemodynamic assessment typically reveals high *E*-wave velocities and early closure of the mitral valve, sometimes with diastolic mitral regurgitation due to markedly elevated left ventricular diastolic pressures. A short pressure halftime of the aortic regurgitant jet (<200 ms) and holodiastolic flow reversal in the descending aorta may also be seen. Transesophageal echocardiography may be necessary to confirm the diagnosis, especially if the transthoracic study is suboptimal.

Prosthetic valve dysfunction should be suspected in any patients with prior valve surgery who present with acute and subacute shortness of breath. The

common causes of acute prosthetic valve dysfunction include thrombosis, infective endocarditis, structural valve failure, and valve dehiscence. Long-standing prosthetic valve pathologies like pannus formation and patient-prosthetic mismatch can also predispose to acute deterioration with other precipitating conditions (like infection, arrhythmia). Identification of prosthetic valve dysfunction and differentiation from physiologic states (such as elevated transvalvular gradients due to a high-flow state in a septic patient) require a high level of imaging expertise. Retrieval of operative/procedural records and prior echocardiograms can be crucial for decision-making. Transthoracic echocardiography can be limited by the acoustic windows as well as reverberation and shadowing artifacts created by prosthetic material. Therefore, the threshold for obtaining transesophageal echocardiogram in any patient with suspected prosthetic valve dysfunction should be low.

Left-sided prosthetic valve regurgitation can be intraprosthetic or paraprosthetic. Of note, endocarditis of the prosthetic valve commonly results in paravalvular involvement and is less likely to produce vegetations compared to native valve endocarditis. Echocardiography supplemented by 3D imaging can identify the anatomic cause of valvular dysfunction, especially with the mitral valve pathology, and can help to quantify the degree of regurgitation. In patients with large paraprosthetic leaks abnormal mobility of the valve ("rocking") is commonly seen. Quantitative assessment of paraprosthetic mitral valve regurgitation is typically possible using Doppler-derived measurements similar to native valve regurgitation. Quantification is more difficult in paraprosthetic aortic valve regurgitation; using the degree of prosthetic valve regurgitation circumference on the short-axis view has been suggested but it lacks rigorous validation [9]. Three-dimensional planimetry of the vena contracta area may also be feasible and can be especially useful for multiple jets. Increased transvalvular gradients are commonly seen with prosthetic valve regurgitation in the absence of obstruction. Careful assessment of the pressure halftime (for mitral regurgitation) and dimensionless velocity index and acceleration time (for aortic valve) helps in differential diagnosis.

Left-sided prosthetic valve obstruction causes elevated transvalvular gradients; as mentioned above, it should be differentiated from other causes of elevated gradients such as patient-prosthetic mismatch, pathologic prosthetic valve regurgitation, and high-flow states. Prosthetic valve thrombosis has been traditionally associated with mechanical valves but it has been increasingly recognized with bioprosthetic valve, including transcatheter valves (Fig. 2.9). The mitral valve can be evaluated with high accuracy using transesophageal echocardiography while the assessment of a prosthetic aortic valve, especially in patients with both mitral and aortic prosthetic valves, can be very challenging and may require other imaging modalities (such as fluoroscopy for assessment of mechanical leaflet mobility or CT scan for assessment of mechanical and bioprosthetic aortic valves).

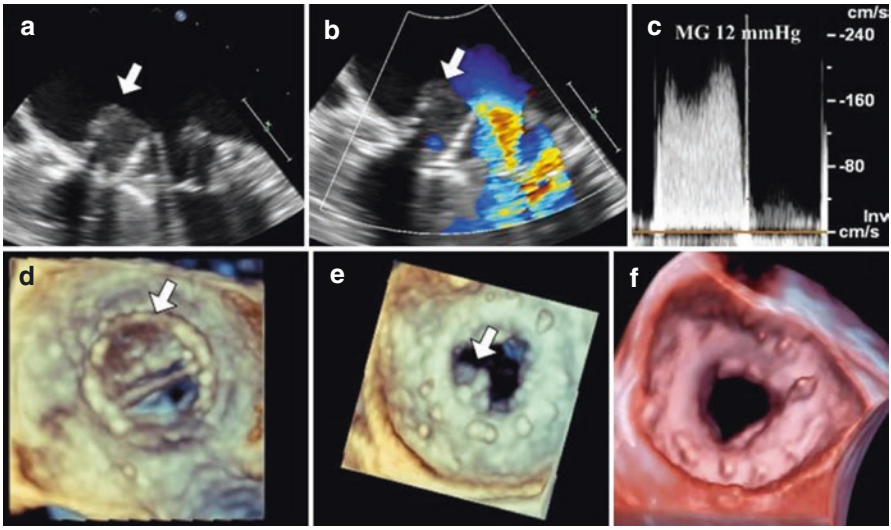

Fig. 2.9 Prosthetic mitral valve thrombosis. A patient with mechanical mitral valve thrombosis (panels **a**–**d**). A large thrombus (arrow) is seen on 2D transesophageal echocardiogram (panel **a**) that obstructs the flow (arrow) and results in filling only through the opening of the non-obstructed strut of the valve (panel **b**). Elevated transmitral gradients are seen (panel **c**). Three-dimensional transesophageal echocardiogram confirms immobility of the obstructed strut (panel **d**). A patient with bioprosthetic mitral valve thrombosis (panels **e**, **f**). An immobile leaflet of the valve is seen on 3D transesophageal echocardiogram due to thrombosis (panel **e**). Complete restoration of leaflet mobility and normal valve functioning are seen after 6 weeks of anticoagulation with a vitamin K antagonist (panel **f**)

Is There a Heart Failure with Preserved Ejection Fraction?

Heart failure with preserved ejection fraction, also known as "diastolic" heart failure, is a fashionable diagnosis. There is a common misconception that this phenotype is solely related to decreased compliance and impaired relaxation properties of the left ventricle. Interestingly, diastolic dysfunction as assessed by echocardiography is quite prevalent in elderly, mostly asymptomatic population. On the other hand, trials of heart failure with preserved ejection fraction enrolled a significant proportion of patients that lacked well-established echocardiographic markers of diastolic dysfunction [13]. In reality, heart failure with preserved ejection fraction is a complex phenotype with varying contribution of cardiac, vascular, and extracardiac components. Echocardiographic assessment of patients with suspected heart failure, in addition to confirming preserved ejection fraction, should focus on the evidence of structural heart disease and hemodynamic assessment. Patients with this phenotype commonly have enlarged left atrium, left ventricular hypertrophy, and decreased e' velocities. Assessment of the right ventricle and estimation of the

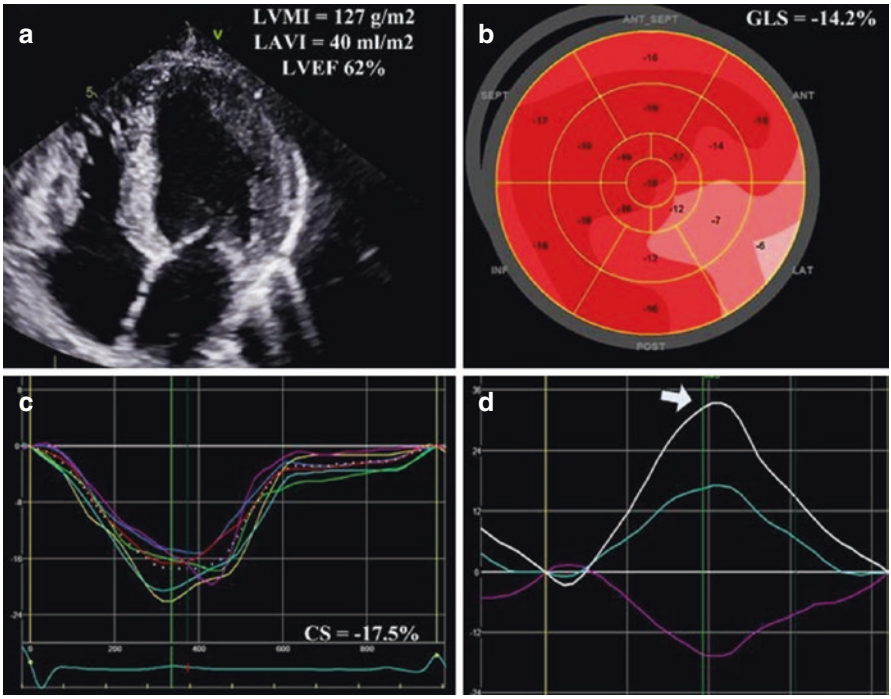

Fig. 2.10 Echocardiographic findings in a patient with heart failure with preserved ejection fraction. Two-dimensional echocardiogram demonstrates increased left ventricular mass, enlarged left atrium, and preserved left ventricular ejection fraction (panel **a**). Global longitudinal strain is significantly decreased (panel **b**). There is also impairment of the circumferential strain (panel **c**) while the left ventricular twist is exaggerated (panel **d**, arrow)

pulmonary pressures provide important clinical information. While traditional echocardiographic markers of diastolic dysfunction may be useful in these patients their accuracy is limited. Isolated application of diastolic indices (such as *E*/*e′* ratio) in patients with preserved ejection fraction and unexplained dyspnea showed poor discrimination in identifying patients with heart failure as confirmed with invasive estimation of left ventricular filling pressures [14]. More importantly, studies have identified specific patterns of impaired myocardial mechanics characteristic for this phenotype using speckle-tracking echocardiography [15]. Many traditional cardiovascular risk factors affect the inner layer myocardial performance resulting in attenuation of the global longitudinal strain early in the disease course while circumferential strain and left ventricular twist are preserved or exaggerated. It has also been suggested that decrease in circumferential strain may indicate the transition to the clinical phenotype of heart failure with preserved ejection fraction (Fig. 2.10) [16]. In addition, heterogeneity of the longitudinal strain pattern with apical sparing and increased LVEF to longitudinal strain ratio may suggest the presence of cardiac amyloidosis. Speckle-tracking echocardiography may also help in

differentiating restrictive cardiomyopathy from constrictive pericarditis. While longitudinal strain is a highly reproducible tool which has been integrated into the clinical guidelines other aspects of myocardial mechanics obtained by speckle-tracking echocardiography are less reproducible and require further validation before widespread clinical use [15].

Heart failure societies have recognized the entity of heart failure with midrange ejection fraction. While it could truly be an overlap between two distinct heart failure phenotypes the best clinical approach to this entity is unknown. Moreover, further echocardiographic studies may shift the traditional thinking about heart failure from left ventricular ejection fraction estimation to more precise characterization of myocardial mechanics [15].

References

1. Mandavia DP, Hoffner RJ, Mahaney K, Henderson SO. Bedside echocardiography by emergency physicians. Ann Emerg Med. 2001;38:377–82.
2. Argulian E, Messerli F. Misconceptions and facts about pericardial effusion and tamponade. Am J Med. 2013;126:858–61.
3. Argulian E, Herzog E, Halpern DG, Messerli FH. Paradoxical hypertension with cardiac tamponade. Am J Cardiol. 2012;110:1066–9.
4. Eisenberg MJ, Oken K, Guerrero S, Saniei MA, Schiller NB. Prognostic value of echocardiography in hospitalized patients with pericardial effusion. Am J Cardiol. 1992;70(9):934.
5. Merce J, Sagrista-Sauleda J, Permanyer-Miralda G, Soler-Soler J. Should pericardial drainage be performed routinely in patients who have a large pericardial effusion without tamponade? Am J Med. 1998;105:106–9.
6. Halpern DG, Argulian E, Briasoulis A, Chaudhry F, Aziz EF, Herzog E. A novel pericardial effusion scoring index to guide decision for drainage. Crit Pathw Cardiol. 2012;11:85–8.
7. Ristic AD, Imazio M, Adler Y, et al. Triage strategy for urgent management of cardiac tamponade: a position statement of the European Society of Cardiology Working Group on Myocardial and Pericardial Diseases. Eur Heart J. 2014;35:2279–84.
8. Lang RM, Badano LP, Mor-Avi V, et al. Recommendations for cardiac chamber quantification by echocardiography in adults: an update from the American Society of Echocardiography and the European Association of Cardiovascular Imaging. J Am Soc Echocardiogr. 2015; 28:1–39.e14
9. Lancellotti P, Price S, Edvardsen T, et al. The use of echocardiography in acute cardiovascular care: recommendations of the European Association of Cardiovascular Imaging and the Acute Cardiovascular Care Association. Eur Heart J Acute Cardiovasc Care. 2015;4(1):3–5.
10. Hoffmann R, Barletta G, von Bardeleben S, et al. Analysis of left ventricular volumes and function: a multicenter comparison of cardiac magnetic resonance imaging, cine ventriculography, and unenhanced and contrast-enhanced two-dimensional and three-dimensional echocardiography. J Am Soc Echocardiogr. 2014;27:292–301.
11. Amsallem M, Sternbach JM, Adigopula S, et al. Addressing the controversy of estimating pulmonary arterial pressure by echocardiography. J Am Soc Echocardiogr. 2016;29:93–102.
12. Seo Y, Iida N, Yamamoto M, Machino-Ohtsuka T, Ishizu T, Aonuma K. Estimation of central venous pressure using the ratio of short to long diameter from cross-sectional images of the inferior vena cava. J Am Soc Echocardiogr. 2017;30:461.
13. Argulian E, Messerli FH. Misconceptions and facts about 'diastolic' heart failure. Am J Med. 2014;127:1144–7.

14. Santos M, Rivero J, McCullough SD, et al. *E*/*e′* ratio in patients with unexplained dyspnea: lack of accuracy in estimating left ventricular filling pressure. Circ Heart Fail. 2015;8: 749–56.
15. Claus P, Omar AM, Pedrizzetti G, Sengupta PP, Nagel E. Tissue tracking technology for assessing cardiac mechanics: principles, normal values, and clinical applications. JACC Cardiovasc Imaging. 2015;8:1444–60.
16. Kraigher-Krainer E, Shah AM, Gupta DK, et al. Impaired systolic function by strain imaging in heart failure with preserved ejection fraction. J Am Coll Cardiol. 2014;63:447–56.

Chapter 3
The Arrhythmia Patient in the CCU – Impact of Echocardiography

Alan Sugrue, Subir Bhatia, Vaibhav Vaidya, and Sam Asirvatham

Abstract Echocardiography is an essential tool in patients with cardiac arrhythmias, particularly in the critical care environment. It plays an important role in the etiological assessment, prognosis, and risk stratification of patients with arrhythmias. In this chapter, we discuss the key role of echocardiography in the arrhythmic patient in the coronary care unit.

Keywords Atrial fibrillation · Syncope · Ventricular tachycardia

Introduction

Echocardiography is an essential part of both the cardiologist and electrophysiologist armamentarium, particularly in the coronary care unit and in patients with cardiac arrhythmias. Historically, the use of echocardiography in patients with arrhythmias dates back to the 1980s where M mode was used to augment clinical decision-making in patients with wide complex tachycardias [1]. The expansion of echocardiography techniques and the availability of multiple echocardiography modalities (transthoracic, transesophageal, pocket-sized devices) have shaped echocardiography to be a critical tool for day-to-day practice. Echocardiography is particularly an attractive imaging modality; it is inexpensive, noninvasive and can be rapidly performed at the bedside.

A. Sugrue · S. Bhatia · V. Vaidya
Division of Heart Rhythm Services, Department of Cardiovascular Diseases, Mayo Clinic, Rochester, MN, USA
e-mail: Sugrue.Alan@mayo.edu; Bhatia.Subir@mayo.edu; Vaidya.Vaibhav@mayo.edu

S. Asirvatham (✉)
Division of Heart Rhythm Services, Department of Cardiovascular Diseases, Mayo Clinic, Rochester, MN, USA

Division of Pediatric Cardiology, Department of Pediatrics and Adolescent Medicine, Mayo Clinic, Rochester, MN, USA
e-mail: Asirvatham.Samuel@mayo.edu

E. Herzog, E. Argulian (eds.), *Echocardiography in the CCU*,
https://doi.org/10.1007/978-3-319-90278-4_3

Cardiac arrhythmias are common in the critical care setting and are often a consequence of or associated with a wide spectrum of structural heart disease, both congenital and acquired. Echocardiography enables easy, safe anatomical and functional assessment for structural heart disease through examination of the left and right cardiac chambers, myocardium, pericardium, cardiac valves, and great vessels. This assessment can help determine the etiologies of arrhythmias through detection of structural heart disease. Further, it can help augment medical decisions, guide prognosis and risk stratification. In this chapter, we discuss the role of echocardiography in the critical care setting focusing on patients with cardiac arrhythmias. Specifically, we discuss tachycardias (particularly atrial fibrillation and ventricular tachycardia), cardiac arrest, implantable cardioverter defibrillator (ICD) shocks, and bradyarrhythmias. Finally, we examine the emerging role of echocardiography in patients post-cardiac ablation.

Atrial Fibrillation

Echocardiography is fundamental to the management of patients with atrial fibrillation (AF) in both the acute and chronic setting. In the acute critical care setting, echocardiography has the ability to not only detect abnormalities in cardiac function and structure, but also guide management decisions (rate vs. rhythm control), as well as aid in risk stratification (Table 3.1). While transthoracic echocardiography (TTE) is often the first-line modality, transesophageal echocardiography (TEE) is useful for thrombus and valvular disease assessment.

Etiology

Determining underlying abnormities which could predispose to AF is vital. Echocardiography should be used to help identify valvular heart disease (in

Table 3.1 Echocardiographic features in atrial fibrillation and their corresponding clinical values

Echocardiogram feature	Value
Ejection fraction (EF)	Guide pharmacological therapy
Mitral valve	
Stenosis	Guide anticoagulation
Regurgitation	Assess EF to ensure no left ventricular dysfunction
E/*e′* ratio	Assess for diastolic dysfunction
Left atrial volume index	Guide pharmacological therapy
Large transmitral A wave	May derive benefit from sinus rhythm
Thrombus	Contraindication to DC cardioversion
Spontaneous echo contrast	Risk factor for thrombus formation

particular mitral valve disease), and assess for diastolic dysfunction, left ventricular systolic dysfunction, atrial size, and right-heart function.

In the assessment of the mitral valve, one should pay close attention to the mitral valve morphology, annulus, commissures, and papillary muscles. If *mitral regurgitation (MR)* is present, determination of whether it is due to a primary and secondary etiology is important. A *high ejection fraction (EF)*, often in the range of 60–75%, is often observed in MR. Therefore the observation of a normal EF in a patient with MR (50–65%) should imply left ventricular (LV) dysfunction, which would consequently impact treatment decisions (as discussed below). *Mitral stenosis* (Fig. 3.1), if present, can be detected by the classic hockey stick deformity of the mitral valve leaflets in the parasternal long-axis view or fish mouth on short axis and its presence has significant implications, particularly in regard to anticoagulation.

Global LV systolic assessment also has important etiologic, prognostic, and management implications and should be calculated from *end-diastolic volume* and *end-systolic volumes* (disc summation or biplane Simpson method are the most commonly used). The validity of systolic function indices in patients with AF is limited due to loss of synchronized atrial contraction, altered left atrial pressure, and irregular RR intervals [2]. Therefore understanding how and when to acquire measurements in order to accurately identify LV dysfunction in AF patients is critical. Present consensus opinion, published by the American Society of Echocardiography and the European Association of Cardiovascular Imaging [3], suggests a minimum of five beats in AF patients. Assessment of diastolic function is equivocally important, as up to 70% of patients with heart failure with a preserved ejection fraction (HFpEF) have a history of AF [4]. For assessment of diastolic dysfunction, the mitral inflow is fundamental; however in AF, atrial contraction is lost. Consequently, there is no *transmitral A (mitral end-diastolic inflow) velocity* (Fig. 3.2) and no *pulmonary Ar (pulmonary vein reversal flow) velocity* which means these indices cannot be applied. Thus, different parameters have been proposed. The *E/e′ ratio* (Fig. 3.2) has been demonstrated to be an accurate estimate of LV filling pressures in patients with AF and is largely used in

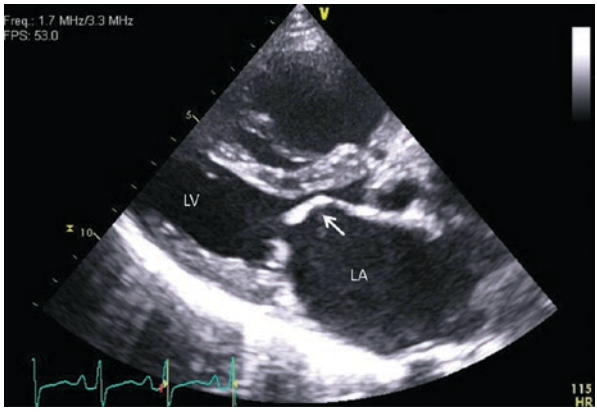

Fig. 3.1 Mitral stenosis on parasternal long axis. Arrow—classic "hockey stick" shape of the anterior leaflet of the mitral valve. Note that the LA is dilated. *LA* left atrium, *LV* left ventricle

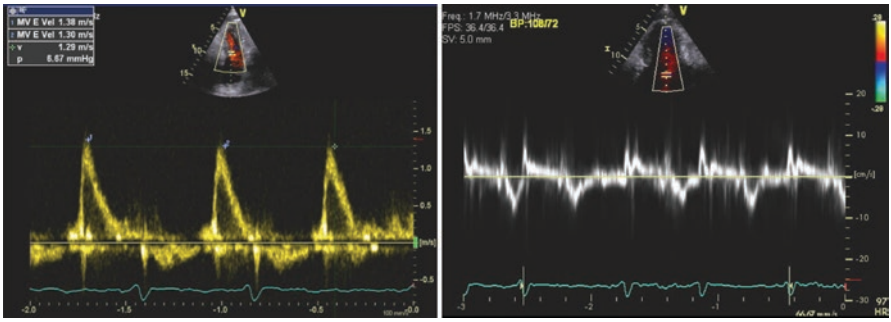

Fig. 3.2 Transmitral pulsed-wave Doppler spectral tracing demonstrating *E* wave with loss of *A* wave in a patient with atrial fibrillation (left). Mitral annular tissue Doppler spectral tracing showing *E′* velocity = 0.08 m/s. *E*/*e′* is 16, suggestive of increased left ventricular filling pressures (right)

clinical practice [5]. Lastly, *RA volume* should be assessed and is a key measure that is advised by the 2015 ASE/EACVI recommendations [3].

Management

The echocardiogram can facilitate patient discussions and should play a part of shared decision-making when it comes to management of AF (Fig. 3.3). In hemodynamically stable patients in the critical care setting, rate control is often the preferred choice; however, there are many benefits to rhythm control and this approach is often underutilized.

Rate Control

If a rate control strategy is employed, in patients with a reduced EF, beta-blockers or digoxin would be the preferred agent. Of note, digoxin should not be used as monotherapy [6]. In the acute setting, such as critically ill patients and those with severely impaired LV systolic function, intravenous amiodarone can be used and has been shown to be reasonably efficacious [7].

Rhythm Control

Echocardiography can help with antiarrhythmic drug selection and selection of appropriate candidates.

Firstly, assessment of left atrial (LA) size is critical as the presence of an enlarged left atrium (defined as *LA volume index of >34 ml/m*^{2}) decreases the probability that

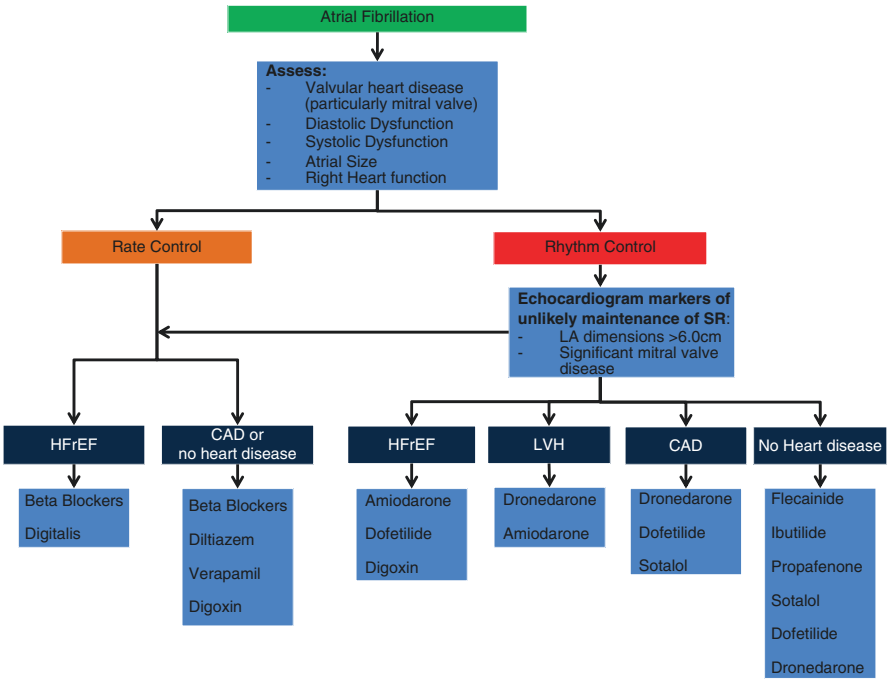

Fig. 3.3 Management of atrial fibrillation. *SR* sinus rhythm, *HFrEF* heart failure with reduced ejection fraction, *CAD* coronary artery disease, *LVH* left ventricular hypertrophy, *LA* left atrium

long-term maintenance of sinus rhythm will be successful, with severe atrial enlargement >60 mm defining those at greatest risk [8]. In these patients the goal of achieving sinus rhythm may be unfeasible and a rhythm approach may not be the best option. Secondly, examination of a prior echocardiogram when the patient is in sinus rhythm (if available) may highlight the relative atrial contribution to left ventricular filling. In patients with a *relatively high/large transmitral A wave*, the contribution of left atrial systole to left ventricular filling is greater and these patients may derive hemodynamic benefit from rhythm control.

In guiding antiarrhythmic drug selection, echocardiography is invaluable. In a patient with *reduced EF*, dofetilide and amiodarone are the only approved drug options. Importantly, class I drugs and dronedarone are contraindicated in patients with ischemic or structural heart disease because of concerns for ventricular proarrhythmia and increased mortality [9]. If left ventricular hypertrophy is detected (*>1.4 cm interventricular septal thickness*), class I and class III antiarrhythmics should be avoided and amiodarone would be the drug of choice. Although not widely studied in this population, dronedarone is reported to be a reasonable option [10]. Those with no underlying structural heart disease have the most options for rhythm drug therapy with class IC or class III antiarrhythmics preferred (particularly sotalol and dofetilide).

Anticoagulation

Apart from helping guide rate or rhythm control, echocardiography can augment clinical decisions regarding anticoagulation by assisting in reducing thromboembolic (TE) complications with cardioversion and enhancing TE risk stratification.

In the cardioversion setting, TEE is the backbone imaging modality and provides excellent identification and characterization of the left atrial appendage (LAA) with accurate thrombosis detection (Fig. 3.4) [11]. The finding of thrombus on TEE is an absolute contraindication to DC cardioversion. Echocardiography can also detect *spontaneous echo contrast* (SEC), which is considered to be a strong risk factor for, and often the preceding stage to, thrombus formation [12]. Guidelines do not address whether patients with SEC without thrombus can be safely cardioverted and clinical practice in this regard varies. TEE also enables assessment of other factors associated with TE, specifically reduced *LAA flow velocity* [13] (less than 20 cm/s) and complex aortic atheroma or plaque [14]. In terms of further TE risk stratification, echocardiography was historically limited to detection of a reduced EF which would give a point per the CHA_2DS_2-VASc score. Although there have been emerging studies on other echocardiographic factors which could further augment and suggest the likelihood of LAA thrombus [15, 16], these are not widely used clinically at present. Lastly, it is important to be cognizant that application of the CHA_2DS_2-VASc score for the decision regarding anticoagulation presumes that the underlying AF is *not* due to valvular heart disease. AF is defined as *valvular* when associated with rheumatic mitral stenosis, a mechanical or bioprosthetic heart valve, or a mitral valve repair. These patients generally all require anticoagulation with the CHA_2DS_2-VASc score not applicable.

Cardiac Arrest

Cardiac arrest management is driven by Advanced Cardiac Life Support Algorithms (ACLS) and while echocardiography does not have a defined role (at present) it can

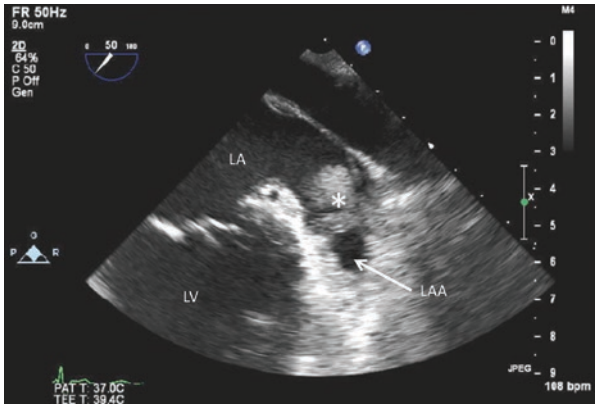

Fig. 3.4 Transesophageal echocardiogram demonstrating echo-dense mass within the left atrial appendage (LAA) consistent with LAA thrombus (labeled with an asterisk). *LA* left atrium, *LAA* left atrial appendage, *LV* left ventricle

Table 3.2 Etiologies for cardiac arrest and their corresponding echocardiographic features. *RV* right ventricle, *RA* right atrium, *LV* left ventricle, *IVC* inferior vena cava

Etiology	Echocardiogram feature
Tamponade	Swinging heart
	Right ventricular diastolic collapse
	Pseudosystolic anterior motion of mitral valve
	Enlarged non-pulsatile vena cava
Cardiac ischemia	Regional wall motion abnormalities
	Mitral valve papillary muscle rupture
	Ventricular septal defect
	Free wall rupture
Pulmonary embolism	RV dilation (especially compared to the LV)
	RA dilatation
	Flat intraventricular septum
	Akinetic RV
Hypovolemia	Small, hyperkinetic left ventricle
	End-systolic cavity obliteration ("kissing" trabecular muscles)
	Hypercontractile ventricle
	Flattened and small IVC

play a key role in enabling early identification of the precipitating etiology and thereby increase the likelihood of a favorable outcome (Table 3.2).

During Cardiac Arrest

The main advantage of focused echocardiography during resuscitation is the ability to gather rapid and real-time evaluation through the detection of *spontaneous cardiac movement* (SCM) , and identify reversible causes that can help narrow a differential diagnoses. Performing echocardiography in the cardiac arrest setting is challenging and requires significant skill and expertise. If performed it should be focused and not interfere with chest compressions and ACLS algorithms. Forward planning is essential with depth and gain settings pre-optimized and one should attempt a subcostal window first as this often yields the most useful views with the least interruption to ACLS algorithms. The 10-s pulse check has been proposed as a time in which it could be useful to perform a focused echocardiography exam [17]. The absence of SCM predicts a low likelihood of survival and can aid in the decision to terminate resuscitation [18]. It is also particularly valuable in the setting of pulseless electrical activity (PEA), where it can help differentiate between pseudo-PEA (presence of SCM with no central pulse) vs. true PEA [19].

Echocardiography can also assess for reversible causes particularly tamponade, coronary artery disease, pulmonary embolism, and hypovolemia.

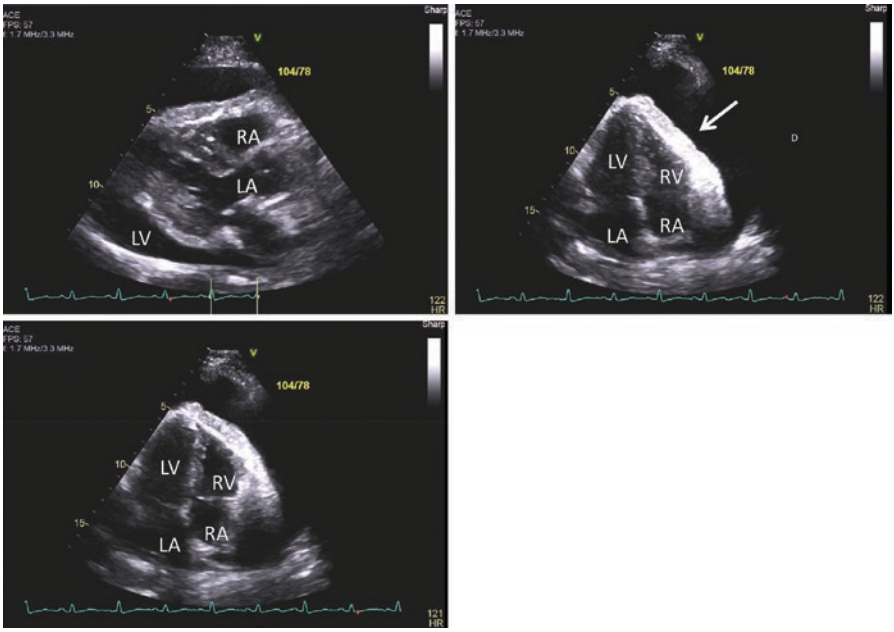

Fig. 3.5 Cardiac tamponade. Parasternal long axis (top left) showing the pericardial effusion. The apical four camber in diastole (top right) and systole (bottom) showing collapse of RV (arrow). *LA* left atrium, *RA* right atrium, *LV* left ventricle, *RV* right ventricle

- Tamponade (Fig. 3.5)
- Echocardiographic features that would suggest a hemodynamically significant pericardial fluid collection include the presence of a *swinging heart, right ventricular diastolic collapse, right atrial diastolic collapse, pseudosystolic anterior motion of mitral valve*, and an *enlarged non-pulsatile vena cava* (all parts of the respiratory cycle). It should be noted that cardiac tamponade is a clinical diagnosis and echocardiographic features may aid in diagnosis but do not secure the diagnosis alone.
- Cardiac Ischemia from Coronary Artery Disease
- Echocardiography may reveal *regional wall motion abnormalities* (RWMAs) which could be due to either previous Myocardial infarction (MI) or new ischemia. In addition to detecting potential ischemia itself, it can also enable timely identification of MI complications (mitral valve papillary muscle rupture, ventricular septal defect, free wall rupture) causing hemodynamic instability and cardiac arrest.
- Pulmonary Embolism (PE)
- Any PE that causes an arrest will generally be large and significant. Often one will see a *dilated right ventricle (RV)* (especially compared to the left ventricle) and this may be accompanied by *Right Atrial dilatation* (Fig. 3.6). Additionally, the intraventricular septum will appear flattened with an *akinetic RV* and in some cases McConnell's sign will be observed (akinesis of the mid free wall and hypercontractility of the apical wall).
- Hypovolemia

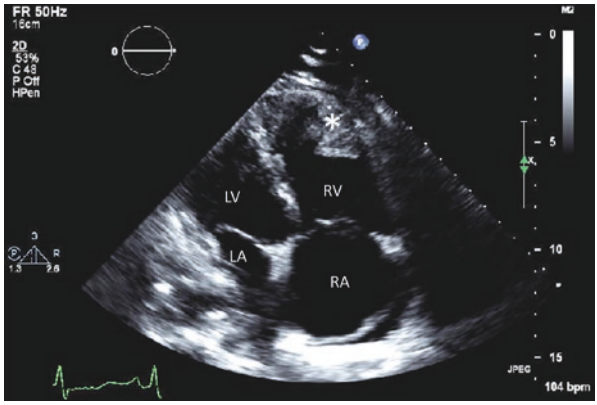

Fig. 3.6 Apical four-chamber view showing right atrial and ventricular dilation in the setting of a pulmonary embolism and a right ventricular thrombus. Asterisk showing thrombus. *LA* left atrium, *RA* right atrium, *LV* left ventricle, *RV* right ventricle

- A number of echocardiographic parameters have been identified as indicative of hypovolemia, particularly in critically ill patients. These include the presence of a small, *hyperkinetic left ventricle* often with *end-systolic cavity obliteration* ("kissing" trabecular muscles) and a *hypercontractile ventricle*. While assessment of the inferior vena cava (IVC) is difficult in an arrest situation, a finding of *flattened and small IVC* means the patient is likely hypovolemic.

Post-arrest

Post-return of spontaneous circulation, echocardiography helps in further determination of the cause of the arrest and can guide hemodynamic support (i.e., vasopressors) [20]. Post-arrest, a 12-lead electrocardiogram (ECG) should be performed to identify ischemic or conduction defects. However, ECG changes may be difficult to interpret post-arrest, since many patients will have an acute ischemia-reperfusion syndrome. Echocardiography can remediate this deficiency: the *finding of LV dysfunction* or *regional wall motion abnormalities* aids in identifying those who should undergo immediate angiography. Post-cardiac arrest myocardial dysfunction occurs in one-third of patients with a variety of patterns observed, including global hypokinesis (17.2%), regional wall motion abnormalities (13.4%), and abnormalities like stress-induced cardiomyopathy (4.8%, Fig. 3.7) [21]. Early echocardiography enables the extent of myocardial dysfunction to be quantified and helps determine if vasopressors or inotropes are needed to maximize cardiac output and reperfusion.

Ventricular Tachycardia

Ventricular tachycardia (VT) occurs across a range of individuals with and without structural heart disease. VT is a clinical spectrum of premature ventricular

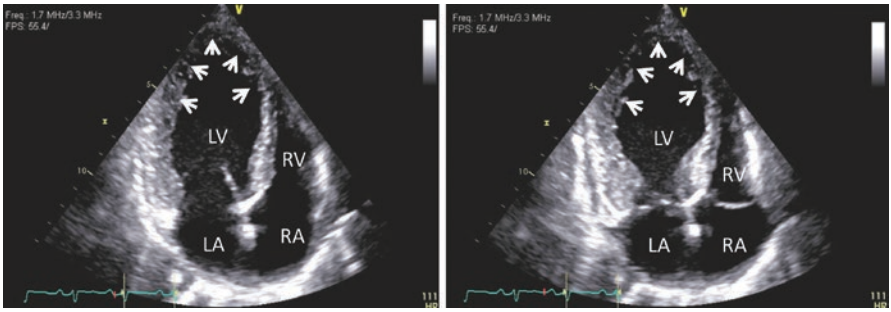

Fig. 3.7 Apical four-chamber view showing stress-induced cardiomyopathy in systole (left) and diastole (right). Arrows indicating ballooning. *LA* left atrium, *RA* right atrium, *LV* left ventricle, *RV* right ventricle

complexes (PVCs), monomorphic ventricular tachycardia (MVT), and polymorphic ventricular tachycardia (PVT). Echocardiography plays a key role in the assessment of VT by enabling identification of structural heart disease, assessing possible underlying etiologies such as scar and false tendons, as well as guiding therapeutic interventions. In the management of patients with VT, there has been significant growth and value placed on other imaging modalities, such as cardiac MRI or nuclear imaging; however echocardiography is still essential as it can be easily obtained and is less costly. Thus, it remains an important first-line imaging modality and an option that should be considered in all patients.

Outflow Tract (Idiopathic) VT

OT-VT is commonly encountered in the critical care setting and tends to exclusively occur in those patients without any structural heart disease. The most common sites of OT-VT are the left and right outflow tracts (LVOT and RVOT, respectively), with the right more common (60–80%). There are other variants of OT-VT described with origins from the pulmonic valve [22], the aortic sinus of Valsalva [23], near the His bundle [24], and the epicardium of the ventricles [25]. While there are specific nuisances to the surface electrocardiogram, many which are beyond the scope of this chapter [26], it is worthwhile reviewing some of the more basic features which can help guide echocardiography in these patients. Firstly, any VT that originates from the LVOT and RVOT will tend to have an inferior axis, which is defined by a QRS with tall positive R waves in leads II, III, and aVF and negative QS complexes in leads aVR and aVL. If the origin is from the RVOT, the ECG will typically display an LBBB pattern and R-wave transition in lead V4 or greater (in addition to the inferior axis), while LVOT will typically have an RBBB pattern with R-wave transition in leads at V3 or earlier.

While most OT-VT tends to be "benign" there are some dangerous structural heart disease mimickers that need to be excluded and evaluated for. The finding of

a completely normal heart on echocardiogram is reassuring that the underlying mechanism of the OT-VT is likely triggered by automaticity. This is valuable information, as it precludes the need for extensive evaluation for structural heart disease and consideration of an implantable cardiac defibrillator to treat further episodes. Consequently, patient management should focus on refinement of potential triggers particularly reducing excess catecholamines by changing or altering vasopressors (if the patient is receiving).

On the other hand if the echocardiogram shows *reduced LV or RV function* this would not be generally consistent with an idiopathic cause and raises concern for a structural process. Assessment for underlying arrhythmogenic right ventricular cardiomyopathy (ARVC) is critical, as it classically presents with RVOT-VT and is a well-described "dangerous" mimicker. ARVC (Fig. 3.8) is diagnosed by a Task Force Criteria in which echocardiography plays a key role by helping identify RV functional and structural alterations [27]. Features that would suggest ARVC are *regional and global RV dilatation with increased RV inflow tract, outflow tract, and longitudinal dimensions*. It is important that all RV regions are visualized as the presence of abnormal regional wall motion is a prerequisite for the diagnosis regardless of dilatation and systolic function. *RV fractional area change* has been shown to be a useful correlate of global RV function and is decreased in individuals with ARVC compared with controls [28]. However, complete and accurate RV assessment can be difficult due to its retrosternal position and complex geometry, and subsequently there has been a rise in cardiac MRI as the chosen modality for RV assessment [27]. If the RV images are suboptimal contrast can improve identification of the free wall of the RV and enable better wall motion analysis. Nevertheless, echocardiography still plays a decisive initial role as access to cardiac MRI can be limited and is prone to false positives especially if there is an overreliance on detection of intramyocardial fat and wall thinning. Further, MRI is expensive (especially for serial evaluation) and many of these patients have cardiovascular implantable electronic devices that limit MRI use.

Another potential mimicker that needs to be considered is cardiac sarcoidosis (CS). Echocardiographic findings in CS tend to be better appreciated in more

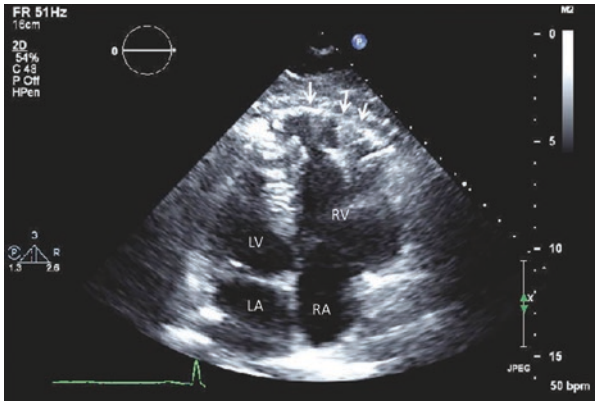

Fig. 3.8 Apical four-chamber view showing arrhythmogenic right ventricular cardiomyopathy. Note dilation of the RV with trabeculations and outpouchings involving the right ventricular apex (highlighted with arrows). *LA* left atrium, *RA* right atrium, *LV* left ventricle, *RV* right ventricle

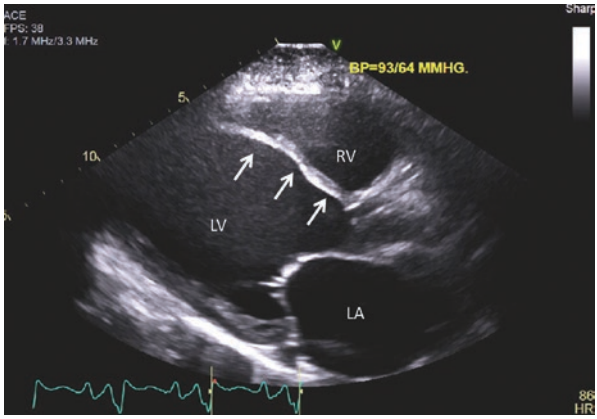

Fig. 3.9 Parasternal long axis showing cardiac sarcoid. Note dilation of the LV with septal thinning (arrows). *LA* left atrium, *LV* left ventricle, *RV* right ventricle

advanced disease, as early disease tends to be focal and patchy [29]. *Interventricular thinning (particularly basal)* is the most typical feature observed (Fig. 3.9) [30]. A potential clue to CS is regional wall motion abnormalities or myocardial thinning appearing in a noncoronary distribution.

Lastly, acute myocarditis is another consideration which can rarely present with OT-VT. The echocardiogram is helpful in the diagnosis but not usually diagnostic. Typical findings would be *severe global hypokinesis (with a normal wall thickness) with abnormal diastolic filling*; however, there can be regional variations which are often reflective of the focal nature of myocarditis. When it comes to LVOT VT, considerations of the above also are important but these are less described.

Moderator Band VT

The moderator band (MB) of the RV can be a source of ventricular arrhythmias (VA) in patients without structural heart disease (Fig. 3.10). It is a muscular structure encompassing RV Purkinje fibers that connect the anterior papillary muscle to the free wall of the ventricle. VA that can arise from the MB include monomorphic VT and idiopathic VF. VT arising from the MB tends to be LBBB morphology with a left superior frontal plane axis, a sharp downstroke of the QRS in the precordial leads, and a relatively narrow QRS width [31]. The MB is generally easily detected by echocardiography based upon its location in the RV and is often seen as a thick echo-dense structure.

Monomorphic VT

Monomorphic VT (MVT) occurs largely in those patients with structural cardiac disease, with the majority caused by reentry around a region of ventricular scar.

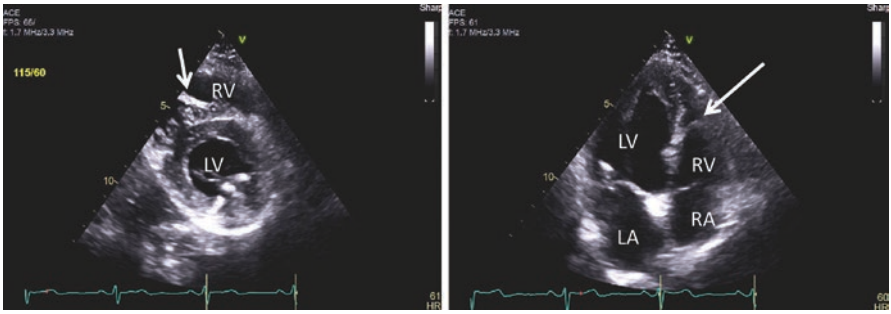

Fig. 3.10 Moderator band (arrow) detected on both short-axis (left) and four-chamber views (right). *LA* left atrium, *RA* right atrium, *LV* left ventricle, *RV* right ventricle

Etiology

Echocardiography is a key modality to help identify underlying arrhythmogenic substrate. The etiology of MVT can be broadly divided into an ischemic (coronary artery disease) and nonischemic, with coronary artery disease constituting the large majority of MVT cases. While MVT can occur in the acute stage of a myocardial infarction, this is uncommon with most episodes occurring during the subacute and chronic phases, with a reported median time of 3 years. Interestingly, the development of arrhythmogenic substrate can be influenced by the primary reperfusion method that the patient received with patients who received early reperfusion therapy likely to have smaller and "patchy" myocardial scar formation. Again like OT-VT, an understanding of the surface ECG can enable a focused and effective echocardiogram and confirm initial suspicions of the arrhythmia origin. In MVT, QRS duration is affected by the proximity of the origin of the VT to the septum. Post-MI VT generally arises from the LV or the intraventricular septum. VTs with RBBB patterns always arise in the LV, while VTs with LBBB patterns arise from, or adjacent to, the LV septum. The presence of the QS complex in any ECG lead suggests the focus of wave front and could provide areas to focus echocardiography. Echocardiography should also be used to assess LVEF and identify *regions of wall motion abnormalities*, areas of *myocardial thinning*, or *aneurysms* that may have developed. *Myocardial scar tissue* can be identified as thinned myocardium with an end-diastolic wall thickness of <6 mm. It usually appears brighter than normal myocardium and with greater intensity of *backscattered echo signals*. Regional contractile function, more specifically the observation of akinesia or dyskinesia, has been correlated with transmural scar tissue, whereas preserved contractile function or mild hypokinesia is considered normal [32]. More advanced techniques such as LV strain, strain rate, and torsion have been used to assess scar but may not be feasible in the critically care setting [33]. While echocardiography is a useful first-line tool, it is important to note that it does have limitations in terms of defining transmural extent and intramyocardial location of scar.

There is a broad differential for nonischemic etiologies, and therefore echocardiography plays a critical role for identifying specific characteristics that may guide the determination of the underlying etiology. There are many echocardiographic features described for the differing etiologies which would be beyond the scope of this chapter; however there are a few critical and distinctive features which are noteworthy and highlighted in Fig. 3.11.

Management

Echocardiography can help augment and define management strategies in addition to guiding risk assessment, particularly for ablation procedures (Fig. 3.12). If an antiarrhythmic drug approach is used, knowledge of the patient's EF is imperative. If *EF is <40%,* lidocaine or amiodarone are the best options. An EF >40% opens up other possibilities such as procainamide and sotalol, with the caveat that class Ic drugs are contraindicated in patients with CAD. The identification of *thrombus* (mobile or mural LV wall) is a contraindication to an ablation procedure. Additionally, the presence of a thrombus has clinically relevant consequences in

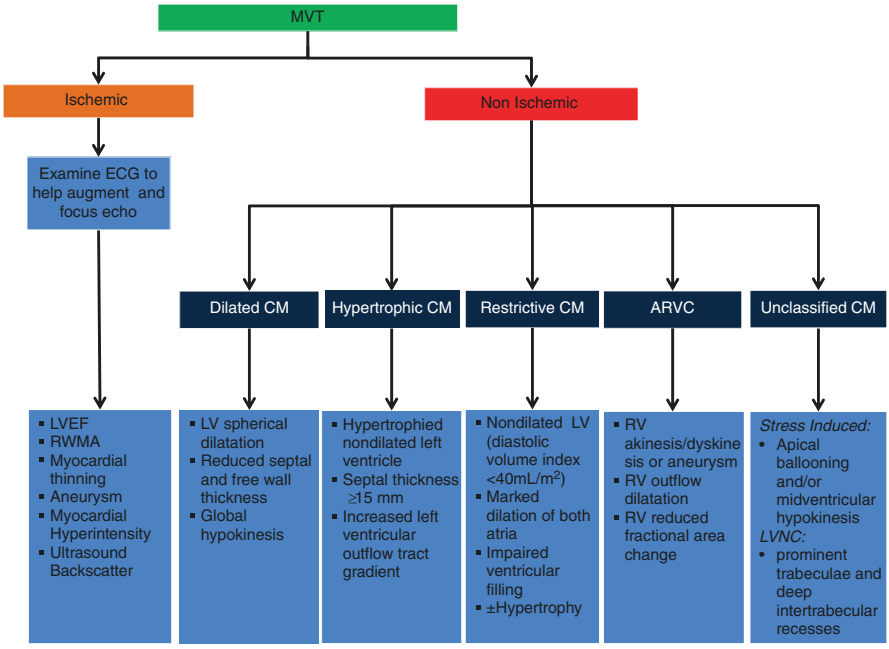

Fig. 3.11 Echocardiographic features of the different etiologies of monomorphic ventricular tachycardia (MVT). *ECG* electrocardiogram, *LVEF* left ventricular ejection fraction, *RWMA* regional wall motion abnormalities, *LV* left ventricle, *CM* cardiomyopathy, *RV* right ventricle, *ARVC* arrhythmogenic right ventricular cardiomyopathy, *LVNC* left ventricular non-compaction cardiomyopathy

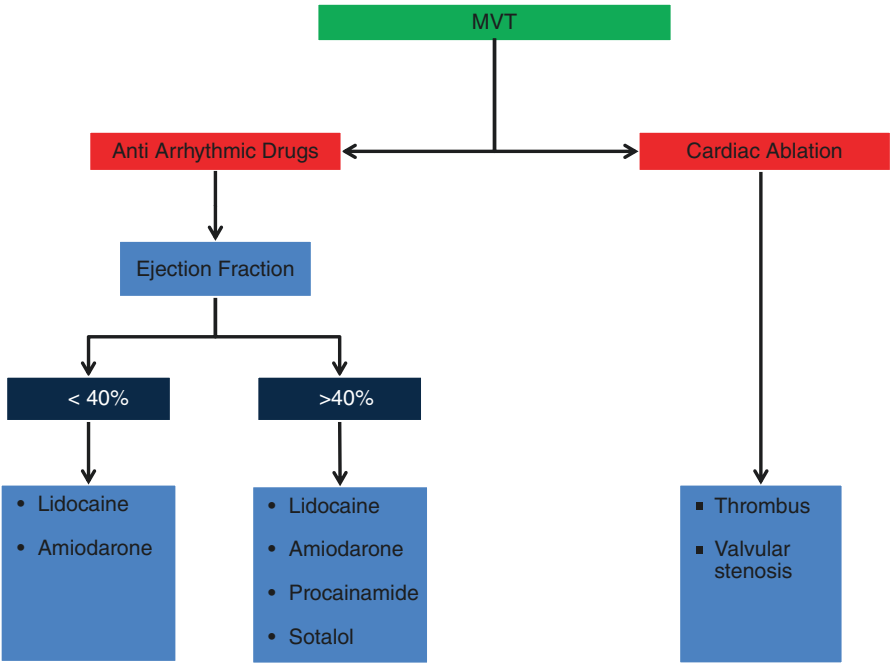

Fig. 3.12 Role of echocardiography in the management and risk assessment of patients with MVT

terms of risk of systemic embolization and implications for antithrombotic management. A thrombus would typically be observed at the apex but visualization of the LV apex on echocardiography can be difficult as imaging can be confounding by foreshortening and near-field ring-down artifacts. In these situations, decreasing the depth and increasing the probe frequency may help. Additionally, contrast can enable complete visualization of the apex and identify filling defects suggestive of thrombus. The presence of valvular stenosis or calcification may influence the decision for a retrograde aortic versus transseptal ablation approach, if that is appropriate.

Polymorphic VT

Echocardiography is generally performed in PVT to detect any structural heart disease; however this is rarely detected. Most PVT occurs in the setting of prolonged QT and due to underlying channelopathies such as long QT syndrome and Brugada. However, it can occur during episodes of acute myocardial ischemia and PVT is typically associated with signs or symptoms of recurrent myocardial ischemia [34]. Echocardiography is valuable in these scenarios by enabling early detection of RWMA which can occur prior to the onset of electrocardiographic changes or

development of symptoms. However, overall echocardiography has high sensitivity but a relatively lower specificity for the detection of ischemia [35].

Left Ventricular Assist Device

Cardiac arrhythmias are one of the most common untoward effects of left ventricular assist device (LVAD) therapy, with estimates suggesting an incidence of 4.66 events per patient year [36, 37], with a majority of these ventricular arrhythmias. There are a variety of potential mechanisms for ventricular arrhythmias in LVAD patients and echocardiography plays a key role in this evaluation.

In those LVADs that are continuous-flow pumps, arrhythmias can be precipitated by "suction events" [38–40]. In this scenario, excessive ventricular unloading occurs in the setting of suboptimal left ventricular preload. As a consequence, the ventricular chamber collapses and subsequently the inflow cannula makes direct contact with the ventricular wall inciting a ventricular arrhythmia. Echocardiography is crucial in helping identify arrhythmias precipitated by this mechanism by enabling visualization of the inflow cannula to ensure that its position and direction are appropriate (it may even visualize a "suction" event). In addition to these "suction" events, abnormality of the inflow cannula orientation or placement can precipitate arrhythmias, particularly if it becomes angulated in a small ventricle and subsequently makes contact with the septum [41]. Apically inserted inflow cannula can be adequately imaged in standard or modified 2D parasternal and apical TTE views. The inflow cannula should be aligned with the mitral valve opening with a properly aligned inflow cannula showing laminar flow from the ventricle to the device. Turbulence and elevated Doppler velocity suggest obstruction of the inflow cannula from either thrombus or intermittent obstruction by LV wall [42].

Although intrinsic myocardial scarring related to the patient's underlying cardiomyopathic process, rather than the apical cannula, has been shown to be the dominant VT substrate in LVAD patients [43], reentry involving apical scarring around the inflow cannula is an important consideration [44, 45]. Echocardiography is useful to help differentiate these as it can assess for deteriorating cardiomyopathy or aid in the detection of new/worsening scar (as discussed previously). Of note patients with apical scar VT related to the inflow cannula tend to have an RBBB that is superiorly directed, with late precordial transition between V3 and V5 [44].

Ischemic Premature Ventricular Contractions

Premature ventricular contractions (PVCs) are ubiquitous and many patients in the critical care setting develop PVCs or runs of NSVT for a variety of reasons. Often when these are frequent and persistent there is concern that underlying ischemia may be the driver of these ventricular beats. Echocardiography is particularly useful in this scenario when performed at the time of the PVCs/VT. Detection of a

wall motion abnormality that corresponds with the exit site of the PVC/VT on the surface ECG would be suggestive that the PVC/VT is related to possible underlying ischemia.

Central Venous Catheters

Central venous catheters (CVCs) are a critical element to the management of patients in the critical care setting by providing robust venous access for a number of different indications, including dialysis, drug administration, and/or hemodynamic monitoring. While many different types of catheters exist (tunneled or non-tunneled, multi-lumen, dialysis catheters, and peripherally inserted central catheters) ventricular dysrhythmias are a well-recognized complication both acutely during insertion and from short-term or long-term use [46].

While the optimal positioning of the tip of a CVC is a controversial subject [47], the finding of the CVC tip (either accidentally or intentionally placed) on the right side of the heart is worrisome because of the potential cardiac-related complications. Contact of the guidewire and/or catheter with the internal myocardial surface can precipitate cardiac arrhythmias. While clinical acumen often dominates detection of the CVC as a precipitant for the arrhythmia, echocardiography is useful as it can enable direct visualization of catheter tip movement and its location. Therefore in the critical care setting for a patient with central venous access that is experiencing recurrent arrhythmias, consideration of the CVC tip as the precipitant is important and echocardiography can help in this regard.

ICD Shocks

In a patient who presents with ICD shocks, particularly recurrent ICD shocks or storm, echocardiography can enable evaluation of changes or development of new underlying arrhythmogenic substrate (see MVT section). Many of these patients will have known structural heart disease and a factor for precipitant of arrhythmias, such as electrolyte imbalance, ischemia, congestive heart failure (CHF) exacerbation, and medication noncompliance. While the impact of LV shocks on cardiac function is controversial, there is growing evidence that it can transiently impair cardiac function and hemodynamics especially in patients with systolic dysfunction. There is also impairment of LV diastolic dysfunction, irrespective of baseline LVEF [48].

Bradyarrhythmias

Patients with symptomatic bradycardia often require close monitoring in the critical care setting. Echocardiography evaluation can help define and guide underlying determination of the underlying etiology.

Sinus Node Dysfunction

CCU care for patients with sinus node dysfunction (SND) is rare due to its often slow progressive nature. Most intrinsic SND is due to idiopathic degenerative disease and the echocardiogram may not reveal any definitive substrate abnormalities; thus it is often not part of the initial workup. Nevertheless, echocardiography can still be of some value if physical signs or surface ECG suggests an ischemic, infiltrative, or inflammatory cause. Acute myocardial infarction, particular anterior MIs, can lead to sinus arrest or slowing of the sinus rate. Cardiomyopathies and infiltrative disorders can result in SND with rare causes such as myotonic dystrophy or Friedreich's ataxia. Further, sinus venous and secundum atrial septal defects can be associated with SND.

Atrioventricular Conduction Abnormities

An atrioventricular (AV) block is defined as a delay or interruption of an atrial impulse to the ventricles due to an anatomic or a functional impairment in the conduction system. Again like SND, it is unlikely that these patients will require critical care admission but in cases of more advanced AV block (second or third degree) the symptoms experienced by patients can be variable particularly in the presence of comorbid conditions. In these situations, clinical evaluation with a thorough history and exam may identify an underlying systemic disorder of which echocardiography can confirm clinical suspicions. Of particular importance is infiltrative disorders and possible exposure to ticks (Lyme disease).

Complete heart block is one of the most common findings in patients with CS and should be considered especially in younger patients. It is usually caused by involvement of the *basal septum by scar tissue*, granulomas, or involvement of the nodal artery causing ischemia in the conduction system. Although echocardiography may not be of value in detecting early-stage disease, if a patient has more significant cardiac involvement this may be detected.

Lastly, Lyme disease may be suggested by clinical history and positive titers, and patients generally have a normal echocardiogram. In some cases it will be helpful to define further cardiac involvement, in particular pericardial involvement, which may manifest as pericardial effusion. Lyme myocarditis may be suggested by left ventricular dysfunction with regional wall motion abnormalities [49].

Post-cardiac Catheter Ablation

With tremendous growth in cardiac ablation technology, and improved outcomes compared to antiarrhythmic drugs, there has been a rise in the number of cardiac ablations performed, particularly complex ablations such as ventricular tachycardia [50]. Although cardiac ablation is generally successful, complications may

occur with acute cardiac tamponade one of the most common life-threatening complications occurring with an incidence of 1.3% [51], and is associated with an increase in mortality [52]. This may be detected during the procedure and, if present, a drain can be placed in the electrophysiology lab. Echocardiography can be used to ensure that there is no residual or new fluid accumulation before pulling the drain. However, there is newer evidence to suggest that early removal of pericardial drains (i.e., before leaving the EP lab) after cardiac tamponade appears to be safe and effective [53].

Conclusion

Echocardiography is an extremely useful tool in patients with cardiac arrhythmias. It is an advantageous imaging modality as it is cheap, easily obtainable, portable, and causes minimal patient harm. Echocardiography enables easy and safe anatomical and functional assessment for structural heart disease and enables identification of underlying arrhythmogenic substrate. Furthermore, it can help augment medical decisions, guide prognosis and risk stratification in the arrhythmia patient.

References

1. Wren C, Campbell RW, Hunter S. Role of echocardiography in differential diagnosis of broad complex tachycardia. Br Heart J. 1985;54(2):166–72.
2. Kotecha D, Mohamed M, Shantsila E, Popescu BA, Steeds RP. Is echocardiography valid and reproducible in patients with atrial fibrillation? A systematic review. EP Europace. 2017:eux027.
3. Lang RM, Badano LP, Mor-Avi V, Afilalo J, Armstrong A, Ernande L, et al. Recommendations for cardiac chamber quantification by echocardiography in adults: an update from the American Society of Echocardiography and the European Association of Cardiovascular Imaging. Eur Heart J Cardiovasc Imaging. 2015;16(3):233–71.
4. Donal E, Lund LH, Oger E, Reynaud A, Schnell F, Persson H, et al. Value of exercise echocardiography in heart failure with preserved ejection fraction: a substudy from the KaRen study. Eur Heart J Cardiovasc Imaging. 2015;17(1):106–13.
5. Punjani S, Wu W-C, Cohen S, Sharma SC, Choudhary G. Echocardiographic indices of diastolic function relate to functional capacity and quality of life in ambulatory men with atrial fibrillation. J Am Soc Echocardiogr. 2011;24(5):533–40.e3.
6. Turakhia MP, Santangeli P, Winkelmayer WC, Xu X, Ullal AJ, Than CT, et al. Increased mortality associated with digoxin in contemporary patients with atrial fibrillation: findings from the TREAT-AF study. J Am Coll Cardiol. 2014;64(7):660–8.
7. Sleeswijk ME, Van Noord T, Tulleken JE, Ligtenberg JJ, Girbes AR, Zijlstra JG. Clinical review: treatment of new-onset atrial fibrillation in medical intensive care patients: a clinical framework. Crit Care. 2007;11(6):233.
8. Brodsky MA, Allen BJ, Capparelli EV, Luckett CR, Morton R, Henry WL. Factors determining maintenance of sinus rhythm after chronic atrial fibrillation with left atrial dilatation. Am J Cardiol. 1989;63(15):1065–8.
9. Køber L, Torp-Pedersen C, McMurray JJ, Gøtzsche O, Lévy S, Crijns H, et al. Increased mortality after dronedarone therapy for severe heart failure. N Engl J Med. 2008;358(25):2678–87.

10. Chung R, Houghtaling PL, Tchou M, Niebauer MJ, Lindsay BD, Tchou PJ, et al. Left ventricular hypertrophy and antiarrhythmic drugs in atrial fibrillation: impact on mortality. Pacing Clin Electrophysiol. 2014;37(10):1338–48.
11. Manning WJ, Weintraub RM, Waksmonski CA, Haering JM, Rooney PS, Maslow AD, et al. Accuracy of transesophageal echocardiography for identifying left atrial thrombi: a prospective, intraoperative study. Ann Intern Med. 1995;123(11):817–22.
12. Black IW, Hopkins AP, Lee LC, Walsh WF. Left atrial spontaneous echo contrast: a clinical and echocardiographic analysis. J Am Coll Cardiol. 1991;18(2):398–404.
13. Goldman ME, Pearce LA, Hart RG, Zabalgoitia M, Asinger RW, Safford R, et al. Pathophysiologic correlates of thromboembolism in nonvalvular atrial fibrillation: I. Reduced flow velocity in the left atrial appendage (The Stroke Prevention in Atrial Fibrillation [SPAF-III] study). J Am Soc Echocardiogr. 1999;12(12):1080–7.
14. Celeste F, Muratori M, Mapelli M, Pepi M. The evolving role and use of echocardiography in the evaluation of cardiac source of embolism. J Cardiovasc Echogr. 2017;27(2):33.
15. Ayirala S, Kumar S, O'Sullivan DM, Silverman DI. Echocardiographic predictors of left atrial appendage thrombus formation. J Am Soc Echocardiogr. 2011;24(5):499–505.
16. Ono K, Iwama M, Kawasaki M, Tanaka R, Watanabe T, Onishi N, et al. Motion of left atrial appendage as a determinant of thrombus formation in patients with a low CHADS2 score receiving warfarin for persistent nonvalvular atrial fibrillation. Cardiovasc Ultrasound. 2012;10(1):50.
17. Breitkreutz R, Walcher F, Ilper H, Seeger FH, Price S, Via G, et al. Focused echocardiography in life support: the subcostal window. Eur J Trauma Emerg Surg. 2009;35(4):347–56.
18. Tsou P-Y, Kurbedin J, Chen Y-S, Chou EH, Lee M-tG, Lee MC-H, et al. Accuracy of point-of-care focused echocardiography in predicting outcome of resuscitation in cardiac arrest patients: A systematic review and meta-analysis. Resuscitation. 2017;114:92–9.
19. Labovitz AJ, Noble VE, Bierig M, Goldstein SA, Jones R, Kort S, et al. Focused cardiac ultrasound in the emergent setting: a consensus statement of the American Society of Echocardiography and American College of Emergency Physicians. J Am Soc Echocardiogr. 2010;23(12):1225–30.
20. Stub D, Bernard S, Duffy SJ, Kaye DM. Post cardiac arrest syndrome. Circulation. 2011;123(13):1428–35.
21. Cha K-C, Hwang SO, Kim HI, Kim OH, Cha YS, Kim H, et al. Echocardiographic patterns of post-cardiac arrest myocardial dysfunction. Resuscitation. 2018;124:90–5.
22. Mulpuru SK, Konecny T, Madhavan M, Kapa S, Noseworthy PA, McLeod CJ, et al. Atypical variants of right ventricular outflow arrhythmias. J Cardiovasc Electrophysiol. 2014;25(12):1321–7.
23. Ouyang F, Fotuhi P, Ho SY, Hebe J, Volkmer M, Goya M, et al. Repetitive monomorphic ventricular tachycardia originating from the aortic sinus cusp: electrocardiographic characterization for guiding catheter ablation. J Am Coll Cardiol. 2002;39(3):500–8.
24. Yamauchi Y, Aonuma K, Takahashi A, Sekiguchi Y, Hachiya H, Yokoyama Y, et al. Electrocardiographic characteristics of repetitive monomorphic right ventricular tachycardia originating near the His-bundle. J Cardiovasc Electrophysiol. 2005;16(10):1041–8.
25. Chun KR, Satomi K, Kuck KH, Ouyang F, Antz M. Left ventricular outflow tract tachycardia including ventricular tachycardia from the aortic cusps and epicardial ventricular tachycardia. Herz. 2007;32(3):226–32.
26. Padmanabhan D, Sugrue A, Gaba P, Asirvatham SJ. Outflow tract ventricular arrhythmias. Herzschrittmacherther Elektrophysiol. 2017;28(2):177–86.
27. Marcus FI, McKenna WJ, Sherrill D, Basso C, Bauce B, Bluemke DA, et al. Diagnosis of arrhythmogenic right ventricular cardiomyopathy/dysplasia: proposed modification of the Task Force Criteria. Eur Heart J. 2010;31(7):806–14.
28. te Riele ASJM, Tandri H, Sanborn DM, Bluemke DA. Noninvasive Multimodality Imaging in ARVD/C. J Am Coll Cardiol Img. 2015;8(5):597–611.
29. Mehta D, Lubitz SA, Frankel Z, Wisnivesky JP, Einstein AJ, Goldman M, et al. Cardiac involvement in patients with sarcoidosis: diagnostic and prognostic value of outpatient testing. Chest. 2008;133(6):1426–35.

30. Ayyala US, Nair AP, Padilla ML. Cardiac sarcoidosis. Clin Chest Med. 2008;29(3):493–508, ix.
31. Sadek MM, Benhayon D, Sureddi R, Chik W, Santangeli P, Supple GE, et al. Idiopathic ventricular arrhythmias originating from the moderator band: electrocardiographic characteristics and treatment by catheter ablation. Heart Rhythm. 2015;12(1):67–75.
32. Rösner A, Avenarius D, Malm S, Iqbal A, Bijnens B, Schirmer H. Severe regional myocardial dysfunction by stress echocardiography does not predict the presence of transmural scarring in chronic coronary artery disease. Eur Heart J Cardiovasc Imaging. 2015;16(10):1074–81.
33. Aarsæther E, Rösner A, Straumbotn E, Busund R. Peak longitudinal strain most accurately reflects myocardial segmental viability following acute myocardial infarction—an experimental study in open-chest pigs. Cardiovasc Ultrasound. 2012;10(1):23.
34. Wolfe CL, Nibley C, Bhandari A, Chatterjee K, Scheinman M. Polymorphous ventricular tachycardia associated with acute myocardial infarction. Circulation. 1991;84(4):1543–51.
35. Sabia P, Afrookteh A, Touchstone DA, Keller MW, Esquivel L, Kaul S. Value of regional wall motion abnormality in the emergency room diagnosis of acute myocardial infarction. A prospective study using two-dimensional echocardiography. Circulation. 1991;84(3 Suppl):I85–92.
36. Kirklin JK, Naftel DC, Kormos RL, Stevenson LW, Pagani FD, Miller MA, et al. Fifth INTERMACS annual report: risk factor analysis from more than 6,000 mechanical circulatory support patients. J Heart Lung Transplant. 2013;32(2):141–56.
37. Rosenbaum AN, Kremers WK, Duval S, Sakaguchi S, John R, Eckman PM. Arrhythmias in patients with cardiac implantable electrical devices after implantation of a left ventricular assist device. ASAIO J. 2016;62(3):274–80.
38. Vollkron M, Voitl P, Ta J, Wieselthaler G, Schima H. Suction events during left ventricular support and ventricular arrhythmias. J Heart Lung Transplant. 2007;26(8):819–25.
39. Andersen M, Videbæk R, Boesgaard S, Sander K, Hansen PB, Gustafsson F. Incidence of ventricular arrhythmias in patients on long-term support with a continuous-flow assist device (HeartMate II). J Heart Lung Transplant. 2009;28(7):733–5.
40. Reesink K, Dekker A, Van der Nagel T, Beghi C, Leonardi F, Botti P, et al. Suction due to left ventricular assist: implications for device control and management. Artif Organs. 2007;31(7):542–9.
41. Estep JD, Stainback RF, Little SH, Torre G, Zoghbi WA. The role of echocardiography and other imaging modalities in patients with left ventricular assist devices. J Am Coll Cardiol Cardiovasc Imaging. 2010;3(10):1049–64.
42. Stainback RF, Estep JD, Agler DA, Birks EJ, Bremer M, Hung J, et al. Echocardiography in the management of patients with left ventricular assist devices: recommendations from the American Society of Echocardiography. J Am Soc Echocardiogr. 2015;28(8):853–909.
43. Sacher F, Reichlin T, Zado ES, Field ME, Viles-Gonzalez JF, Peichl P, et al. Characteristics of ventricular tachycardia ablation in patients with continuous flow left ventricular assist devices. Circ Arrhythm Electrophysiol. 2015;8(3):592–7.
44. Moss JD, Flatley EE, Beaser AD, Shin JH, Nayak HM, Upadhyay GA, et al. Characterization of ventricular tachycardia after left ventricular assist device implantation as destination therapy: a single-center ablation experience. JACC Clin Electrophysiol. 2017;3(12):1412–24.
45. Pedretti S, Cipriani M, Bonacina E, Vargiu S, Ad VG, Frigerio M, et al. Refractory ventricular tachycardia caused by inflow cannula mechanical injury in a patient with left ventricular assist device: catheter ablation and pathological findings. J Arrhythmia. 2017;33(5):494–6.
46. Ng PK, Ault MJ, Ellrodt AG, Maldonado L. Peripherally inserted central catheters in general medicine. Mayo Clin Proc. 1997;72(3):225–33.
47. Vesely TM. Central venous catheter tip position: a continuing controversy. J Vasc Interv Radiol. 2003;14(5):527–34.
48. Toh N, Nishii N, Nakamura K, Tada T, Oe H, Nagase S, et al. Cardiac dysfunction and prolonged hemodynamic deterioration after implantable cardioverter-defibrillator shock in patients with systolic heart failure. Circ Arrhythm Electrophysiol. 2012;5(5):898–905.

49. Malawista M. Lyme carditis: cardiac abnormalities of Lyme disease. Ann Intern Med. 1980;93(Part 1):8–16.
50. Sapp JL, Wells GA, Parkash R, Stevenson WG, Blier L, Sarrazin JF, et al. Ventricular tachycardia ablation versus escalation of antiarrhythmic drugs. N Engl J Med. 2016;375(2):111–21.
51. Cappato R, Calkins H, Chen SA, Davies W, Iesaka Y, Kalman J, et al. Updated worldwide survey on the methods, efficacy, and safety of catheter ablation for human atrial fibrillation. Circ Arrhythm Electrophysiol. 2010;3(1):32–8.
52. Cappato R, Calkins H, Chen SA, Davies W, Iesaka Y, Kalman J, et al. Prevalence and causes of fatal outcome in catheter ablation of atrial fibrillation. J Am Coll Cardiol. 2009;53(19):1798–803.
53. Pedersen ME, Leo M, Kalla M, Malhotra A, Stone M, Wong K, et al. Management of tamponade complicating catheter ablation for atrial fibrillation: early removal of pericardial drains is safe and effective and reduces analgesic requirements and hospital stay compared to conventional delayed removal. JACC Clin Electrophysiol. 2017;3(4):367–73.

Chapter 4
Echocardiography in Patients with Syncope

Karthik Seetharam, Brandon W. Calenda, and Farooq A. Chaudhry[†]

Abstract Syncope is defined as a temporary, abrupt loss of consciousness with spontaneous return to baseline. This chapter offers a framework for a focused approach to syncope. A detailed history and physical examination establishes the pretest probability that the syncope is of cardiac origin. Although echocardiography is not indicated for many cases of syncope, it can be a valuable tool to risk stratify syncope when it is suspected to be of cardiac origin. Transthoracic echo (TTE) is an efficient means of rapidly identifying structural heart disease, which suggests a higher probability of cardiogenic syncope and places the patient in a higher risk category than a patient with a structurally normal heart.

Keywords Syncope · Arrhythmia · Cardiomyopathy

Introduction

Syncope is defined as a temporary, abrupt loss of consciousness with spontaneous return to baseline. It contributes to approximately 3% of emergency-department admissions as well as 6% of total hospital admissions in the United States [1]. The cost of medical care for this condition approaches two billion dollars annually [2]. Although it is a common medical problem, syncope is really an umbrella term representing a multitude of disorders and frequently presents a diagnostic challenge. Many institutions lack a standardized approach because there is no "gold standard" diagnostic test for the cause of syncope [3].

[†]Deceased

Dedication: This chapter is dedicated to the memory of Dr. Farooq Chaudhry who was a cherished colleague in the Division of Cardiology at Mount Sinai Hospital. His untimely passing in 2017 has left a void in our hearts and minds.

K. Seetharam · B. W. Calenda (✉) · F. A. Chaudhry
Mount Sinai School of Medicine, New York, NY, USA
e-mail: brandon.calenda@mountsinai.org

E. Herzog, E. Argulian (eds.), *Echocardiography in the CCU*,
https://doi.org/10.1007/978-3-319-90278-4_4

This chapter offers a framework for a focused approach to syncope. A detailed history and physical examination establish the pretest probability that the syncope is of cardiac origin. Although echocardiography is not indicated for many cases of syncope, it can be a valuable tool to risk stratify syncope when it is suspected to be of cardiac origin. Transthoracic echo (TTE) is an efficient means of rapidly identifying structural heart disease, which suggests a higher probability of cardiogenic syncope and places the patient in a higher risk category than a patient with a structurally normal heart.

Mechanisms of Syncope

Syncope can be broadly classified based on the underlying mechanism [4]. They can be subdivided into neurally mediated syncope, orthostatic syncope, and cardiogenic syncope (Fig. 4.1). Frequently, a detailed history and physical examination are sufficient to identify the cause of syncope. When there is sufficient suspicion of cardiogenic syncope, an electrocardiogram and/or echocardiogram may be appropriate for further risk stratification.

Neurally Mediated Syncope

Neurally mediated or "reflex syncope" accounts for 45% of cases of known syncope [5]. It mainly presents with prodromal symptoms such as nausea, flushing, warmth, and diaphoresis. It is associated with prolonged standing, emotional stress, urination, coughing, swallowing, or carotid stimulation. It is the most common cause of syncope regardless of age and gender. Neurally mediated syncope is driven by imbalance in the autonomic nervous system leading to excess parasympathetic activation. It can manifest as a vasodepressor (vasodilatory, hypotensive) response or as cardioinhibitory (vagally mediated bradycardia). It is also one of the most common

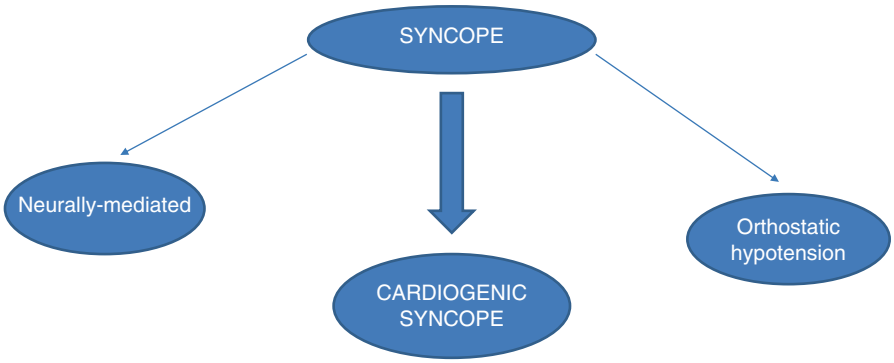

Fig. 4.1 Mechanisms of syncope

causes of recurrent syncope [6]. Regardless, the prognosis is very good and the mortality is low [7]. This cause of syncope typically does not warrant echocardiographic evaluation or inpatient admission.

Orthostatic Hypotension

Orthostatic hypotension is defined as a symptomatic drop in blood pressure with postural changes [3]. Similar to neurally mediated and cardiogenic syncope, there are a number of causes [8]. It is frequently seen in the elderly following postural changes due to age-related degeneration of the autonomic nervous system. Pathological conditions such as parkinsonism, multisystem atrophy, peripheral neuropathies, and diabetes can cause orthostatic hypotension due to alterations in the autonomic nervous system regulation and loss of compensatory mechanisms. It can also result from a number of medications such as diuretics, nitrates, antidepressants, and antipsychotics when it carries a favorable prognosis [9]. As with neurally mediated syncope, this diagnosis can be made by history and physical examination, and does not merit echocardiographic evaluation unless concomitant structural heart disease is suspected.

Cardiogenic Syncope

Cardiac disorders are the most common causes of syncope occurring in the critical care setting, and contribute to nearly 80% of intensive care unit admissions for syncope [10]. Identification and timely assessment of cardiogenic syncope are critical because the associated morbidity and mortality are higher compared to other causes of syncope [11]. Cardiac syncope can be broadly subdivided into arrhythmias or obstruction in blood flow (Fig. 4.2).

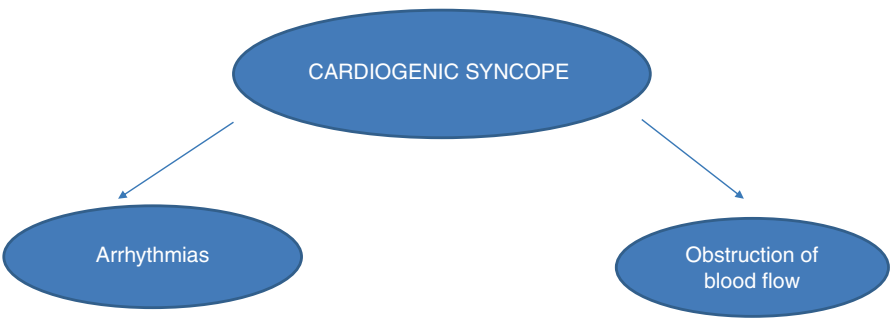

Fig. 4.2 General mechanisms of cardiac syncope

Disorders of Heart Rhythm

Cardiac arrhythmias are the most common cause of cardiogenic syncope [3]. Severe rhythm disturbances may mediate syncope by causing an acute drop in cardiac output due to abrupt decreases or increases in heart rate with resulting cerebral hypoperfusion. Among cardiac arrhythmias, severe bradyarrhythmia and asystolic pauses are frequently encountered. Common causes for bradyarrhythmia include sick sinus syndrome, Mobitz type II block, and complete heart block [3]. Tachyarrhythmias (ventricular and supraventricular) are the second most common cause of cardiac arrhythmia causing cardiogenic syncope [12]. Medications, particularly AV nodal blockers, QT interval prolonging drugs, and antiarrhythmics are important causes of arrhythmia [3]. Arrythmogenic syncope is considered an important risk factor for sudden cardiac death [13].

Obstruction of Blood Flow

Obstructive cardiac lesions presenting with syncope can be potentially life threatening but can be readily identified by transthoracic echo. For example, syncope is well established as a very high-risk presenting symptom in patients with severe aortic stenosis. Furthermore, other common conditions such as cardiac tamponade, hypertrophic cardiomyopathy, mitral stenosis, and massive pulmonary embolism may be lethal if not recognized and treated promptly. These findings are summarized in Table 4.1.

Table 4.1 High-risk cardiac lesions and their echocardiographic correlates

Structural heart disease which may present with syncope	Associated echo findings
Severe aortic stenosis	Calcified aortic valve with reduced excursion, elevated velocities across aortic valve
Hypertrophic obstructive cardiomyopathy	LV hypertrophy, elevated velocities in LV outflow tract, abnormal papillary muscles, early aortic valve closure
Cardiac tamponade	Early diastolic collapse of RV, systolic collapse of RA, enhanced ventricular interdependence, IVC plethora
Mitral stenosis	Thickened, domed mitral valve with elevated gradient
Massive pulmonary embolism	RV dilation, dysfunction
Anomalous origin of coronary arteries	Echo may be normal
Severe pulmonary hypertension	High-velocity tricuspid regurgitation jet, dilated pulmonary artery, early closure of pulmonic valve, elevated pulmonic regurgitant end-diastolic velocity
Arrhythmogenic right ventricular cardiomyopathy (ARVC)	Dilated RV, RV wall motion abnormalities

Diagnosis: History and Physical Examination

A proper and detailed medical history is paramount in distinguishing possible cardiogenic syncope from more benign causes of syncope. The historical features which distinguish cardiac syncope from neurally mediated or orthostatic syncope are summarized in Table 4.2.

Attention should be paid to eliciting the setting of syncope, prodromal symptoms, medications, associated medical conditions, and family history of malignant arrhythmia, structural heart disease, or sudden death. Many patients with cardiogenic syncope may present with loss of consciousness during exercising or lying flat [14]. These patients are typically asymptomatic prior to the event, although some may experience palpitations just prior to the event [15]. If the history does not clearly suggest a neurally mediated or orthostatic cause of syncope, then cardiogenic syncope should be considered, particularly in older patients. Any information regarding previous history of heart disease, cardiac surgeries, and family history of heart disease, medications, and comorbidities should be noted.

On physical exam, one can seek out clues suggesting structural heart disease such as murmurs, gallops, distended jugular veins, cyanosis, or clubbing.

How to Differentiate Noncardiac Syncope from Cardiogenic Syncope

Demographics are important in establishing the probability of cardiac syncope. Patients with cardiac syncope are more frequently male, typically greater than 60 years of age [16]. In patients with a history of heart disease or congenital heart

Table 4.2 Historical clues to distinguish cardiac from noncardiac causes of syncope

Features suggesting cardiac causes of syncope	Features suggesting noncardiac causes
Older age (greater than 60 years)	Younger age
Known coronary disease, reduced ventricular function, or structural heart disease	No known cardiac disease
Exertional or supine syncope	Syncope from standing position or after positional changes
Absent or minimal prodrome, usually palpitations	Prodrome of nausea, warmth, sweating
Family history of sudden death	Triggers such as pain, dehydration, emotional stress, coughing, laughing, swallowing, urinating
One or fewer prior episodes of syncope	Multiple, recurrent episodes of syncope
Abnormal cardiac physical examination	Normal physical examination

disease, they tend to be younger than 50 years. Patients with cardiac syncope usually do not have a history of recurrent syncope, and typically have only one or two prior episodes [16].

Patients with noncardiac syncope are usually of younger age and frequently have no history of cardiac disease. These patients may have a history of frequent and recurrent syncope. Syncope often occurs in standing position or in association with pain or emotional duress. They may also have a history of physical triggers such as coughing, laughing, and urination.

Role of ECG for Syncope

An ECG is essential in the evaluation of syncope. It should be the first diagnostic test performed for suspected cardiogenic syncope. It is a low-cost, easily available, and reproducible test that can detect the presence of arrhythmia and may provide clues to the presence of underlying structural heart disease. The gold standard for the diagnosis of cardiogenic syncope is when a relationship between symptoms and documented arrhythmia on ECG is seen [17]. However, some patients may have arrhythmias such as prolonged asystole (>3 s), rapid supraventricular tachycardias (SVTs) (>160 b.p.m. for >32 beats), or ventricular tachycardia seen on ECG when asymptomatic. This can also be considered diagnostic for arrhythmogenic syncope [18]. However, if a patient presents with syncope and a normal ECG, cardiogenic syncope cannot be ruled out. Continuous monitoring may be required in these cases. If cardiogenic syncope is suspected, echocardiography can provide valuable prognostic information, whether or not the initial ECG is abnormal.

Role of Echocardiography for Syncope

Transthoracic echocardiography should be considered in the setting of suspected cardiogenic syncope or structural heart disease in the setting of syncope [16]. If the history, physical, and ECG clearly point towards a noncardiac cause of syncope, then there is no role of echocardiogram as part of the evaluation (Fig. 4.3). If, however, the initial evaluation is equivocal and there are historical, exam, or ECG features suggesting cardiac syncope, then transthoracic echocardiogram is reasonable [16]. Given the noninvasive nature, low risk, and relatively low cost of TTE, it can be a valuable test for suspected cardiac syncope.

In certain conditions, echocardiography is instrumental in making the final diagnosis. Conditions such as severe aortic stenosis, cardiac tamponade, hypertrophic obstructive cardiomyopathy, mitral stenosis, or atrial myxoma can be definitively diagnosed by TTE. Other findings such as reduced LV ejection fraction can help inform prognosis, as discussed below.

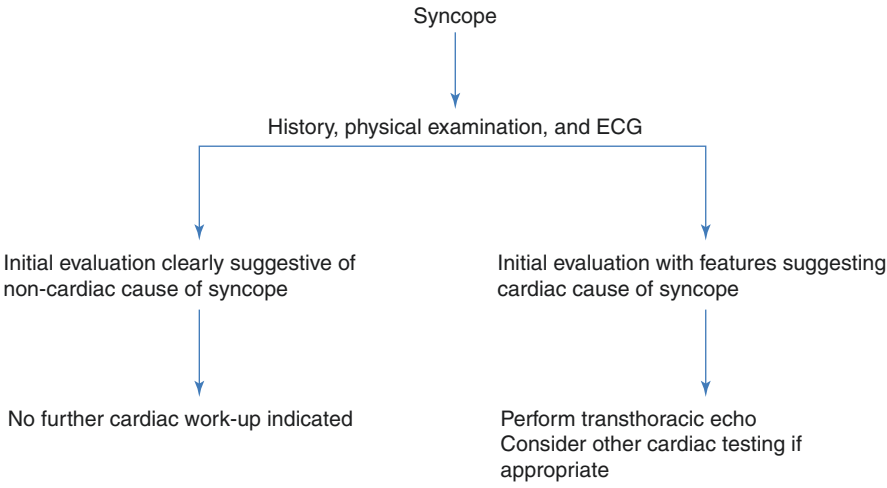

Fig. 4.3 A diagnostic approach to syncope

Echocardiography and Risk Stratification in Syncope

Although echocardiography may not always indicate a clear cause for syncope, echo remains an important tool for risk stratification in the setting of syncope. Patients with reduced left or right ventricular function and/or evidence of prior myocardial infarction may be at higher risk for adverse events in the short and long terms. Ejection fraction can also be used as a predictor of arrhythmia in certain subset of patients with an unremarkable initial ECG [19].

Quantifying risk in syncope is an area of ongoing research. There are a number of clinical risk scores which have been validated in cases of syncope, though the studies are heterogeneous and difficult to compare [16]. Syncope risk scores incorporating echocardiographic findings have not been well described.

In the setting of syncope and known pulmonary embolism, the presence of right ventricular dilation or dysfunction on transthoracic echo adds significant prognostic information and may help guide the decision to perform thrombolysis. Echocardiography is the best imaging study to detect right ventricular dysfunction during acute PE [20]. In cases of submassive pulmonary embolism, thrombolysis may be offered if RV dysfunction or dilation is present [20].

High-Risk Features Meriting Admission or Extended Observation

The 30-day mortality for syncope is less than 1% [20]. Despite the overall favorable prognosis, risk stratification is essential to determine which patients would benefit from higher levels of monitoring, including inpatient or intensive care admissions.

Table 4.3 European Society of Cardiology guidelines for cardiogenic syncope admission

Severe structural or coronary artery disease including:
• Heart failure • Reduced ejection fraction • Previous myocardial infarction
Clinical features suggesting arrhythmic syncope:
• Exertional syncope, syncope while supine, palpitations prior to syncope • Family history of sudden cardiac death • History of non-sustained ventricular tachycardia
High-risk ECG features:
• Bifascicular block (LBBB or RBBB with left hemi-block) • Prolonged QRS duration • ECG suggestive of pre-excitation, Brugada pattern • Arrhythmogenic ventricular cardiomyopathy
Other important comorbidities:
• Severe anemia • Electrolyte imbalance

Table 4.4 Canadian Cardiovascular Society criteria for syncope admission

Major risk factors (should have urgent, inpatient cardiac evaluation):
• Abnormal ECG (acute or old infarct, tachyarrhythmia, bradyarrhythmia, or conduction disease
• History of significant structural heart disease or arrhythmia
• Hypotension (systolic blood pressure < 90 mmHg)
Minor risk factors (can consider urgent inpatient evaluation):
• Age >60
• Associated dyspnea
• Anemia
• Hypertension
• Cerebrovascular disease
• Family history of sudden death
• Syncope while supine, exercising, or without prodrome

The presence of high-risk echocardiographic features is among some of the criteria which would generally merit expedited workup with inpatient admission for syncope, according to the guidelines set forth by the European Society of Cardiology (ESC) and Canadian Cardiovascular Society (CCS) [3, 21]. These features are delineated in Tables 4.3 and 4.4.

Role of Advanced Echocardiography in Syncope

Exercise stress testing can be considered in situations of exertional syncope. However, exercise stress echocardiography should be reserved for individual cases

in which exercise would be expected to provide incremental information above and beyond the resting echocardiogram, as may be seen in dynamic intracavitary or LV outflow tract obstruction.

Transesophageal echocardiography (TEE) is generally not indicated for the evaluation of syncope unless there are specific structural features that would be better identified on TEE, such as atrial myxoma or mitral valve pathology not well characterized on TTE.

Conclusion

The CCU should be equipped to provide rapid and immediate access to echocardiography for all patients with possible cardiogenic syncope. There are several "can't miss," life-threatening causes of cardiogenic syncope, most of which can be rapidly identified or excluded with a good-quality transthoracic echo. Even when the echocardiogram does not indicate a clear cause for the syncope, the presence or absence of high-risk features can help risk stratify the patient and aid in selecting optimal monitoring and follow-up.

References

1. Grubb BP, Karabin B. Syncope: evaluation and management in the geriatric patient. Clin Geriatr Med. 2012;28(4):717–28.
2. Grossman SA, Chiu D, Lipsitz L, Mottley JL, Shapiro NI. Can elderly patients without risk factors be discharged home when presenting to the emergency department with syncope? Arch Gerontol Geriatr. 2014;58(1):110–4.
3. The Task Force for the Diagnosis and Management of Syncope of the European Society of Cardiology (ESC). Guidelines for the diagnosis and management of syncope (version 2009). Eur Heart J. 2009;30(21):2631–71.
4. Brignole M, Hamdan MH. New concepts in the assessment of syncope. J Am Coll Cardiol. 2012;59(18):1583–91.
5. Mitro P, Kirsch P, Valocik G, Murin P. A prospective study of the standardized diagnostic evaluation of syncope. Europace. 2011;13(4):566–71.
6. Ruwald MH, Hansen ML, Lamberts M, et al. Comparison of incidence, predictors, and the impact of co-morbidity and polypharmacy on the risk of recurrent syncope in patients <85 versus >/=85 years of age. Am J Cardiol. 2013;112(10):1610–5.
7. D'Ascenzo F, Biondi-Zoccai G, Reed MJ, et al. Incidence, etiology and predictors of adverse outcomes in 43,315 patients presenting to the Emergency Department with syncope: an international meta-analysis. Int J Cardiol. 2013;167(1):57–62.
8. Freeman R, Wieling W, Axelrod FB, et al. Consensus statement on the definition of orthostatic hypotension, neurally mediated sncope and the postural tachycardia syndrome. Auton Neruosci. 2011;161(1–2):46–8.
9. van Dijk N, Quartieri F, Blanc JJ, et al. Effectiveness of physical counterpressure maneuvers in preventing vasovagal syncope the physical counterpressure manoeuvres trial (PC-Trial). J Am Coll Cardiol. 2006;48(8):1652–7.

10. Silverstein MD, Singer DE, Mulley AG, Thibault GE, Barnett GO. Patients with syncope admitted to medical intensive care units. JAMA. 1982;248(10):1185–9.
11. Soteriades ES, Evans JC, Larson MG, et al. Incidence and prognosis of syncope. N Engl J Med. 2002;347(12):878–85.
12. Davis S, Westby M, Pitcher D, Petkar S. Implantable loop recorders are cost-effective when used to investigate transient loss of consciousness which is either suspected to be arrhythmic or remains unexplained. Europace. 2012;14(3):402–9.
13. Bhat PK, Pantham G, Laskey S, Como JJ, Rosenbaum DS. Recognizing cardiac syncope in patients presenting to the emergency department with trauma. J Emerg Med. 2014;46(1):1–8.
14. Del Rosso A, Ungar A, Maggi R, et al. Clinical predictors of cardiac syncope at initial evaluation in patients referred urgently to a general hospital: the EGSYS score. Heart. 2008;94(12):1620–6.
15. Sule S, Palaniswamy C, Aronow WS, et al. Etiology of syncope in patients hospitalized with syncope and predictors of mortality and rehospitalization for syncope at 27-month follow-up. Clin Cardiol. 2011;34(1):35–8.
16. Writing Committee M, Shen WK, Sheldon RS, et al. 2017 ACC/AHA/HRS guideline for the evaluation and management of patients with syncope: executive summary: a report of the American College of Cardiology/American Heart Association Task Force on Clinical Practice Guidelines and the Heart Rhythm Society. Heart Rhythm. 2017;14(8):e218–54.
17. Krahn A, Klein G, Norris C, Yee R. The etiology of syncope in patients with negative tilt table and electrophysiologic testing. Circulation. 1995;92:1819–24.
18. Krahn AD, Klein GJ, Yee R, Skanes AC. Detection of asymptomatic arrhythmias in unexplained syncope. Am Heart J. 2004;148(2):326–32.
19. Sarasin FP, Junod AF, Carballo D, Slama S, Unger PF, Louis-Simonet M. Role of echocardiography in the evaluation of syncope: a prospective study. Heart. 2002;88(4):363–7.
20. Piazza G, Goldhaber SZ. Management of submassive pulmonary embolism. Circulation. 2010;122(11):1124–9.
21. Sheldon RS, Morillo CA, Krahn AD, et al. Standardized approaches to the investigation of syncope: Canadian Cardiovascular Society position paper. Can J Cardiol. 2011;27(2):246–53.

Chapter 5
Echocardiography in Cardiac Arrest and Resuscitation

Soheila Talebi, Edgar Argulian, and Eyal Herzog

Abstract Sudden cardiac arrest carries a grave prognosis. The management of cardiac arrest is algorithmic because providers typically have limited knowledge of the patient's past medical history. Peri-resuscitation echocardiography provides an invaluable real-time bedside diagnostic tool that can identify some of the potentially reversible causes of cardiac arrest and can be regarded as analogous to pulse oximetry or ECG monitoring.

Keywords Cardiac arrest · Resuscitation · Arrhythmia

Introduction

Sudden cardiac arrest carries a grave prognosis, with less than 12% of patients surviving to hospital discharge [1]. The management of cardiac arrest is algorithmic because providers have limited knowledge of the patient's past medical history. Cardiac arrest environment typically involves many staff members gathered around the patient, including medical doctors, nurses, and technicians. This makes management of medical cardiac arrest challenging: multiple providers perform critical tasks simultaneously. The cardiac arrest team leader is responsible for coordinating the team and ensuring compliance with accepted guidelines. Current advance life support (ALS) guidelines prioritize chest compressions and, when appropriate, timely defibrillation. In parallel to resuscitation, attempts should be made to elucidate and address the cause of the arrest. Early identification of the precipitating cause increases the likelihood of a favorable outcome [1].

In patients with a primary electrical cause of the arrest definitive treatment generally involves reversing the electrical abnormality by cardioversion, defi-

S. Talebi · E. Argulian · E. Herzog (✉)
Mount Sinai St. Luke's Hospital, New York, NY, USA
e-mail: Sohelia.Talebi@mountsinai.org; Edgar.Argulian@mountsinai.org; Eyal.Herzog@mountsinai.org

E. Herzog, E. Argulian (eds.), *Echocardiography in the CCU*,
https://doi.org/10.1007/978-3-319-90278-4_5

brillation, or pacing. In contrast, in patients with pulseless electrical activity or asystole, potentially treatable causes should be immediately excluded and reversed. Some potentially treatable underlying conditions such as hypoxia, hypothermia, and metabolic derangements can be diagnosed at bedside and by review of the laboratory data. Other causes like severe hypovolemia, tamponade, pulmonary embolism, and coronary thrombosis may be less obvious upon initial evaluation. Moreover, in the stressful environment of resuscitation, differential diagnosis based solely on history and physical examination may be ineffective and inaccurate [1].

Role of Echocardiography in Cardiac Arrest

Echocardiography is one of the most powerful diagnostic and monitoring tools available to the emergency and critical care provider. Mobility and relatively low cost of echocardiographic machines, including handheld devices, allow their use virtually everywhere. In expert hands, echocardiography may provide instantaneous and accurate assessment of cardiac structure and function as well as hemodynamics, with minimal risk to the patient. If there is any change in patient's condition or a need to follow up previously detected abnormalities it can be easily and safely repeated to accelerate the decision-making process [2].

Although persistent or developing hemodynamic instability is considered a class I indication for echocardiography, current resuscitation guidelines do not recommend its routine use during cardiac arrest. Appropriately applied and interpreted cardiovascular ultrasound can diagnose/exclude some potentially reversible causes of cardiac arrest and guide lifesaving therapeutic interventions. The current American Society of Echocardiography guidelines recommend limited, focused transesophageal echocardiography during intraoperative cardiac arrest [1], and International Liaison Committee on Resuscitation (ILCOR) guidelines support this recommendation for nontraumatic cardiac arrest when appropriately trained personal is present [3]. Peri-resuscitation echocardiography provides an invaluable real-time bedside diagnostic tool that can identify some of the potentially reversible causes of cardiac arrest and can be regarded as analogous to pulse oximetry or ECG monitoring [4].

Challenges of Imaging During Cardiac Arrest

Acquisition of echo images during cardiac arrest is challenging and should be done in a way that minimizes interruptions in cardiopulmonary resuscitation (CPR). The number of factors including supine positioning, positive pressure ventilation, lung injury (pneumothorax/pneumomediastinum), trauma (head and neck, thoracic), and

presence of lines/dressings and/or drains can interfere with image acquisition. Limited time available for interpretation of echocardiographic data in a critically ill patient can further challenge the examiner [5].

Goals of Echocardiography in Cardiac Arrest

In the settings of cardiac arrest, a comprehensive transthoracic echocardiography (TTE) study is neither necessary nor relevant. Excessive time spent scanning and distracting the team from performing high-quality CPR can be detrimental. Instead, fast and focused ultrasound examination used as an extension of the clinical examination should aim at ruling in or ruling out potential causes of the cardiac arrest. In hemodynamically unstable patients, early and rapid identification of the precipitating cause may assist in treatment decisions and may prevent progression to full cardiac arrest. In patients with cardiac arrest, the examiner must be aware of the importance of uninterrupted chest compressions during CPR. The 10-s pulse check is a useful time window during which focused echocardiography can be performed by a provider experienced in echocardiography and trained in ALS compliance. Given the brief time available, forward planning is essential. Gain and depth settings must be pre-optimized. The subcostal window often yields the most useful views with the least interruption to CPR. However, in experienced hands, other views can also be sought (apical and parasternal) and echocardiography can be performed with ongoing compressions. It is crucial for examiners to be able to obtain nonstandard views of the heart in order to acquire optimal images for interpretation in a given situation. The findings during focused echocardiography should be communicated to the team leader. While the benefits of the routine use of cardiac ultrasound in patients with cardiac arrest are unclear we believe that bedside echocardiography can be safely incorporated into the resuscitation algorithm.

Figure 5.1 outlines the use of bedside TTE during cardiac arrest. Our five recommendations for bedside TTE during resuscitation of patient with cardiac arrest are as follows:

1. Obtaining information by echocardiography should not interrupt resuscitation.
2. Transthoracic echocardiography should be done during the 10-s pulse check window.
3. Goal of focused echocardiographic evaluation in life support is to improve resuscitative efforts but not to terminate resuscitation.
4. The findings of focused echocardiography should be communicated to the team leader.
5. Images must be stored for review.

Figure 5.2 is our group proposal of incorporating bedside TTE to the advanced cardiac life support (ACLS) circular algorithm in adult cardiac arrest.

In summary: Bedside TTE can provide highly relevant information in the hands of experienced examiners, specifically in patients with PEA arrest and asystole [6–8].

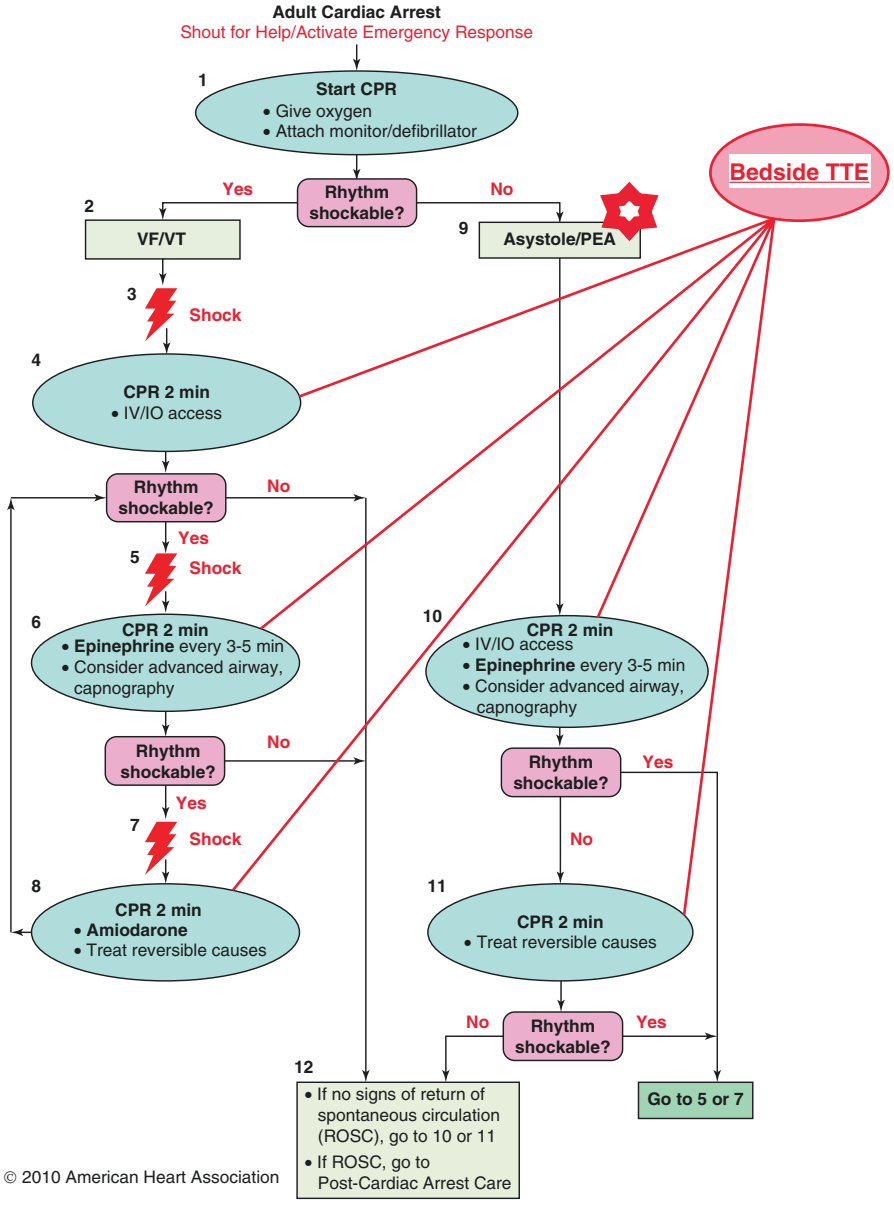

Bedside TTE may provide important information in Asystole/PEA

- Obtain information by TTE should not interrupt resuscitation
- TTE should be done during the 10-second pulse check
- Goal of TTE evaluation is to improve resuscitative efforts, not to terminate resuscitation
- The findings of TTE should be communicated to the team leader
- Images must be stored for review

Fig. 5.1 Incorporated bedside TTE to advanced cardiac life support (ACLS) algorithm in adult cardiac arrest—2015 update

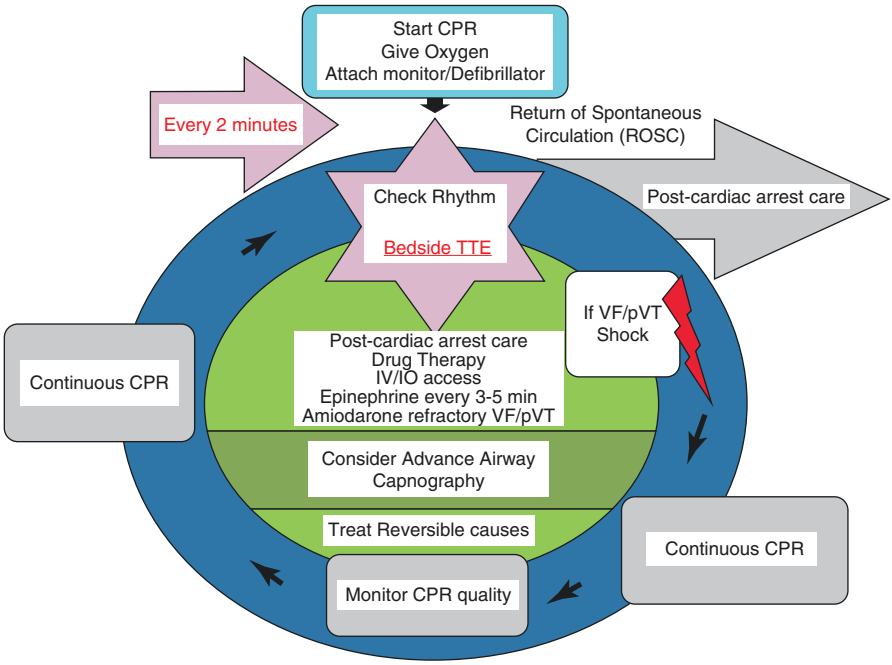

Fig. 5.2 Incorporated bedside TTE to advanced cardiac life support (ACLS) circular algorithm in adult cardiac arrest—2015 update

Training for Advanced Cardiac Life Support Echocardiography

Pocket-sized imaging devices have been recommended as a tool for fast initial screening in the emergency settings. Technical characteristics and image quality of these new miniaturized echocardiographic systems are usually sufficient for the qualitative (but not quantitative) evaluation of ventricular function, pericardial and pleural effusions, and possibly valvular disease. Because an experienced echocardiographer is not a standard part of the cardiac arrest team, it is imperative to train non-cardiologist providers in bedside-focused cardiac ultrasound.

Focused ultrasound is now considered a routine part of advanced trauma life support in patients with traumatic cardiac arrest, and in some hospitals in the intensive care setting. In order to ensure a basic competence level of the examiner a training program should be available to clinicians who wish to practice echocardiography in the cardiac arrest settings. A training protocol will guide the examiner through obtaining quick-look views during the 10-s pulse check and minimizing the interruptions in CPR. Both individual competence and competence of the team can be formally assessed through a certification process. The certification process therefore supports the concept of the patient-centric approach which is pivotal to acute/critical care medicine. The certification should be limited to the clinical questions that can potentially be answered in such settings. When appropriate training is undertaken, peri-resuscitation echocardiography does not interfere with high-quality cardiopulmonary

resuscitation (CPR), and may potentially improve decision-making. Specific training in advanced cardiac life support compliance is required, even with experienced practitioners in order to ensure that images are obtained and recorded only during the pulse/rhythm check. These courses are now administered by the UK Resuscitation Council and endorsed by the British Society of Echocardiography. Focused echocardiographic evaluation in life support (FEEL) has been developed, as an adjunct to resuscitation in an ALS-compliant manner. The use of FEEL is to improve resuscitative efforts but not to terminate resuscitation. The consultation via network connections enables discussion with the most competent colleagues in the hospital, with direct visualization of the echocardiographic images, which may further improve interpretation of the findings and adjust decision-making [9].

Ethical Points

While it is acknowledged that simple and fast cardiovascular ultrasound procedures may be helpful in many cases, it should be used wisely and cautiously. It is important to emphasize that emergency echocardiography should only be performed by an examiner who is adequately trained in image acquisition and interpretation in acute/critical settings. Poor-quality images or image misinterpretation may be misleading and may result in poor outcome. Stored images obtained during resuscitation can be viewed later during case review and root cause analysis. If there are plans to do potential semi-invasive procedures (e.g., TEE), informed consent should be secured from the family, whenever applicable.

Role of Echocardiography in Typical Clinical Scenarios Leading to Cardiac Arrest

Hypovolemia

Inadequate circulating volume is one of the causes of pulseless electrical activity (PEA) in cardiac arrest. In circulatory failure state, determination of hypovolemia can be challenging. Physical examination is not a sensitive way to identify hypovolemia in patients with occult volume loss and no external bleeding. In critically ill patients, a number of parameters in echocardiography have been found to indicate severe hypovolemia. A small left ventricle with systolic cavity obliteration is suggestive of hypovolemia. In addition, in spontaneous breathing patients a small inferior vena cava (IVC) diameter with inspiratory collapse can be a sign of hypovolemia. These patients need aggressive volume resuscitation and correction of the cause of hypovolemia [10]. Figure 5.3 shows TTE findings of a 72-year-old woman with past medical history of hypothyroidism, hypertension, and coronary artery disease who had cardiac arrest secondary to wide complex tachycardia. Bedside transthoracic echocardiography revealed marked left ventricle hypertrophy with a small cavity size and mid left ventricular obliteration during systole.

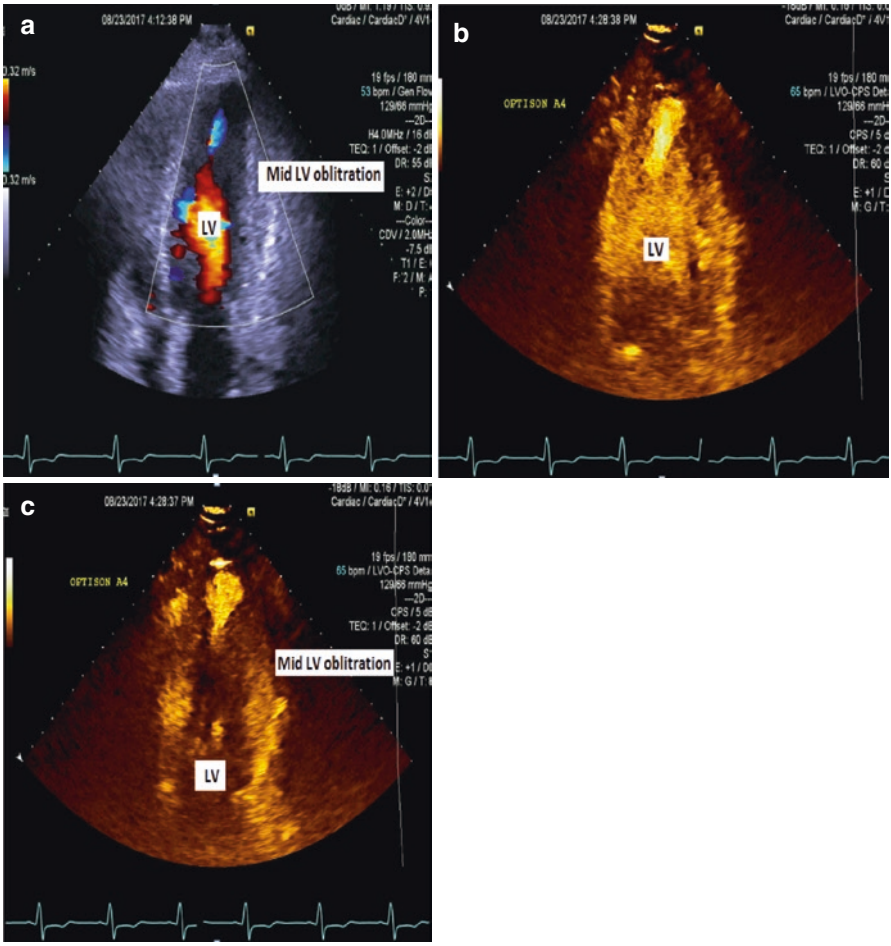

Fig. 5.3 A 72-year-old woman with past medical history of hypothyroidism, hypertension, and coronary artery disease admitted for severe diarrhea and progressive shortness of breath. She had a cardiac arrest secondary to wide complex tachycardia. Bedside transthoracic echocardiography showed the following: (**a**) Apical four-chamber view: severe left ventricle hypertrophy with small cavity and turbulent flow in mid-ventricle. (**b**) Apical four-chamber view in diastole after contrast injection. (**c**) Apical four-chamber view in systole after contrast injection showing mid left ventricular obliteration. *LV* left ventricle

Pulmonary Embolism

Massive pulmonary embolism (PE) is a well-known reversible cause of cardiac arrest, typically PEA or asystole. Thrombolytic therapy increases the chance of successful resuscitation in patients presenting with hemodynamic instability as a consequence of acute pulmonary embolism. A sudden increase in afterload can result in acute dilation of the right ventricle while the absence of signs of right ventricular overload or dysfunction effectively excludes PE as a cause of cardiac arrest. Occasionally, clots can be visible in the right ventricle, right atrium, right ventricular outflow tract, or pulmonary arteries on the ultrasound examination [11].

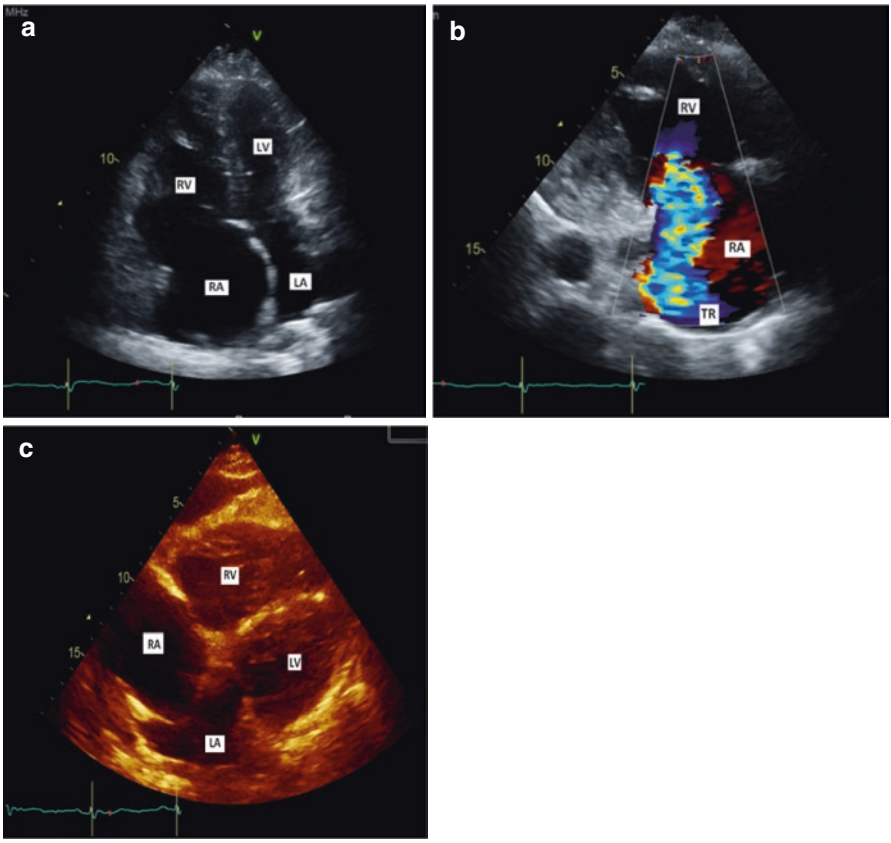

Fig. 5.4 A 67-year-old man with multiple comorbidities who was brought post-cardiac arrest. Initial rhythm was pulseless electrical activity. He had history of hip surgery 2 weeks ago. Bedside transthoracic echocardiography revealed the following: (**a**) Apical four-chamber view: right atrial and right ventricular dilation, and bulging of the interatrial septum toward left atrium. (**b**) Right ventricle inflow view: Severe tricuspid regurgitation. (**c**) Subxiphoid four-chamber view: right atrial and right ventricular dilation. *LV* left ventricle, *LA* left atrium, *RV* right ventricle, *RA* right atrium, *TR* tricuspid regurgitation

Figure 5.4 demonstrates TTE imaging of a 67-year-old man with multiple comorbidities who was brought to hospital after resuscitation from cardiac arrest. His initial rhythm was pulseless electrical activity (PEA). He had a history of hip surgery 2 weeks before his admission. Bedside transthoracic echocardiography showed right ventricular dilation with IVC engorgement.

Pericardial Tamponade

Pericardial tamponade is a life-threatening clinical syndrome caused by pericardial accumulation of fluid, pus, blood, clots, or gas that leads to compression of the heart. Increase in pericardial pressure impairs cardiac filling and ultimately causes cardiogenic shock and cardiac arrest. Echocardiography should be obtained

immediately if pericardial tamponade is suspected. Acute pericardial tamponade is a clinical diagnosis based on tachycardia (>100 beats/min), hypotension (<100 mmHg systolic), pulsus paradoxus (>10 mmHg drop in blood pressure on inspiration), and neck vein distention with elevated jugular venous pressure. The traditional clinical features are often difficult to ascertain in the peri-resuscitation state. Echocardiography is the diagnostic method of choice in suspected cardiac tamponade and should be performed without delay. The most common finding is a pericardial effusion. During resuscitation, demonstration of a pericardial collection should lead to consideration of cardiac arrest secondary to tamponade, especially in patients with recent procedure, chest surgery, or chest trauma [11, 12]. The size of the effusion can be misleading, as it is the rate of accumulation of fluid that determines the clinical course. Echocardiographic features routinely sought in tamponade such as the presence of a swinging heart, right ventricular diastolic collapse, right atrial collapse, and enlarged non-pulsatile vena cava may not be universally present. The reciprocal changes in the size of cardiac chambers and transvalvular flows may be difficult to interpret in cardiac arrest. Figure 5.5 shows the TTE

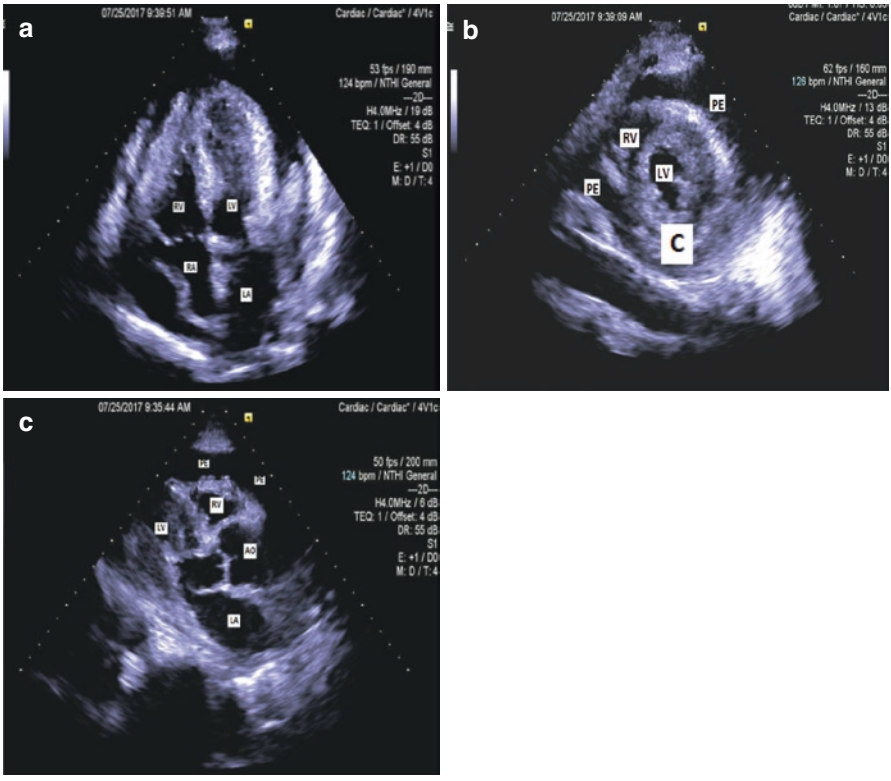

Fig. 5.5 A 24-year-old woman with past medical history of mitral valve prolapse and recent symptoms of upper respiratory infection presents to the emergency department post-cardiac arrest. Transthoracic echocardiography revealed the following: (**a**) Apical four-chamber view: large pericardial effusion with right atrial and right ventricular collapse. (**b**) Parasternal short-axis view: Large pericardial effusion. (**c**) Parasternal long-axis view: large pericardial effusion. *LV* left ventricle, *LA* left atrium, *RV* right ventricle, *RA* right atrium, *AO* aorta, *PE* pericardial effusion

findings of a 24-year-old woman with past medical history of mitral valve prolapse and recent symptoms of upper respiratory infection who was brought to the emergency department after cardiac arrest. The initial cardiac rhythm was asystole. Transthoracic echocardiography revealed large pericardial effusion suggestive of tamponade etiology for cardiac arrest.

Coronary Artery Disease

Coronary artery disease (CAD) is the major cause of cardiac arrest in the Western world, either as a result of severe ventricular dysfunction, acute arrhythmia, or complications arising from prior myocardial infarction (MI). Although myocardial ischemia is often heralded by typical symptoms and ECG findings, these are not always present in unexplained cardiac arrest. Bedside TTE in patients with a shockable rhythm can be used to look for segmental wall motion abnormalities as a surrogate for CAD being the primary cause of cardiac arrest following the return of spontaneous circulation (ROSC). In cases where a wall motion abnormality is documented, CAD would be suspected as the primary cause of the arrest and early revascularization may be necessary. Bedside TTE can also be used for evaluation of mechanical complications of AMI such as acute VSD and papillary muscle rupture [13]. Figure 5.6 shows the bedside TTE findings after ROSC including left ventricle systolic dysfunction and hypokinesia of the anterior wall along with an apical ventricular septal defect. Figure 5.7 demonstrates the echocardiographic findings of a 58-year-old man with a history of gastritis and schizophrenia brought to emergency department after witnessing cardiac arrest. Patient was reportedly out with a friend and complained of severe shortness of breath and chest pain. On arrival the patient had agonal breathing but still had a pulse. Patient subsequently went into PEA arrest. Bedside transthoracic echocardiogram after ROSC showed a flail anterior mitral leaflet with severe mitral regurgitation.

Monitoring Cardiac Output

Detection of cardiac output during cardiac arrest is generally performed by palpating central pulses and/or noninvasive blood pressure measurements; however, both of these methods may not be accurate. Although intensive care unit patients frequently have an arterial pressure transducer and therefore these inaccuracies may be irrelevant, this is not necessarily true in the non-ICU settings. Here, focused echocardiography has been shown to identify the presence or absence of cardiac kinetic motion during resuscitation. Furthermore, echocardiography especially TEE has the potential to define the efficiency of the chest compressions and the optimal duration of the resuscitation maneuvers [14].

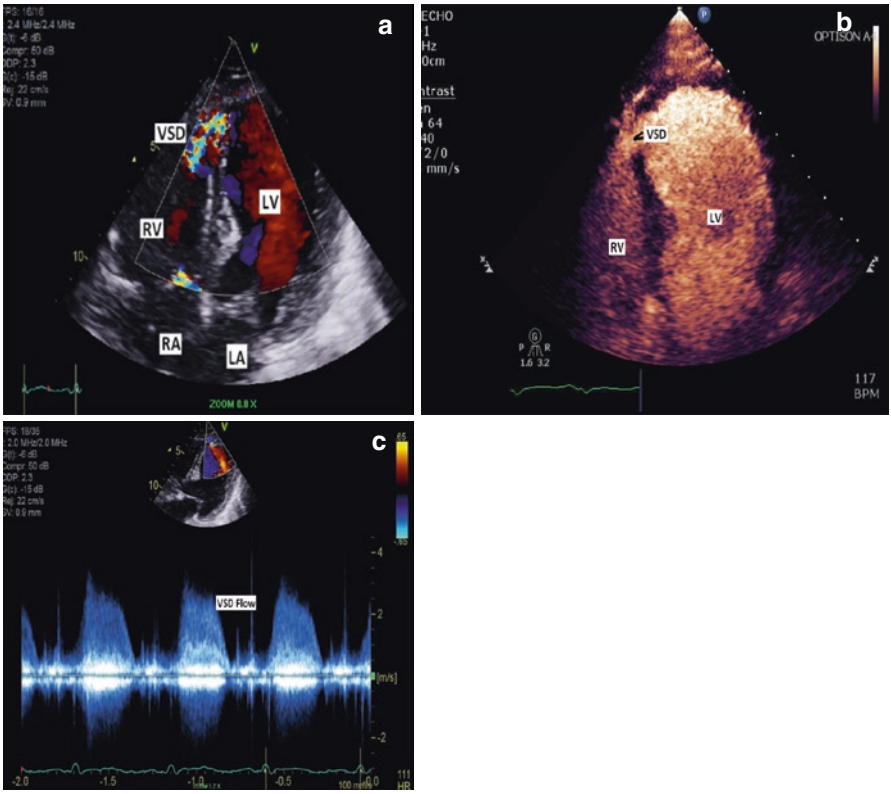

Fig. 5.6 A 71-year-old woman with past medical history of hypertension and hypothyroidism who presented with a chief complain of epigastric pain. She had cardiac arrest on arrival to emergency department. Bedside transthoracic echocardiogram revealed the following: (**a**) Apical four-chamber view: left ventricular systolic dysfunction and apical ventricular septal color flow. (**b**) Apical four-chamber view: apical ventricular septal defect with contrast. (**c**) Ventricular septal defect Doppler flow. *LV* left ventricle, *LA* left atrium, *RV* right ventricle, *RA* right atrium, *VSD* ventricular septal defect

Identifying Cardiac Rhythm

The ECG has been regarded as the gold standard in the diagnosis of asystole or ventricular fibrillation; however, studies have shown that echocardiography may be more accurate.

Confirmation that a "flat line" is truly asystole is an important step in the ACLS protocol. Fine ventricular fibrillation (VF) can be misdiagnosed as asystole on the cardiac monitor and/or electrocardiogram. The distinction between them has an important impact on patient management and prognosis. Bedside TTE can demonstrate subtle disorganized cardiac twitching consistent with ventricular fibrillation. Distinguishing VF from asystole with echocardiography is also more challenging than identifying more obvious causes of cardiopulmonary arrest such as cardiac

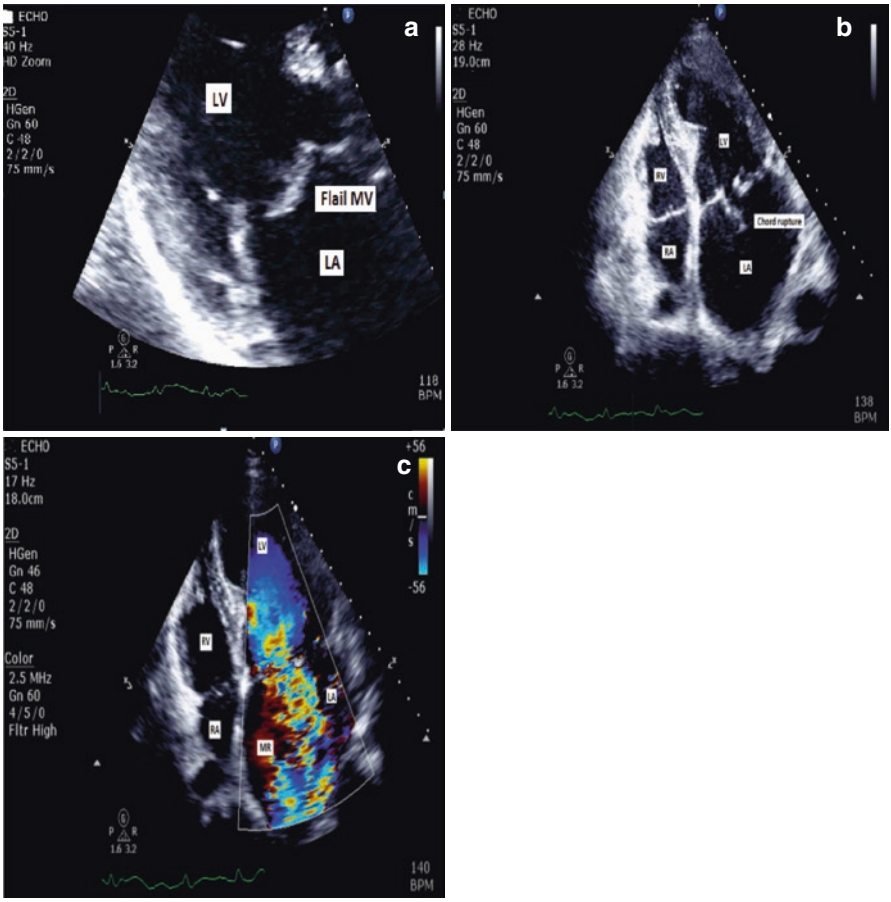

Fig. 5.7 A 58-year-old man with a history of gastritis and schizophrenia brought to emergency department after witnessing cardiac arrest. On arrival, the patient had agonal breathing but still had a pulse. Subsequently, the patient experienced cardiac arrest. Bedside transthoracic echocardiogram showed the following: (**a**) Parasternal long-axis view: flail anterior mitral leaflet. (**b**) Apical four-chamber view: flail anterior mitral leaflet and left atrium enlargement. (**c**) Apical four-chamber view: flail anterior mitral leaflet with severe mitral regurgitation. *LV* left ventricle, *LA* left atrium, *RV* right ventricle, *RA* right atrium, *MV* mitral valve, *MR* mitral regurgitation

tamponade and examiner should be familiar with the subtle cardiac movements. The sensitivity and specificity of TTE for diagnosing VF in the settings of cardiac arrest are currently unknown [15, 16].

Despite the absence of a pulse with a PEA rhythm, bedside TTE may demonstrate organized cardiac activity—this scenario is described as "pseudo-PEA." In true PEA, the patient has cardiac electrical activity without any mechanical contraction. In pseudo-PEA, the patient has cardiac electrical activity with no palpable pulses, but myocardial contractions can be seen by echocardiography. The outcomes of these patient groups are significantly different. Finding of coordinated cardiac activity confers a better outcome and should potentially be regarded as an indication to continue

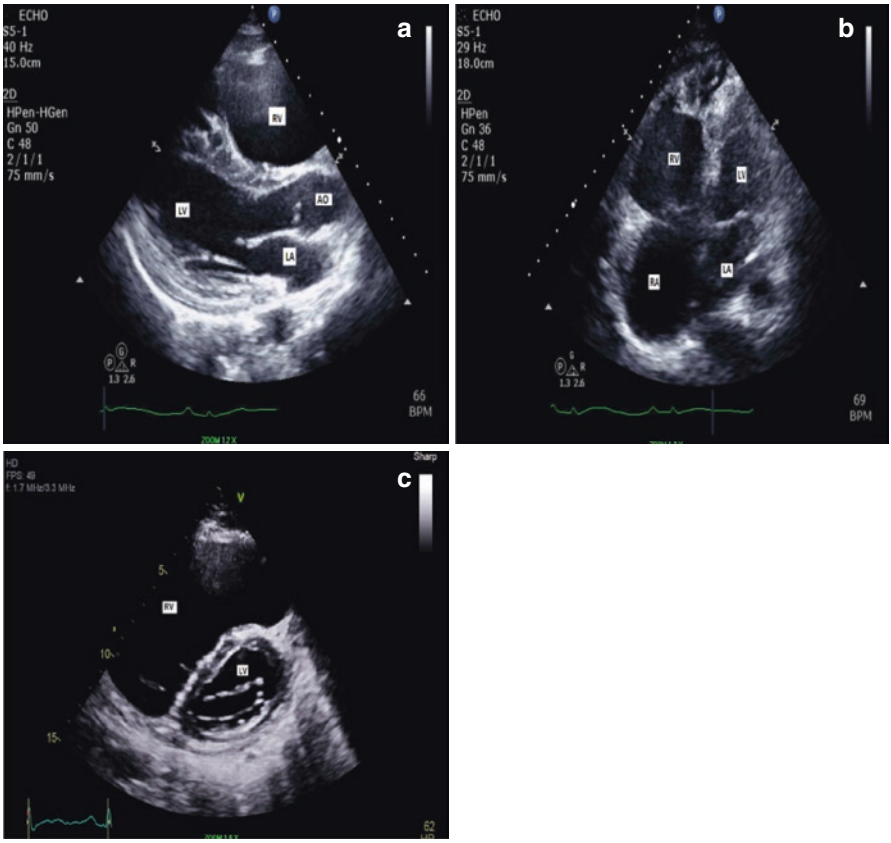

Fig. 5.8 A 35-year-old man was brought to emergency department after an out-of-hospital cardiac arrest. On arrival no pulse was detectable and telemetry was suggestive of asystole. Transthoracic echocardiography revealed the following: (**a**) Parasternal long-axis view: severe right ventricular dilation and myocardial twitching. (**b**) Apical four-chamber view: severe right ventricular and right atrial dilation. (**c**) Parasternal short-axis view: severe right ventricular dilation. *LV* left ventricle, *LA* left atrium, *RV* right ventricle, *RA* right atrium

resuscitation efforts [17–19]. Figure 5.8 illustrates the bedside echocardiography findings of a 35-year-old-man who was brought to emergency department after an out-of-hospital arrest. On arrival the pulse was undetectable and telemetry was suggestive of asystole. Transthoracic echocardiography showed myocardial twitching, and severe right ventricle dilation. The patient was successfully defibrillated.

Transesophageal Echocardiography

Transesophageal echocardiography (TEE) can be very useful in the emergency settings, when TTE is nondiagnostic. In patients with cardiac arrest TTE image acquisition is technically difficult due to ongoing CPR, gastric air, and presence of the

defibrillator pads. The quality of images is better with TEE compared to TTE in patient with recent chest surgery, chest deformity, and emphysema. TEE allows the examiner to visualize the heart, even during chest compressions, to evaluate the quality of compressions and to see subtle contractility. Patients can be electrically cardioverted with the probe in place as it is electrically isolated. In certain clinical scenarios, the combination of TTE and TEE may be necessary to confirm or reject the suspected diagnoses such as acute aortic syndrome, acute prosthetic valve dysfunction, or aortic transection due to chest trauma [20, 21].

Conclusion

The choice of imaging modality during cardiac arrest should be based on not only sensitivity and specificity of the modality but also its accessibility in the resuscitation field. Bedside echocardiography is an invaluable tool to rapidly assess cardiac structure and function, pulmonary pathology, and fluid status in the settings of cardiac arrest and the peri-resuscitation period. ALS-compliant focused echocardiography can be taught to nonexpert practitioners.

Even though the performance of peri-resuscitation echocardiography has been recommended by some researchers [3], there is no agreement on the examiners' training and the evaluation of their respective competencies. It is very likely that echocardiography will become a standard part of the evaluation of cardiac arrest patients as image quality of handheld devices improves and the number of physicians who are familiar with their use increases.

The routine incorporation of echocardiography into the ALS algorithm should be studied further in different settings (e.g., in-hospital and out-of-hospital cardiac arrest). Lightweight, handheld echocardiography machines provide a good opportunity to extend research in this field beyond the hospital setting and assess the benefit of bedside TTE in out-of-hospital resuscitation. Although some studies suggest that focused echocardiography can be performed in an ALS-compliant manner and that clinicians can potentially predict the outcome depending on the echocardiography findings, none have yet shown that the use of focused echocardiography improves outcomes.

References

1. Link MS, Berkow LC, Kudenchuk PJ, Halperin HR, Hess EP, Moitra VK, et al. Part 7: adult advanced cardiovascular life support: 2015 American Heart Association Guidelines Update for Cardiopulmonary Resuscitation and Emergency Cardiovascular Care. Circulation. 2015;132(18 Suppl 2):S444–64.
2. Zafiropoulos A, Asrress K, Redwood S, Gillon S, Walker D. Critical care echo rounds: echo in cardiac arrest. Echo Res Pract. 2014;1(2):D15–21.

3. Timerman S, Gonzalez MM, Mesquita ET, Marques FR, Ramires JA, Quilici AP, Timerman A. The International Liaison Committee on Resuscitation (ILCOR). Roll in guidelines 2005–2010 for cardiopulmonary resuscitation and emergency cardiovascular care. Arq Bras Cardiol. 2006;87(5):e201–8.
4. Long B, Alerhand S, Maliel K, Koyfman A. Echocardiography in cardiac arrest: an emergency medicine review. Am J Emerg Med. 2018;36(3):488–93.
5. Price S, Uddin S, Quinn T. Echocardiography in cardiac arrest. Curr Opin Crit Care. 2010 Jun;16(3):211–5.
6. Arntfield RT, Millington SJ. Point of care cardiac ultrasound applications in the emergency department and intensive care unit—a review. Curr Cardiol Rev. 2012;8(2):98–108.
7. Neskovic AN, Flachskampf FA, Picard MH. Emergency echocardiography. 2nd ed. Boca Raton: CRC Press; 2016.
8. Greenstein YY, Martin TJ, Rolnitzky L, Felner K, Kaufman B. Goal-directed transthoracic echocardiography during advanced cardiac life support: a pilot study using simulation to assess ability. Simul Healthc. 2015;10(4):193–9; quiz 199–201
9. Breitkreutz R, Walcher F, Seeger FH. Focused echocardiographic evaluation in resuscitation management: concept of an advanced life support-conformed algorithm. Crit Care Med. 2007;35(5 Suppl):S150–61.
10. Neskovic AN, Flachskampf FA, Picard MH, editors. Emergency echocardiography: principles and practice. Boca Raton: CRC Press; 2017.
11. Amico AF, Nardi F. Clinical cardiac imaging in cardiac arrest and periarrest. Minerva Cardioangiol. 2017;65(6):621–8.
12. Adler Y, Charron P, Imazio M, Badano L, Barón-Esquivias G, Bogaert J, Brucato A, Gueret P, Klingel K, Lionis C, Maisch B, Mayosi B, Pavie A, Ristić AD, Sabaté Tenas M, Seferovic P, Swedberg K, Tomkowski W. 2015 ESC guidelines for the diagnosis and management of pericardial diseases. Rev Esp Cardiol (Engl Ed). 2015;68(12):1126.
13. Guidelines for the appropriate use of bedside general and cardiac ultrasonography in the evaluation of critically ill patients—Part II: Cardiac ultrasonography.
14. Amaya SC, Langsam A. Ultrasound detection of ventricular fibrillation disguised as asystole. Ann Emerg Med. 1999;33(3):344–6.
15. Flato UA, Paiva EF, Carballo MT, Buehler AM, Marco R, Timerman A. Echocardiography for prognostication during the resuscitation of intensive care unit patients with non-shockable rhythm cardiac arrest. Resuscitation. 2015;92:1–6.
16. Querellou E, Meyran D, Petitjean F, Le Dreff P, Maurin O. Ventricular fibrillation diagnosed with trans-thoracic echocardiography. Resuscitation. 2009;80(10):1211–3.
17. Paradis N, Halperin H, Kern K, Wenzel V, Chamberlain D, editors. Etiology, electrophysiology, and myocardial mechanics of pulseless electrical activity. Cambridge: Cambridge University Press; 2007. p. 426–46.
18. Myerburg RJ, Halperin H, Egan DA, Boineau R, Chugh SS, Gillis AM, Goldhaber JI, Lathrop DA, Liu P, Niemann JT, Ornato JP, Sopko G, Van Eyk JE, Walcott GP, Weisfeldt ML, Wright JD, Zipes DP. Pulseless electric activity definition, causes, mechanisms, management, and research priorities for the next decade: report from a National Heart, Lung, and Blood Institute Workshop. Circulation. 2013;128(23):2532–41.
19. Hernandez C, Shuler K, Hannan H, Sonyika C, Likourezos A, Marshall J. C.A.U.S.E.: Cardiac arrest ultra-sound exam—A better approach to managing patients in primary non-arrhythmogenic cardiac arrest. Resuscitation. 2008 Feb;76(2):198–206.
20. Fair J, Mallin M, Mallemat H, Zimmerman J, Arntfield R, Kessler R, Bailitz J, Blaivas M. Transesophageal echocardiography: guidelines for point-of-care applications in cardiac arrest resuscitation. Ann Emerg Med. 2018;71(2):201–7.
21. Blaivas M. Transesophageal echocardiography during cardiopulmonary arrest in the emergency department. Resuscitation. 2008 Aug;78(2):135–40.

Chapter 6
Echocardiography in a Patient with a New Murmur

Julie Friedman and Muhamed Saric

Abstract Heart murmurs are common in cardiac care unit (CCU) patients. As many of CCU patients are intubated and unable to provide medical history, the physical exam becomes crucial in piecing together a patient's medical history. Once a new murmur is identified, echocardiography can be a helpful tool in the critical care setting to further elucidate the cardiac abnormalities of a CCU patient. Whereas many patients have murmurs representing manifestations of chronic diseases, this chapter focuses on the diagnosis and etiology of murmurs that are presumably new at the time of CCU admission and represent an acute change in clinical status.

Keywords Murmur · Aortic valve disease · Mitral valve disease

Introduction

Heart murmurs are common in cardiac care unit (CCU) patients. As many of CCU patients are intubated and unable to provide medical history, the physical exam becomes crucial in piecing together a patient's medical history. Once a new murmur is identified, echocardiography can be a helpful tool in the critical care setting to further elucidate the cardiac abnormalities of a CCU patient. Whereas many patients have murmurs representing manifestations of chronic diseases, this chapter focuses on the diagnosis and etiology of murmurs that are presumably new at the time of CCU admission and represent an acute change in clinical status.

The majority of new native valve murmurs represent nonstenotic lesions and they are related primarily to acute valvular regurgitation. On the contrary, new prosthetic valve murmurs may be either stenotic, such as in acute prosthetic valve stenosis, or

J. Friedman · M. Saric (✉)
New York University Langone Medical Center, New York, NY, USA
e-mail: julie.friedman@nyumc.org; muhamed.saric@nyumc.org

E. Herzog, E. Argulian (eds.), *Echocardiography in the CCU*,
https://doi.org/10.1007/978-3-319-90278-4_6

regurgitant, as in infective endocarditis. Other new murmurs that may present in a CCU patient include that of ventricular septal rupture and left ventricular outflow tract (LVOT) obstruction, both of which are described in this chapter as well.

Genesis and Types of Heart Murmurs

Murmurs are defined as sounds heard in addition to the sequence of two to three heart sounds during each heartbeat [1]. The two normal heart sounds in adults—the first heart sound (S_1) and the second heart sound (S_2)—are produced mainly by the closure of the atrioventricular (tricuspid and mitral) and semilunar (aortic and pulmonary) valves, respectively. Sometimes, an additional heart sound associated with the ventricles filling up with blood may be heard. It is referred to as S_3 when it occurs in early diastole and S_4 when heard in late diastole after atrial contraction. In children it can be normal to hear an S_3 but in adults it often represents pathology. When an S_3 or S_4 heart sound is heard together with the two normal heart sounds, it is referred to as a "gallop." A combination of $S_1 + S_2 + S_3$ is a ventricular ("Kentucky") gallop. In contrast, a combination of $S_4 + S_1 + S_2$ is an atrial ("Tennessee") gallop [2].

Murmurs are thought to be the result of abnormal movement of blood across valves and between cardiac chambers which result in turbulence of blood flow. The turbulence creates vibrations in the heart chambers and outflow tracts that are detected via auscultation with a stethoscope. The intensity of a murmur can vary greatly depending on the size of the orifice which blood is flowing through, the pressure gradient across the narrowing, and the volume of blood flowing across the site. Heart murmurs can be systolic, diastolic, or continuous (Table 6.1) and they can be reported with accompanying intensity grades (Table 6.2).

When clinically insignificant, murmurs are referred to as being "innocent"; they are caused by increased flow or turbulence across anatomically normal valves or other cardiovascular structures. Some systolic murmurs may be clinically innocent, while all diastolic and continuous murmurs are abnormal. Pathological murmurs occur as a result of either diseased cardiac valves or abnormal communications between cardiac chambers, blood vessels, or both. These lesions may be congenital or acquired, and have unique hemodynamic consequences.

Table 6.1 Types of heart murmurs

	Start	End
Systolic murmurs		
Midsystolic	After S1	Before S2
Pansystolic (holosystolic)	At or after S1	At S2
Late systolic	Middle or late systole	At S2
Diastolic murmurs		
Early diastolic	At S2	Before next S1
Mid-diastolic	Shortly after S2	Before next S1
Late diastolic (presystolic)	Late diastole	At next S1
Continuous murmurs	Begin in systole and continue through the cardiac cycle	

Table 6.2 Intensity and grades of heart murmurs

Grade	Murmur intensity	Comments
I	Very faint	
II	Quiet murmur	As loud as S1, S2
III	Moderately loud murmur	Louder than S1, S2
IV	Loud murmur	With thrill
V	Very loud murmur	Heard even with stethoscope barely on the chest
VI	Extremely loud	Heard even without stethoscope

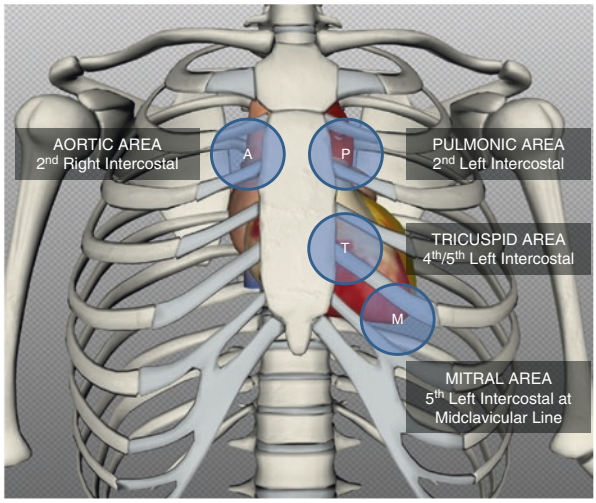

Fig. 6.1 Cardiac auscultation areas. The background thorax image with permission from BioDigital.com. *Abbreviations*: *A* aortic area, *M* mitral area, *P* pulmonic area, *T* tricuspid area

Detection of a Heart Murmur

Clinicians will often first detect murmurs via auscultation using a stethoscope. The invention of the stethoscope is often credited to René Laënnec who, in 1816, created the monaural stethoscope as a means of amplifying heart sounds without requiring physical contact. In 1851, Arthur Leared invented the binaural stethoscope and then in 1852 George Cammann, who was a practicing physician in New York City, perfected the binaural stethoscope which is most reminiscent of the modern-day auscultation device used by medical professionals today [3].

The standard stethoscope often includes both a shallow bell (for low-frequency sounds) and a thin, stiff diaphragm (for high-frequency sounds). Clinicians routinely assess at least four surface anatomical areas with the stethoscope when evaluating for murmurs as shown in Fig. 6.1. Murmurs are then further described based on their intensity (grade), pitch (frequency), configuration, timing, quality, and radiation (Table 6.3).

Table 6.3 Murmur types and conditions

Murmur type	Associated abnormality
Systolic	
Early systolic	Mitral regurgitation
	Tricuspid regurgitation
	Ventricular septal rupture
	Aortic stenosis
Midsystolic	Aortic stenosis
	Dynamic LVOT obstruction
Late systolic	Mitral valve prolapse
Holosystolic	Mitral regurgitation
	Tricuspid regurgitation
	Ventricular septal rupture
Diastolic	
Early diastolic	Aortic regurgitation
Mid-diastolic	Rheumatic mitral stenosis
Late diastolic	Rheumatic mitral stenosis
Continuous	
	Patent ductus arteriosus
	Arteriovenous fistula

Role of Echocardiography After Detection of a Heart Murmur

Once detected, murmurs are typically further characterized via echocardiography which can help evaluate the primary lesion in terms of cause and severity, define the lesion's hemodynamic significance, detect coexisting abnormalities, evaluate the size and function of cardiac chambers, and establish a reference point for future comparisons.

Modern ultrasound machines have become smaller and more portable allowing the exams to be performed at the patient's bedside. In recent years, there has also been an increasing use of handheld pocket scanners as partial replacement tools for auscultation. While these tools cannot replace the detail obtained in a formal echocardiogram, there has been an increasing reliance on these tools to confirm pathology suspected based on auscultatory findings and these have become an extension of the physical exam in the critical care setting.

New murmurs in the CCU are most often of a regurgitant variety as a result of acute infective endocarditis, acute type A aortic dissection, or sequelae of an acute myocardial infarction. Acute valve stenosis is typically seen only with prosthetic valves and can occur in the setting of acute valve thrombosis which is a devastating and life-threatening condition. Other murmurs such as that of a new dynamic LVOT obstruction or ventricular septal rupture have distinctive murmurs which are important to recognize and are discussed in this chapter.

New Murmur After an Acute Myocardial Infarction

Myocardial Infarction

Myocardial infarction (MI) is a clinical or pathologic event caused by myocardial ischemia, resulting in myocardial necrosis or injury. The American College of Cardiology and the American Heart Association endorse the Third Universal Definition of Myocardial Infarction which defines an MI as a typical rise and/or fall of cardiac troponin with at least one value above the assay's upper reference limit, accompanied by at least one other feature of ischemia (e.g., typical symptoms or ECG changes) [4]. Acute MIs—often in the form of ST-elevation MI (STEMI)—make up a high percentage of admissions to cardiac intensive care units (ICUs).

The new murmurs that arise as a consequence of an acute MI are related to mechanical complications of the infarct. The most common lesions are acute mitral regurgitation (MR), a ventricular septal rupture (VSR), and LV wall rupture. MR and VSR, but not LV rupture typically present as a new heart murmur. Papillary muscle rupture (and resulting mitral regurgitation) typically occurs 2–7 days after MI, ventricular septal defects typically occur 3–7 days after MI, and LV free wall rupture often occurs 5–14 days after MI (Table 6.4) [5].

Acute Mitral Regurgitation

Clinical Presentation

Acute MR in the setting of an acute MI (or endocarditis, which is discussed in subsequent section) often presents as a cardiac emergency with the sudden onset and rapid progression of hypotension, pulmonary edema, and signs and symptoms of cardiogenic shock. Acute MR due to MI is related to papillary muscle rupture.

The murmur of acute MR may be systolic, midsystolic, or holosystolic. It is often best heard along the left sternal border and may radiate to the back. However, since the pressure within the left atrium markedly increases during ventricular systole and the pressure gradient between the LA and LV diminishes or disappears by the end of systole, the systolic murmur is often soft, low pitched, and decrescendo. An important point to keep in mind while in the ICU is that the approximately 50% of

Table 6.4 Myocardial infarction related murmurs

Complication type	Complication onset days after MI
Papillary muscle rupture	2–7 days
Ventricular septal rupture	3–7 days
Free wall rupture	5–14 days

patients with moderate-to-severe acute MR will have no audible murmur and therefore the intensity of the murmur does not necessarily correlate with the severity of the valve lesion [6]. The presumed mechanism is thought to be secondary to a relatively low systolic pressure gradient between the left ventricle and left atrium due to the combination of low systemic blood pressure and elevated left atrial pressure. An S_3 can commonly be heard but may be difficult to appreciate as these patients are often quite tachycardic.

Pathophysiology and Anatomic Considerations

The mitral valve apparatus consists of the mitral annulus, anterior and posterior leaflets, chordae tendineae, papillary muscles, and underlying ventricular wall (Fig. 6.2). Mitral regurgitation can occur as a complication of acute myocardial infarction by several mechanisms: (1) papillary muscle or chordal rupture, (2) papillary muscle displacement, and (3) LV dilatation/aneurysm.

Papillary muscle rupture is the primary mechanism of acute MR related to MI. The other two mechanisms (papillary muscle displacement and LV dilatation) typically lead to subacute or chronic MR murmur. Partial or complete rupture of a papillary muscle can have catastrophic effects. Additionally, there is a wide range of infarction size that can be associated with papillary muscle rupture. Many patients may have very limited overall left ventricular dysfunction from their MI and, in the setting of acute severe mitral regurgitation, may actually have a hyperdynamic LV which can further limit identification of wall motion abnormalities. It is for these reasons that echocardiography can be quite helpful in diagnosing this potentially life-threatening condition.

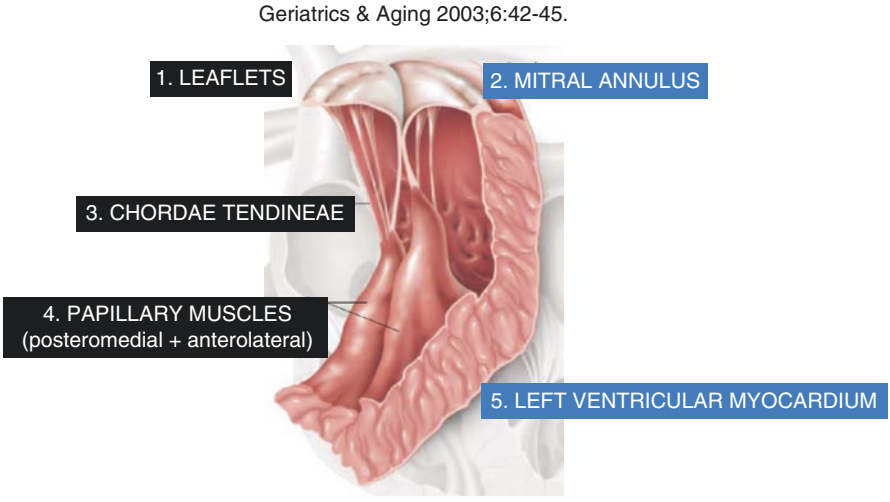

Fig. 6.2 Mitral valve apparatus. Based on the image of the mitral valve apparatus with permission from *Geriatrics & Aging* journal

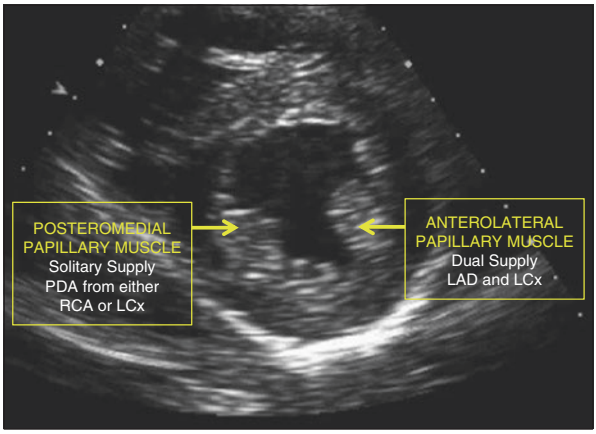

Fig. 6.3 Papillary muscle blood supply. Short-axis TTE view at the level of papillary muscle; note the solitary blood supply of the posteromedial papillary muscle vs. dual blood supply of the anterolateral papillary muscle. *Abbreviations*: *LAD* left anterior descending artery, *LCx* left circumflex artery, *PDA* posterior descending artery, *RCA* right coronary artery

The posteromedial (PM) papillary muscle has solitary blood supply from the posterior descending artery whereas the anterolateral (AL) papillary muscle has a dual blood supply from the left anterior descending and left circumflex arteries (Fig. 6.3) [7]. It is for this reason that rupture of the PM papillary muscle occurs at a much higher frequency than that of the AL papillary muscle. It is rare that acute rupture of a papillary muscle involves the entire body of the papillary muscle; more commonly, only one of the subheads of the muscle is involved resulting in a partial leaflet flail. It is important to note, however, that chordae to both leaflets arise from each papillary muscle such that, in cases of complete rupture, both leaflets are often affected.

Echo Findings

The jet of acute MR from papillary muscle rupture is most often eccentric and directed opposite to that of the partial flail leaflet (Figs. 6.4 and 6.5). Given the eccentric nature, the severity of the regurgitant jet may often be underestimated. Associated findings include a small inferior wall motion abnormality, a mass (the ruptured papillary muscle) attached to flail segments of the leaflets often seen in the LA in systole and in the LV in diastole. Given the acuity of the regurgitant lesion, the LA is often nondilated. For this reason, the detection of an eccentric mitral regurgitation jet with a relatively normal-sized left atrium should raise suspicion for acute mitral regurgitation and, in the proper clinical context of myocardial ischemia or infarction, is concerning for papillary muscle rupture.

As discussed in the auscultatory findings, the murmur of acute MR is either soft or absent because of rapid pressure equilibration between LV and LA in systole. Echocardiographically, this is visualized on spectral Doppler tracings as a low-velocity triangular systolic flow velocity pattern (Fig. 6.6). This is often accompanied by a prominent, rapidly decelerating early diastolic (E) wave, which corresponds to auscultatory S_3 sound.

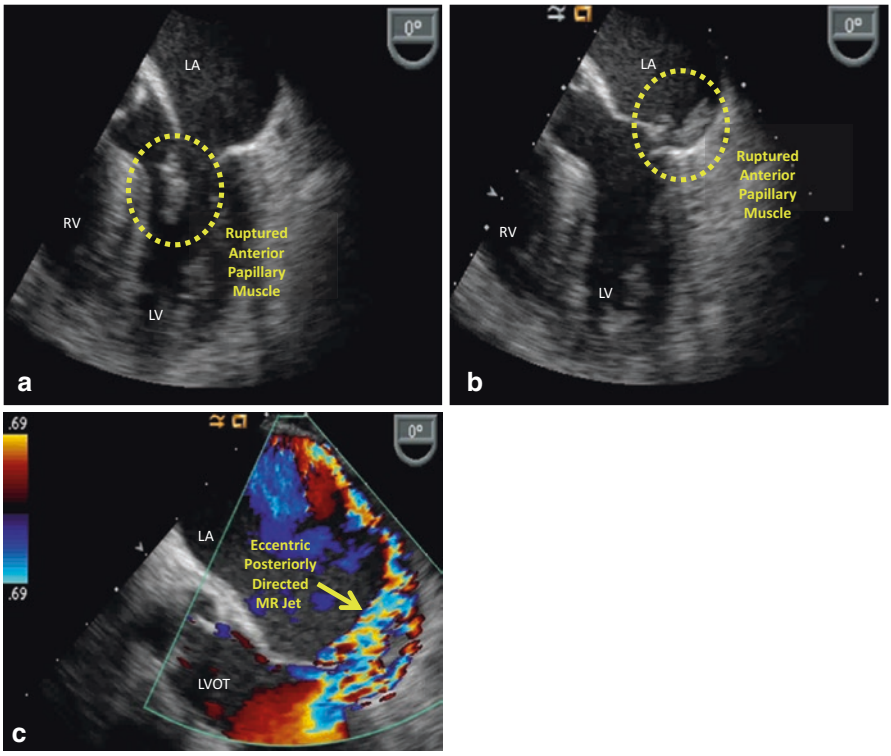

Fig. 6.4 Ruptured anterior papillary muscle on TEE. Panel (**a**): Ruptured anterior papillary muscle in the left ventricle during diastole. Panel (**b**): Ruptured anterior papillary muscle in the left atrium during systole. Panel (**c**): Color Doppler imaging showing very severe eccentric, posteriorly directed, mitral regurgitation. In this condition, a murmur of severe acute mitral regurgitation may be heard. *Abbreviations*: *LA* left atrium, *LV* left ventricle, *LVOT* left ventricular outflow tract, *MR* mitral regurgitation, *RV* right ventricle

Ventricular Septal Rupture

Clinical Presentation

The classic presentation of someone with ventricular septal rupture (VSR) is that of acute onset of hemodynamic compromise with hypotension, biventricular failure (right greater than left), and a new harsh murmur soon after an MI. It is yet another rare, but lethal complication of acute myocardial infarction and is often seen 3–5 days after acute MI. VSR is an utmost emergency and thus the prompt diagnosis is crucial for prompt surgical or percutaneous VSR closure.

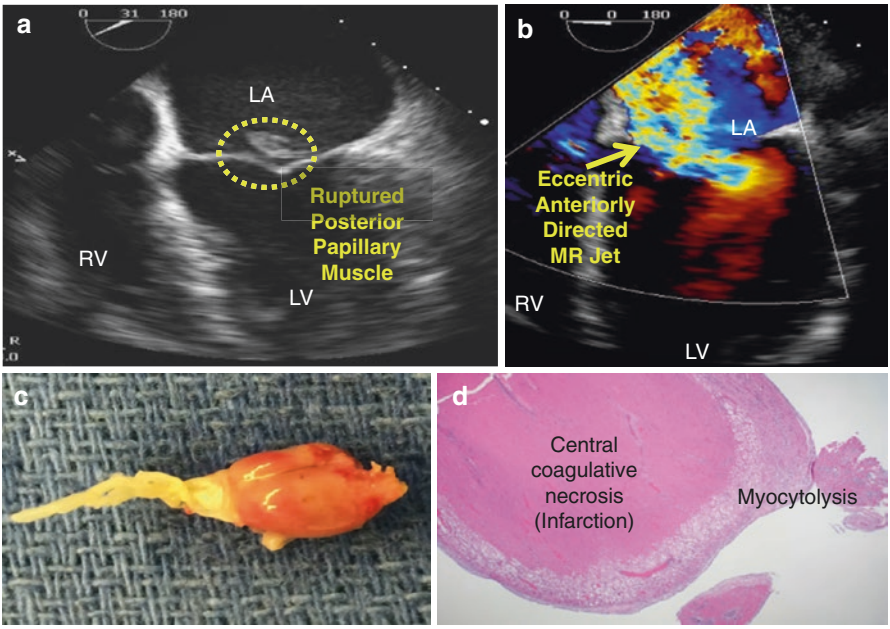

Fig. 6.5 Ruptured posterior papillary muscle. Panel (**a**): Ruptured posterior papillary muscle in the left atrium during systole on TEE. Panel (**b**): Color Doppler imaging showing eccentric, anteriorly directed, mitral regurgitation jet on TEE. Panel (**c**): Gross surgical specimen of a ruptured papillary muscle. Panel (**d**): Histology of a necrotic, ruptured papillary muscle. In this condition, a murmur of severe acute mitral regurgitation may be heard. *Abbreviations*: *LA* left atrium, *LV* left ventricle, *MR* mitral regurgitation, *RV* right ventricle

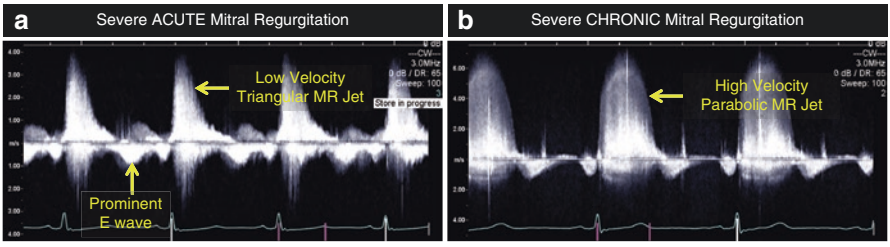

Fig. 6.6 Acute vs. chronic MR on spectral Doppler. Panel (**a**): Continuous-wave Doppler across the mitral valve in severe acute mitral regurgitation. Note that the low-velocity, rapidly dissipating LV to LA systolic gradient may result in a soft or even absent mitral regurgitation murmur. Panel (**b**): Continuous-wave Doppler across the mitral valve in severe chronic mitral regurgitation. *Abbreviations*: *E wave* early diastolic flow, *MR* mitral regurgitation

Murmur of Acute VSR

The murmur of VSR is very loud, harsh in character, holosystolic, and often heard throughout the precordium. Up to 50% of patients with acute VSR have a detectable thrill.

Pathophysiology

VSR develops after transmural infarction of the ventricular septum and can occur at any anatomic location along the septum. It can result from an MI of any of the coronary arteries as the septal blood supply comes from branches of the left anterior descending artery, the posterior descending branch of the right coronary artery, or the left circumflex artery when it is dominant (Fig. 6.7) [7]. However, septal rupture tends to occur most frequently with anterior MIs. The newly formed communication between the right and left ventricles results in left-to-right shunting of blood from the high-pressure LV to the lower pressure right ventricle (RV) [8].

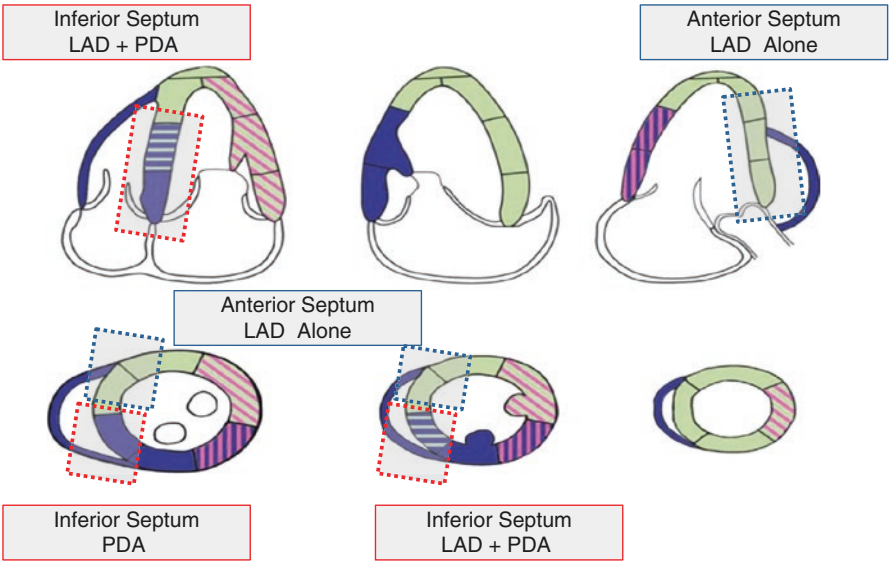

Fig. 6.7 Coronary territories of septum. Note the difference in the blood supply between the anterior and the inferior interventricular septum. The image with permission from the Journal of American Society of Echocardiography. *Abbreviations*: *LAD* left anterior descending artery, *PDA* posterior descending artery

Echo Findings

The key to identifying a VSR by echocardiography is noting a high-velocity, left-to-right systolic jet on continuous-wave Doppler and systolic turbulence on the RV side of the septum on color Doppler imaging. As this can be challenging to identify, it is often necessary to use nonconventional imaging planes, scanning up and down the septum with color Doppler imaging, to identify the pathologic left-to-right flow. Once the site of rupture is identified with color flow, color can then be turned off and anatomic imaging undertaken to help identify the site of dropout of the ventricular septum with 2D imaging. These defects may often be serpiginous through the myocardium and can range in size from millimeters to several centimeters making it challenging to visualize the chamber connection on echo (Fig. 6.8).

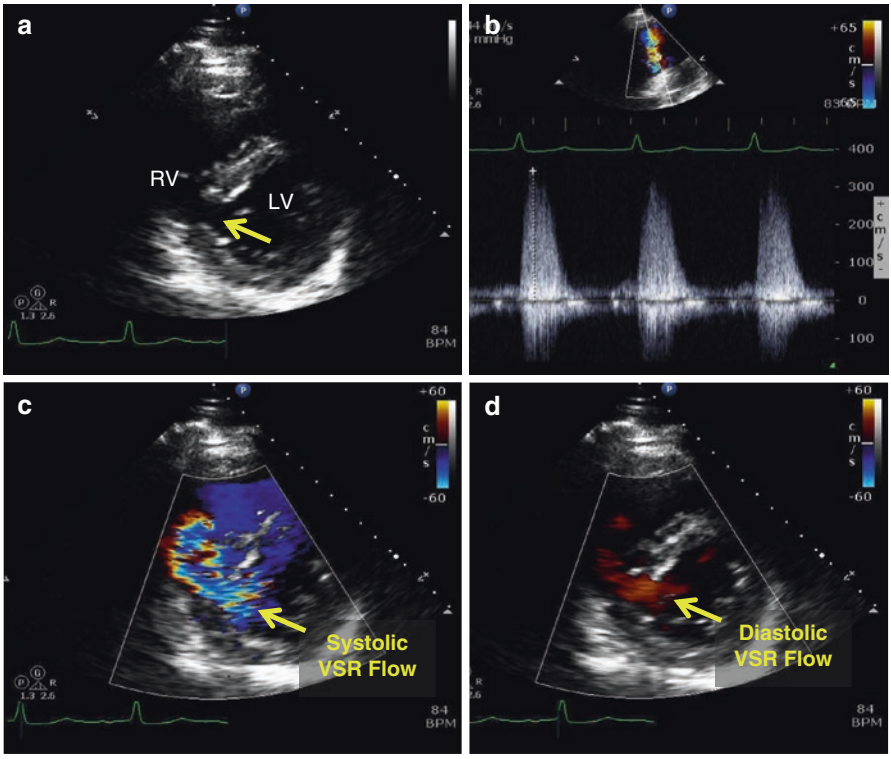

Fig. 6.8 Ventricular septal rupture (VSR) on echo. Panel (**a**): Parasternal short-axis TTE view of VSR identifying dropout of the ventricular septum. Panel (**b**): Spectral Doppler confirms high-velocity systolic flow across VSR. Panel (**c**): Color Doppler imaging showing high-velocity systolic flow across VSR. Panel (**d**): Color Doppler imaging showing low-velocity diastolic flow across VSR. In this condition, a harsh holosystolic murmur is typically heard. *Abbreviations*: *LV* left ventricle, *RV* right ventricle, *VSR* ventricular septal rupture

New Murmur in a Febrile Patient

Infective Endocarditis

Clinical Presentation

Infective endocarditis is an infection of the endocardial surface of the heart, most commonly referring to an infection of one or more of the heart valves or of an intracardiac device (pacing wires, catheters, conduits, etc.). It is an uncommon infectious disease with an annual incidence ranging from 3 to 7 per 100,000 person-years in the most contemporary population [9]. The presentation can vary from a subacute or chronic disease with nonspecific symptoms to an acute, rapidly progressive infection with hemodynamic consequences resulting from valvular dysfunction. Cardiac complications occur in up to half of patients and can result in these patients requiring ICU-level care for heart failure from valvular dysfunction or conduction abnormalities from paravalvular abscesses.

Murmur in Infective Endocarditis

The presence of a new regurgitant murmur in a febrile patient should raise suspicion for infective endocarditis. Left-sided valvular lesions are more common than right-sided ones. Thus, one may expect to hear the murmur of aortic or mitral regurgitation. Right-sided lesions are typically associated with intravenous drug users (tricuspid valve involvement and less commonly pulmonic valve) but can also be found in those with right-sided indwelling catheters (such as hemodialysis catheters) or intracardiac devices (pacemakers, defibrillators). It is important to keep in mind that even though most right-sided lesions are found in the setting of intravenous (IV) drug use, it is still much more common for an IV drug user to present with left-sided rather than right-sided valvular disease.

Echocardiographic Features of Vegetations

One of the major Duke criteria for infective endocarditis is the echocardiographic finding of evidence of endocardial involvement [10]. To that end, the findings of abscess, new partial dehiscence of prosthetic valve, or visualization of a vegetation support a diagnosis of infective endocarditis in the ICU in the setting of a new regurgitant murmur.

A vegetation is typically an irregularly shaped, echogenic, highly mobile mass that may be attached to any area of the valve leaflet, although lesions at the coaptation line are most common (Fig. 6.9). Since the vegetation is a discrete structure, it may often only be seen in certain tomographic planes and thus slow scanning between the standard image planes is crucial to help increase the probability of identifying a valvular vegetation. Most vegetations are highly mobile and tend to

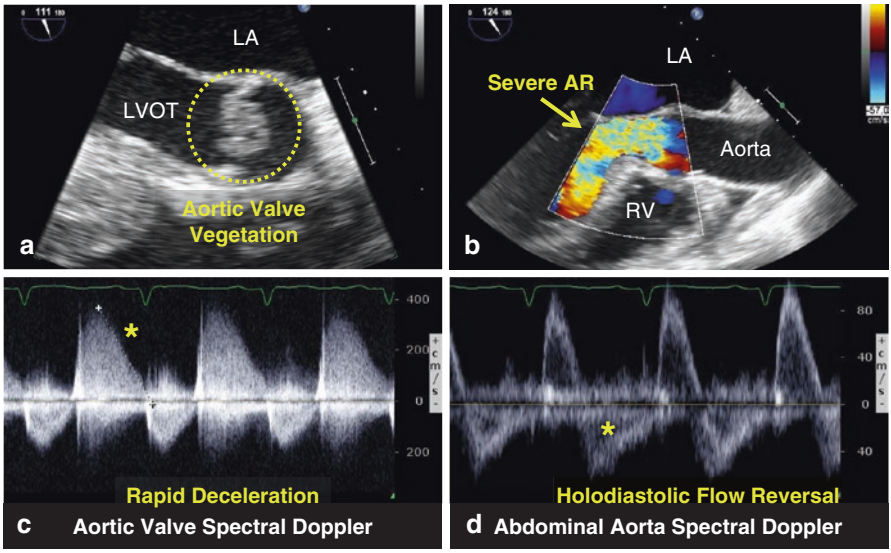

Fig. 6.9 Aortic valve endocarditis on TEE. Panel (**a**): Large aortic valve vegetation. Panel (**b**): Color Doppler imaging showing turbulent flow of severe aortic regurgitation. Panel (**c**): Spectral Doppler tracing showing rapid deceleration of flow in severe acute aortic regurgitation. Panel (**d**): Spectral Doppler tracing showing holodiastolic flow reversal in the abdominal aorta, consistent with severe aortic regurgitation. In this condition, a murmur of severe acute aortic regurgitation may be heard. *Abbreviations*: *AR* aortic regurgitation, *LA* left atrium, *LV* left ventricle, *LVOT* left ventricular outflow tract, *RV* right ventricle

have motion that is independent of the movement of the valve itself. The movement is often described as fluttering, oscillating, or chaotic. Vegetations tend to form on the upstream side of a valve so they will be seen on the atrial side of the mitral or tricuspid valve and on the ventricular size of the aortic or pulmonic valve [11]. These vegetations can be associated with acute regurgitant valvular lesions. Acute aortic regurgitation, similar to acute MR as described previously, will be associated with a rapidly decelerating aortic valve spectral Doppler tracing due to the rapid pressure equalization between the LV and the aorta in systole. Classic echocardiographic findings in severe aortic regurgitation include a holodiastolic flow reversal seen on spectral Doppler tracings of the distal thoracic aorta and proximal abdominal aorta and a wide vena contracta.

There are no single pathognomonic findings on the echocardiogram that will definitively define an identified mass as a vegetation. Vegetations begin as a microscopic focus of infection and gradually develop over time into a well-formed mass. Therefore, at early stages they may be too small to be reliably seen. It is classically felt that a vegetation needs to be at least 3–6 mm in size in order to be reliably seen with standard imaging techniques on transthoracic echocardiography.

There are other echogenic abnormalities that can be seen and mistaken for vegetation and it is important to identify these entities to improve the specificity of echocardiography. Findings that may be mistaken for a vegetation include papillary

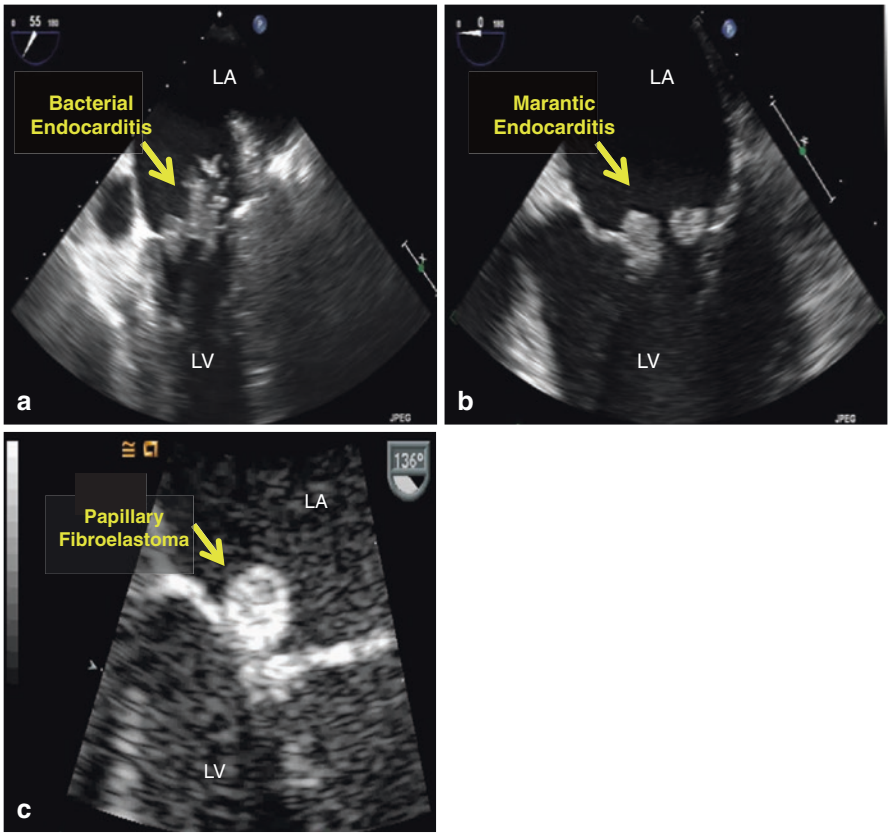

Fig. 6.10 Vegetation masqueraders on TEE involving the mitral valve. Panel (**a**): Bacterial endocarditis. Note the shaggy appearance of the vegetation on the atrial side of the mitral valve. Panel (**b**): Marantic (nonbacterial, thrombotic) endocarditis. Note the so-called kissing lesions on either leaflet of the mitral valve. Panel (**c**): Papillary fibroelastoma. Note the well-circumscribed rounded appearance of the papillary fibroelastoma attached to the atrial surface of the mitral valve. In this condition, a murmur of severe acute mitral regurgitation may be heard. *Abbreviations*: *LA* left atrium, *LV* left ventricle

fibroelastoma, myxomatous mitral valve disease, nonbacterial thrombotic endocarditis (marantic endocarditis), thrombus (especially with prosthetic valves), beam-width artifact, and Lambl's excrescence (Fig. 6.10).

New Murmur in Patient with Shock

Many of the patients who are critically ill in the ICU with a presentation of shock may have no murmur on physical exam. Others may have murmur from non-cardiogenic causes such as the flow murmur often appreciated in septic shock. The etiologies of murmurs with cardiogenic shock include the already discussed

murmur of acute mitral regurgitation (due to acute MI or mitral valve endocarditis) and the murmur of acute aortic regurgitation (due to aortic valve endocarditis). Additional etiologies of shock-associated murmurs include left ventricular outflow tract (LVOT) obstruction and type A aortic dissection.

Stress Cardiomyopathy with LVOT Obstruction

Clinical Presentation

LVOT obstruction can be either a preexisting condition (such as in a patient with hypertrophic obstructive cardiomyopathy) or newly developed such as in a patient presenting with a stress cardiomyopathy (also referred to as Takotsubo cardiomyopathy or apical ballooning syndrome). Stress cardiomyopathy is a clinical syndrome characterized by transient focal LV dysfunction in the absence of obstructive coronary artery disease and is often on the differential of acute MI. The true incidence of this phenomenon is likely on the range of 1–2% of those presenting with troponin-positive acute coronary syndrome, but ICU studies have found that up to 28% of those patients admitted with a noncardiac diagnosis were found with stress cardiomyopathy [12].

A subset of this population will develop a dynamic LVOT obstruction felt to be induced by basal hyperkinesis in the setting of apical hypokinesis. One of the early signs of this may be the appreciation of a systolic murmur and the presence of the LVOT obstruction can contribute to the development of shock in an ICU patient. Echocardiographic findings can help support this diagnosis which can have major implications in medical management.

Murmur of LVOT Obstruction

The murmur of LVOT obstruction is typically a high-pitched, crescendo-decrescendo, midsystolic murmur that is best appreciated at the left lower sternal border. It can often be mistaken for the murmur of aortic stenosis (AS) given similar qualities; however, unlike the murmur of AS, this murmur does not radiate to the carotid arteries. Maneuvers that alter afterload and preload can also help differentiate the murmur of LVOT obstruction from others such as AS. The LVOT murmur will increase with Valsalva maneuver (decrease in preload) and will decrease with handgrip (increase in afterload).

Echocardiographic Features of LVOT Obstruction

In the transthoracic parasternal long-axis or apical three-chamber view, one will often see the classic finding of systolic anterior motion of the mitral valve (SAM) with apposition of the mitral leaflet and septum in mid to late systole (mitral-septal

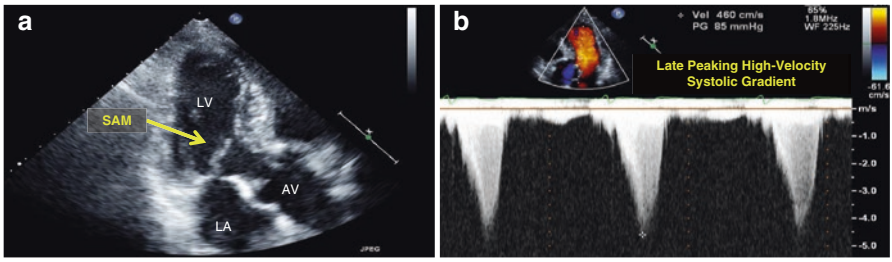

Fig. 6.11 LVOT obstruction and SAM on TTE. Panel (**a**): Systolic anterior motion of the mitral valve with mitral-septal contact. Panel (**b**): Late-peaking, high-velocity systolic gradient consistent with LVOT obstruction. In this condition, the characteristic late-peaking systolic murmur is heard. *Abbreviations*: *AV* aortic valve, *LA* left atrium, *LV* left ventricle, *SAM* systolic anterior motion of the mitral valve

contact). Given its greater temporal resolution, M-mode recordings may be helpful to better identify the mitral-septal contact. M-mode can also be helpful in identifying mid-systolic abrupt partial closure of the aortic valve with coarse fluttering of the aortic valve leaflets in late systole that results from this late systolic dynamic outflow obstruction. The degree of SAM may not be uniform from medial to lateral across the mitral leaflets, so it is important to image in multiple planes with slight adjustments in transducer angulation to demonstrate the presence and extent of dynamic outflow obstruction.

While 2D and M-mode imaging can provide clues to the presence of an outflow obstruction, Doppler studies can be used to identify the site of obstruction and the severity of obstruction. Using pulsed-wave Doppler from the apical approach, the sample volume is moved slowly from the apex up to the base while recording the velocity at each step. At the site of obstruction, the velocity increases abruptly and this velocity reflects the degree of obstruction. Continuous-wave Doppler will reveal a late-peaking high-velocity systolic jet (Fig. 6.11).

Type A Aortic Dissection

Clinical Presentation

Aortic dissection is a rare, yet life-threatening condition for which the early and proper diagnosis is crucial for survival. The classic presentation of acute aortic dissection is with severe chest pain and acute hemodynamic compromise. Progressive hemodynamic decline and death in patients with type A dissection can result from several mechanisms: (1) rupture of the dissection into the pericardium resulting in cardiac tamponade, (2) dissection into the aortic valve leading to severe aortic regurgitation, and (3) obstruction of the coronary artery ostia leading to acute myocardial infarction [13].

Pathophysiology

The primary event is an intimal tear in the aortic wall, followed by degeneration of the aortic media (cystic and medial necrosis) and ultimately the passage of blood into the media via the tear further separating the intima from the surrounding media and/or adventitia, thus creating a false channel. This channel can remain localized or can propagate downstream.

Murmur of Type A Aortic Regurgitation

Aortic regurgitation is very frequently present in cases of type A aortic dissection as patients have either chronic AR due to aortic dilation over time or more acute AR due to retrograde extension of the dissection resulting in inadequate leaflet support. The murmur of acute AR is often low pitched and early diastolic whereas the murmur of chronic AR tends to be high pitched and holodiastolic. Given the increased blood volume crossing the aortic valve, a soft systolic murmur may be heard as well. This combination of a soft systolic and a low-pitched diastolic aortic murmur is often referred to as a "to-and-fro" murmur of acute AR. Additionally, similar to the murmur of acute MR, the murmur of acute AR may be faint or absent as a result of an equalization of the pressures between the aorta and the LV.

Echocardiographic Features of Type A Aortic Dissection

Echocardiography, transesophageal more so than transthoracic, can be used to identify the dissection flap, which is a mobile flap separating the true and false lumens of the aorta in the setting of a dissection (Fig. 6.12). The dissection flap typically

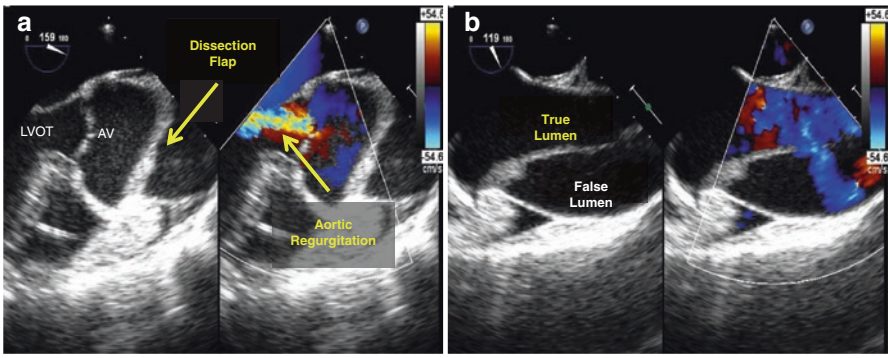

Fig. 6.12 Type A aortic dissection on TEE. Panel (**a**): Dissection flap with color Doppler imaging of aortic regurgitation jet. Panel (**b**): True and false lumens of aorta in setting of aortic dissection and color Doppler imaging showing flow from true to false lumen. In this condition, a murmur of severe acute aortic regurgitation may be heard. *Abbreviations*: *AV* aortic valve, *LVOT* left ventricular outflow tract

moves towards the false lumen in systole due to systolic expansion of the true lumen. The flap's motion is often independent of the aorta itself and should be visualized in more than one view to confirm its presence and to prevent mistaking beam-width artifacts and reverberations for dissection. In addition to helping determine the location of the true and false lumens, echocardiography can be useful to identify complications of type A aortic dissection such as acute AR, pericardial effusion (and resultant tamponade physiology), and LV dysfunction (in the case of coronary ostia dissection).

New Murmur in Patient with Known Prosthetic Valve

Valve Thrombosis

Whereas the majority of new murmurs in the CCU are regurgitant murmurs as described above, there is one important exception to this rule which is the stenotic murmur of prosthetic valve thrombosis.

Clinical Presentation

Valve thrombosis is more likely to occur with mechanical than bioprosthetic valves. Critical valve thrombosis, while rare, can be devastating, and is most often the result of inadequate anticoagulation. What is more commonly seen is prosthetic valve degeneration, pannus formation, and less critical thrombosis. Prosthetic valve thrombosis should be on the differential of a patient with a prosthetic valve who presents with a change in the quality of the mechanical valve closing clicks, new heart failure symptoms, a new stenotic murmur, or a stroke or other thromboembolic event.

Murmur of Prosthetic Valve Stenosis

The murmur of prosthetic valve stenosis is similar to the murmur of native valve stenosis. In addition, there may be absence of mechanical leaflet clicks.

Echocardiographic Features of Prosthetic Valve Stenosis

In general, the echocardiographic features used to identify native valve stenosis can be applied to the evaluation for prosthetic valve stenosis. Since prosthetic valves are inherently narrower than the native valves at baseline, the maximum velocity tends to be somewhat higher across a prosthetic valve than a healthy native valve. The

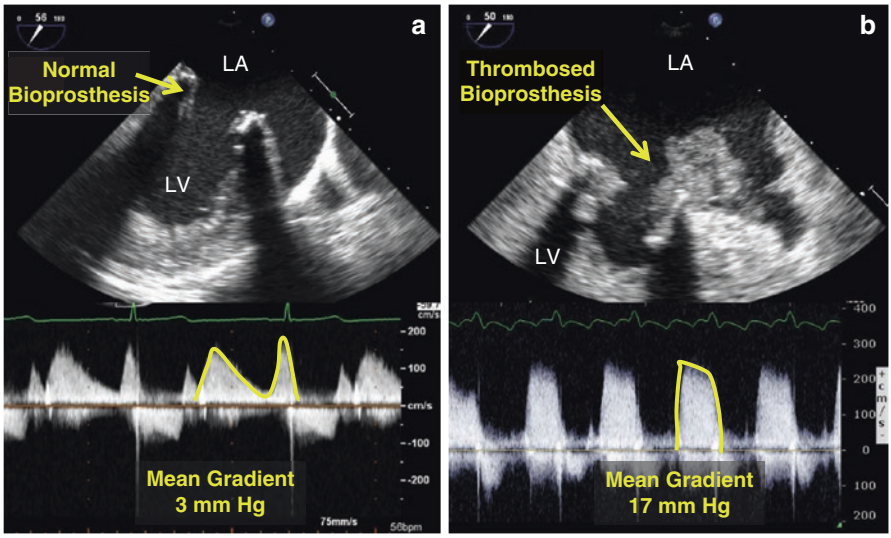

Fig. 6.13 Mitral prosthetic valve thrombosis on TEE. Panel (**a**): Normal mitral valve prosthetic function with corresponding low LA-LV gradient during diastole. Panel (**b**): Prosthetic mitral valve thrombosis with corresponding high LA-LV gradient during diastole consistent with marked prosthetic stenosis. In this condition, a murmur of severe mitral stenosis may be heard. *Abbreviations*: *LA* left atrium, *LV* left ventricle, *mmHg* millimeters of mercury

function of the prosthetic valve is assessed via determination of the peak velocity, peak and mean gradient, effective orifice area (EOA), Doppler velocity index (DVI), as well as contour of the jet velocity (Fig. 6.13) [14]. In general, prosthetic valve obstruction should be suspected when there is a significant increase in mean transvalvular gradient when compared with baseline (after exclusion of other causes such as a high output state).

References

1. Lessard E, Glick M, Ahmed S, Saric M. The patient with a heart murmur: evaluation, assessment and dental considerations. J Am Dent Assoc. 2005;136:347–56; quiz 80–1
2. Bickley LS, Szilagyi PG, Bates B. Bates' guide to physical examination and history-taking. 11th ed. Philadelphia: Wolters Kluwer Health/Lippincott Williams & Wilkins; 2013.
3. David L, Dumitrascu DL. The bicentennial of the stethoscope: a reappraisal. Clujul Med. 2017;90:361–3.
4. Thygesen K, Alpert JS, Jaffe AS, et al. Third universal definition of myocardial infarction. J Am Coll Cardiol. 2012;60:1581–98.
5. Lavie CJ, Gersh BJ. Mechanical and electrical complications of acute myocardial infarction. Mayo Clin Proc. 1990;65:709–30.
6. Bursi F, Enriquez-Sarano M, Nkomo VT, et al. Heart failure and death after myocardial infarction in the community: the emerging role of mitral regurgitation. Circulation. 2005;111:295–301.

7. Lang RM, Badano LP, Mor-Avi V, et al. Recommendations for cardiac chamber quantification by echocardiography in adults: an update from the American Society of Echocardiography and the European Association of Cardiovascular Imaging. Eur Heart J Cardiovasc Imaging. 2015;16:233–70.
8. Birnbaum Y, Fishbein MC, Blanche C, Siegel RJ. Ventricular septal rupture after acute myocardial infarction. N Engl J Med. 2002;347:1426–32.
9. Baddour LM, Wilson WR, Bayer AS, et al. Infective endocarditis in adults: diagnosis, antimicrobial therapy, and management of complications: a scientific statement for healthcare professionals from the American Heart Association. Circulation. 2015;132:1435–86.
10. Mylonakis E, Calderwood SB. Infective endocarditis in adults. N Engl J Med. 2001;345:1318–30.
11. Nishimura RA, Otto CM, Bonow RO, et al. AHA/ACC guideline for the management of patients with valvular heart disease: a report of the American College of Cardiology/American Heart Association Task Force on Practice Guidelines. J Am Coll Cardiol. 2014;63:e57–185.
12. Park JH, Kang SJ, Song JK, et al. Left ventricular apical ballooning due to severe physical stress in patients admitted to the medical ICU. Chest. 2005;128:296–302.
13. Goldstein SA, Evangelista A, Abbara S, et al. Multimodality imaging of diseases of the thoracic aorta in adults: from the American Society of Echocardiography and the European Association of Cardiovascular Imaging: endorsed by the Society of Cardiovascular Computed Tomography and Society for Cardiovascular Magnetic Resonance. J Am Soc Echocardiogr. 2015;28:119–82.
14. Zoghbi WA, Chambers JB, Dumesnil JG, et al. Recommendations for evaluation of prosthetic valves with echocardiography and doppler ultrasound: a report From the American Society of Echocardiography's Guidelines and Standards Committee and the Task Force on Prosthetic Valves, developed in conjunction with the American College of Cardiology Cardiovascular Imaging Committee, Cardiac Imaging Committee of the American Heart Association, the European Association of Echocardiography, a registered branch of the European Society of Cardiology, the Japanese Society of Echocardiography and the Canadian Society of Echocardiography, endorsed by the American College of Cardiology Foundation, American Heart Association, European Association of Echocardiography, a registered branch of the European Society of Cardiology, the Japanese Society of Echocardiography, and Canadian Society of Echocardiography. J Am Soc Echocardiogr. 2009;22:975–1014; quiz 82–4

Chapter 7
Echocardiography in Acute Neurologic Syndrome

Gregory Katz and Muhamed Saric

Abstract Stroke is the third leading cause of mortality in the high-income countries. While acute neurologic syndromes can be divided into stroke and non-stroke causes, stroke from a cardiac source is the focus of this review. The chapter outlines cardiovascular conditions with high and moderate thromboembolic risk including the descriptions of key anatomic features and echocardiographic findings.

Keywords Stroke · Atrial fibrillation · Thrombus

Introduction

Stroke is the third leading cause of mortality in the high-income countries, and an estimated 6.9 million Americans over the age of 20 have had strokes. There are approximately 800,000 strokes annually, which accounts for over $35 billion in direct and indirect costs. While acute neurologic syndromes can be divided into stroke and non-stroke causes, stroke from a cardiac source will be the focus of this review.

Stroke Subtypes

Strokes can be divided into two distinct subtypes, ischemic and hemorrhagic. Approximately 87% of strokes are ischemic, and some hemorrhagic strokes result from conversion of an ischemic stroke [1]. Ischemic strokes can be further subdivided into five different subtypes based on the Trial of Org 10,172 in Acute Stroke Treatment (TOAST) criteria. Strokes from pathologies of the heart and aorta fall into two groups: (1) established cardioembolic strokes and (2) cryptogenic strokes, some of which are cardioembolic (Fig. 7.1).

G. Katz · M. Saric (✉)
New York University Langone Medical Center, New York, NY, USA
e-mail: muhamed.saric@nyumc.org

E. Herzog, E. Argulian (eds.), *Echocardiography in the CCU*,
https://doi.org/10.1007/978-3-319-90278-4_7

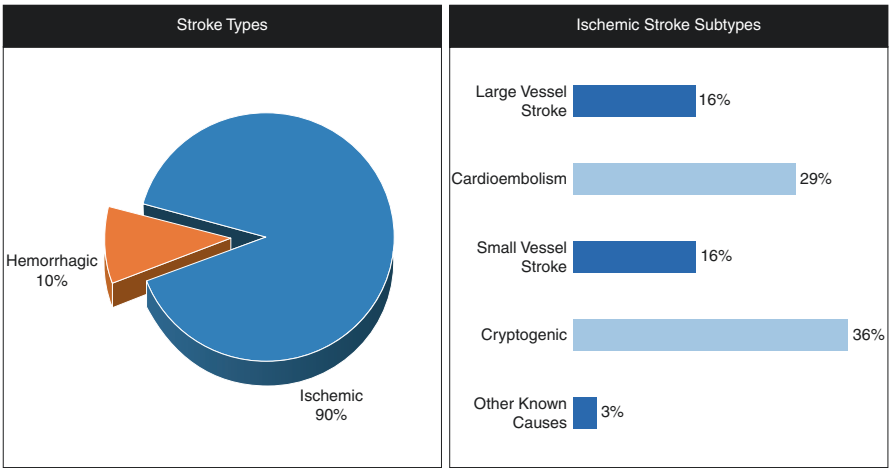

Fig. 7.1 Prevalence of hemorrhagic and ischemic strokes. (*Left panel*) Breakdown of stroke types and relative prevalence. (*Right panel*) Different subtypes of ischemic stroke. Strokes with cardiac involvement include cardioembolism and some cryptogenic strokes

Table 7.1 Factors suggesting stroke of cardioembolic etiology

Factors suggesting stroke of cardioembolic etiology
Abrupt onset of symptoms with lack of preceding TIA
Striking severity of stroke (NIHSS > 10, age > 70)
Previous infarctions in various arterial distributions
• Multiplicity in space (infarct in both anterior and posterior circulation)
• Multiplicity in time (infarct of different age)
Other signs of systemic thromboembolism
Territorial distribution of infarcts involving cortex or subcortical large lenticulostriate area
Hyperdense MCA sign (without severe ipsilateral internal carotid stenosis)
Rapid recanalization of occluded major brain artery (evaluated with repeat neurovascular ultrasound)

Echocardiography is used for identifying cardiac sources of embolism and abnormalities of the aorta that can present with focal neurologic findings, which can be suspected based on several clinical characteristics (Table 7.1). Features suggesting a stroke that is potentially cardioembolic include abrupt onset of symptoms, severe neurologic symptoms at the onset (severity of stroke with NIH Stroke Scale > 10), infarction in multiple cerebrovascular beds, concomitant infarctions in non-cerebrovascular territories, territorial distribution of the infarcts involving cortex or subcortical large lenticulostriate area, hyperdense middle cerebral artery sign, and rapid recanalization of occluded major brain artery (Fig. 7.2) [2].

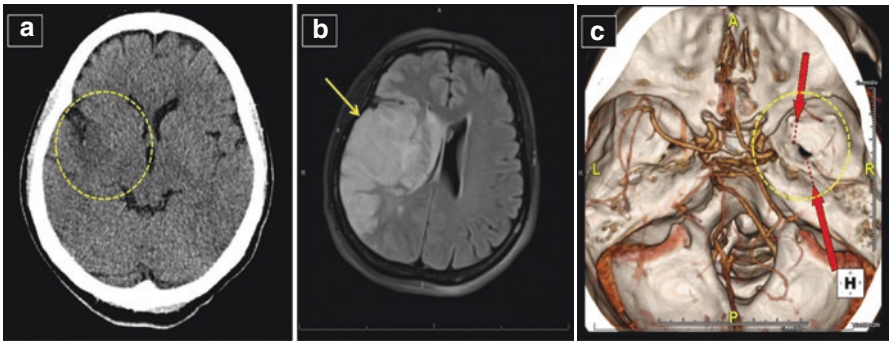

Fig. 7.2 Ischemic stroke on radiologic imaging. (**a**) Dense MCA sign found on noncontrast head CT scan. (**b**) Brain MRI demonstrating right MCA stroke. (**c**) Cerebral angiographic reconstruction demonstrating 100% occlusion of the right MCA. *MCA* Middle cerebral artery, *CT* Computed tomography, *MRI* Magnetic resonance imaging

Embolism from a cardiac source accounts for 15–40% of ischemic strokes, and diagnosis relies on identifying a potential etiology in the absence of identifiable cerebrovascular occlusive disease [3]. In patients with acute neurologic syndromes, the primary role of echocardiography is to identify the existence of a cardiac source of embolism, evaluate the likelihood that the source is a potential cause of the syndrome, and guide treatment strategies.

Cardioembolic Stroke

Not all cardiac sources have an equal embolic potential. Thrombi, vegetations, tumor fragments, and atherosclerotic debris have the highest embolic potential. These and less likely cardiac sources based on their embolic potential are listed in (Table 7.2). Acute aortic dissection with or without extension into the carotid arteries is also an important cause of acute neurologic syndromes, and its identification with echocardiography will also be discussed in this chapter. Dedicated guidelines of the European Society of Cardiology (ESC) [4] and the American Society of Echocardiography (ASE) [5] provide in-depth recommendations on proper use of echocardiography in identifying a cardiac source of embolism.

High Embolic Risk Cardiovascular Conditions

These include the tetrad of thrombi, vegetations, tumors, and aortic atheroma.

Table 7.2 Cardiac sources of stroke classified by embolic potential

High embolic potential	Moderate embolic potential
Intracardiac thrombi • Atrial arrhythmias—atrial fibrillation, atrial flutter • Ischemic heart disease—recent MI, chronic ischemic cardiomyopathy with LV thrombus • Nonischemic cardiomyopathy with LV thrombus • Prosthetic valves and devices	*Septal defects and anomalies* • Patent foramen ovale • Atrial septal aneurysm • Atrial septal defect
Intracardiac vegetations • Native valve endocarditis • Prosthetic valve endocarditis • Nonvalvular endocarditis	*Precursors of intracardiac thrombi* • Spontaneous echo contrast (smoke) • Left ventricular aneurysm without apparent thrombus • Mitral valve prolapse
Intracardiac tumors • Myxoma • Papillary fibroelastoma • Other tumors	*Intracardiac calcifications* • Mitral annular calcification • Calcific aortic stenosis
Aortic pathology • Aortic atheroma • Aortic dissection	*Valvular abnormalities* • Fibrin strands • Lambl's Excrescence

Thrombi

The risk of acute neurologic syndrome from atrial arrhythmias is primarily dictated by its risk of development of a thrombus in the left atrium, or more precisely, in the left atrial appendage (LAA); these thrombi are the most common source of cardiogenic embolism [6]. Regional or focal left ventricular myocardial wall motion abnormalities in the setting of an acute myocardial infarction or severe left ventricular dysfunction also provide a nidus for left ventricular thrombus formation due to development of blood stasis.

Atrial Arrhythmias

The link between atrial fibrillation and ischemic stroke is complex but important. Atrial fibrillation is the most common cardiac dysrhythmia, and the annual risk of stroke in atrial fibrillation ranges from 1% in low-risk patients to 15% in the highest-risk group. The majority of all cardioembolic events in atrial fibrillation are linked to thrombi in the left atrial appendage (LAA). The percentage of thrombi in the LAA vs. thrombi in the body of the left atrium (LA) is dependent on the type of atrial fibrillation. In nonvalvular atrial fibrillation, about 90% of all thrombi are located in the LAA. In contrast, in patient with valvular atrial fibrillation (primarily defined as atrial fibrillation in patients with rheumatic mitral valve disease), only 2/3 of all thrombi are in the LAA, the remainder being in the body of the LA.

LAA and LA thrombus formation is primarily a result of increased stasis, since the other aspects of Virchow's triad, endothelial injury and hypercoagulability, are not as clinically relevant in these patients. When left atrial appendage emptying velocity is brisk, thrombus formation is generally prevented; when atrial dysfunction occurs, generally from atrial fibrillation, left atrial enlargement, or mitral valve disease, the emptying velocity is diminished and the LAA becomes a potential nidus for thrombus development. Transesophageal echocardiography is the gold standard test for identifying LAA thrombi.

Key Anatomic Features

The left atrial appendage can occur in four distinct morphologic shapes: cactus, chicken wing, windsock, and cauliflower. The size of the left atrium should also be quantitatively evaluated in patients with suspected cardioembolic stroke.

Echocardiography Findings

The presence of spontaneous echo contrast (SEC) or smoke in the LAA is a sign of erythrocyte rouleaux formation indicative of blood stasis. SEC can progress to sludge (very dense smoke) and to true thrombus (Fig. 7.3). Thrombus is most frequently visualized in the LAA but can also be found in the true LA cavity. The presence of SEC, sludge, and thrombus have all been linked to increased risk of systemic embolism. LAA emptying velocity should be evaluated with pulsed wave Doppler on TEE, with the highest risk of embolism seen with values less than 20 cm/s.

Alternative Imaging

In patients who are unable to tolerate or have a contraindication to TEE, cardiac computed tomography scan can be used to evaluate for presence of thrombus in the LA and LAA with reasonably high accuracy.

Myocardial Infarction and Heart Failure

The incidence of left ventricular thrombus following myocardial infarction varies from 7% to 20% among different studies, with the highest prevalence in patients with anterior or apical infarction and those with reduced ejection fractions [7, 8]. Patient with left ventricular aneurysm may have incidence of thrombus as high as 50%. Current reperfusion therapies have reduced the prevalence of left ventricular thrombus following myocardial infarction. Chronic

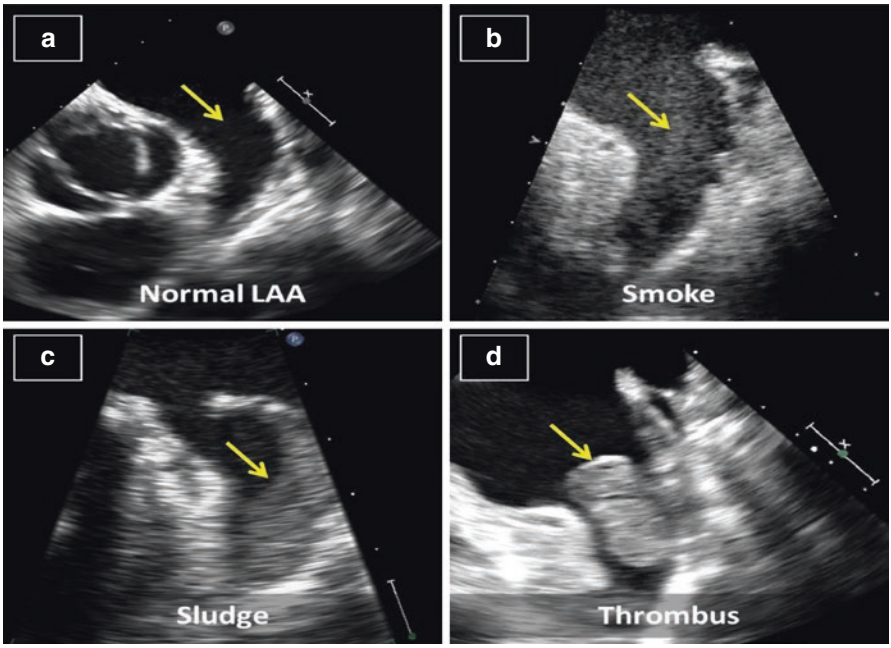

Fig. 7.3 Left atrial appendage pathology. (**a**) LAA without presence of clot. (**b**) Smoke in the LAA. (**c**) LAA demonstrating presence of sludge. (**d**) Thrombus in the LAA. *LAA* Left atrial appendage

cardiomyopathies are also associated with increased risk of left ventricular thrombus, with risk increasing with ventricular enlargement, decrease in cardiac output with resultant stasis, and apical variant of hypertrophic cardiomyopathy with apical outpouching.

Key Anatomic Features

Thrombi in the left ventricle come in three distant morphologic appearances

1. Flat mural thrombus—flat and parallel to the endocardium with only one surface exposed to blood
2. Protruding thrombus—multiple surfaces exposed to blood
3. Mobile thrombus—independent motion of all or part of thrombus

Although mobile or protruding thrombi are the most likely to embolize, embolic events can also occur in patients with flat mural thrombi.

Echocardiography Findings

Left ventricular thrombus is defined as a discrete echo-dense mass in the left ventricle with distinct margins from the endocardium and that is seen during both systole and diastole. It should be located by an area of the LV wall where the myocardium is hypokinetic or akinetic. Echocardiography must visualize a thrombus in two orthogonal views to adequately exclude artifacts and make an accurate diagnosis.

The use of echocardiographic microbubble contrast agents has greatly improved the ability of echocardiography to adequately identify a left ventricular thrombus (Fig. 7.4a,b). A low threshold to utilize echo contrast helps to reduce the likelihood of a technically difficult study leading to inadequate diagnosis. Moving the echocardiographic focal zone to the apex and reducing the aliasing velocity may help to better define any thrombi in the left ventricle.

Transesophageal echocardiography is of little marginal utility in identifying an LV thrombus due to poor views of the apex and its distance away from the transducer in the esophagus.

Alternative Imaging

Cardiac magnetic resonance imaging has a higher sensitivity and specificity than echocardiography to identify a left ventricular thrombus, although the ease of use may limit its applicability in the acute setting (Fig. 7.4c).

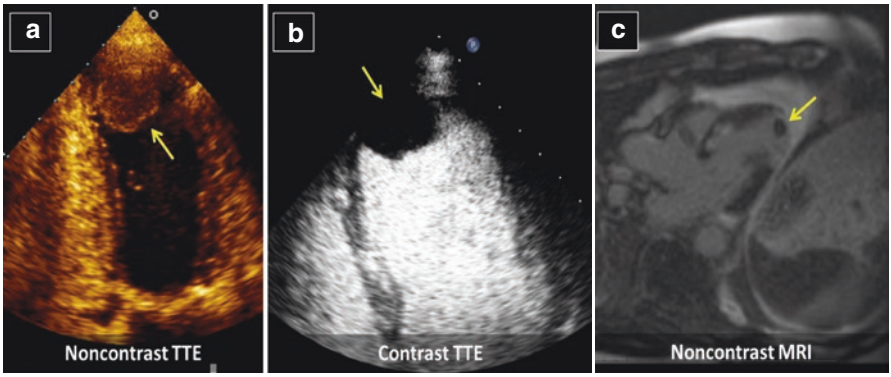

Fig. 7.4 Left ventricular thrombus. (**a**) TTE demonstrating thrombus in the LV apex. (**b**) Echocardiography contrast can enhance ability to detect thrombus on TTE. (**c**) MRI demonstrating presence of apical LV thrombus. *TTE* Transthoracic echocardiogram, *LV* Left ventricle, *MRI* Magnetic resonance imaging

Vegetations

Endocarditis

Both infective and noninfective endocarditis can be a cause of acute neurologic events. In most cases, positive blood cultures and echocardiographic evidence are able to make the diagnosis of infective endocarditis (IE). Systemic embolism is a very common consequence of IE, and stroke may be the first clinical manifestation in some instances. The majority of cases of systemic embolism occur before the initiation of antimicrobial therapy. While TTE imaging is highly specific for making a diagnosis of endocarditis, it lacks sensitivity, particularly in the setting of prosthetic valves, and is also less effective in evaluating leaflet or cusp perforation. In these cases, TEE should be considered the first-line test. Noninfective endocarditis—also known as marantic endocarditis—leads to the formation of fibrin- and platelet-rich valvular vegetations that have a high risk of systemic embolization. Marantic endocarditis occurs in the setting of severe systemic disease or hypercoagulable state (such as antiphospholipid syndrome).

Key Anatomic and Hemodynamic Features

Acute severe valvular regurgitation can occur in IE due to leaflet perforation, and IE should be considered as a potential cause of acute valvular insufficiency. Clues that can help to distinguish acute aortic insufficiency include normal left ventricular size, narrow pulse pressure, and hypotension, which occur in the setting of acutely elevated LVEDP impairing forward flow and stroke volume. Early closure of the mitral valve and poor coaptation of the aortic valve leaflets can also be seen in acute aortic regurgitation. Acute mitral regurgitation can be suspected based on normal left atrial and left ventricular size, markedly elevated left atrial pressure, and clinical features of pulmonary edema or large left atrial V waves on pressure monitoring.

Echocardiography Findings

Valvular vegetations, intracardiac abscess, prosthetic valve dehiscence, and the presence of new valvular insufficiency can all be used to make the diagnosis of IE.

Vegetations typically appear as a mass with echogenic properties that are different than the underlying tissue, adherent to a valve leaflet, and independently mobile from the valve (Fig. 7.5a). While most commonly found on valves, vegetations can also be less frequently seen on the mural endocardium or the papillary muscles. Healed vegetations generally appear more echogenic and calcified compared to acute vegetations. Infective endocarditis vegetations are more commonly on the

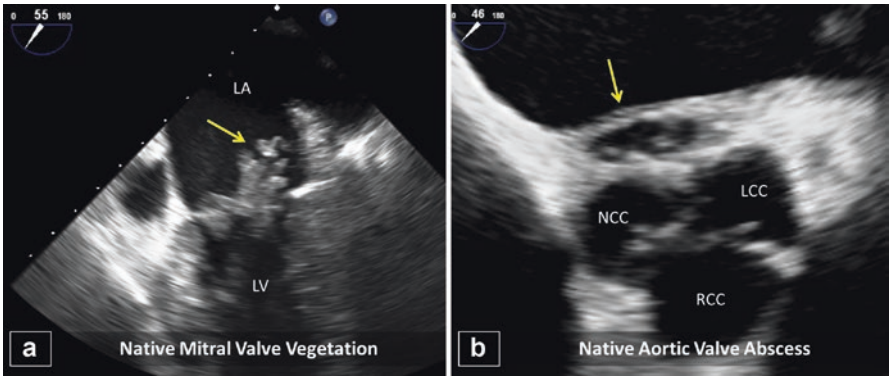

Fig. 7.5 Endocarditis. (**a**) Vegetation visualized on atrial side of the mitral valve on TEE. (**b**) Abscess formation adjacent to the aortic valve. *TEE* Transesophageal echocardiogram, *LA* Left atrium, *LV* Left ventricle, *NCC* Noncoronary cusp, *RCC* Right coronary cusp, *LCC* Left coronary cusp

atrial side of the atrioventricular valves and the ventricular side of the semilunar valves.

Abscesses are echolucent or echogenic heterogeneous spaces that are generally adjacent to valvular structures. While they are mainly paravalvular, they can affect any myocardial region. They are most commonly identified on the aortic valve and can result in fistula and pseudoaneurysm formation (Fig. 7.5b).

Mechanical mitral valve prosthesis adds additional diagnostic complexity and is better visualized with TEE than with TTE due to shadowing from the prosthesis. In the right clinical context, paravalvular regurgitation should be suspected as the echocardiographic manifestation of IE.

Differential Diagnosis

Differential diagnosis of endocarditis includes a number of entities that can be confused for vegetations, so a thorough understanding of the patient's clinical scenario is vital for accurate interpretation. On native valves, mitral annular calcification with mobile components, redundant chordae, Lambl's excrescences, and papillary fibroelastoma can be mistaken for vegetations. Findings on prosthetic valves that can be mistaken for a vegetation of IE include prosthetic valve strands, mitral subvalvular tissue remnants, and microcavitations (Fig. 7.6).

Alternative Imaging

Echocardiography is the imaging modality of choice for the diagnosis of endocarditis. There is no role for either CT or CMR in adding diagnostic utility to echocardiography.

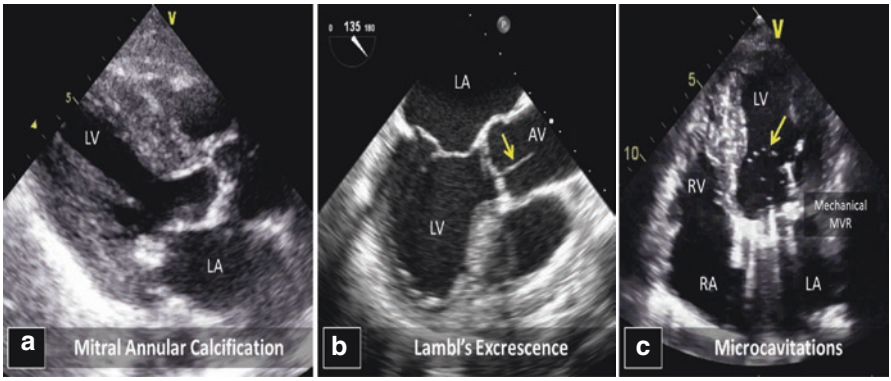

Fig. 7.6 Ancillary pathologies. (**a**) Severe mitral annular calcification can be mistaken for vegetation from endocarditis. (**b**) Large Lambl's excrescence visualized on the aortic valve. (**c**) Microcavitations from mechanical mitral valve prosthesis can mimic vegetation. *LA* Left atrium, *LV* Left ventricle, *AV* Aortic valve, *RV* Right ventricle, *RA* Right atrium, *MVR* Mitral valve replacement

Prosthetic Valves

Prosthetic valves represent a major source of embolism leading to acute neurologic syndrome, and the presence of a prosthetic valve or intracardiac device in the setting of an acute embolic event should raise suspicion for device contribution.

Prosthetic valve thrombosis more commonly occurs in the tricuspid and mitral positions than aortic, and annual incidence is as high as 1%. Thrombosis and embolism can occur in the absence of obstructive symptoms such as dyspnea or heart failure and generally happen in the setting of subtherapeutic anticoagulation.

Key Anatomic and Hemodynamic Features

Prosthetic heart valve thrombosis or vegetation can be associated with symptoms of flow obstruction, including a new murmur, dyspnea, heart failure, and cardiogenic shock. Right-sided prosthetic valve thrombosis can only lead to acute neurologic syndrome in the presence of an intracardiac or intrapulmonary shunt.

Echocardiography Findings

Both TTE and TEE should be performed in patients with suspected prosthetic valve thrombosis. In cases of severe obstruction, TTE will reveal abnormal transvalvular color flow jet, elevated transprosthetic valve gradients, and reduced effective orifice area. TEE is generally the test of choice to visualize restricted leaflet motion,

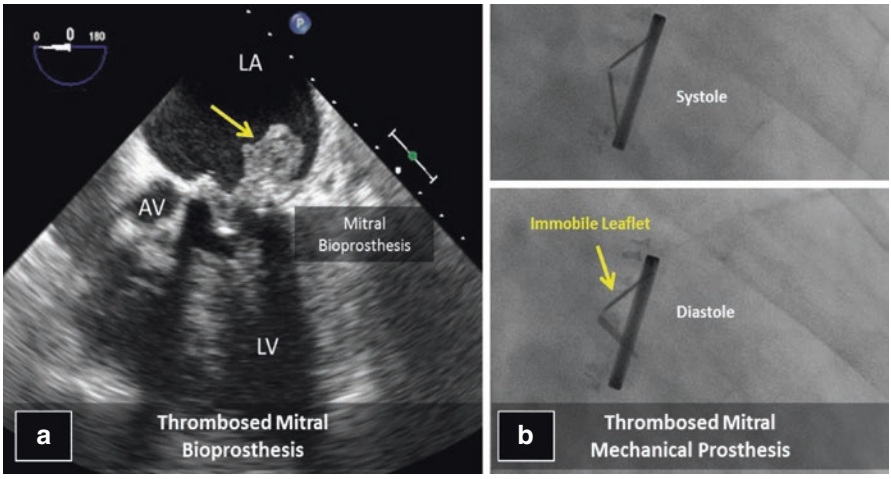

Fig. 7.7 Prosthetic valves. (**a**) Thrombosis on mitral valve bioprosthesis visualized on TEE. (**b**) Mechanical valve thrombosis on cinefluoroscopy demonstrating impaired leaflet mobility during diastole leading to impaired flow (*bottom image*). Normal systolic leaflet closure is maintained (*upper image*). *LA* Left atrium, *AV* Aortic valve, *LV* Left ventricle, *TEE* Transesophageal echocardiogram

abnormal central regurgitation, loss of physiologic regurgitant jets, and direct visualization of thrombus (Fig. 7.7a). Diagnosis of partial valve thrombosis is challenging even with TEE and high clinical suspicion must be present.

Differential Diagnosis

Differential diagnosis of prosthetic valve thrombosis includes prosthetic valve vegetation or fibrin strand. The hemodynamic consequences of valve thrombosis can also be seen in prosthetic valve stenosis and patient-prosthesis mismatch. Pannus formation, the development of fibrous tissue growth around a prosthetic valve, can also cause elevated prosthetic valve gradients, but is not associated with systemic thromboembolism or acute neurologic syndromes.

Alternative Imaging

Cinefluoroscopy is often used to evaluate for mechanical prosthetic valve thrombosis. Its role is very limited in identifying prosthetic vegetation or intracardiac device thrombus or vegetation per se (Fig. 7.7b). Gated cardiac CT can also be useful to demonstrate reduced leaflet motion.

Intracardiac Tumors

Primary cardiac tumors are rare diagnoses, and most are benign in nature with the majority of complications arising from their embolic potential. Myxoma and papillary fibroelastoma (PFE) are the two most common intracardiac tumors as well as the intracardiac tumors with the highest embolic potential; as a result they frequently present with complications from an embolic event. Embolic events due to tumors can either be due to a piece of the tumor itself or due to embolism of an associated thrombus. The most common malignant cardiac tumor is metastatic disease, which is 20-fold more common than primary benign cardiac tumors, although less frequently associated with embolic disease. Primary malignant cardiac tumors tend to occur on the right side of the heart and more commonly present with pulmonary rather than systemic embolism. The most common metastatic malignant tumors of the heart are from melanoma and tumors of the lung, breast, colon, and stomach.

Key Anatomic and Hemodynamic Features

Cardiac myxomas are the most common benign cardiac tumor, more common in women, and seen most frequently in the left atrium. Less commonly, patients can have multiple myxomas, and approximately 7% of myxomas are associated with Carney complex, an autosomal dominant disorder with cardiac and skin myxomas as well as adrenocortical disease leading to Cushing syndrome. Myxomas can be large at times, leading to obstruction of the mitral valve and mimicking the clinical symptoms and Doppler signs of mitral stenosis.

PFEs are the second most common cardiac tumor and predominantly located on the cardiac valves, most frequently aortic and then mitral. PFEs are derived from endocardium and are avascular. They rarely cause valvular dysfunction and tend to be located on the aortic side of the aortic valve and ventricular side of the mitral valve, which is the opposite of what is commonly seen with infective endocarditis. Although frequently asymptomatic, the most common presenting symptoms from PFEs are stroke, TIA, and myocardial infarction from tumor embolization.

Echocardiography Findings

Cardiac myxomas usually have a stalk attached near the fossa ovalis; they can also be seen in the left ventricle, right atrium, and, less commonly, right ventricle. Myxomas often appear pedunculated with a surface that is smooth or friable and can have necrotic areas with focal calcifications. Frequently, myxomas are partly vascularized which will lead to partial opacification on echo contrast imaging. Partial

opacification can differentiate myxomas from thrombi and malignant tumors, which are not opacified and completely opacified, respectively (Fig. 7.8).

PFEs are often mobile with a clear border and can appear homogenously textured. They are typically described as resembling a sea anemone with multiple papillary fronds attached to the endocardium by a short pedicle (Fig. 7.9). While PFEs can grow larger than 20 mm in size, they are more commonly 8–9 mm in length. TTE and TEE have sensitivities for detection of approximately 62% and 77%, respectively.

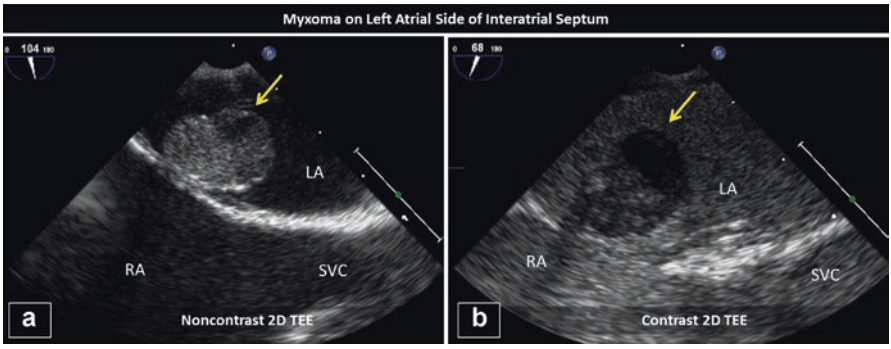

Fig. 7.8 Myxoma. (**a**) Left atrial myxoma adherence to the interatrial septum visualized on TTE. (**b**) Echocardiographic contrast demonstrating partial opacification of left atrial myxoma. *TEE* Transesophageal echocardiogram, *LA* Left atrium, *RA* Right atrium, *SVC* Superior vena cava

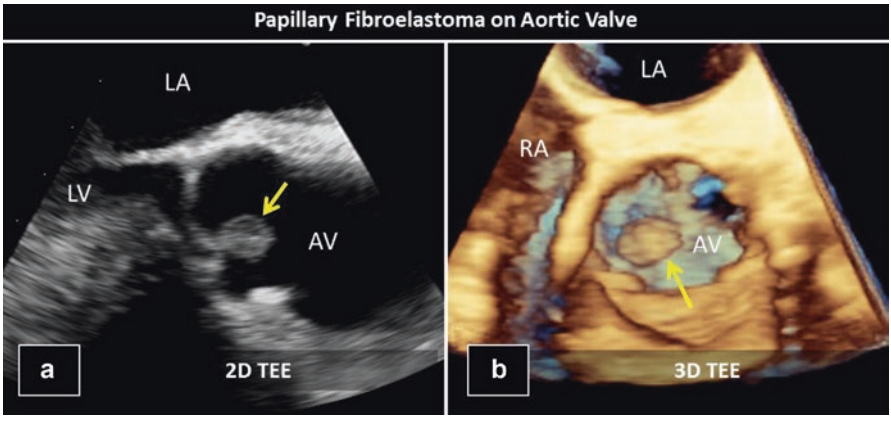

Fig. 7.9 PFE. (**a**) Papillary fibroelastoma on the aortic side of the aortic valve on two dimensional imaging. (**b**) PFE visualized on 3-D TEE. *LA* Left atrium, *LV* Left ventricle, *AV* Aortic valve, *TEE* Transesophageal echocardiogram

Differential Diagnosis

As previously discussed, the most common intracardiac masses are myxomas and PFEs. Differential diagnosis for intracardiac masses includes primary and secondary and for valvular lesions also includes vegetations, valvular strands, and Lambl's excrescences.

Alternative Imaging

To define tissue characteristics of intracardiac tumors, cardiac magnetic resonance imaging provides improved discrimination and tissue resolution. Myxomas, metastatic disease, and primary cardiac tumors are often better visualized with MRI. Since PFEs are commonly on valves, their mobility is better visualized on TTE and TEE than alternative imaging.

Aortic Pathologies

Imaging of the aorta is a vital part of evaluating neurologic symptoms due to suspected cardioembolism. Atherosclerotic plaque of the aorta is the most common etiology of aortic embolism and can occur due to either thromboemboli (aortic thromboembolism syndrome or ATS) or cholesterol emboli (cholesterol emboli syndrome or CES). ATS is due to embolism from a thrombus overlying an atherosclerotic plaque leading to acute ischemia or a target organ, whereas CES is due to embolism of multiple small cholesterol crystals that lead to a shower of emboli that can cause symptoms due to smaller vessel occlusion and end organ damage caused by either occlusion or inflammatory response.

Neurologic symptoms are frequently seen in patients with aortic dissection and may occur in the absence of chest or back pain. As many as 29% of patients with acute aortic dissection develop neurologic symptoms, and a third of this group does not experience pain. Neurologic sequelae of aortic dissection include ischemic stroke, spinal cord ischemia, ischemic neuropathy, hypoxic encephalopathy, syncope, and seizures [9]. Rapid and accurate diagnosis in the setting of an acute aortic dissection is vital as mortality increases about 1% per hour prior to initiating appropriate treatment. The DeBakey and Stanford classification schemes are the most widely used to classify the location of dissection and decide on medical versus surgical management.

Key Anatomic and Hemodynamic Features

Atherosclerotic plaques are manifestations of atherosclerosis that develop over a lifelong process, starting with asymptomatic plaque development that can progress and lead to symptoms of atherosclerosis and atheroembolic disease over time.

In an aortic dissection, a tear in the aortic intima leads to the creation of a false lumen that can rapidly propagate throughout the aorta, both proximally and distally. Symptoms and signs are generally the result of branches of the aorta that are involved either through propagation of the dissection or via occlusion of blood flow and the resultant hypoperfusion. When dissection occurs near the aortic valve, acute aortic regurgitation can occur, the hemodynamics of which have been previously discussed. Pericardial effusion, with or without organization, may also be seen in these cases and can lead to cardiac tamponade and hemodynamic collapse.

Echocardiography Findings

Aortic atheroma pathologies are the following: severe plaque (Fig. 7.10a), intramural hematoma (Fig. 7.10b), and penetrating ulcer (Fig. 7.10c).

Atherosclerotic plaques are located in the aortic intima and can progress from atheromas to fibroatheromas and subsequently to complex plaques with hemorrhage, ulcerations, and overlying thrombi. The risk of embolism increases with the amount of plaque present, and plaque typically increases in quantity, moving proximal to distal through the aorta.

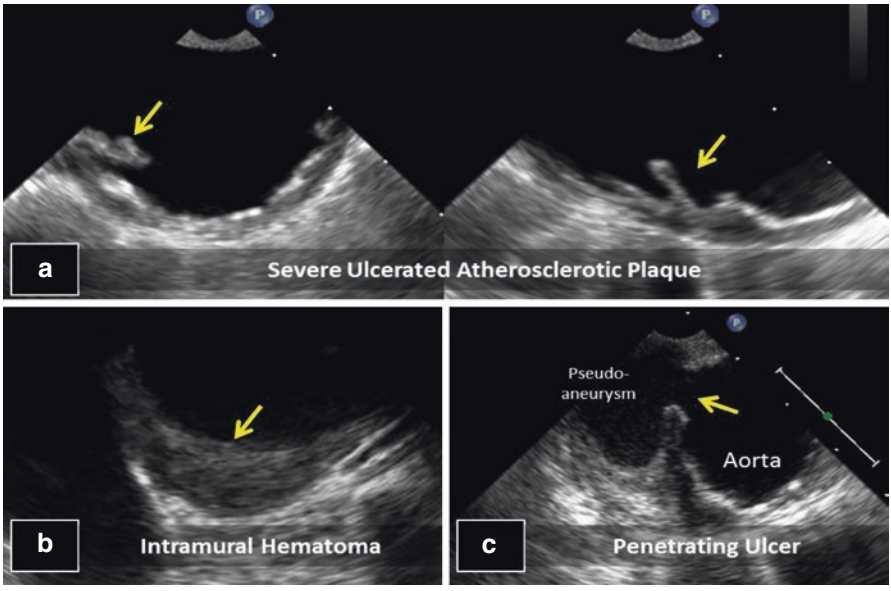

Fig. 7.10 Atheroma triad. (**a**) Severe ulcerated atherosclerotic plaque in the aorta visualized in multiple planes on transesophageal echocardiogram. (**b**) Intramural hematoma in the wall of the aorta due to rupture of vasa vasorum. (**c**) Penetrating ulcer in the aorta leading to creation of pseudoaneurysm outpouching

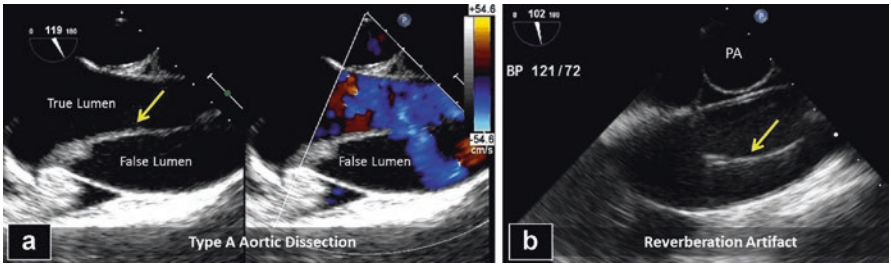

Fig. 7.11 Dissection. (**a**) Type A aortic dissection with separation of aorta into true and false lumen with color Doppler flow demonstrating communication between lumens. (**b**) Reverberation artifact from pulmonary artery mimicking aortic dissection. *PA* Pulmonary artery

The diagnosis of aortic dissection is made when a true and false lumen is separated by an intimal flap and can be visualized within the aorta. In most cases, the false lumen flow is detectable via color Doppler but may be absent in cases of false lumen thrombosis or retrograde dissection. Particular attention should be paid to presence of aortic root dilation, aortic regurgitation, and pericardial effusion (Fig. 7.11a).

The ascending aorta is best imaged on TTE on the parasternal long axis but can sometimes also be seen on apical five-chamber views and subxiphoid views. The sensitivity of TTE for type A dissection is as high as 78% in older case series and can be improved with the use of echo contrast. If clinically suspected, however, even negative contrast TTE does not rule out an ascending dissection, and in these cases TEE has a much higher sensitivity for detection, approaching 98% in some series.

Artifacts in the aorta are common, with some series estimating incidence at 44–53%, and as many as 3.5% of clinically suspected cases were mistakenly diagnosed due to artifacts. In the aortic root, reverberations are from the left atrium; in the ascending aorta, reverberations are noted from the pulmonary artery. Typically, reverberations are distinguishable from dissection flap based on their location and movement on M-mode echocardiography (Fig. 7.11b).

Differential Diagnosis

Acute aortic dissection exists on a continuum of acute aortic syndromes that include intramural hematoma and penetrating atherosclerotic ulcer. Intramural hematoma is characterized by circular or crescentic thickening of the aortic wall, generally greater than 5 mm in thickness. Penetrating atherosclerotic ulcer is generally visualized as a crater-like outpouching with jagged edges in the aortic wall and is associated with severe and diffuse atherosclerosis.

Alternative Imaging

Evaluation of atherosclerotic plaque can be accomplished with TEE, CT, or CMR. Alternative imaging modalities are more useful for distal aortic plaque beyond the areas reached by TEE. CT and CMR are both imaging modalities associated with extremely high sensitivity and specificity in the diagnosis of acute aortic dissection and may be more accurate choices for making a diagnosis if readily available and without contraindications, such as impaired renal function.

Moderate Embolic Risk Cardiovascular Lesion

Intracardiac shunt leading to the potential for systemic embolization can occur in the setting of a patent foramen ovale or an atrial septal defect. In the setting of acute neurologic syndrome of a suspected cardiogenic etiology, it is imperative to exclude the etiologies of higher cardioembolic potential before concluding that an intracardiac shunt is responsible and treatment should be considered.

Patent Foramen Ovale and Atrial Septal Defect

Paradoxical embolism in a patient with a patent foramen ovale (PFO) or atrial septal defect (ASD) has been associated with increased risk of stroke, particularly in young patients [10]. Although PFOs are found in as many as 25% of the normal population, some data suggest a prevalence of up to 40% in young patients with acute neurologic ischemia. A PFO is a remnant of fetal circulation to enable circulatory bypass of the lungs commonly found in adults and is normally kept closed by the positive left-to-right atrial pressure gradient. In settings of increased right atrial pressure (commonly Valsalva maneuver and acute or chronic pulmonary hypertension), a right-to-left shunt can occur resulting in acute stroke from paradoxical thromboembolism. The presence of atrial septal aneurysm (ASA) can cause retraction of the septum primum, resulting in a larger interatrial shunt and increasing risk of stroke. The ASA may lead to increased risk by funneling thrombotic remnant toward the PFO.

Key Anatomic and Hemodynamic Features

The foramen ovale anatomy can vary considerably from small tunnels of communication to wide open PFO with ridge on the left atrial side. ASA is diagnosed if there is fixed displacement of the fossa ovalis toward the right or left atria or a combined total excursion of the right and left of >15 mm from the midline (Fig. 7.12).

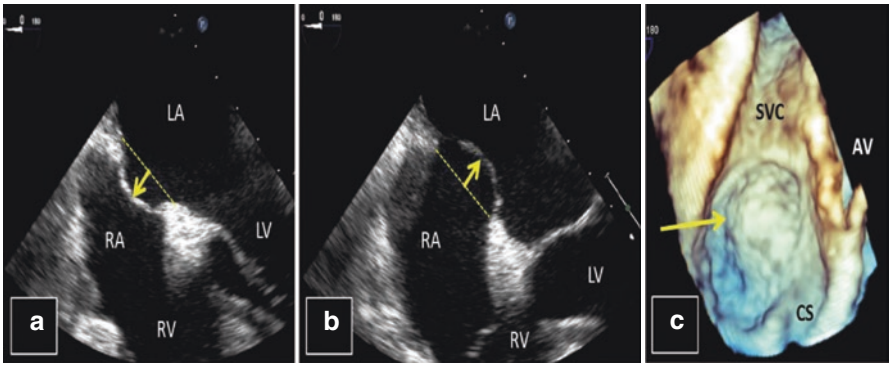

Fig. 7.12 ASA. (**a**) Atrial septal aneurysm when bowing into the right atrium. (**b**) Atrial septal aneurysm bowing into the left atrium. (**c**) 3D view of atrial septal aneurysm bowing into the right atrium. *RA* Right atrium, *RV* Right ventricle, *LA* Left atrium, *LV* Left ventricle, *CS* Coronary sinus, *AV* Aortic valve, *SVC* Superior vena cava

Echocardiography Findings

To assess for a PFO, the presence of a right-to-left shunt must be detected. Routine color Doppler evaluation is the primary means of visualization, and agitated saline injection and lowering the Nyquist limit can both provide increased sensitivity of evaluation.

Agitated saline can be injected intravenously for the purpose of finding intracardiac or intrapulmonary shunts. Injections should be performed both at rest and with Valsalva maneuver. Deviation of the interatrial septum to the left atrial side can be used as confirmation of adequate rise in right atrial pressure. The presence of a PFO is suggested by the presence of microbubbles in the left side of the heart within three cardiac cycles of injection (Fig. 7.13). Current guidelines likely overemphasize the importance of timing of the appearance of bubbles in the left heart (early with intracardiac shunt and late with intrapulmonary shunt) as well as the importance of counting bubbles for quantitative evaluation (>20 bubbles means a large shunt). Improved discrimination can be accomplished via evaluation of the pattern of bubbles appearance; a PFO will appear as a puff and have rapid bubble disappearance, while a pulmonary arteriovenous malformation will demonstrate a progressive increase in bubbles that disappear very late. TEE should be performed when shunt is detected on TTE to confirm the presence of a PFO, exclude other shunts, and plan for potential closure if clinically indicated. If planning to perform Valsalva maneuver during a TEE, it can be helpful to provide the patient with instructions on Valsalva maneuver or coughing prior to procedural sedation.

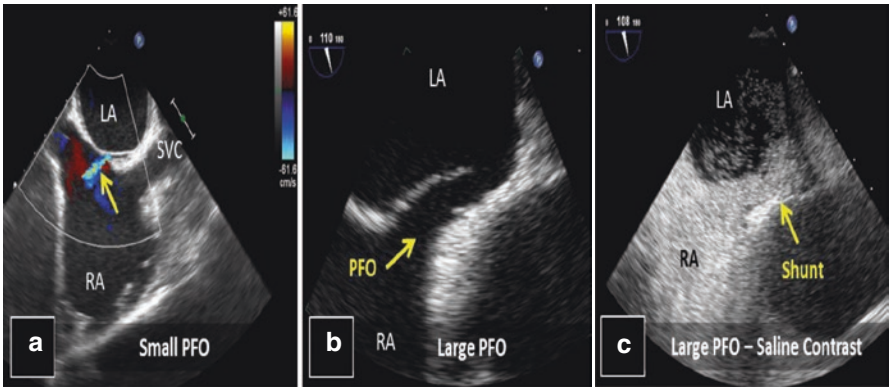

Fig. 7.13 PFO. (**a**) Small PFO visualized with color Doppler. (**b**) Large PFO can be visualized without assistance of color Doppler or agitated saline. (**c**) Communication between right and left atrium in large PFO with significant proportion of bubbles crossing the interatrial septum during bubble study. *PFO* Patent foramen ovale, *LA* Left atrium, *RA* Right atrium, *SVC* Superior vena cava

Alternative Imaging

Transcranial Doppler can often provide a clue to the existence of a right-to-left shunt by detecting microbubbles in the middle cerebral artery (MCA) after injection of intravenous fluid; however TEE remains the gold standard test for detection.

Other Conditions

Several other conditions of low embolic potential should be considered in the differential diagnosis of acute neurologic syndrome from a suspected cardiac etiology. These can be further characterized according to the etiology of embolism.

- Precursor lesions to thromboembolism, such as SEC representing smoke or sludge in the left atrial appendage or LV aneurysm in the absence of frank clot demonstrated with echo contrast or CMR.
- Etiologies that increase intracardiac calcification such as severe mitral annular calcification or calcific aortic stenosis.
- Valvular abnormalities such as fibrin strands or large Lambl's excrescences comprise a group of intracardiac findings with relatively low embolic potential that should be considered in the differential diagnosis of acute neurologic syndrome from a suspected cardiac etiology.

Although these lower-risk lesions can be a cause of systemic embolism, it is imperative on the clinician to rule out the intracardiac etiologies that are more frequently associated with distal embolic phenomena.

References

1. Stroke Facts | cdc.gov. https://www.cdc.gov/stroke/facts.htm. Accessed 12 Nov 2017.
2. Celeste F, Muratori M, Mapelli M, Pepi M. The evolving role and use of echocardiography in the evaluation of cardiac source of embolism. J Cardiovasc Echogr. 2017;27(2):33–44. https://doi.org/10.4103/jcecho.jcecho_1_17.
3. Benjamin EJ, Blaha MJ, Chiuve SE, et al. Heart disease and stroke statistics-2017 update: a report from the American Heart Association. Circulation. 2017;135(10):e146–603. https://doi.org/10.1161/CIR.0000000000000485.
4. Pepi M, Evangelista A, Nihoyannopoulos P, et al. Recommendations for echocardiography use in the diagnosis and management of cardiac sources of embolism European Association of Echocardiography (EAE) (a registered branch of the ESC). Eur J Echocardiogr. 2010; 11(6):461–76. https://doi.org/10.1093/ejechocard/jeq045.
5. Saric M. Guidelines for the use of echocardiography in the evaluation of a cardiac source of embolism. J Am Soc Echocardiogr. 2016;29:1–42. https://doi.org/10.1016/j.echo.2015.09.011.
6. Fuster V, Ryden LE, Cannom DS, et al. ACC/AHA/ESC 2006 guidelines for the management of patients with atrial fibrillation executive summary: A report of the American College of Cardiology/American Heart Association Task Force on practice guidelines and the European Society of Cardiology Committee for Practice Guidelines (Writing Committee to Revise the 2001 Guidelines for the Management of Patients with Atrial Fibrillation) developed in collaboration with the European Heart Rhythm Association and the Heart Rhythm Society. Eur Heart J. 2006;27(16):1979–2030. https://doi.org/10.1093/eurheartj/ehl176.
7. Weinsaft JW, Kim HW, Shah DJ, et al. Detection of left ventricular thrombus by delayed-enhancement cardiovascular magnetic resonance. J Am Coll Cardiol. 2008;52(2):148–57. https://doi.org/10.1016/j.jacc.2008.03.041.
8. Senior R, Becher H, Monaghan M, et al. Contrast echocardiography: evidence-based recommendations by European Association of Echocardiography. Eur J Echocardiogr. 2008; 10(2):194–212. https://doi.org/10.1093/ejechocard/jep005.
9. Flemming KD, Brown RD, Friedrich I, Sirch J, Erbguth FJ. Acute cerebral infarction caused by aortic dissection: caution in the thrombolytic era. Stroke. 1999;30(2):477–8. https://doi.org/10.1161/01.str.0000254594.33408.b1.
10. Kerut EK, Norfleet WT, Plotnick GD, Giles TD. Patent foramen ovale: a review of associated conditions and the impact of physiological size. J Am Coll Cardiol. 2001;38(3):613–23. http://www.ncbi.nlm.nih.gov/pubmed/11527606. Accessed 12 Nov 2017.

Part II
Application of Echocardiography in the CCU

Chapter 8
Hemodynamic Assessment in the CCU by Echocardiography

Yuvrajsinh J. Parmar, Craig Basman, and Itzhak Kronzon

Abstract Cardiac hemodynamics and intracardiac pressures can be assessed non-invasively with echocardiography. The simplified Bernoulli equation can be used for the majority of calculation for inter-chamber gradients. These measurements can aid in the assessment and management of patients in the cardiac intensive care unit. This chapter will focus on the hemodynamic assessment of the cardiac intensive care patient using Doppler and other echocardiographic techniques.

Keywords Doppler · Cardiac output · Intra cardiac gradients

Introduction

Cardiac hemodynamics and intracardiac pressures can be assessed noninvasively with echocardiography. The simplified Bernoulli equation can be used for the majority of calculation for inter-chamber gradients. These measurements can aid in the assessment and management of patients in the cardiac intensive care unit. This chapter will focus on the hemodynamic assessment of the cardiac intensive care patient using Doppler and other echocardiographic techniques.

Evaluation of Right Atrial Pressure

The inferior vena cava size and change with respiration can be used to evaluate right atrial pressures. The inferior vena cava can be visualized with the transducer in the subxiphoid position traveling through the liver into the right atrium. The ultrasound transducer is placed perpendicular to the inferior vena cava. Normally, the inferior vena cava is <2.1 cm when measured 1–2 cm prior to entering the right atrium, and

Y. J. Parmar · C. Basman · I. Kronzon (✉)
Department of Cardiology, Hofstra University School of Medicine, Lenox Hill Hospital—Northwell Health, New York, NY, USA
e-mail: ikronzon@northwell.edu

E. Herzog, E. Argulian (eds.), *Echocardiography in the CCU*,
https://doi.org/10.1007/978-3-319-90278-4_8

Table 8.1 Inferior vena cava (IVC) size and respiratory variation in the evaluation of right atrial (RA) pressure

Inferior vena cava size and collapsibility	Estimate of right atrial pressure
Dilated (>2.1 cm) and little collapsibility (<50%)	Elevated (10–20 mmHg)
Normal (<2.1 cm) but little collapsibility (<50%) Dilated (>2.1 cm) but collapsible (>50%)	Intermediate (5–10 mmHg)
Normal (<2.1 cm) and collapsible (>50%)	Normal/low (0–5 mmHg)

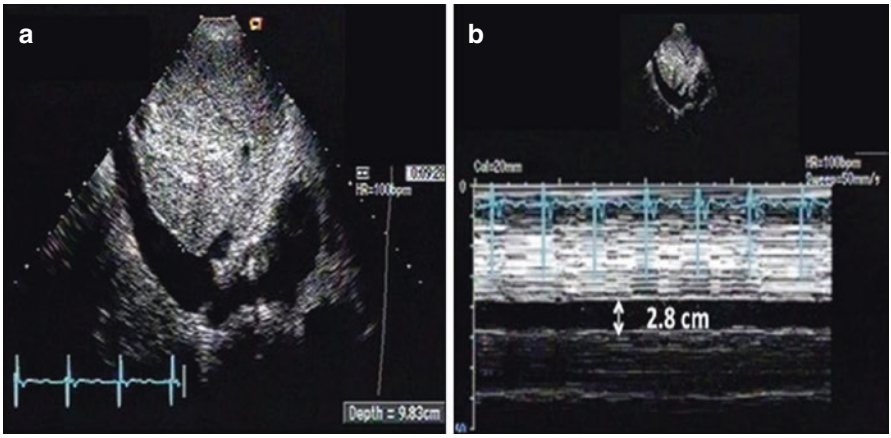

Fig. 8.1 Assessment of right atrial pressure (RAP). (**a**) The inferior vena cava (IVC) is markedly dilated at its entrance to the right atrium (2.8 cm). (**b**) The M-mode recorded demonstrates lack of respiratory variations in diameter. RAP is estimated to be 15–20 mmHg

there is a decrease of 50% or more in its diameter with inspiration. A dilated inferior vena cava and failure to collapse with respiration and the "sniff test" suggests elevated right atrial pressures [1–3]. M-mode echocardiography can be particularly helpful to measure the size and changes of its diameter during inspiration. Table 8.1 displays inferior vena cava characteristics (diameter and respiratory changes) and estimated right atrial pressure. Figure 8.1 shows a two-dimensional image and M-mode echocardiogram of a patient with a markedly elevated right atrial pressure.

Evaluation of Right Ventricular Systolic Pressure

The tricuspid valve during systole can be used to estimate the right ventricular systolic pressure. During systole, the tricuspid valve is closed, and there is a pressure gradient between the right ventricle and right atrium. Approximately 80% of adults have some degree (usually trace to mild) of tricuspid regurgitation. Continuous wave Doppler can be used to measure the peak velocity of this tricuspid regurgitant

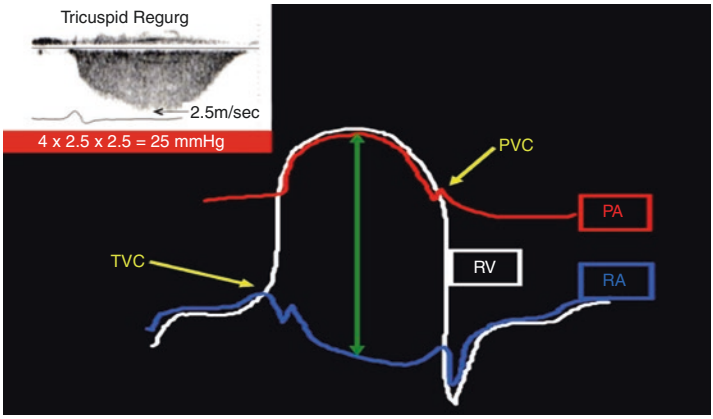

Fig. 8.2 Assessment of right ventricular (RV) systolic pressure (see text). The diagram shows normal right-sided pressures with no significant systolic gradient across the pulmonic valve and no significant diastolic gradient across the tricuspid valve. The gradient across the tricuspid valve in systole (*green arrow*) is responsible for the tricuspid regurgitation velocity seen in the *upper left corner*. With a peak regurgitant velocity of 2.5 m/s, the gradient between the right ventricle and right atrium is 25 mmHg. Other abbreviations: *PA* Pulmonary artery pressure, *PVC* Pulmonic valve closure, *RA* Right atrial pressure, *TVC* Tricuspid valve closure

jet. In the absence of pulmonic stenosis, the right ventricular systolic pressure can be used to estimate pulmonary artery systolic pressure. Figure 8.2 shows the superimposed pressure curves of the right atrium, right ventricular, and pulmonary artery pressure. This peak velocity can be used to estimate the gradient between the right ventricle and right atrium by using the simplified Bernoulli equation. The right ventricular systolic pressure (RVSP) therefore will equal the tricuspid regurgitant (TR) gradient plus the right atrial pressure (RAP).

$$\text{RVSP} = \text{TR gradient} + \text{RAP}$$

In a patient with ventricular septal defect (VSD) with a left-to-right shunt, the right ventricular systolic pressure can be calculated after measuring the gradient across the VSD in systole. In the absence of aortic stenosis, the systolic pressure in the left ventricle equals the systemic systolic blood pressure. Thus, the right ventricular systolic pressure (RVSP) equals systolic blood pressure (SBP) minus the systolic ventricular septal defect (SVSD) gradient.

$$\text{RVSP} = \text{SBP} - \text{SVSD gradient}$$

Figure 8.3 shows an example of calculating right ventricular systolic pressure in a patient after a myocardial infarction that developed a VSD with a left-to-right shunt.

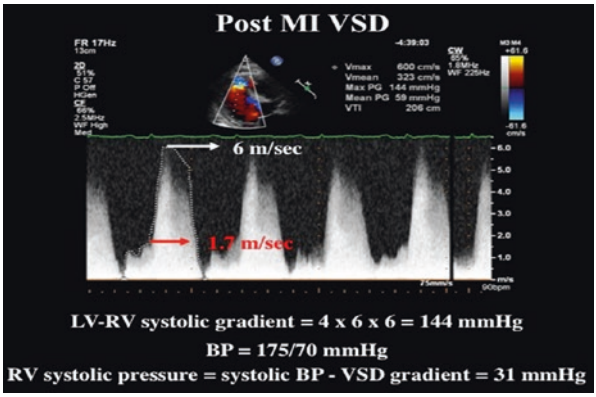

Fig. 8.3 Assessment of right ventricular systolic pressure in a patient with a ventricular septal defect after myocardial infarction. Note that there is flow in both systole (*white arrow*) and diastole (*red arrow*). Other abbreviations: *LV* Left ventricle, *RV* Right ventricle

Evaluation of Right Ventricular Diastolic Pressure

The right ventricular diastolic pressure is similar to the right atrial pressure in the absence of tricuspid stenosis. Therefore, the right ventricular diastolic pressure (RVDP) equals right atrial pressure (RAP). One can use the IVC dimensions to estimate the RAP and substitute that number for RVDP.

$$\text{RVDP} = \text{RAP}$$

The RVDP can also be calculated in the presence of a ventricular septal defect with left-to-right shunt. If the left ventricular diastolic pressure is higher than the right ventricular diastolic pressure, then there is continuous diastolic flow from left ventricle to right ventricle. If the left ventricular diastolic pressure is known, then the RVDP can be calculated as the left ventricular diastolic pressure (LVDP) minus the ventricular septal defect (VSD) diastolic gradient.

$$\text{RVDP} = \text{LVDP} - \text{VSD diastolic gradient}$$

Evaluation of Pulmonary Artery Systolic Pressure

It can be assumed that the pulmonary artery systolic pressure equals the right ventricular systolic pressure in the absence of pulmonic stenosis. Therefore, the pulmonary artery systolic pressure (PASP) equals the tricuspid regurgitation (TR) gradient plus the right atrial pressure (RAP).

$$\text{PASP} = \text{TR gradient} + \text{RAP}$$

However, in the presence of pulmonic stenosis, the gradient across the pulmonic valve must be accounted for. It is still possible to calculate the PASP by first

calculating the pulmonic stenosis gradient. In these patients, the pulmonary artery systolic pressure (PASP) equals the right ventricular systolic pressure (RVSP) minus the pulmonic stenosis (PS) gradient.

$$\text{PASP} = \text{RVSP} - \text{PS gradient}$$

Evaluation of Pulmonary Artery Diastolic Pressure

The velocity of pulmonic regurgitation can be used to calculate the gradient between the pulmonary artery and the right ventricle. The majority of patients normally have some degree (trace to mild) of pulmonic regurgitation. Thus, the pulmonary artery diastolic pressure (PADP) equals the end pulmonary regurgitation gradient plus the right ventricular diastolic pressure (RVDP).

$$\text{PADP} = \text{PR gradient} + \text{RVDP}$$

Since the right atrial pressure is approximately equal to the right ventricular diastolic pressure, this equation can be simplified to the pulmonary artery diastolic pressure (PADP) equaling the pulmonic regurgitation (PR) gradient plus right atrial pressure (RAP).

$$\text{PADP} = \text{PR gradient} + \text{RAP}$$

The ability to measure the pulmonic regurgitation velocity may be particularly helpful in the evaluation of the pulmonary artery pressure in patients who do not have a sufficient tricuspid regurgitation jet. Figure 8.4 shows a continuous wave Doppler tracing of pulmonic valve flow in a patient evaluated for significant pulmonary

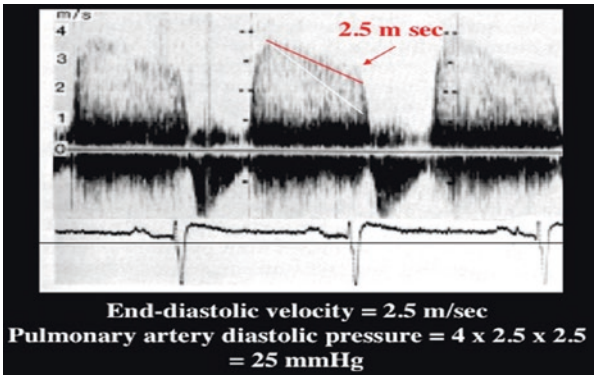

Fig. 8.4 Assessment of pulmonary artery diastolic pressure in a patient with pulmonary hypertension. The continuous wave Doppler of the pulmonic valve shows an end-diastolic velocity of 2.5 m/s. This indicates an end-diastolic gradient of 25 mmHg between the pulmonary artery and the right ventricle

hypertension who did not have tricuspid regurgitation. The end-diastolic velocity of the pulmonic regurgitant flow is 2.5 m/s, which indicates an end-diastolic gradient of 25 mmHg across the pulmonic valve. Therefore, the diastolic pulmonary artery pressure is at least 25 mmHg (25 mmHg plus the right ventricular diastolic pressure or right atrial pressure).

Evaluation of Mean Pulmonary Arterial Pressure

An estimation of pulmonary artery (PA) pressures in the absence of tricuspid or pulmonic regurgitation can be obtained with M-mode echocardiography and pulse wave Doppler. Normally atrial contraction produces a premature opening movement of the pulmonic valve, since the diastolic pressure is lower in the pulmonary artery than the right atrial/ventricular pressure after atrial contraction. In severe pulmonary hypertension, the elevated pulmonary pressures do not allow the atrial contraction to cause movement of the pulmonary leaflet. The characteristic M-mode pattern of the pulmonic valve in patients with severe pulmonary HTN includes an absence of "a" deflection during atrial contraction. The elevated pulmonary pressures can cause premature closure of the pulmonary valve during systole, which appears as the "flying W" on M-mode echocardiography (Fig. 8.5).

Mean PA pressures can be obtained by measuring the systolic acceleration time of the antegrade flow velocity measured by pulse wave Doppler just proximal to the pulmonic valve. The acceleration time is inversely proportional to the mean PA pressure [4]. The equation used for this estimation is:

$$\mathrm{PAMP} = 79 - \left(0.45 \times \mathrm{AcT}\right)$$

where PAMP is mean PA pressure in mmHg and AcT is acceleration time in milliseconds.

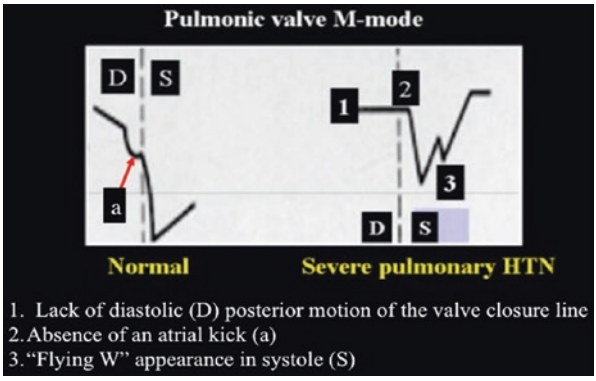

Fig. 8.5 A comparison M-mode echocardiography of the pulmonic valve in individuals with and without severe pulmonary hypertension

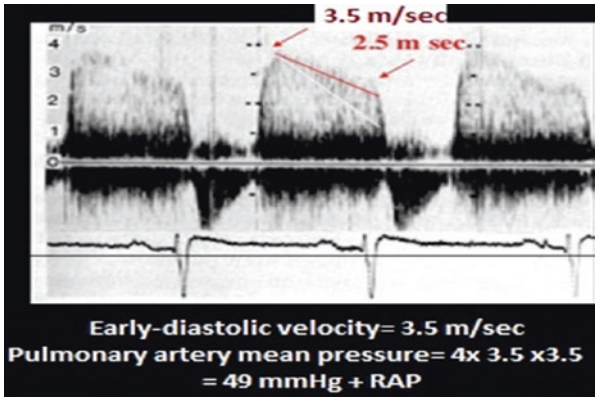

Fig. 8.6 Assessment of pulmonary artery mean pressure in a patient with pulmonary hypertension. The continuous wave Doppler of the pulmonic valve shows an early diastolic velocity of 3.5 m/s. This indicates an early diastolic gradient of 49 mmHg between the pulmonary artery and the right ventricle

A normal acceleration time is greater than 120 ms, and values less than 90 ms are associated with a PA mean pressure greater than 40 mmHg.

Mean PA pressure can also be estimated from the pulmonic regurgitation jet. Figure 8.6 shows a continuous wave Doppler tracing of pulmonic valve flow in a patient evaluated for significant pulmonary hypertension who did not have tricuspid regurgitation. The early diastolic velocity of the pulmonic regurgitant flow is 3.5 m/s, which indicates an early diastolic gradient of 49 mmHg across the pulmonic valve. Therefore, the mean pulmonary artery pressure is at least 49 mmHg (49 mmHg plus the right ventricular diastolic pressure or right atrial pressure).

Evaluation of Left Ventricular Systolic Pressure

In patients without aortic valve or left ventricular outflow obstruction, the gradient between the left ventricle and the aorta during systole is negligible. Therefore, left ventricular systolic pressure (LVSP) is equal to the systolic blood pressure (SBP).

$$\text{LVSP} = \text{SBP}$$

In patients with outflow obstruction (i.e., aortic valve, subvalvular or supravalvular stenosis), there is a gradient between the left ventricle and the ascending aorta. Since the systolic ascending aortic pressure equals the systolic blood pressure, the left ventricular systolic pressure (LVSP) equals the systolic blood pressure (SBP) plus the systolic pressure gradient across the aortic valve (or other subvalvular or supravalvular sites).

$$\text{LVSP} = \text{SBP} + \text{aortic valve gradient}$$

The gradient across the aortic valve can be measured with continuous wave Doppler. While cardiac catheterization records the peak-to-peak gradient (P2P), which is the gradient between peak aortic systolic pressure and peak left ventricular systolic

pressure, Doppler echocardiography measures the maximum instantaneous gradient (MIG). The value of the MIG is typically higher than the P2P (Fig. 8.7). In most cases of severe aortic stenosis, the P2P is approximately 70% of the MIG. After the mean pressure gradient is calculated with Doppler echocardiography, the P2P can be estimated by taking 70% of the MIG. This number is then added to systolic blood pressure to calculate left ventricular systolic pressure.

$$\text{LVSP} = \text{SBP} + 70\%\text{MIG}$$

The mitral regurgitant jet can be used to help estimate LVSP and gradients across the aortic valve. Continuous wave Doppler of the mitral regurgitant jet is used to estimate the gradient between the left ventricle and left atrium. The left ventricular systolic pressure (LVSP) equals the mitral regurgitation gradient plus the left atrial pressure.

$$\text{LVSP} = \text{MR systolic gradient} + \text{LAP}.$$

The mitral regurgitant jet can also be used to estimate the gradient in a patient with aortic stenosis. Figure 8.8 shows the MR jet in a patient with aortic stenosis, with a

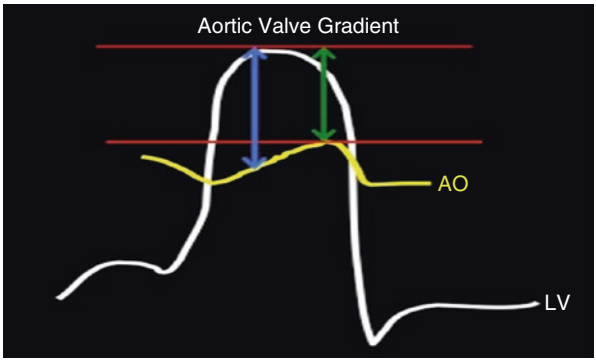

Fig. 8.7 Left-sided pressure curves in aortic stenosis demonstrating maximum instantaneous gradient (*blue arrow*) and the peak-to-peak gradient (*green arrow*)

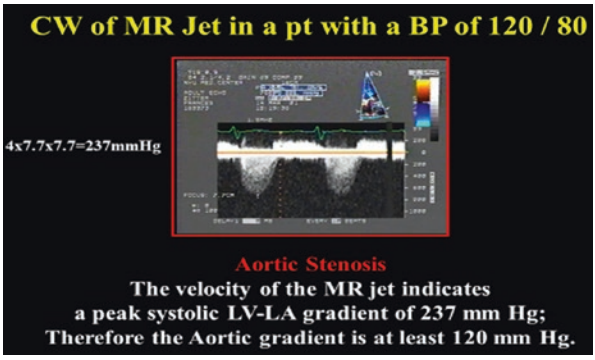

Fig. 8.8 The velocity of the MR jet indicates a peak systolic LV-LA gradient of 237 mmHg. The aortic gradient is therefore 237 mmHg + LAP – 120 mmHg (SBP)

blood pressure of 120/80 mmHg. The LVSP can be calculated based on the MR jet (see above). Aortic gradient can be calculated from the LVSP and SBP.

$$\text{Aortic gradient} = \text{LVSP} - \text{SBP}$$

Evaluation of Left Ventricular Diastolic Pressure

Similar to the right atrial and ventricular diastolic pressure, the gradient between the left atrium and the left ventricle during diastole is small and can be ignored in the absence of mitral stenosis. Therefore, the left atrial pressure (LAP) can be estimated and will approximate left ventricular diastolic pressure (LVDP).

$$\text{LVDP} = \text{LAP}$$

In patients who have aortic regurgitation, the regurgitant jet velocity is a function of the diastolic gradient between the aorta and the left ventricle. If the aortic diastolic pressure is known, then the left ventricular end-diastolic pressure (LVEDP) equals the diastolic blood pressure (DBP) minus the aortic regurgitation gradient (AR) at end diastole. In most patients, the aortic pressure equals the cuff pressure in the arm.

$$\text{LVEDP} = \text{DBP} - \text{end diastolic AR gradient}$$

In patients with VSD with a left-to-right shunt, the LVEDP can be calculated if the RA pressure (RAP), which estimates RV diastolic pressure (in the absence of tricuspid stenosis), is known. In these patients, the addition of the RAP and the VSD end-diastolic gradient equals the LVEDP.

$$\text{LVEDP} = \text{RAP} + \text{VSD}\,\text{end} - \text{diastolic gradient}$$

Figure 8.9 demonstrates a continuous wave Doppler tracing taken from a patient with both aortic stenosis and aortic regurgitation. The aortic stenosis peak velocity jet is 4 m/s, and aortic regurgitation end-diastolic velocity is also 4 m/s. The blood pressure during the examination was 150/80 mmHg. Therefore, the left ventricular systolic pressure equals the systolic blood pressure (150 mmHg) plus 70% of the aortic systolic gradient. Since the maximum instantaneous aortic gradient is 64 mmHg, the peak-to-peak gradient is 70% of 64 mmHg, which is 45 mmHg. The left ventricular systolic pressure is therefore 150 + 45 = 195 mmHg. The left ventricular diastolic pressure equals the diastolic blood pressure (80 mmHg) minus the aortic diastolic gradient (64 mmHg), which equals 16 mmHg. Therefore, this patient's left ventricular pressure is 195/16 mmHg.

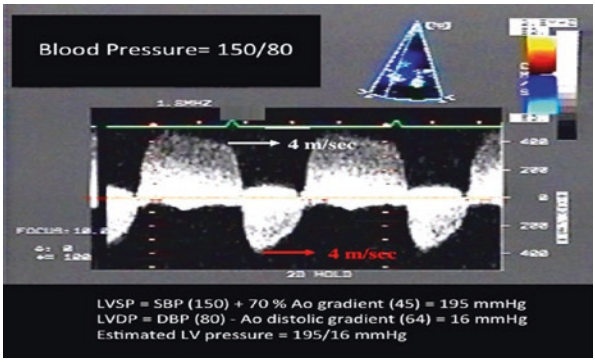

Fig. 8.9 Continuous wave Doppler (CW) in the calculation of left ventricular (LV) pressures in a patient with aortic stenosis and insufficiency (see text). Aortic stenosis peak velocity (*red arrow*) and aortic regurgitation end-diastolic velocity (*white arrow*) both measure to be 4 m/s. Other abbreviations: *Ao* Aorta, *LVSP* Left ventricular systolic pressure, *LVDP* Left ventricular diastolic pressure, *SBP* Systolic blood pressure, *DBP* Diastolic blood pressure

Evaluation of Left Atrial Pressure

Doppler echocardiography is useful to estimate left ventricular filling pressures. Pulse wave Doppler of the transmitral and pulmonary venous flow, along with tissue Doppler of the lateral and septal mitral annulus, allows for the estimation of LAP. Under normal flow patterns, the pressure in the left atrium is generally between 6 and 12 mmHg. Impaired relaxation results in a flow pattern with a low *E*-wave and high *A*-wave on pulse Doppler and corresponds to an atrial pressure of ~13–19 mmHg (minimal elevation left atrial pressure). In pseudonormalization of transmitral flow, the *E*–*A* ratio is between 9 and 14 with a low *E*′. This corresponds to an elevated left atrial pressure ranging from 20 to 24 mmHg. Lastly, a restrictive pattern with a high *E*-wave, low *A*-wave, and rapid transmitral deceleration time (<150 ms) occurs when the left atrial pressure is usually at least 25 mmHg. A simpler alternative to calculating left atrial pressure uses the ratio of the transmitral flow *E*-wave velocity and the tissue Doppler (*E*′). In general, as the left atrial pressure increases, *E*-wave becomes higher and the *E*′ becomes lower. An *E*/*E*′ ratio of less than 9 is associated with normal left atrial pressures, where as a ratio of greater than 14 is highly specific for elevated left atrial pressures (>14 mmHg). An equation reported by Nagueh et al. [5] describes the relation between LAP and *E*/*E*′.

$$\mathrm{LAP} = 1.24\left[\left(E / E'\right) + 1.9\right]$$

The simplified equation that may be used is:

$$\mathrm{LAP} = E / E' + 4\,\mathrm{mmHg}$$

In patients with mitral regurgitation (without aortic stenosis), the left atrial pressure during ventricular systole (LAS) equals the systolic blood pressure (SBP) minus the mitral regurgitation (MR) gradient.

$$\text{LAS} = \text{SBP} - \text{MR gradient}$$

In patients with mitral stenosis, the left atrial pressure during ventricular diastole (LAD) equals the left ventricular end-diastolic pressure (LVEDP) plus the mean transmitral gradient.

$$\text{LAD} = \text{LVEDP} + \text{transmitral gradient}$$

Left atrial pressure can also be estimated with the use of flow propagation velocity (V_p) of the mitral inflow obtained by color M-Mode. The V_p measures that rate at which red blood cells reach the LV apex from the mitral valve during early diastole. V_p is an indirect measurement of LV relaxation rate. Therefore a lower V_p means that LV relaxation is higher, which corresponds to elevated filling pressures.

$$\text{PAWP} = 4.6 + 5.27 \times E / V_p$$

where V_p is the flow propagation velocity of the mitral inflow obtained by color M-Mode in cm/sec. E is the peak blood flow velocity of the mitral inflow in cm/s.

It is important to note that for the use of Doppler echocardiography, the estimation of left atrial pressure assumes absence of atrial fibrillation, ventricular pacing, left bundle branch block, left ventricular assist device, or mitral valve disease.

Calculation of Cardiac Output

Cardiac output (CO) may be calculated by measuring either pulmonary or systemic blood flow. In the absence of shunts, the pulmonary blood flow is equal to systemic blood flow (SBF). The left ventricular outflow tract blood flow is often used to calculate the stroke volume. The LVOT flow can be calculated by the cross-sectional area (CSA) times the velocity time integral (VTI) of the LVOT. The cardiac output can then be calculated by multiplying the stroke volume with the heart rate (HR) (Fig. 8.10).

$$\text{SV} = \text{CSA}_{\text{LVOT}} \times \text{VTI}_{\text{LVOT}}$$

$$\text{CO} = \text{SV} \times \text{HR}$$

Calculation of cardiac output can be done using the right ventricular outflow tract blood flow or the flow in the pulmonary artery as well.

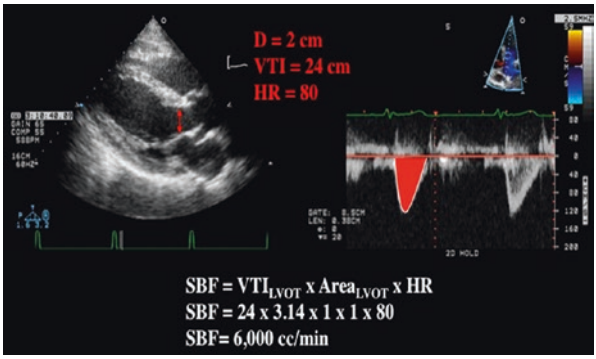

Fig. 8.10 Calculation of systemic blood flow. The diameter (*D*) is measured at the LVOT in parasternal long-axis view (*left*), and the VTI (*right*) is determined by pulse wave Doppler at the LVOT

Calculation of Shunt Flow

Calculating shunt flow in patients with atrial or ventricular septal defects can be performed by subtracting the systemic blood flow (SBF) from the pulmonary blood flow (PBF) (Fig. 8.11).

$$\text{Shunt flow} = \text{PBF} - \text{SBF}$$

Alternatively, the shunt flow can be estimated by multiplying the defect orifice area (DOA) by the shunt velocity time integral (VTI) and heart rate (HR). Figure 8.10 is an example of the calculation of ASD flow with a left-to-right shunt with an orifice area of 1.2 (radius of 0.6 cm), a VTI of 80 cm, and HR of 80 bpm. Using the equation below, the shunt flow is calculated.

$$\text{Shunt flow} = \text{DOA} \times \text{VTI}_{\text{shunt}} \times \text{HR}$$

Estimation of Pulmonary Vascular Resistance (PVR)

Pulmonary vascular resistance is defined as the ratio between the pressure gradient and the blood flow across the pulmonary vascular tree, measured in Wood's units. Invasively, PVR can be calculated using the following equation:

$$\text{PVR} = \left(\text{PAMP} - \text{LAMP}\right) / \text{PBF}$$

where PAMP = pulmonary artery mean pressure in mmHg, LAMP = left atrial mean pressure in mmHg, and PBF = pulmonary blood flow in L/min.

The PVR is directly related to the PA pressure (and therefore to the maximal TR jet velocity) and inversely related to the stroke volume in the RVOT (which can be measured noninvasively by pulse wave Doppler, using the VTI at the RVOT, just proximal to the pulmonic valve). PVR can therefore be calculated by Doppler using the following equation [6]:

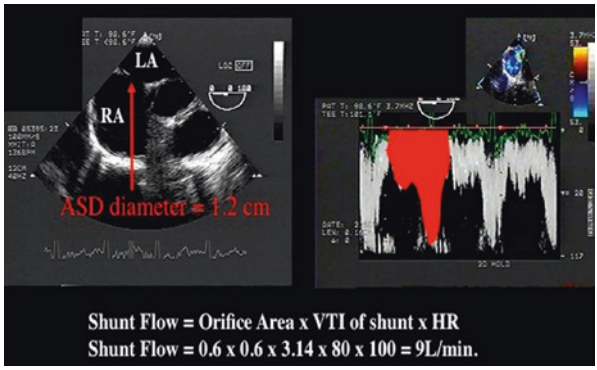

Fig. 8.11 Calculation of ASD with left-to-right shunt flow. The *red arrow* marks the ASD orifice diameter (*left*). The VTI of the shunt flow is shown in the shaded red area (*right*)

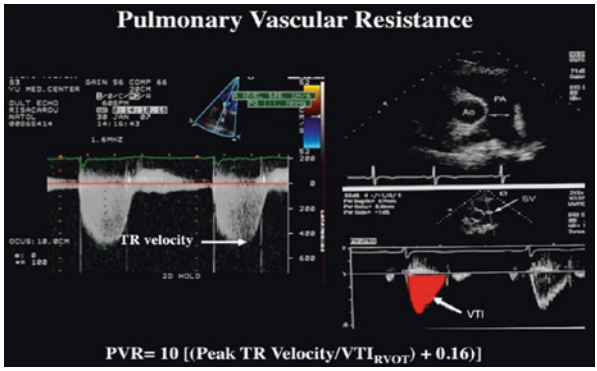

Fig. 8.12 Noninvasive calculation of PVR in Wood's units using the peak TR velocity and VTI at the RVOT

$$\mathrm{PVR} = 10\left[\left(\text{peak TR Velocity} / \mathrm{VTI}_{\mathrm{RVOT}}\right) + 0.16\right]$$

where PVR is expressed in Wood's units, TR = tricuspid regurgitation in m/s, and $\mathrm{VTI}_{\mathrm{RVOT}}$ = velocity time integral at the right ventricular outflow tract in centimeters (Fig. 8.12).

Conclusion

With the use of Doppler Echocardiography, intracardiac pressures can be assessed noninvasively. The hemodynamic information obtained with the use of echocardiography can be comparable to invasive methods. It is therefore important to obtain a full echocardiographic exam in cardiac patients hospitalized in the cardiac critical care unit. This information can be especially helpful in the assessment and management of CCU patients without invasive hemodynamic monitoring.

References

1. (2007) Doppler echocardiography and color flow imaging: comprehensive non invasive hemodynamic assessment, chapter 4. In: Oh JK, Seward JB, Tajik JA (eds) The echo manual, 3rd edn. Lippinkot Williams and Wilkins, Philadelphia, PA. pp 59–79.
2. Otto C, editor. Textbook of clinical echocardiography. 5th ed. Philadelphia, PA: Elsevier–Saundres; 2013. p. 159.
3. Rudski LG, Lai WW, Afilalo J, Hua L, Handschumacher MD, Chandrasekaran K, Solomon SD, Louie EK, Schiller NB. Guidelines for the echocardiographic assessment of the right heart in adults: a report from the American Society of Echocardiography endorsed by the European Association of Echocardiography and the Canadian Society of Echocardiography. J Am Soc Echocardiogr. 2010;23:685–713.
4. Mahan G, Dabestani A, Gardin J, et al. Estimation of pulmonary artery pressure by pulsed Doppler echocardiography. Circulation. 1983;68(suppl III):367.
5. Nagueh SF, Middleton KJ, Kopelen HA, et al. Doppler tissue imaging: a noninvasive technique for evaluation of LV filling pressure. J Am Coll Cardiol. 1997;30:1527–33.
6. Scapellato F, Temporrelli PL, Eleuteri E, et al. Accurate noninvasive assessment of pulmonary vascular resistance in patients with chronic heart failure. Am J Cardiol. 2001;37:1813–9.

Chapter 9
Cardiac Point of Care Ultrasound in the CCU

Allison Selby, Eyal Herzog, and Edgar Argulian

Abstract Point-of-care cardiac ultrasound (POCUS) is becoming more commonly used in the assessment of patients as an adjunct to the physical examination, particularly in critically ill patients. Improving technology has made these devices smaller and portable with improved ease of use by cardiologists, as well as critical care and emergency room physicians. The use of cardiac POCUS can improve diagnostic accuracy and provide valuable diagnostic information that can significantly impact medical management.

Keywords Point of care · Pericardial effusion · Chest pain

Introduction

Point-of-care cardiac ultrasound (POCUS) is a practice with growing indications and utility when used at the bedside in critically ill patients. The development of handheld, battery-powered devices has led to more frequent use, including use by non-cardiologists in the emergency department and the critical care setting. The Society of Critical Care Medicine and American College of Emergency Physicians have published guidelines for the use of POCUS and recognized its potential advantages [1]. The utility of POCUS is to answer a particular clinical question, to improve diagnostic accuracy, and to help augment physical examination findings. POCUS can provide valuable information in the critically ill patient, where ultrasound findings can impact medical management [2].

POCUS has been shown to be useful in the evaluation of hypotensive, cardiac arrest, trauma, chest pain, and cardiac surgery patients [3]. In these instances, a critically ill or unstable patient can be rapidly evaluated with a bedside ultrasound to assist in confirming physical examination findings and ruling out diagnoses rapidly. POCUS is particularly useful in hypotensive patients, where an assessment of left ventricular (LV) function, right ventricular (RV) function, presence of a pericardial

A. Selby · E. Herzog · E. Argulian (✉)
Mount Sinai St. Luke's Hospital, New York, NY, USA
e-mail: Edgar.Argulian@mountsinai.org

E. Herzog, E. Argulian (eds.), *Echocardiography in the CCU*,
https://doi.org/10.1007/978-3-319-90278-4_9

effusion, and assessment of IVC size can help establish a diagnosis not clearly suggested by physical examination findings alone.

Point-of-Care Cardiac Ultrasound Devices

POCUS can have a number of different meanings. Other terms used to describe it include handheld ultrasound, hand-carried cardiac ultrasound, focused echocardiography, bedside cardiac ultrasound, and quick look cardiac ultrasound [4]. There are also different machines used to perform these exams ranging from small handheld, battery-powered machines to portable ultrasound machines. These devices typically range from 2 to 12 pounds and can cost between $8,000 and $30,000. Advances in technology have also promoted the use of application-based ultrasonography, where the operator's smartphone or tablet can be turned into a portable ultrasound with the connection of a transducer. Some newer devices have touch screens. There are also capabilities to upload images wirelessly to a cloud database [5]. Some devices also have compatibility with different types of probes. Phased array probes are used in cardiac studies as well as lung ultrasound. Linear array probes are useful for vascular studies. Curved array probes which are useful in abdominal studies are also available for certain devices.

The handheld devices vary widely in terms of their imaging capability. The handheld machines typically include 2D and color Doppler imaging and can be carried by the examiner. These smaller devices are an ideal adjunct to the physical examination to answer a particular clinical question; however, most handheld devices do not have the capability to visualize all abnormalities. The lack of spectral and tissue Doppler and acquisition of 3D images render these smaller devices unable to provide a complete echocardiographic examination in the assessment of particular cardiac diseases. As handheld devices continue to be developed, future devices will likely include spectral Doppler [5]. A limitation of these smaller, handheld devices is small screens and more limited imaging quality. Zooming capabilities, lowering sector width, adjusting gray scale, altering ultrasound beam focus, and adjusting transducer frequency are also limited on these devices, which can result in lower image quality. These characteristics combined can make interpretation of findings difficult by practitioners with limited experience in echocardiography interpretation and image acquisition [4].

Some larger, portable machines include spectral Doppler and M-mode as well. There are also differences between the meaning of limited echocardiography and focused echocardiography; the latter being a brief exam performed to answer a specific clinical question, the former referring to a study including a brief number of images. Limited echocardiography typically includes a full range of cardiac studies including 2D, color Doppler, spectral Doppler, and M-mode and is typically performed by a sonographer or a Level II/III echocardiographer. POCUS can be performed by a practitioner with POCUS training with a limited scope of interpretation. The documentation also varies between limited echocardiography and

POCUS—the former requiring a formal report to be documented; the latter documenting findings as part of the physical examination findings [4]. POCUS is not equivalent to an echocardiographic exam and is frequently followed up by a complete TTE to confirm POCUS findings and to look for other abnormalities not easily identified by POCUS.

Assessment of Left Ventricular Function

Physical examination findings in the detection of LV systolic dysfunction have variable sensitivity and specificity and are dependent on the skill and level of training of the examiner as well as the overall degree of heart failure [2]. Studies have shown variable sensitivity (SN) and specificity (SP) in heart failure physical examination signs, with an S3 having sensitivity of 11–51% and 85–98% specificity. In addition, a displaced apical impulse is not easily appreciated by examiners [6]. It is in these patients, with minimal physical examination findings suggestive of LV systolic dysfunction, in which POCUS can be particularly helpful in providing an assessment of ejection fraction and the presence of elevated left ventricular filling pressures.

The echocardiographic assessment of the critically ill patient is often difficult. Patients in the ICU are frequently intubated with limited mobility which can limit the acquisition of high-quality images and can make certain echocardiographic views very difficult to obtain. Several studies have shown that a subjective, visual assessment of ejection fraction obtained in the parasternal long-axis view (PLAX) is adequate in these patients [7]. The parasternal view can be obtained with the patient supine and is less dependent on patient position or body habitus. An example of a patient with severe LV dysfunction in the PLAX view is shown in Fig. 9.1. Apical views are more difficult to obtain and commonly require change in patient position to the left lateral decubitus position which may be limited in ICU patients. Issues such as apical foreshortening can lead to inaccurate interpretation of LV function. Technical aspects of acquiring apical images such as transducer penetration is limited on smaller, handheld devices which degrade image quality and the ability to accurately interpret images. With all of these factors considered, the PLAX view is recommended in the assessment of LV function by less experienced users [4]. The PLAX view also allows for visualization of the E-point septal separation (EPSS) which is another marker of LV dysfunction on echocardiography. The EPSS is the closest distance between the anterior mitral leaflet and the interventricular septum. When LV function is decreased, the mitral valve opens slower and not as wide, making the EPSS larger [7]. A value of EPSS of 7 mm or larger was significantly associated with severe LV dysfunction (EF less than or equal to 30%) in a study as performed by ED ultrasound fellows [8].

In addition to the visual assessment of LV ejection fraction, other POCUS findings can suggest clinically significant LV systolic function. The detection of left atrial enlargement (LAE) on POCUS is a clinically significant marker of increased LV filling pressures and carries prognostic significance in patients with

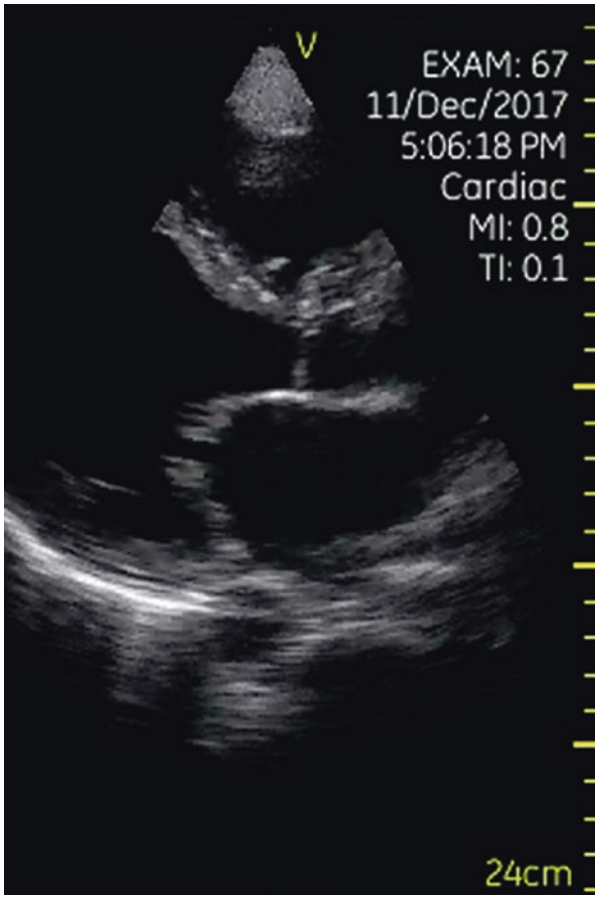

Fig. 9.1 PLAX view of a patient with dilated cardiomyopathy and severe LV dysfunction

cardiomyopathy, mitral valve disease, and atrial fibrillation. Using a parasternal long-axis view, an assessment of the LA anteroposterior diameter compared to a 4 cm reference standard can be quickly obtained [2]. Furthermore, criteria proposed by Kimura et al. compared the size of the left atrium to that of the overlying aorta obtained in a single PLAX view at end diastole. A ratio >1 signifies at least moderate LAE and thus can suggest clinically significant heart failure [9]. The presence of pulmonary vascular congestion and pleural effusions can also be easily detected by POCUS and assist in identifying acute decompensated heart failure. Pulmonary edema is manifest on ultrasonography by the presence of B-lines, believed to be caused by pleural thickening and interstitial edema [10]. They appear as "comet-tail" artifacts on ultrasound and tend to have a higher specificity for acute decompensated heart failure when found at the lung apices as compared to the lung bases [11]. Pleural effusions can also be identified on POCUS. The presence of bilateral effusions often suggests acute decompensated heart failure [2], particularly when present along with the other findings previously mentioned. On

echocardiography, a left-sided pleural effusion can be visualized in the PLAX view, posterior to the descending thoracic aorta. A right-sided pleural effusion is best visualized in the subcostal view.

A rapid echocardiographic assessment of LV function is invaluable and can lead to significant changes in medical management depending on the echocardiographic findings. Therefore, this has become an area of interest, for both cardiologists and non-cardiologists alike in the critical care and emergency room settings. Studies have been performed comparing LV function evaluation by intensivists with limited training in echocardiography versus experienced cardiologists, as differences in level of training in interpretation of ejection fraction is a concern, especially since one's interpretation can considerably impact treatment. Some studies have shown emergency department (ED) and intensive care unit (ICU) physicians are capable of assessing LV function accurately. One study in which medical ICU physicians performed limited bedside TTE in 44 critically ill patients showed a statistically significant agreement between intensivist and echocardiographer interpretation of degree of LV dysfunction (divided into normal, mild-moderately decreased, and severely decreased). In addition, intensivists correctly identified normal LV function in 92% of patients and abnormal LV function in 80% of patients; both of which achieved statistical significance [12]. In another study, 115 patients were assessed for LV ejection fraction by emergency physicians who had undergone a 3-hour training session in limited echocardiography. Results of this study showed 86.1% overall agreement between the emergency physicians and formal echocardiograms interpreted by a staff cardiologist [13]. The best correlation between both groups was in the normal EF category, followed by the poor EF category, with the least correlation in the moderate EF category. Detection of LV dysfunction by POCUS rather than waiting for formal standard echocardiography and reporting can reduce the time until implementing appropriate medical management; one study showing an average time difference of 18 h [4].

A study by Panoulas et al. showed that POCUS after physical examination improved sensitivity and specificity in detection of LV systolic dysfunction from 26% SN, 85% SP to 74% SN, 94% SP in medical students and junior doctors with 2 hours of POCUS training [14]. In another study by Kimura et al., 13 internal medicine residents with 2 h of POCUS 2D imaging training evaluated outpatients including subsets of patients with asymptomatic LV dysfunction. After US use, accuracy of detecting LV dysfunction improved in 10 out of 13 residents. In addition, adequate image quality was noted in 82% of resident-obtained ultrasounds [15]. These studies, among others, have shown an increase in diagnostic accuracy in detection of LV dysfunction even when performed by non-cardiology personnel after brief training.

Assessment of Valvular Disease

The ability to detect valvular disease by physical examination alone depends on a number of factors, including examiner skill, patient's body habitus, severity of lesions, and the number of valvular lesions present. When there is doubt in the identity of a murmur,

POCUS can provide more information. The addition of color Doppler to POCUS increases the sensitivity of identifying valvular lesions. However, not all of the handheld devices have spectral Doppler; therefore quantitation of lesion severity is limited, and often referral for a complete echocardiogram is recommended in these cases.

Significant valvular stenosis can be identified with POCUS by demonstration of restricted aortic and mitral valve leaflet motion in acquired images. POCUS findings of restricted aortic leaflet opening has a sensitivity and specificity of 85% and 89%, respectively, similar to the physical exam findings of a late-peaking systolic murmur [2]. A study was performed using pocket-sized echocardiograms for visual assessment of aortic stenosis (AS) severity using a scoring system to define aortic leaflet mobility. Leaflets were given a score of 0, 1, or 2 based on no restriction, mild, or severe, respectively. The study found that in the diagnosis of severe AS, a visual AS score $\geq$4 had sensitivity of 85% and specificity of 89% of identifying severe aortic stenosis. In addition, the diagnosis of moderate to severe AS, defined as a score $\geq$3, had sensitivity of 84% and specificity of 90% [16]. POCUS can be helpful in these cases by helping to select appropriate patients to be referred for formal echocardiography. Color Doppler can also be performed on these handheld devices and can demonstrate turbulence through the affected valve which can also suggest clinically significant stenosis.

POCUS can be utilized in the identification of regurgitant lesions. 2D visualization of leaflets showing mitral valve prolapse or leaflet malcoaptation can clue the examiner into the presence of a regurgitant lesion. The addition of color Doppler can identify even mild mitral regurgitation with 82% and 93% sensitivity and specificity. Exact determination of lesion severity is likely best interpreted by an expert in the field. The significance of identifying mildly regurgitant lesions and referral for formal echocardiography is not clearly understood and may not be cost-effective as these lesions are often not significant, particularly if LV function is preserved [2]. Identification of moderate or severe lesions on POCUS may affect medical management. Figure 9.2 demonstrates a parasternal long-axis (PLAX) view of a patient with severe mitral regurgitation performed on a handheld echo machine.

POCUS can be used to detect valvular insufficiency in patients with endocarditis, though it is similar to transthoracic echocardiogram in that the ability to detect vegetations is limited. POCUS can be used to augment the physical exam in these cases. However, the absence of spectral Doppler on most handheld devices limits the determination of lesion severity which is often assessed by valvular gradients. In instances of hypertrophic obstructive cardiomyopathy (HOCM), POCUS has been shown to be useful in identifying septal hypertrophy as well as systolic anterior motion of the mitral leaflet (SAM) in 2D images. Septal hypertrophy is defined as a septal thickness of >15 mm [17]. In devices with M-mode capability, the degree of SAM can be further defined and graded depending on the degree of septal contact with the anterior mitral valve leaflet; Grade II being <30% and Grade III being >30% contact during systole. The limitations of evaluation of HOCM by POCUS is the lack of availability of M-mode imaging on many devices as well as the lack of spectral Doppler to quantify left ventricular outflow tract (LVOT) gradients. POCUS has been shown to be useful in this diagnosis in some case reports [18].

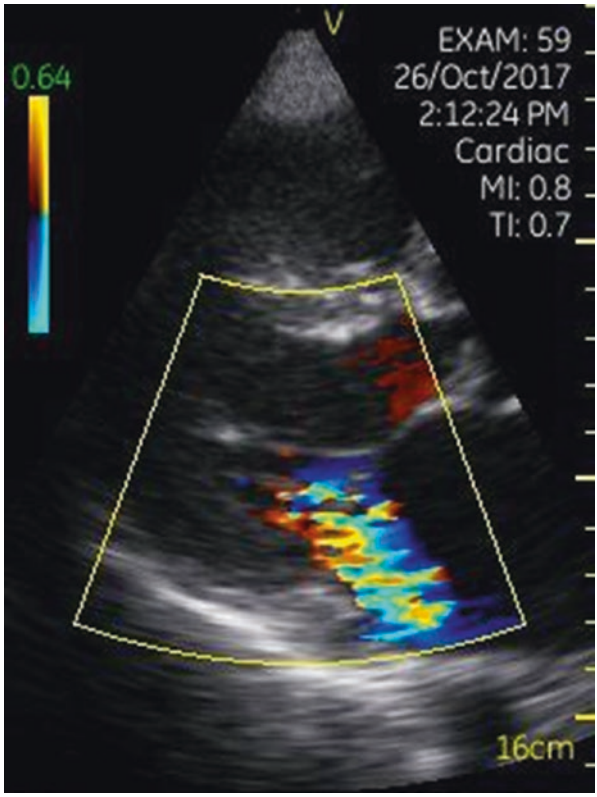

Fig. 9.2 PLAX view showing severe mitral regurgitation on handheld echo

Use of POCUS for assessment of valvular disease can lead to false-positive ultrasound exams. These false positives can lead to further evaluation with a transthoracic echocardiogram, which might not necessarily be needed. In a study by Martin et al., 354 patients underwent POCUS performed by hospitalists in the assessment of LV function, pericardial disease, cardiomegaly, and valvular disease. While the assessment of the other factors was more accurate when physical examination was augmented with POCUS, the detection of AI, MR, and AS was not improved with the use of this tool [19]. The role for POCUS in the assessment of valvular disease still requires further investigation.

Assessment of Right Ventricular Function

Physical examination findings suggestive of RV enlargement, including left parasternal heave and right-sided S3 occur relatively infrequently and have minimal accuracy [2]. The assessment of right-sided cardiac structures by POCUS is helpful in the evaluation of a hypotensive patient in whom pulmonary embolism (PE) is suspected. Right ventricular enlargement, new tricuspid regurgitation, or a

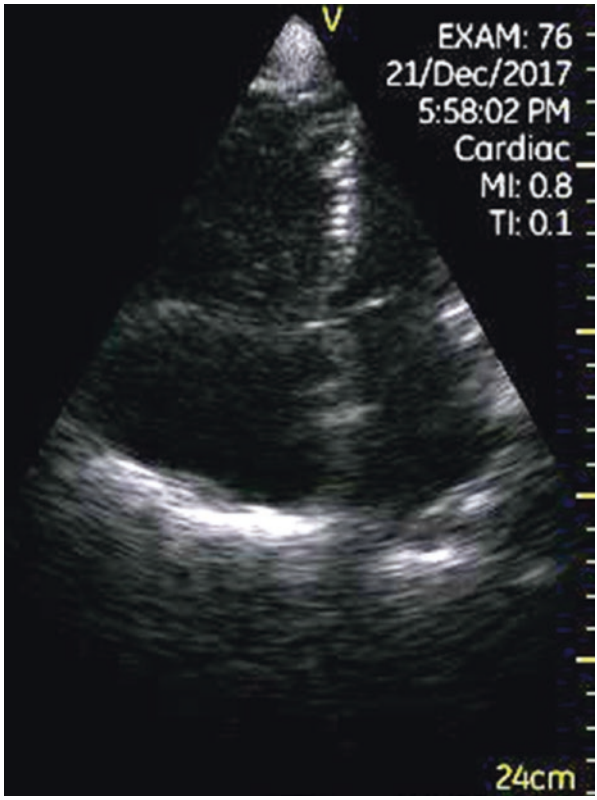

Fig. 9.3 Apical four-chamber view of a patient with marked RV enlargement by handheld echo

hyperdynamic LV is present in 27–55% cases of PE, and the presence of these signs might have a significant impact on medical management, including consideration of thrombolytic administration in the unstable patient [3]. The absence of these signs, however, is not sufficient to rule out the diagnosis. The right ventricle can be assessed in the PLAX, parasternal short axis (PSAX), apical four-chamber views, and subcostal views, all of which can be acquired on POCUS devices. Determination of RV size is best evaluated on PSAX and apical four-chamber views. Visually, the normal right ventricle is less than 2/3 the size of the left ventricle. Moderate dilatation is defined with an RV/LV ratio of >2/3, whereas severe dilatation is when the RV is the same size or larger than the LV, with an RV/LV ratio >1 [20]. Example of a patient with severe RV enlargement is shown in Fig. 9.3. As with apical views in the assessment of LV function, apical foreshortening can distort the shape of the right ventricle, leading to misinterpretation of RV size and function. In addition, septal flattening or a "D-shaped septum" can be seen in the parasternal short axis (PSAX) view which can suggest RV pressure overload in cases of acute PE and pulmonary hypertension. An example of D-shaped septal flattening in a patient with severe pulmonary hypertension is shown in Fig. 9.4. Without the availability of spectral Doppler on most handheld devices limits the ability to quantitate pulmonary hypertension, which is identified using continuous wave (CW) Doppler through

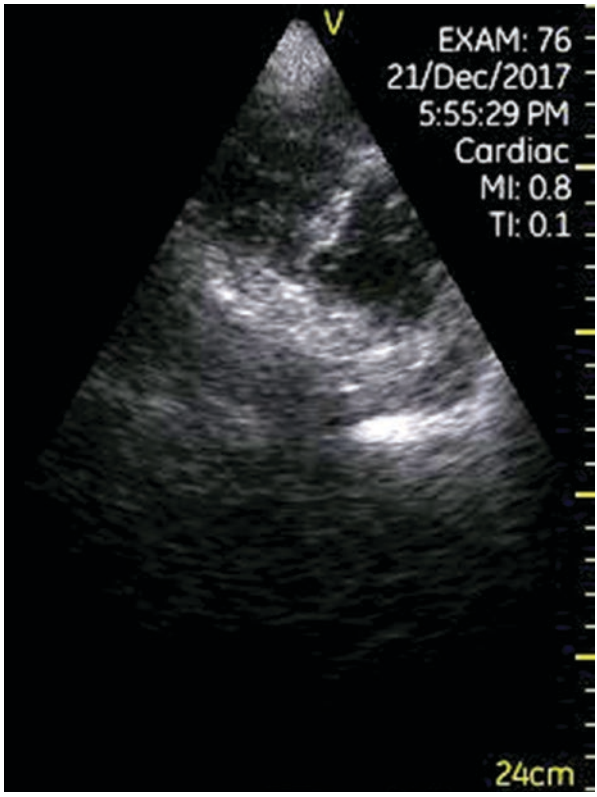

Fig. 9.4 PSAX view showing D-shaped septal flattening in a patient with severe pulmonary hypertension

the tricuspid jet on standard echocardiography. The use of POCUS in the evaluation of the hypotensive patient in the ICU setting is particularly helpful in cases of PE when the patient may not be hemodynamically stable to go to CT scan.

Combination of POCUS with venous ultrasonography may increase the sensitivity of detecting PE when the diagnosis remains uncertain with echocardiography alone. A single ICU-based study looked at the incidence of acute cor pulmonale (ACP) combined with venous ultrasonography in a population of 173 patients with PE. The echocardiographic criterion for ACP was the right to left ventricular end-diastolic area ratio over or equal to 0.6 along with paradoxical septal wall motion. It was found that 100% of patients with proximal (main, right, or left pulmonary artery) embolism or hemodynamic instability had either signs of right heart strain (87%) or DVT (74%) on POCUS [21].

Assessment of Pericardial Disease

Evaluating for the presence of pericardial effusion or cardiac tamponade is critically important for a patient with hypotension. Pericardial effusions can have a varied presentation, ranging from dyspnea to cardiogenic shock. Typical physical exam

findings of Beck's triad and pulsus paradoxus have limited sensitivity [2]. Development of cardiac tamponade depends on the rate of fluid accumulation in the pericardial sac rather than the size of the effusion itself. As cardiac tamponade can progress rapidly to shock, most ED and ICU POCUS protocols include an evaluation for pericardial effusion to quickly rule it out as a diagnosis for the hypotensive patient.

The size of the pericardial effusion can be assessed in multiple views; however, as previously mentioned, the subcostal and PLAX views are more easily obtained. Figure 9.5 shows a subcostal view of a patient with a pericardial effusion. The pericardial effusion should be measured in diastole and is quantified as small if less than 1 cm, moderate if between 1 and 2 cm, and large if greater than 2 cm [22]. Precise measurements and quantification of pericardial effusion may be limited on some handheld devices. In the apical four-chamber view and the subcostal views, RA systolic collapse can also be visualized, which occurs before RV diastolic collapse in pericardial tamponade. Significant RA collapse is defined as collapse in >1/3 of the cardiac cycle. Limitations of POCUS such as lack of ECG gating and M-mode imaging on all devices make this assessment more difficult. RV diastolic collapse is the most specific finding in the diagnosis of cardiac tamponade. RV diastolic collapse can be visualized in the PLAX, subcostal, and apical views. POCUS imaging in pericardial tamponade is limited by the lack of spectral Doppler, rendering respiratory

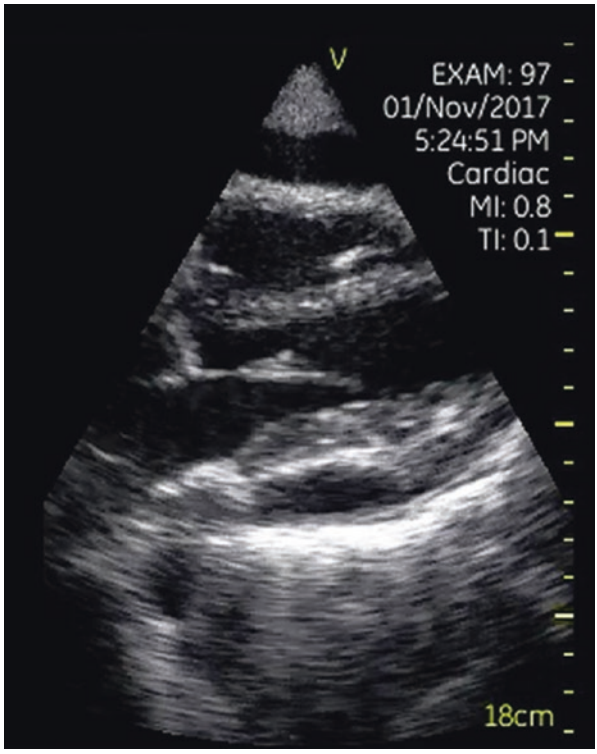

Fig. 9.5 Subcostal view showing a pericardial effusion on handheld echo

variation across the mitral and tricuspid valves unobtainable. In conjunction with IVC plethora and lack of respiratory variation, which will be discussed in a further section, these findings support the diagnosis of cardiac tamponade.

Studies have shown a high degree of sensitivity and specificity in detection of effusions with POCUS by non-cardiologists [23]. In a study by Mandavia et al., echocardiograms performed by emergency medicine physicians with ultrasonography training were reviewed. Of 515 echocardiograms performed, 103 patients were diagnosed with a pericardial effusion. Emergency physicians in this study detected pericardial effusion with a sensitivity of 96%, specificity of 98%, and overall accuracy of 97.5% [24].

Assessment of Volume Status

In the critically ill patient, assessment of hypovolemia and fluid responsiveness is of vital importance as to assess whether a patient needs volume resuscitation or diuresis. Physical examination findings to assess volume status, including jugular venous distention, are sensitive and specific but can be limited in particular patient populations, such as morbidly obese patients with thick necks as well as intubated patients [2]. In these patients, the role of POCUS becomes particularly helpful. Inferior vena cava (IVC) assessment by ultrasound or echocardiography offers an accurate assessment of intravascular volume status. IVC size and respiratory variation have been shown to correlate well with central venous pressure (CVP) [3]. Views of the IVC are obtained in the subcostal view. IVC measurements should be performed just distal to the hepatic vein for the most accurate measurement [25]. Figure 9.6 shows a subcostal view of the IVC by handheld echo. To assess IVC collapsibility and respiratory variation, the examiner should ask the patient to sniff and acquire images simultaneously. This is defined in the American Society of Echocardiography guidelines as follows: IVC diameter ≤2.1 cm collapsing >50% with sniff suggests normal right atrial pressure of 3 mmHg with a range of 0–5 mmHg; IVC diameter >2.1 cm collapsing <50% with sniff suggests high right atrial pressure of 15 mmHg with a range of 10–20 mmHg [26]. The lack of the ability to perform linear measurements on most handheld devices limits an accurate assessment of IVC diameter; however, a visual assessment of size and collapsibility can be performed. A limitation of assessment of IVC diameter is in the instance of mechanically ventilated patients. The increase in intrathoracic pressure that is associated with ventilation causes the IVC to engorge in inspiration due to backflow of pressure to the right atrium. Therefore, RA pressure should not be estimated based on IVC collapsibility and size in intubated patients. However, in patients with an IVC less than 1.2 cm, a RAP less than 10 mmHg can be assumed [25]. Fluid responsiveness can be predicted in these patients using the IVC distensibility index (dIVC), which was shown to be an accurate predictor using a cutoff of 18% [26].

Ultrasound can also be used to find the height of the jugular venous column when physical examination of the neck veins is difficult or equivocal. One ICU-based

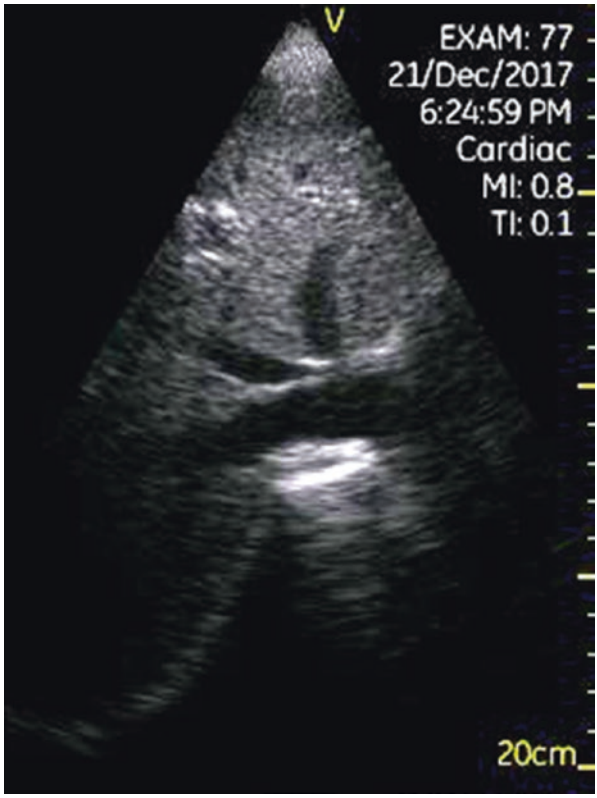

Fig. 9.6 Subcostal view of the IVC by handheld echo

study compared three methods of determining CVP in the critical care setting; measurement of the internal jugular vein height to width ratio (aspect ratio), the inferior vena cava diameter, and the percent collapse of the inferior vena cava with inspiration (collapsibility index) by ultrasound. In this study, it was found that maximal inferior vena cava diameter was a better estimate of central venous pressure than the inferior vena cava collapsibility index or the internal jugular vein aspect ratio [27].

Limitations

POCUS has been demonstrated to be an effective tool in the assessment of left ventricular function, right ventricular function, pericardial effusion and tamponade, volume status, and valvular lesions based on the previously mentioned data. When POCUS is implemented, significant changes in medical management can occur based on these findings. However, the accuracy of the aforementioned structural abnormalities by POCUS is variable. Table 9.1 summarizes the accuracy of POCUS

Table 9.1 Summary of POCUS findings in structural abnormalities

Structural abnormality	Features	Typical views	Limitations
LV Function	Visual estimation, EPSS	PLAX, apical	Poor windows Apical foreshortening
Left atrial enlargement	AP diameter Aorta to LA ratio	PLAX	Poor windows
RV Function	RV enlargement, hypokinesis, septal flattening	PSAX, apical	Apical foreshortening
Valvular disease	Leaflet restriction, leaflet coaptation, calcification, color Doppler findings	PLAX, apical	Lack of spectral Doppler on most devices
Pericardial Effusion	Visual assessment of effusion, size RA/RV collapse	Subcostal	Inability to perform measurements of effusion Lack of spectral Doppler, M-mode, and ECG gating to determine tamponade
CVP	IVC plethora, respiratory variation	Subcostal	Poor windows Difficult in intubated patients

in the assessment of these abnormalities. Based on the available data, the area that requires further study in determination is that of valvular disease. This lack of accuracy in the assessment of valvular disease is due to the fact that most ultrasounds and handheld devices include 2D and color Doppler without spectral Doppler which is used in complete echocardiography to assist in the determination of lesion severity. As technology advances, it is likely that spectral Doppler will be incorporated into newer models.

Another recognized limitation in POCUS is that the quality and interpretation of cardiac ultrasound is dependent on the level of training of the examiner. Numerous studies have shown that physicians of various fields and levels of training can interpret POCUS with acceptable diagnostic accuracy as compared to cardiologists and echocardiographers. At the same time, precise assessment of cardiac abnormalities requires a high degree of expertise in cardiac ultrasound and is beyond the scope of POCUS. Therefore, caution should be exercised when implemented a POCUS program in the critical care and emergency room settings, with careful attention payed to the provider training, scope of practice, documentation, and medicolegal aspects. Overreliance on POCUS findings, especially with less trained examiners, may lead to incorrect diagnosis and management errors.

Conclusions

POCUS has been shown to be an effective tool as an adjunct to the physical examination in critically ill patients. At the hands of a cardiologist, ED physician, or an ICU physician, POCUS has been shown to be performed and interpreted with

reasonable accuracy in the aforementioned clinical conditions. Diagnosing such conditions can significantly impact medical management and reduce the time to change in management. As technology advances, devices for performing POCUS are becoming more advanced with improved image quality and functionality, making more complete assessments possible.

References

1. Whitson MR, Mayo PH. Ultrasonography in the emergency department. Crit Care. 2016;20(1):227. https://doi.org/10.1186/s13054-016-1399-x.
2. Kimura BJ. Point-of-care cardiac ultrasound techniques in the physical examination: better at the bedside. Heart. 2017;103(13):987–94. https://doi.org/10.1136/heartjnl-2016-309915.
3. Arntfield RT, Millington SJ. Point of care cardiac ultrasound applications in the emergency department and intensive care unit—a review. Curr Cardiol Rev. 2012;8(2):98–108.
4. Spencer KT, Kimura BJ, Korcarz CE, Pellikka PA, Rahko PS, Siegel RJ. Focused cardiac ultrasound: recommendations from the American Society of Echocardiography. J Am Soc Echocardiogr. 2013;26(6):567–81. https://doi.org/10.1016/j.echo.2013.04.001.
5. Chamsi-Pasha MA, Sengupta PP, Zoghbi WA. Handheld echocardiography: current state and future perspectives. Circulation. 2017;136(22):2178–88. https://doi.org/10.1161/CIRCULATIONAHA.117.026622.
6. McGee S. Evidence-based physical diagnosis. 3rd ed. Philadelphia, PA: Elsevier Saunders; 2012. p. 320–36.
7. Mark DG, Ku BS, Carr BG, Everett WW, Okusanya O, Horan A, et al. Directed bedside transthoracic echocardiography: preferred cardiac window for left ventricular ejection fraction estimation in critically ill patients. Am J Emerg Med. 2007;25(8):894–900. https://doi.org/10.1016/j.ajem.2007.01.023.
8. McKaigney CJ, Krantz MJ, La Rocque CL, Hurst ND, Buchanan MS, Kendall JL. E-point septal separation: a bedside tool for emergency physician assessment of left ventricular ejection fraction. Am J Emerg Med. 2014;32(6):493–7. https://doi.org/10.1016/j.ajem.2014.01.045.
9. Kimura BJ, Kedar E, Weiss DE, Wahlstrom CL, Agan DL. A bedside ultrasound sign of cardiac disease: the left atrium-to-aorta diastolic diameter ratio. Am J Emerg Med. 2010;28(2):203–7. https://doi.org/10.1016/j.ajem.2008.10.006.
10. Picano E, Pellikka PA. Ultrasound of extravascular lung water: a new standard for pulmonary congestion. Eur Heart J. 2016;37(27):2097–104. https://doi.org/10.1093/eurheartj/ehw164.
11. Liteplo AS, Marill KA, Villen T, Miller RM, Murray AF, Croft PE, et al. Emergency thoracic ultrasound in the differentiation of the etiology of shortness of breath (ETUDES): sonographic B-lines and N-terminal pro-brain-type natriuretic peptide in diagnosing congestive heart failure. Acad Emerg Med. 2009;16(3):201–10. https://doi.org/10.1111/j.1553-2712.2008.00347.x.
12. Melamed R, Sprenkle MD, Ulstad VK, Herzog CA, Leatherman JW. Assessment of left ventricular function by intensivists using hand-held echocardiography. Chest. 2009;135(6):1416–20. https://doi.org/10.1378/chest.08-2440.
13. Randazzo MR, Snoey ER, Levitt MA, Binder K. Accuracy of emergency physician assessment of left ventricular ejection fraction and central venous pressure using echocardiography. Acad Emerg Med. 2003;10(9):973–7.
14. Panoulas VF, Daigeler AL, Malaweera AS, Lota AS, Baskaran D, Rahman S, et al. Pocket-size hand-held cardiac ultrasound as an adjunct to clinical examination in the hands of medical students and junior doctors. Eur Heart J Cardiovasc Imaging. 2013;14(4):323–30. https://doi.org/10.1093/ehjci/jes140.

15. Kimura BJ, Amundson SA, Willis CL, Gilpin EA, DeMaria AN. Usefulness of a hand-held ultrasound device for bedside examination of left ventricular function. Am J Cardiol. 2002;90(9):1038–9.
16. Abe Y, Ito M, Tanaka C, Ito K, Naruko T, Itoh A, et al. A novel and simple method using pocket-sized echocardiography to screen for aortic stenosis. J Am Soc Echocardiogr. 2013;26(6):589–96. https://doi.org/10.1016/j.echo.2013.03.008.
17. American College of Cardiology Foundation/American Heart Association Task Force on Practice Guidelines, American Association for Thoracic Surgery, American Society of Echocardiography, American Society of Nuclear Cardiology, Heart Failure Society of America, Heart Rhythm Society, et al. ACCF/AHA guideline for the diagnosis and treatment of hypertrophic cardiomyopathy: a report of the American College of Cardiology Foundation/American Heart Association Task Force on Practice Guidelines. J Thorac Cardiovasc Surg. 2011;142(6):e153–203. https://doi.org/10.1016/j.jtcvs.2011.10.020.
18. Dinh V, Tseeng S, Jafry Z, Alice B, Schaefer M, Nakashioya J. Cases that count: use of POCUS for the diagnosis and management of hypertrophic obstructive cardiomyopathy: American College of Emergency Physicians; [cited 2017]. https://www.acep.org/_Ultrasound-Section-Microsite/Cases-that-Count--Use-of-POCUS-for-the-Diagnosis-and-Management-of-Hypertrophic-Obstructive-Cardiomyopathy/.
19. Martin LD, Howell EE, Ziegelstein RC, Martire C, Whiting-O'Keefe QE, Shapiro EP, et al. Hand-carried ultrasound performed by hospitalists: does it improve the cardiac physical examination? Am J Med. 2009;122(1):35–41. https://doi.org/10.1016/j.amjmed.2008.07.022.
20. Marcolini E. Critical care emergencies, an issue of emergency medicine clinics of North America. 1st ed. Philadelphia, PA: Elsevier; 2014.
21. Mansencal N, Redheuil A, Joseph T, Vieillard-Baron A, Jondeau G, Lacombe P, et al. Use of transthoracic echocardiography combined with venous ultrasonography in patients with pulmonary embolism. Int J Cardiol. 2004;96(1):59–63. https://doi.org/10.1016/j.ijcard.2003.05.029.
22. Klein AL, Abbara S, Agler DA, Appleton CP, Asher CR, Hoit B, et al. American Society of Echocardiography clinical recommendations for multimodality cardiovascular imaging of patients with pericardial disease: endorsed by the Society for Cardiovascular Magnetic Resonance and Society of Cardiovascular Computed Tomography. J Am Soc Echocardiogr. 2013;26(9):965–1012. e15. https://doi.org/10.1016/j.echo.2013.06.023.
23. Ceriani E, Cogliati C. Update on bedside ultrasound diagnosis of pericardial effusion. Intern Emerg Med. 2016;11(3):477–80. https://doi.org/10.1007/s11739-015-1372-8.
24. Mandavia DP, Hoffner RJ, Mahaney K, Henderson SO. Bedside echocardiography by emergency physicians. Ann Emerg Med. 2001;38(4):377–82. https://doi.org/10.1067/mem.2001.118224.
25. Miller A, Mandeville J. Predicting and measuring fluid responsiveness with echocardiography. Echo Res Pract. 2016;3(2):G1–G12. https://doi.org/10.1530/ERP-16-0008.
26. Mok KL. Make it SIMPLE: enhanced shock management by focused cardiac ultrasound. J Intensive Care. 2016;4:51. https://doi.org/10.1186/s40560-016-0176-x.
27. Prekker ME, Scott NL, Hart D, Sprenkle MD, Leatherman JW. Point-of-care ultrasound to estimate central venous pressure: a comparison of three techniques. Crit Care Med. 2013;41(3):833–41. https://doi.org/10.1097/CCM.0b013e31827466b7.

Chapter 10
Non-cardiac Point of Care Ultrasound in the CCU

Nick Pakzad, Ismini Kourouni, Joseph P. Mathew, and Gopal Narayanswami

Abstract Point-of-care ultrasonography (POCUS) has rapidly emerged as an invaluable tool in the assessment and management of the critically ill CCU patient. Whole-body bedside ultrasound, with evaluation of the heart, lungs, abdomen, and the vascular system, allows for rapid diagnosis and timely treatment of conditions such as shock, acute respiratory failure, and multi-organ dysfunction. Training in POCUS also facilitates improved safety and success of bedside procedures that are routinely performed in the CCU.

Keywords Pleural effusion · Pulmonary edema · Central line

Introduction

Point-of-care ultrasound (POCUS), also referred to as critical care ultrasonography (CCUS) or whole-body ultrasound (WBU), consists of focused ultrasonography performed by a clinician to answer a clinical question or to assist with an invasive procedure. The exam is performed at the bedside and is interpreted in real time by the same clinician, allowing for the rapid and accurate assessment of a patient's condition [1–4]. When performed with a focused clinical question or goal in mind, POCUS serves as a valuable adjunct to the physical exam and significantly increases procedure success rates and safety [5–8].

As the most important innovation in critical care over the past decade, POCUS has enabled expedited and improved quality of care for critically ill patients. The advent of affordable portable ultrasound machines has allowed for widespread training in both cardiac and non-cardiac POCUS and is rapidly becoming the standard of care [1, 9]. In this chapter we describe the role of non-cardiac ultrasound in

N. Pakzad · I. Kourouni · J. P. Mathew (✉) · G. Narayanswami
Division of Pulmonary, Critical Care, and Sleep Medicine, Mount Sinai St. Luke's and Mount Sinai West, New York, NY, USA
e-mail: joseph.mathew@mountsinai.org

E. Herzog, E. Argulian (eds.), *Echocardiography in the CCU*,
https://doi.org/10.1007/978-3-319-90278-4_10

the evaluation and management of the CCU patient presenting with shock, respiratory failure, and multi-organ dysfunction [10].

Basic Principles of Ultrasonography

In order to properly understand and accurately interpret ultrasound (US) images, one must first have knowledge of the basic principles of ultrasonography (USG). This includes familiarity with the equipment and modalities available. Modern-day ultrasound machines use sound waves with frequencies ranging anywhere from 2 to 15 MHz, created by a vibrating crystal within a ceramic transducer. These crystals can send and receive sound waves, and the screen image is created from information on strength, timing, and positioning of the returning sound wave [10, 11].

As ultrasound waves pass through various types of tissue, they are partly reflected at each tissue interface. US waves penetrate well through solid organs and fluid; however, they do not penetrate air or bone; hence the ribs are often a hindrance when performing echocardiography and thoracic ultrasonography. The bone typically has a white leading edge and then a black shadow due to near total reflection of US waves. Air is completely reflected back to the transducer. If air is in the way of sound waves, it generates "A-lines" or "air lines" which are a reverberation artifact [11].

When performing B-mode ultrasonography, bright structures such as the diaphragm and pleura are referred to as *hyperechoic*, as they represent echogenic structures that transmit and reflect US waves. On the other hand, *anechoic* or black regions occur when US waves encounter a structure, such as a fluid cavity, which does not reflect any waves and does not return back to the transducer. US waves propagate well through fluid, and hence this is an excellent medium to see other nearby structures. Low amplitude US waves are translated into shades of gray or *hypoechoic* regions. Lastly, lines occur at boundaries between two markedly different tissue reflectors, delineating the two structures. Soft tissue often has white, gray, and black planes and borders, representing different speeds of propagation and reflection of US waves [11]. Table 10.1 lists examples of structures of different echogenicity.

Equipment and Image Acquisition

Portable ultrasound machines offer an array of transducers (also called probes), all with different indications based on the frequency of US waves they emit and their footprint (Table 10.2). *Linear array* transducers emit high-frequency US waves (5–15 MHz), providing excellent resolution of superficial structures. In the CCU, this

Table 10.1 Differences in tissue echogenicity

Grayscale	Terminology	Structure	Example
	Anechoic	Pure fluid	Pleural or pericardial effusion
			Ascites
			Bladder
			Veins and arteries
	Hypoechoic	Thick fluid, thrombosis, consolidation, tissue/organs	Hemothorax or hemoperitoneum
			DVT
			Pneumonia
			Liver, spleen, kidney, bowel
			Fat, lymph nodes, nerve
	Hyperechoic	Bone/calculus, strong interface	Ribs, kidney, or gallstones
			Pleura, pericardium
			Diaphragm, nerve, tendon

Table 10.2 Transducer characteristics

Transducer	Frequency	Characteristics	Uses
Linear array 	5–15 MHz	High frequency Excellent resolution of superficial structures Loss of depth	Vascular access DVT study Pleural lines Soft tissue and musculoskeletal imaging
Phased array 	1–5 MHz	Low frequency Small footprint Deep penetration	Cardiac Lung/pleural Abdomen
Microconvex 	5–8 MHz	Small footprint Good resolution	Lung Abdomen Vascular Nerve

(continued)

Table 10.2 (continued)

Transducer	Frequency	Characteristics	Uses
Curvilinear 	1–8 MHz	Low frequency Low resolution Multipurpose Full depth of penetration	Abdominal/ pelvic imaging FAST exam Lung/cardiac

can be used for vascular ultrasonography, specifically for procedural guidance during vascular access and also to assess for deep vein thrombosis (DVT). It can be used to image the pleura and rule out pneumothorax. Due to its poor penetration into the body, it is not used to image deeper structures. *Phased array* transducers are low-frequency transducers (1–5 MHz) that provide good penetration into the body and also have small footprint that allows for image acquisition between the ribs. In the CCU, this can be used to image deeper organs such as the heart, lungs, and abdominal structures. *Curvilinear* transducers are hybrid, multipurpose transducers that image at lower frequencies (1–8 MHz). The larger footprint makes it more ideal for abdominal and pelvic imaging and for performing the FAST (focused abdominal sonography for trauma) exam where the subcostal cardiac view can also be obtained [1, 2, 12–15].

Portable US machines have preset imaging settings (e.g., abdomen vs. cardiac) for each organ, which sets the resolution, frame rates, and the location of the screen marker. This is important because if one is performing cardiac imaging in the abdominal preset, the image will be reversed as the screen marker may be on the opposite side; moreover, the frame rates will be suboptimal for cardiac imaging. All US transducers have a marker that correlates to the marker on the US monitor. The operator should always be aware of the orientation of the probe marker in relation to the marker on the monitor screen. Structures adjacent to the probe marker will appear on the same side of the image as the screen marker, helping to orient the viewer and guide probe manipulations. Structures closest to the footprint of the transducer will appear on the top of the screen (near field) and those furthest away will appear on the bottom (far field). The transducer should be held steady, as if holding a pencil (Fig. 10.1), and should be manipulated gently to allow for optimal image acquisition [11].

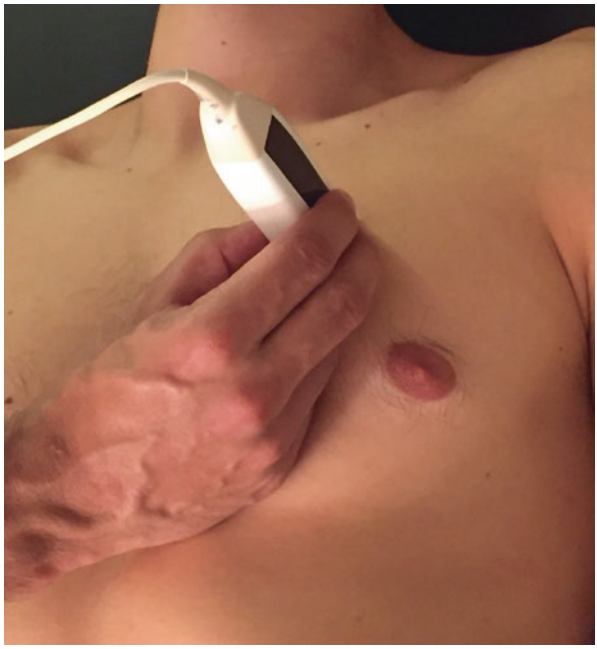

Fig. 10.1 Proper technique for holding the probe. Resting palm of hand on the patient's body allows for greater control

Obtaining quality images will involve optimizing the gain and depth of the imaging. *Gain* adjusts the brightness of the entire image and should be adjusted such that there is maximal resolution between the different tissues that are imaged. Failure to adjust gain can lead to misinterpretation of image. *Depth* is manipulated on the console such that the structure of interest should always be in the center of the screen. The depth of interrogation is usually shown on a scale on the monitor. The operator should familiarize oneself with other features of the portable US machine such as how to *freeze* and measure structures using the *caliper* button, how to *save* images and clips, and how to utilize features such as *M-mode* and *Doppler*.

Practical Applications of POCUS

The critical care US exam performed in the CCU generally involves scanning the major organ systems that would answer the question about the presenting condition. The main regions that are scanned include thoracic (lung and pleural),

cardiac, limited abdominal, and vascular imaging (DVT assessment). The organ of interest is often scanned first (e.g., the heart in shock or lungs in respiratory failure); however, a standardized multi-organ approach can be used for the critically ill CCU patient. Although a focused exam is often all that is needed, studies have shown that a multi-organ or whole-body approach leads to a more accurate diagnosis [4, 16, 17]. The US exam should always be performed in conjunction with the patient's clinical data and then repeated to reassess the patient.

The most common indication for POCUS in the CCU is cardiopulmonary failure. It is very helpful in the CCU patient who suddenly deteriorates; POCUS can be used to quickly rule out pneumothorax, massive pulmonary embolism (PE), pericardial tamponade, valvular rupture, and intra-abdominal bleeding. In the patient with undifferentiated shock, POCUS can help distinguish between obstructive, cardiogenic, hypovolemic, and distributive shock states [4, 16–18]. In the patient with acute respiratory failure, focused US imaging of the heart, lungs, and deep veins can help differentiate various causes of respiratory failure [19]. Assessing inferior vena cava (IVC) size and variation, as well as imaging the heart and lungs, can help guide fluid resuscitation [13]. Assessing the lungs for extravascular lung water during fluid resuscitation can limit over-administration of fluids and decrease days of ventilator support [20].

Thoracic Ultrasonography

Basic Principles

The lung was traditionally not considered an organ that was amenable for ultrasonography since the lungs are filled with air and US waves cannot be transmitted through air-filled structures. When the lungs become devoid of air and the alveoli displaced by fluid, blood, or pus, US findings change and allow for clinical interpretation. Since air is a near total reflector of US, the healthy or "unhealthy" pleural line serves as the generator of reflecting signs, which can be interpreted. The findings of lung ultrasonography relate to the ratio of air to fluid within the lung. Most lung processes (e.g., pulmonary edema, pneumonia, pneumothorax, pleural effusion, and atelectasis) all extend to the lung periphery allowing the US machine's ability to distinguish air and water to produce artifacts [16, 21]. Lung ultrasonography is therefore based on the clinical interpretation of a number of dynamic artifacts.

Lung and Pleural Examination

A low-frequency phased array transducer (1–5 MHz) or micro-convex (5–8 MHz) transducer is preferable as it fits in the rib interspace [15]. A high-frequency linear array transducer (5–15 MHz) can be used to visualize the superficial pleural line; however, it is limited by the depth of penetration (<8 cm) and the linear trajectory of the US waves [21]. When performing thoracic USG, the transducer is held perpendicular to the body in a longitudinal orientation, with the marker facing cephalad (Fig. 10.2). In most

portable US machines, the abdominal preset can be selected for thoracic USG. With a preset depth of 16 cm and the screen marker in the upper left corner of the monitor, the gain and depth must be further adjusted to optimize and center the image.

A complete lung exam can be performed by dividing the thorax into three zones: anterior, lateral, and posterior zone, demarcated by the anterior and posterior axillary line (Fig. 10.2) and then further into upper and lower zones [15]. Thus, a complete exam consists of 12 imaging regions, 6 in each hemithorax (Fig. 10.3). As a general rule, these lung zones can be assessed by using cephalad to caudal scan lines throughout each lung zone (Fig. 10.4). Alternatively, Lichtenstein describes four points in each hemithorax that can be quickly assessed as part of the BLUE (Bedside Lung Ultrasound in Emergency) protocol (Fig. 10.5), a goal-directed lung ultrasound (LUS) exam that can be performed in <3 min [19].

In each lung zone, identify the ribs and direct the US beam between them. The *anterior lung zone* is assessed for pneumothorax, alveolar-interstitial syndromes

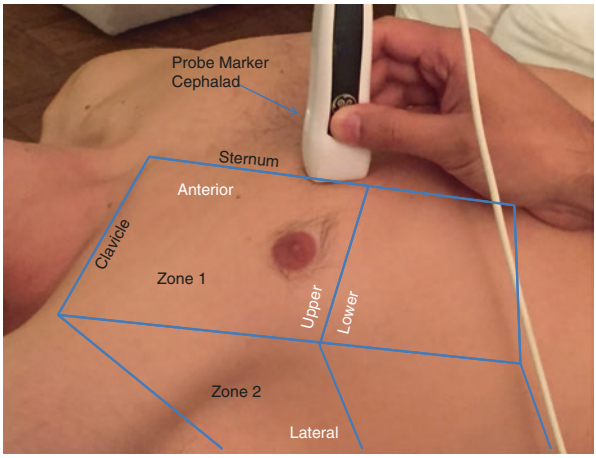

Fig. 10.2 Lung zones for thoracic ultrasonography Zone 3 (posterior) not shown

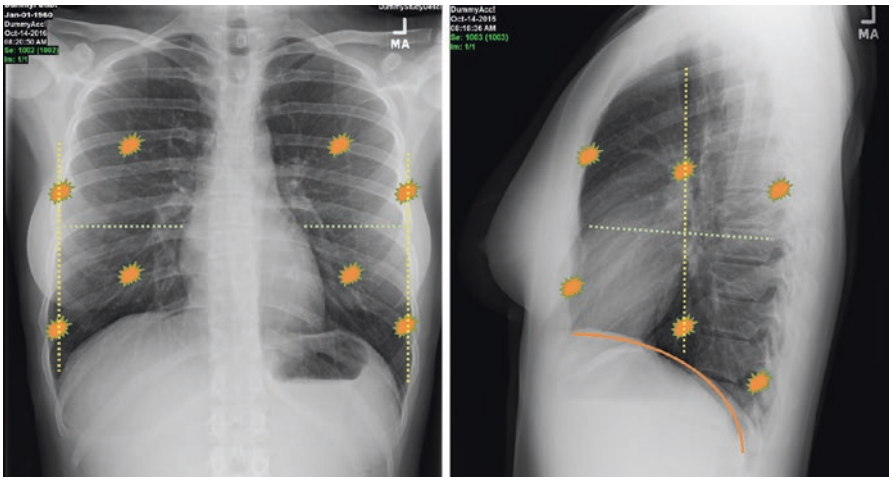

Fig. 10.3 Six scan points in each hemithorax

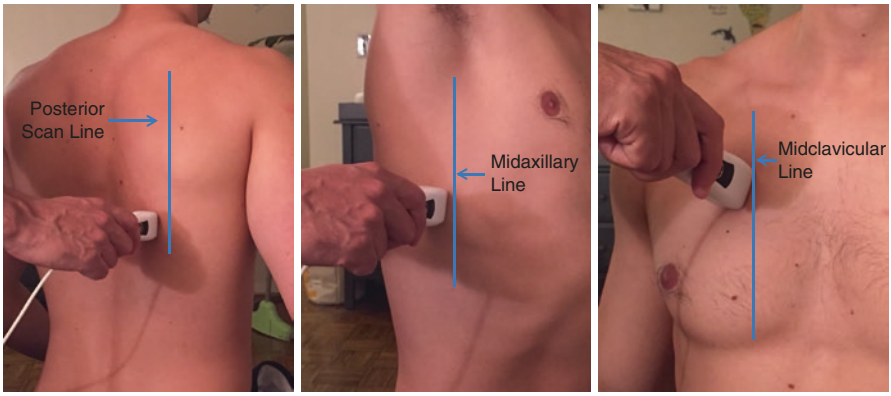

Fig. 10.4 Scan lines to evaluate the three lung zones

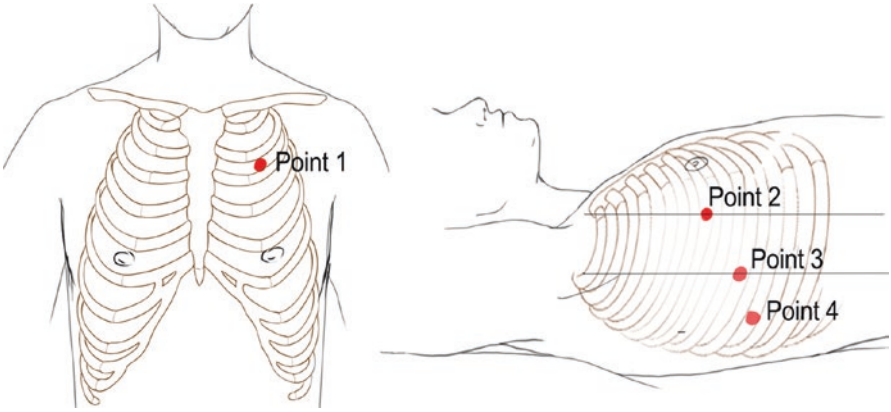

Fig. 10.5 BLUE protocol

such as pulmonary edema, and lung consolidation, which is seen with pneumonia. In the *lateral lung zone*, it is important to identify the kidney, liver or spleen, and the hyperechoic hemidiaphragm as the main anatomical landmarks and then assess for pleural effusions, atelectasis, and consolidation above the hemidiaphragm. The *posterior lung zone* (BLUE point 4) is a forgotten region where dependent pleural effusions and lung consolidation may be seen, so it is important to turn the supine critically ill patient to expose this area.

Normal and Abnormal Lung and Pleural Signs

There are five cardinal signs to look for when performing thoracic ultrasonography. Table 10.3 describes these and additional signs that are described in lung and pleural

Table 10.3 Normal and abnormal signs in lung ultrasonography

Sign	Lung ultrasound pattern	Clinical significance
A-line	Horizontal reflections or reverberations of pleural line Hyperechoic and equal in distance from the skin to pleural line	Present in normal lung "Air" line—indicates air in the lung or pleural space
B-lines	"Comet-tail" or "lung rockets"—vertical hyperechoic reverberation artifacts that arise from the pleural line and extend to the bottom of the screen Move synchronously with the lung sliding and efface A-lines. Implies fluid-filled subpleural interlobular septa	>3 B-lines = interstitial pathology Multiple diffuse B-lines indicate interstitial syndrome Focal B-line can be seen in pneumonia, infarct, cancer
Lung sliding	Sliding or shimmering of the pleural line that occurs with respiration Indicates intact visceral and parietal pleura	Present in normal lung, absent in pneumothorax, apnea, fibrosis, ARDS, pleurodesis
Lung pulse	Subtle rhythmic movement of the visceral upon the parietal pleural with cardiac oscillations	Present in normal lung Rules out pneumothorax
Seashore sign	Normal M-mode image with lines above echogenic pleura and speckled pattern deep to it indicating normal lung sliding	Normal aeration pattern No pneumothorax
Bar code or stratosphere sign	Abnormal M-mode image showing a linear pattern above and below the pleura	Signifies absence of lung sliding; can be seen with pneumothorax
Lung point	Transition point where visceral and parietal pleura separate—image changes from the intermittent presence and then absence of lung sliding	Pathognomonic sign for pneumothorax
Lung hepatization/ consolidation	Loss of aeration of the lung leads to a hyperechoic appearance of the lung; alveoli are filled with fluid or inflammatory cells or are atelectatic	Can be seen with atelectasis or pneumonia
Dynamic air bronchograms	Dynamic echogenic foci within consolidated lung that fluctuate with the respiratory cycle	Seen with pneumonia
Static air bronchograms	Hyperechoic foci which does not move with respiration	Seen with atelectasis
Shred sign	Border between consolidated and aerated lung	Seen with consolidation but not translobar consolidation
Curtain sign	Intermittent obscuration of underlying organs by intervening air-filled lung	Can be normal finding
Hematocrit sign	Effusion is separated into different echogenicity with a layering effect	Seen in hemothorax or highly cellular effusions (e.g., malignant effusion)
Flapping lung (jellyfish sign)	Floating movement of collapsed lung with in a pleura effusion	Atelectatic lung in effusion
Sinusoid sign	In a pleural effusion, M-mode appearance of the pleura moving toward and away from the parietal pleura	Can be used to distinguish pleural thickening from effusion
Plankton sign	Particulate matter in lung effusion	Complex effusion

Table 10.4 Lung ultrasound patterns

Lung Ultrasound pattern	Clinical significance
A lines with lung sliding	Normal aeration pattern
A lines without lung sliding and +lung point	Pneumothorax
B7 lines	Interlobular septal pathology
B3 lines	Alveolar-interstitial syndrome
Focal absence of B-lines	Pulmonary embolus, cancer
Lung hepatization + dynamic air bronchograms	Pneumonia
Lung hepatization ± static air bronchograms	Atelectasis
Anechoic collection without septations	Simple pleural effusion
Echogenic fluid with septations	Complicated effusion

ultrasonography. Table 10.4 summarizes common lung ultrasound patterns seen in common disease processes that may be encountered in the CCU.

Lung Sliding

As the lungs expand during respiration, the visceral pleura surface slides relative to the parietal pleura and chest wall. This creates a subtle shimmering of the hyperechoic pleural line (Fig. 10.6). This is particularly evident using a high-frequency linear array transducer. The presence of lung sliding strongly suggests that two conditions are met: the pleural surfaces are adjacent (i.e., no pneumothorax) and that the patient is ventilating. The presence of lung sliding essentially rules out pneumothorax with 100% certainty at that particular point on the thorax [15, 22]. A similar analogous sign can be from *lung pulse*, which is produced when cardiac motion causes pulsations of the pleural line [23]. Air in the pleural space (i.e., pneumothorax) will cause absence of lung sliding and lung pulse, as the US waves do not propagate through the pleural air. Other conditions that can cause absence of lung sliding include apnea or hypoventilation (e.g., contralateral bronchial intubation), prior pleurodesis, and dense lung consolidation.

A-Lines

A-lines are hyperechoic lines, which are reverberation artifacts of the pleural line (Fig. 10.7). The distance from the transducer to the pleural line and each subsequent A-line will be equal. A-lines can also be thought of as "air" lines, but the air can be either in the pleural space or within the lung parenchyma. The presence of sliding lung determines that the air is in the lung parenchyma and the absence of it indicates that the air maybe in the pleural space. Hence the presence of A-lines and sliding lung means the lungs are normally aerated at that particular site. The standard view of the upper rib, pleural line, A-line, and lower rib has the appearance of a bat flying out of the screen, hence called a *batwing sign* (Fig. 10.8) [19, 21].

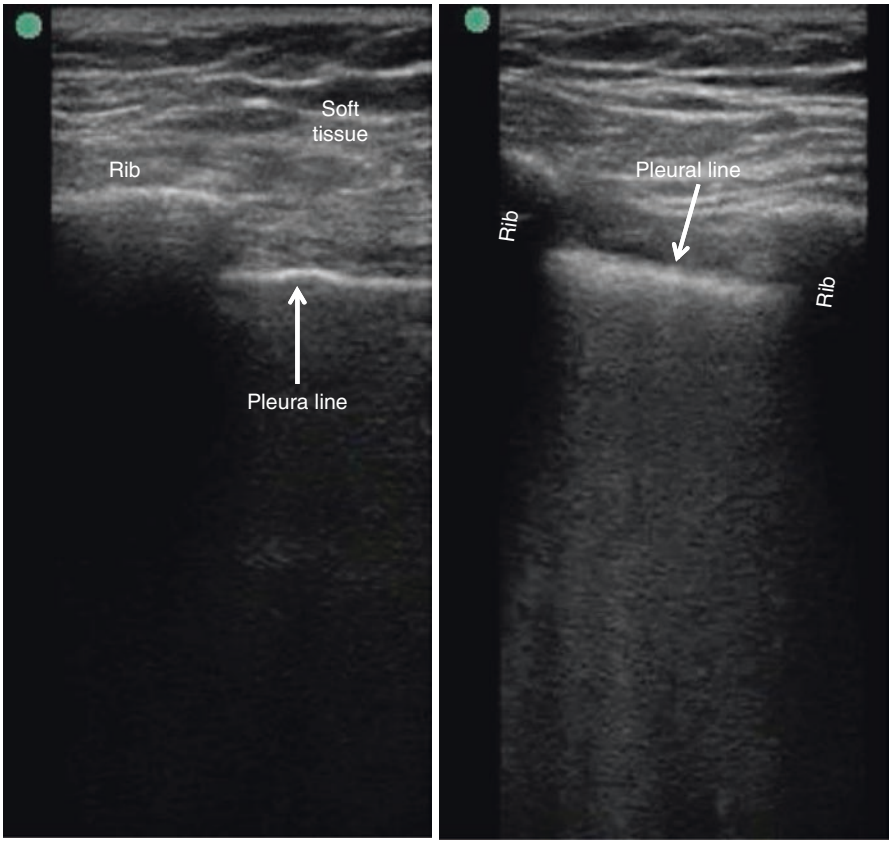

Fig. 10.6 Normal pleural line with lung sliding imaged with linear array transducer

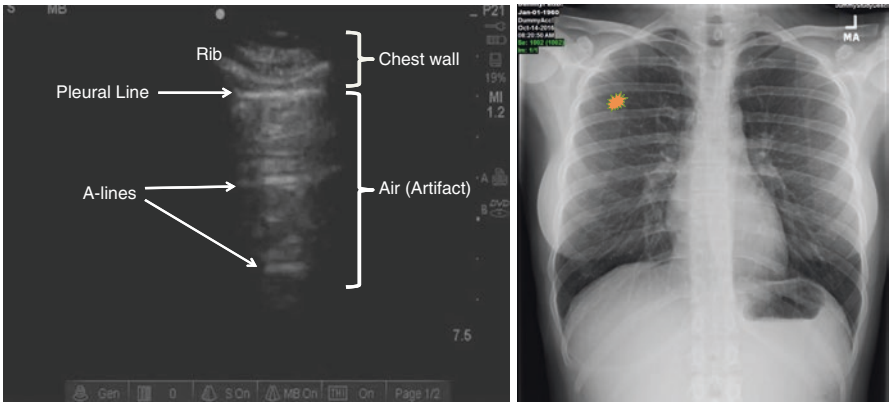

Fig. 10.7 Standard view of A-lines from anterior lung zone imaged with phased array transducer

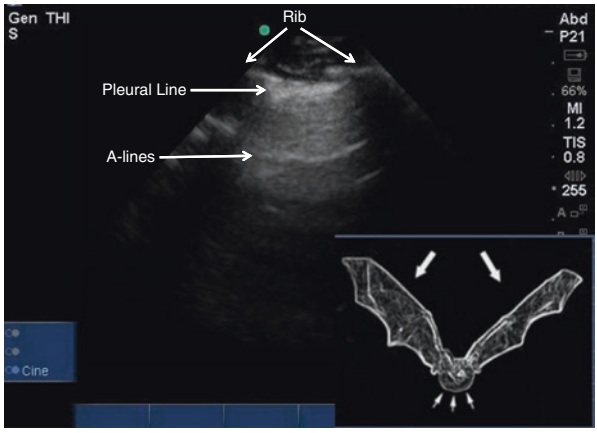

Fig. 10.8 The bat sign is a basic step which allows to locate the lung surface in any circumstance

B-Lines

B-lines, also called comet tails or lung rockets, are vertical ray-like projections that extend from the pleura to the edge of the screen (Fig. 10.9). B-lines move in conjunction with lung sliding and obliterate A-lines. B-lines represent thickening of the interlobular septa or an alveolar filling process (e.g., pneumonia or pulmonary edema). A single B-line in the anterior thorax or a few B-lines in the dependent regions of the thorax may be a normal finding. The presence of >3 B-lines in the anterior lung zones is abnormal. The focal location of B-lines may be suggestive of local infiltration (e.g., focal pneumonia). A generalized bilateral B-line pattern represents an interstitial syndrome such as pulmonary edema, pneumonia, acute respiratory distress syndrome (ARDS), or interstitial lung disease (ILD) [19, 24, 25].

Alveolar Consolidation

When the normally aerated alveoli fill with fluid and inflammatory cells or become atelectatic, US waves can penetrate the lung and reveal echogenic tissue deep to the pleura. Areas of consolidation may have pinpoint hyperechoic opacities corresponding to sonographic air bronchograms, which indicate that air still remains in the bronchioles. It is difficult to distinguish consolidation pattern from pneumonia to atelectasis. Compressive atelectasis is often within a transudative pleural effusion and is associated with volume loss, whereas lung volume is maintained with pneumonia. The term "lung hepatization" is used to describe the hyperechoic solidification of the lung that is seen with pneumonia [15, 19] (Fig. 10.10). Additionally, the presence of mobile or dynamic air bronchograms has a high specificity (94%) for the diagnosis of pneumonia, as compared to static air bronchograms, which is seen in resorptive atelectasis [26]. Figure 10.11 shows an example of lung consolidation in a patient with severe pneumonia with parapneumonic effusion.

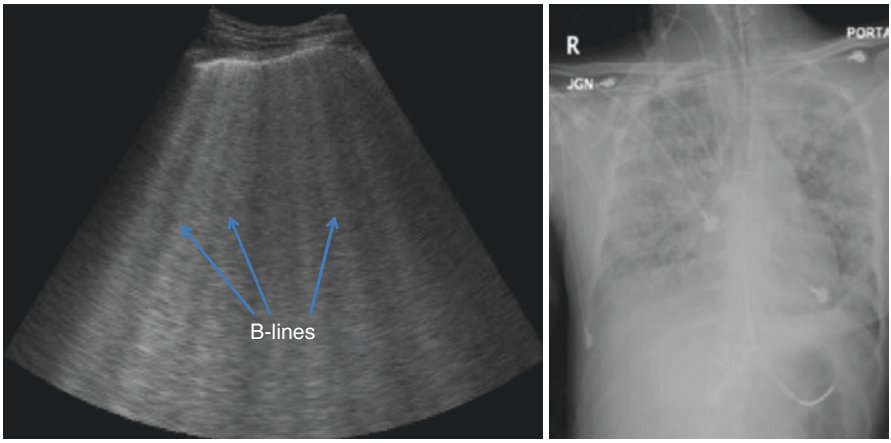

Fig. 10.9 Multiple B-lines in a patient with ARDS

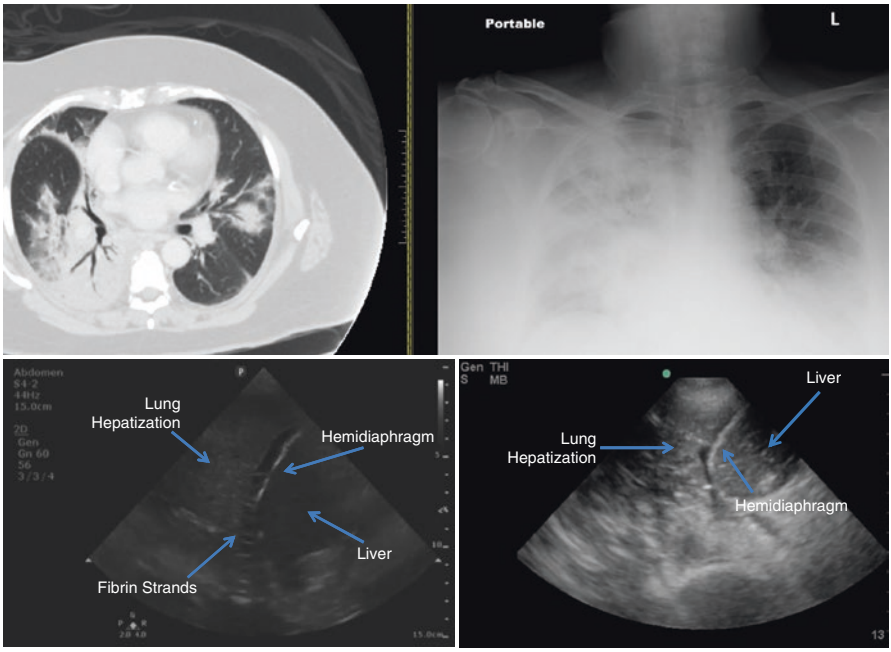

Fig. 10.10 Lung hepatization, indicating loss of aeration due to consolidative process or atelectasis

Pleural Effusion

Ultrasound is a fantastic tool for the rapid diagnosis and characterization of pleural effusion, as well as improving the safety of thoracentesis [7]. It is far superior to the standard chest X-ray (CXR) in differentiating pleural effusions from lung consolidation, which both appear radiopaque on a CXR [27]. Pleural effusion is anechoic

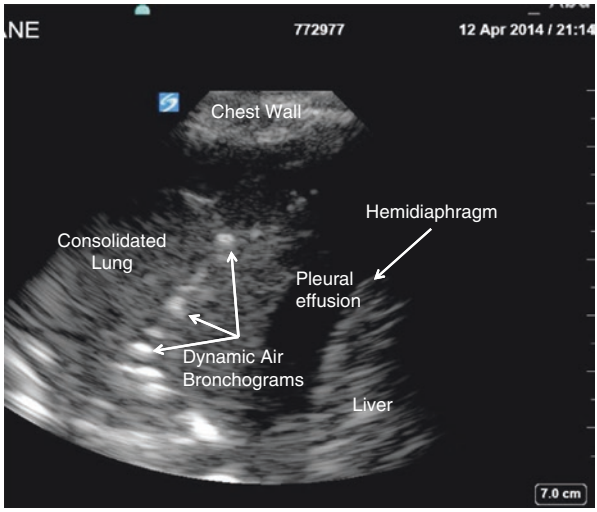

Fig. 10.11 Lung consolidation with sonographic air bronchograms

or hypoechoic on USG, whereas consolidated or atelectatic lung is echogenic. The three main characteristics of a pleural effusion are (1) an anechoic space; (2) anatomic boundaries of the chest wall, diaphragm, and lung; and (3) dynamic changes of the atelectatic lung and diaphragm (Fig. 10.12). Ultrasound can be used to estimate the size of an effusion, as well as whether it is likely to be exudative. Most operators prefer the "eyeball" method to estimate the size of the effusion. One method to quantify the fluid is to measure the horizontal distance from the most cranial aspect of the diaphragm to the nearest segment of the lung in the midaxillary line. This distance (mm) is multiplied by 20 to yield the approximate pleural fluid volume [28, 29].

Simple anechoic fluid suggests a noncomplicated pleural effusion, which may or may not be a transudate. Septated or loculated fluid implies a complicated pleural effusion, which often needs sampling and may warrant chest tube placement or surgical drainage (Fig. 10.13). *Flapping lung* or *jellyfish sign* is the oscillating movement of collapsed lung in a pleural effusion (Fig. 10.14). Strands of echogenic mater floating suggest complex fluid; this is called the *plankton sign* [30]. Similarly, pleural effusions can demonstrate the *hematocrit sign*, where an echogenic or highly cellular effusion (e.g., hemothorax) has gravity-dependent area of increased echogenicity (Fig. 10.14) [30].

Clinical Applications of Thoracic Ultrasonography in the CCU

Detection of Lung Alveolar-Interstitial Syndrome

Various conditions that are encountered in the CCU can lead to an alveolar-interstitial process, including acute pulmonary edema, interstitial pneumonias, and the acute respiratory distress syndrome (ARDS). A diffuse bilateral B-line pattern is

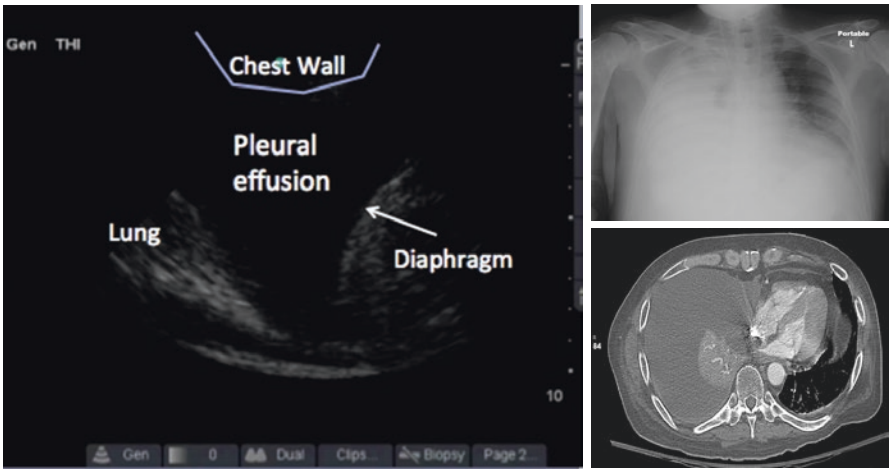

Fig. 10.12 Pleural effusion imaged in the right lateral lung zone imaged with phased array transducer and comparison to CXR and CT scan showing complete opacification of the right hemithorax

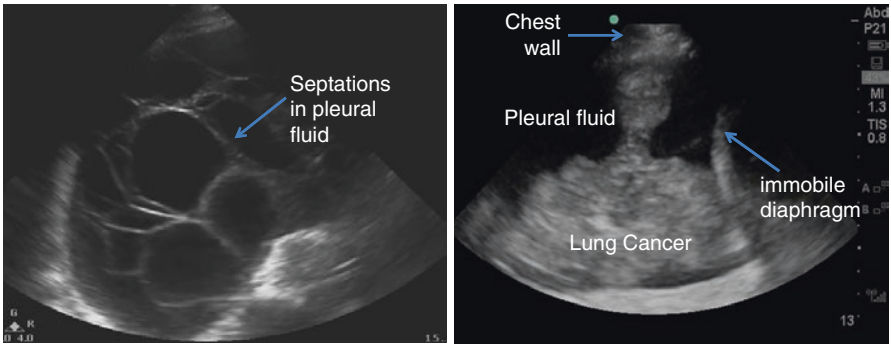

Fig. 10.13 Examples of complex pleural effusions

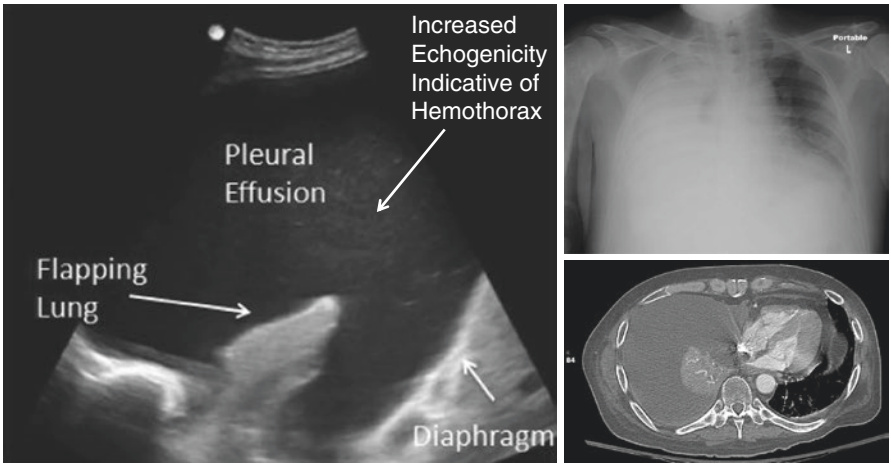

Fig. 10.14 Flapping lung or "jellyfish sign," surrounded by large pleural effusion

seen in patients with both hydrostatic pulmonary edema and the increased permeability edema of ARDS. One can quantify the number of B-lines to assess the degree of lung pathology. *B-7 lines* are 7 mm apart and correspond to edematous or thickened interlobular septa (similar to Kerley B-lines on a CXR or interlobular septal thickening on a CT scan). *B-3 lines* are 3 mm apart and are more confluent, indicating alveolar edema or an alveolar filling process (similar to air space opacities on a CXR or ground glass opacities on a CT scan). The more B-lines that are present anteriorly, the lower the air to fluid and the more severe the lung pathology.

Lung ultrasound (LUS) is very sensitive in detecting early pulmonary vascular congestion, much more than a chest X-ray. This is very helpful during fluid resuscitation, where the appearance of new B-lines corresponds to early pulmonary edema and correlates to elevated pulmonary artery occlusion pressures (PAOP >18 mmHg) [31]. Detection of diffuse B-lines allows the clinician to immediately distinguish acute pulmonary edema from chronic obstructive pulmonary disease (COPD) when the CXR is unhelpful [24]. Similarly, while administering diuretics in the setting of pulmonary edema, the clinician can assess for a reduction in the number of B-lines and also reduction in the volume of pleural effusions. A simplified LUS protocol where only the anterior chest was scanned correlated well with extravascular lung water measured using a transpulmonary thermodilution technique [20]. Recent studies have shown that LUS can be used as a tool in patients on mechanical ventilation for assessing lung recruitment using positive end-expiratory pressure (PEEP) or recruitment maneuvers [32]. Similarly, in patients being weaned from mechanical ventilation, the loss of lung aeration detected using LUS during a spontaneous breathing trial predicted post-extubation respiratory distress [33].

LUS can also help in the differentiation between hydrostatic pulmonary edema and ARDS. In ARDS, subpleural consolidation may be visualized below the pleural line with sparing of certain areas [34]. Performing both cardiac and lung US can also be helpful in the CCU in differentiating cardiogenic pulmonary edema from ARDS and miscellaneous causes of acute hypoxemic respiratory failure [35]. Additionally, assessing the pleura using a linear array transducer can help differentiate the diffuse B-line pattern seen with both pulmonary edema and interstitial lung disease. A smooth pleural line may be seen in pulmonary edema, whereas with lung fibrosis, an irregular or "lumpy bumpy" pleural line will be present. Table 10.5 summarizes main characteristics that can be used to distinguish these entities.

Detection of Pneumothorax

LUS has a high sensitivity (>95%) for the detection of pneumothorax [36]. Pneumothorax can be quickly ruled out in the CCU patient who is decompensating despite mechanical ventilator support or who recently underwent central line placement. The transducer is placed longitudinally in the midclavicular line at the level of the second to third intercostal space. Sequential movement of the transducer inferior and lateral across multiple rib interspaces will allow for a comprehensive

Table 10.5 Differentiating causes of the interstitial syndrome

	Acute pulmonary edema	Chronic heart failure	ARDS	Pulmonary fibrosis
Clinical setting	Acute	Chronic	Acute	Chronic
B-lines number	++++	+/++/+++	++++	+/++/+++
B-lines distribution	Multiple, diffuse, bilateral	Multiple, diffuse, bilateral following dependent regions	Nonhomogeneous distribution, spared areas	More frequently posterior at lung bases
Other lung US signs	Small bilateral pleural effusions	Bilateral pleural effusions	Subpleural consolidations, possible effusion	Irregular pleural line
Echo	Abnormal	Abnormal	Likely normal	Likely normal

examination of the pleural space [15]. Checking for lung sliding before and after central venous catheter (CVC) placement will quickly rule out pneumothorax. The presence of lung sliding carries a 100% negative predictive value in the diagnosis of pneumothorax [22]. In contrast to normal lung, when air is trapped between the visceral and parietal pleural layers, lung sliding will not be detected. Note that absence of lung sliding can also be seen with hypoventilation, massive atelectasis, ARDS, pleural adhesions, and severe lung fibrosis. The presence of B-lines or lung pulse also rules out pneumothorax [23, 25].

If lung sliding is difficult to appreciate, the pleura should be reassessed using a linear array transducer. With normal lungs and pleura, M-mode analysis demonstrates the *seashore sign*, with lines above the hyperechoic pleura and a granular pattern deep to it, representing normal pleural sliding (Fig. 10.15a). In the presence of a pneumothorax, the *stratosphere* or *barcode sign* is seen, with a linear pattern both above and below the pleural line, indicating lack of lung sliding (Fig. 10.15b) [36]. The visualization of the *lung point* may also be used in the diagnosis of pneumothorax, having a specificity of 100% but only moderate sensitivity. The lung point represents the transition point between normal lung sliding and to an area of absent lung sliding (Fig. 10.16) [37]. Lung point is helpful to quantify the size of the pneumothorax and also aids in choosing the location for chest tube placement. LUS can be performed to ensure proper lung aeration after drainage of a pneumothorax and also to evaluate for re-accumulation of air after clamping or removal of a chest tube [38]. Figure 10.17 demonstrates other conditions such as bullous lung disease which can mimic a pneumothorax.

Assessment of Diaphragmatic Function

Phrenic nerve injury or paralysis can occur due to hypothermia or mechanical injury during cardiac surgery or during cardiac ablation procedures. Diaphragmatic function can be quickly assessed in the CCU patient or post-cardiac surgery patient with acute respiratory failure or inability to wean from mechanical ventilation. The

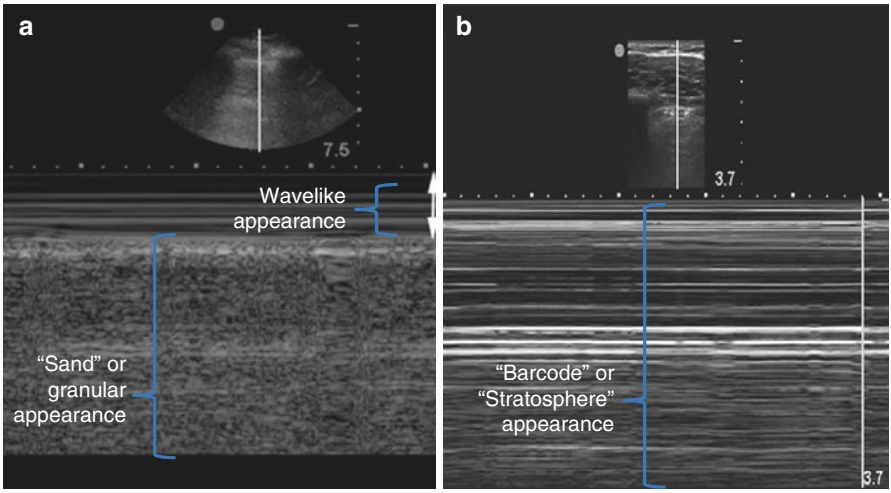

Fig. 10.15 (**a**) Seashore sign. (**b**) Stratosphere or barcode sign

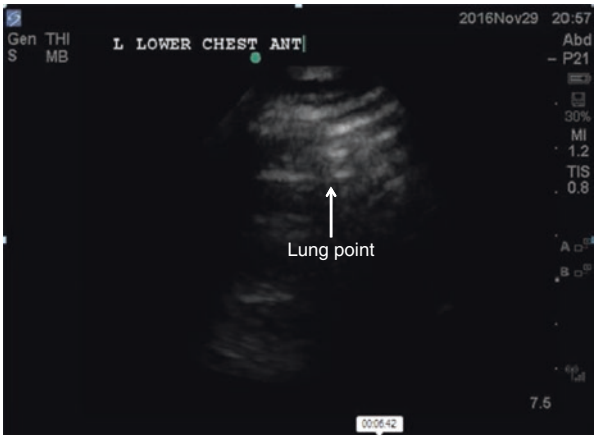

Fig. 10.16 Lung point represents the transition point between normal lung and the pneumothorax

technique involves using the phased array transducer to scan the lateral lung zone, along the anterior or midaxillary line, identifying the liver or spleen. The diaphragm is hyperechoic and easily visualized by ultrasonography. Note the left hemidiaphragm is tougher to locate and may require more posterior imaging. Once visualized, M-mode imaging can be used to measure diaphragmatic excursion. Normal diaphragmatic excursion for a male in quiet breathing is 1.8 cm and 7.5 cm during deep breathing. Sonographically detected diaphragmatic dysfunction, defined as <10 mm or paradoxical motion, can identify patients who are difficult to wean [21]. Figure 10.18 represents 2D and M-mode imaging of the left hemidiaphragm in a patient with amyotrophic lateral sclerosis (ALS). Alternatively, a linear array

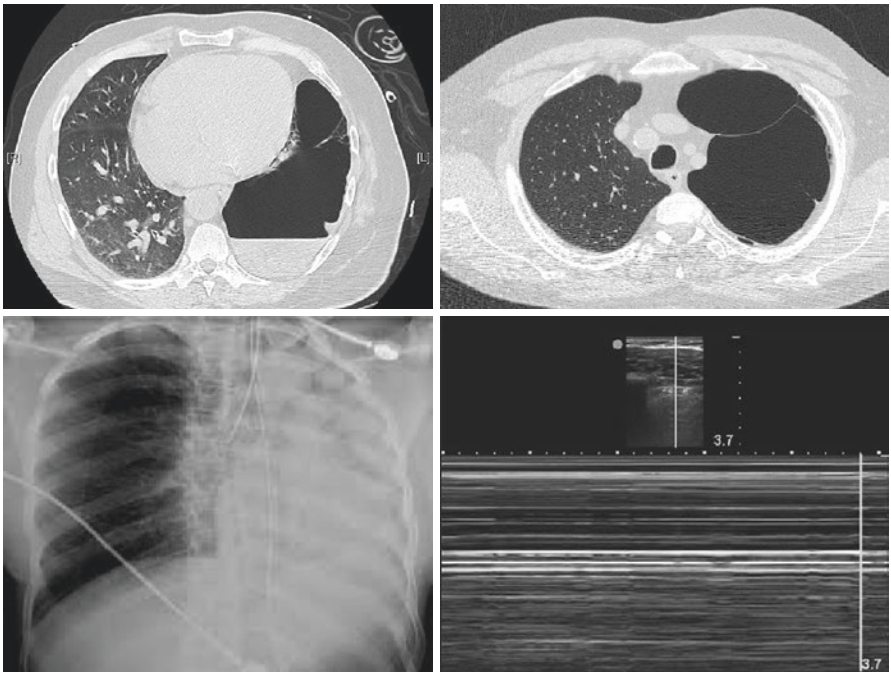

Fig. 10.17 Pneumothorax mimickers on ultrasonography. All may present with lack of lung sliding

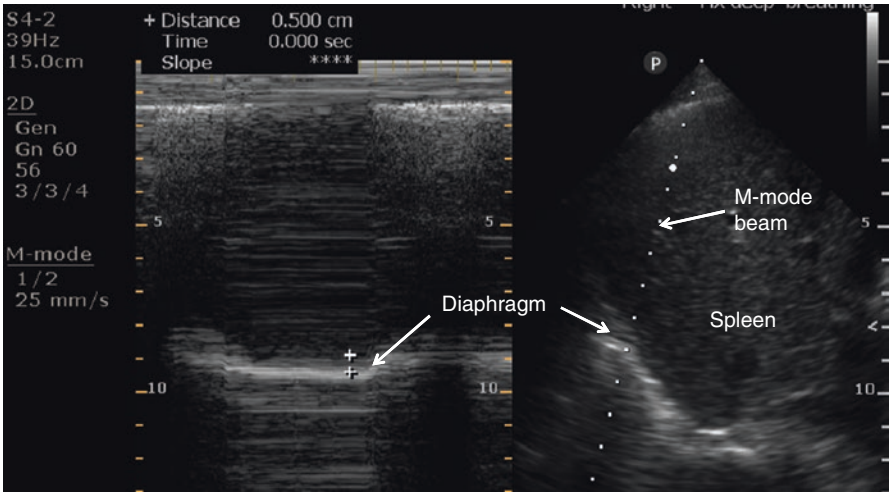

Fig. 10.18 Decreased diaphragmatic excursion on M-mode

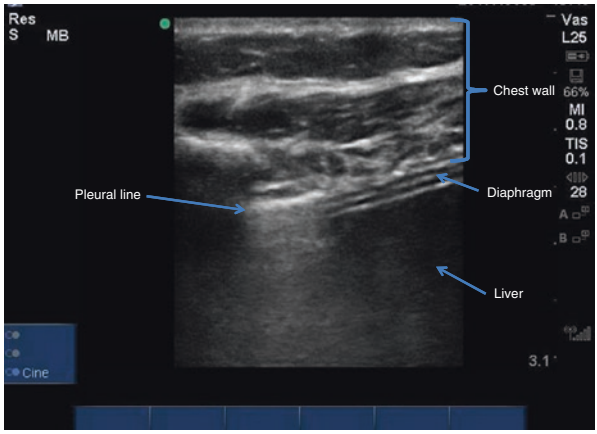

Fig. 10.19 Diaphragm imaged using linear array transducer

transducer can be used to measure diaphragmatic thickness (tdi) at the zone of apposition of the diaphragm to the rib cage (Fig. 10.19). Diaphragmatic thinning and weakening occurs with prolonged mechanical ventilation. Diaphragmatic thickening between end-inspiration and end-expiration (Δtdi > 30%) has been shown to predict extubation success [39].

Rapid Assessment of the Acutely Decompensating CCU Patient

Using the concepts described in this section, one can rapidly evaluate the CCU patient with acute respiratory distress. Bilateral A-line pattern in all three lung zones with presence of sliding lung indicates a normal aeration pattern so the etiology may be due to airways disease (i.e., asthma or COPD) or pulmonary vascular disease or other metabolic causes. A diffuse A-line pattern with lack of sliding lung should prompt the operator to search for lung point to rule out pneumothorax and to perform M-mode analysis to evaluate for barcode sign. A bilateral B-lines pattern with pleural effusions and a smooth pleural line suggest acute cardiogenic pulmonary edema. Bilateral B-lines with subpleural consolidations and areas of sparing are suggestive of ARDS. Unilateral B-lines or a consolidation pattern with dynamic air bronchograms can be seen with pneumonia [15]. Combining thoracic ultrasound with goal-directed echocardiography can detect findings such as right ventricular strain or clot-in-transit, leading to a diagnosis of acute PE [40].

Daniel Lichtenstein developed the BLUE protocol, a simple, goal-directed LUS examination combined with a DVT study for the evaluation of acute respiratory failure. Blinded investigators scanned the four BLUE points and performed compression ultrasound of the lower extremities, following a standardized algorithm (Fig. 10.20). They were able to rapidly make an accurate diagnosis in 90% of the cases. The LUS profiles had very good sensitivity and excellent specificity to diagnose the conditions correlating with each profile [19]. These concepts of thoracic ultrasonography can be easily learned by house staff and other clinicians and utilized to make an accurate diagnosis in patients presenting with dyspnea [41].

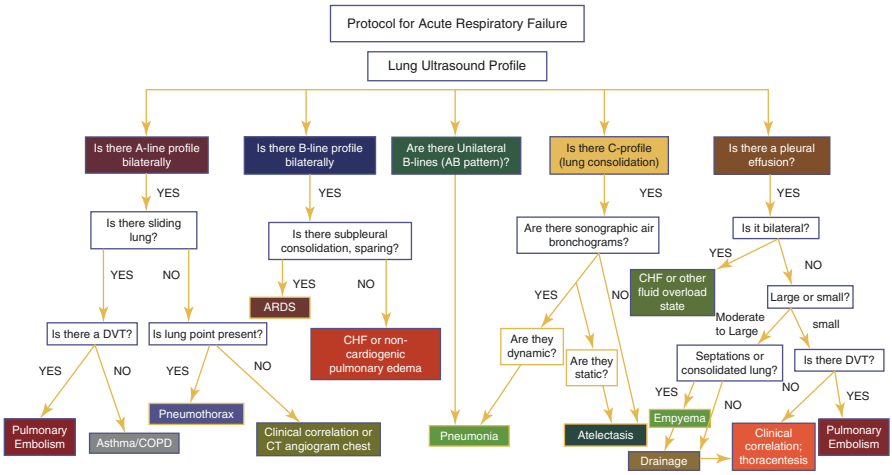

Fig. 10.20 Lung ultrasound profiles and algorithm for the evaluation of acute respiratory failure

Performing Pleural Procedures

Ultrasound assistance has become the standard of care for performing pleural drainage procedures such as thoracentesis and chest tube placement. It increases the success rate and reduces the risk of pneumothorax and organ injury [7]. A systematic approach can be helpful when performing pleural procedures in the CCU [29]:

1. *Locate the anatomical landmarks*. With the phased array transducer and the marker pointing cephalad, locate subdiaphragmatic structures like the kidney and either liver or spleen and then locate the hemidiaphragm. Because other structures are sometimes mistaken for a pleural effusion, confirm that the effusion is truly an anechoic space; identify the boundaries of the chest wall, diaphragm, and lung; and ensure that there are dynamic changes of the atelectatic lung and diaphragm.
2. *Estimate the size of the effusion*. Use the "eyeball" method or quantify the volume is sufficient to safely drain the fluid. Ensure there is no lung in the trajectory of the needle. Assess the US characteristics of the fluid.
3. *Locate the intercostal artery*. Use the linear array transducer and color Doppler to ensure there are no vessels in the trajectory of the needle. This is particularly important in elderly patients where the intercostal vessels can be tortuous.
4. *Measure minimal and maximal distance*. Use the caliper function to estimate the distance from the skin to the pleural space as well as the depth to reach atelectatic lung.
5. *Perform ultrasound-assisted pleural drainage*. Most operators prefer to use US assistance to mark the optimal site for drainage, rather than perform real-time US-guided drainage. Always scan one rib space above and below the chosen site to ensure that this is the most optimal location for needle puncture. Once the site is marked, follow institutional protocol including time-out, full sterile precau-

tions, and application of local anesthesia. Insert the needle along the superior margin of the rib, avoiding the neurovascular bundle that runs along the inferior portion of the rib. Use digital palpation of the rib and intercostal space to assist with needle insertion and advancement. Advance the needle until pleural fluid is reached and aspirated.

IVC Imaging: Evaluating Fluid Status and Fluid Responsiveness in Shock

The inferior vena cava caliber is altered by respiration, blood volume, and right heart failure. The IVC can be used to assess intravascular volume status. Fluid responsiveness is by definition an increase in cardiac output (CO) (generally >15%) after an adequate volume challenge. Interpretation of IVC size and variability is dependent on whether a patient is spontaneously breathing or on mechanical ventilation. In the spontaneously breathing patient, IVC imaging helps estimate RA pressures (i.e., as a "noninvasive" central venous pressure (CVP) reading). In the CCU patient on mechanical ventilation, respiratory variation of the IVC can predict fluid responsiveness, in the appropriate settings.

Technique

With the patient in supine position, the IVC can be visualized from the subcostal cardiac view by placing the phased array transducer in the subxiphoid space with the marker facing the patient's head. Alternatively, obtain a subcostal four-chamber view by positioning the probe flat just below the xiphoid, with the probe marker facing the patient's left side (Fig. 10.21). Identify the right atrium (RA) at the top of the screen and track it while turning the probe counterclockwise and slightly perpendicular to the body such that the marker is facing the patient's head. The IVC will appear within the liver with a hepatic vein joining it and emptying into the RA. Table 10.6 delineates basic characteristics used to identify the IVC and differentiate it from the aorta, which runs alongside the IVC. The IVC diameter can be measured using M-mode imaging by using the caliper feature. The "sniff" maneuver can be used in spontaneously breathing patients to estimate RA pressures. In patients on mechanical ventilation, the maximal and minimal diameter can be calculated to assess for respiratory variability.

Spontaneously Breathing Patient

In the spontaneously breathing patient, IVC size and the degree of collapse correlate to CVP. An IVC >2 cm in diameter, with inspiratory collapse <50%, approximates

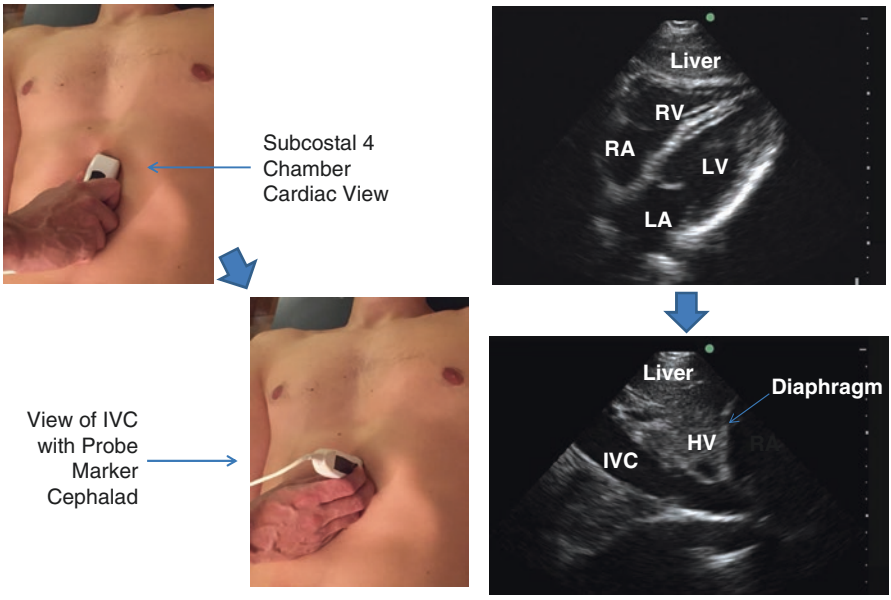

Fig. 10.21 Technique for IVC image acquisition

Table 10.6 Distinguishing inferior vena cava from aorta

	IVC	Aorta
Direction	Goes through the liver	Goes through the liver
Relation to heart	Merges with right atrium	Continues down the heart
Flow	Continuous, changes with respiration	Pulsatile
Walls	Thin walled, may not be visible	Thick walled, hyperechoic
Respiratory variations	May be present	No
Collateral vessels	Subhepatic veins merge with the IVC	Not visible from this approach

a CVP of 15 cmH_2O. When the IVC is narrow (<1.5 cm) and collapses a large amount (>50%), the CVP will be low and a hypovolemic (dehydration, hemorrhage) or distributive (sepsis, anaphylaxis) cause of shock is likely (Table 10.7) [42]. When the IVC is dilated (>3 cm) and non-collapsing, it usually indicates volume unresponsiveness unless the patient has right heart strain. On the other hand, when the IVC is extremely small or a "virtual IVC," it likely indicates that the patient is fluid depleted (Table 10.8).

Mechanically Ventilated Patient

Studies have shown that dynamic measures of fluid responsiveness (e.g., IVC variation) are more reliable than static measures (e.g., CVP) [43]. During mechanical ventilation of a sedated or paralyzed patient, pleural and juxtacardiac pressures

Table 10.7 IVC size, collapsibility, and estimation of CVP in spontaneously breathing patients

IVC diameter (cm)	Inspiratory collapse (%)	CVP (mmHg)
Normal: <2.1	>50%	0–5 (mean 3)
IVC findings other	±	5–10 (mean 8)
High: >2.1	<50%	10–20 (mean 15)

Table 10.8 IVC variability and fluid responsiveness in critically ill patients

Evaluating fluid status via inferior vena cava size and variability
Fluid responsiveness: clinically relevant increase in cardiac output (>15%) after a volume challenge
Spontaneously breathing patients
• Measure IVC size 2–3 cm from the right atrium using M-mode • Static – <1 cm → likely volume depleted – >3 cm → sufficient volume status
Patients on mechanical ventilation (criteria)
• On mechanical ventilation • Tidal volume >8 cc/kg ideal body weight • Passive on ventilator support (no spontaneous breaths) • Normal sinus rhythm
Patient is fluid responsive if
– (Max diameter − min diameter)/min diameter >18% OR – (Max diameter − min diameter)/average diameter >12%

increase during inspiration, causing RA pressures to rise and decreasing filling of the right heart. This causes a reduction in right ventricular stroke volume (SV) and less filling of the left ventricle (LV), thus reducing left ventricular SV several cardiac cycles later. These respiratory changes are exaggerated in the hypovolemic patient, and these variations in SV can be used to predict fluid responsiveness [18]. Respiratory variation of the IVC diameter has been shown to accurately predict fluid responsiveness [13, 44]. Tables 10.7 and 10.8 summarize interpretation of IVC size and variation. Figure 10.22a and b shows examples of IVC diameter measurements with and without respiratory variability using M-mode. Figures 10.23a and b are examples of small collapsible IVCs, as well as large dilated IVC with minimal variability.

Fundamentals of Abdominal Ultrasound in Critical Illness

Abdominal ultrasonography has several applications in the evaluation of the critically ill patient. CCU patients are commonly on dual antiplatelet therapy and anticoagulation and are at high risk for intra-abdominal hemorrhage. Procedures such as cardiac catheterization, intra-aortic balloon pump (IABP) placement, intravascular cooling catheter placement, and femoral arterial sheath placement all increase

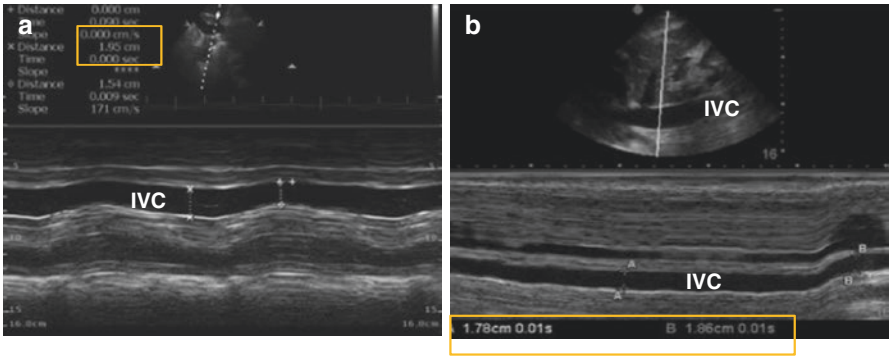

Fig. 10.22 (**a**) M-mode image showing respiratory variation of the IVC. (**b**) M-mode image showing lack of respiratory variability of the IVC

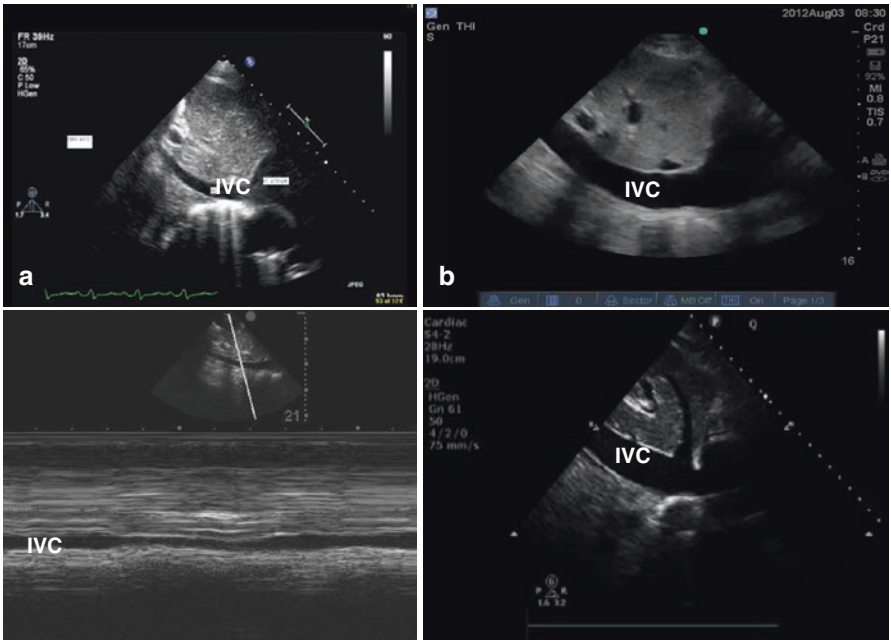

Fig. 10.23 (**a**) Small collapsible IVC. (**b**) Dilated IVC

bleeding risk both during insertion and removal. Intraperitoneal and retroperitoneal hemorrhage should always be ruled out in the CCU patient who is hypotensive.

FAST Exam

The focused assessment with sonography in trauma (FAST) exam is utilized in the assessment of the trauma patient suspected to have intraperitoneal bleeding. With

a minimum of approximately 200 cc, the FAST exam has 90% sensitivity in the detection of abdominal free fluid. Considering the multiple invasive procedures and predilection for bleeding discussed above, the FAST exam is vital for the CCU patient [45]. Given the rapidity and noninvasive nature of the FAST exam, repeat assessments are warranted if there are any concerns regarding intraperitoneal free fluid, as volumes of free fluid less than 200 cc may not be detected on initial examinations [12].

To perform the FAST exam, use a curvilinear or phased array transducer to scan the patient in the supine position. This positioning allows for visualization of the three most dependent areas of the abdominal cavity, as well as the costophrenic angles bilaterally. The addition of the fourth view, the subcostal four-chamber view of the heart and pericardium during the traditional FAST exam of the abdomen allows for further differentiation of a shock state. An extended FAST exam (EFAST) additionally includes two rapid evaluations of the bilateral anterior lung zones in order to evaluate for a pneumothorax (Table 10.9).

The FAST exam begins by placing the transducer (with marker cephalad) in the midaxillary line at the level of the xiphoid process to obtain a coronal view of the right hemidiaphragm, liver, and kidney. The hepatorenal space (Fig. 10.24a), also known as Morrison's pouch, is commonly where free fluid accumulates (Fig. 10.24b). Evaluate for pleural fluid (i.e., hemothorax, Fig. 10.14) by scanning just above the diaphragm from this position. Next move the transducer to the left posterior axillary line, at the level of the xiphoid process. Visualize the left hemidiaphragm, spleen, and kidney and evaluate for free fluid in the splenorenal space. Another quick scan above the hemidiaphragm from this vantage point can assess for pleural fluid in the left hemithorax. Now place the transducer (with marker to patient's left) just superior to the pubic symphysis with the transducer angled toward the patient's feet. This will allow for visualization of the bladder and any free fluid in the pelvis. Adding a subcostal four-chamber cardiac view (with marker to patient's left) to the FAST exam allows for quick assessment for any pericardial effusion and further differentiates etiologies of a shock state. If there is increased echogenicity or layering of the free fluids visualized in the abdomen, it is more indicative of hemoperitoneum than simple ascites (Figs. 10.25a). USG does not have high sensitivity to detect retroperitoneal bleeding (Fig. 10.25b); hence a CT abdomen should be performed.

Ascites

Bedside ultrasonography is an easy way to assess for ascites in the patient with cirrhosis or right heart failure. US also facilitates paracentesis by assisting in selection of the best pocket for sampling and by avoiding nearby structures such as bowel and vasculature (Fig. 10.26). When compared to non-ultrasound-guided paracenteses, US guidance facilitated a 95% success rate, compared to the 61% of traditional methods [46]. Both detection of ascites and procedural competence in US-assisted paracentesis can be easily achieved with appropriate training [47].

Table 10.9 Standardized POCUS protocols in the evaluation of shock

Name	Probe landmarks	Views/structures	Evaluation goals
RUSH exam *R*apid *U*ltrasound in *S*hock	PLAX/PSAX	LV, RV, valves	*Pump*—LV failure, RV strain from PE, tamponade
	A4C/SC views	Pericardium	
	SC	IVC	*Tank*—IVC and IJV collapsibility to evaluate volume status
	Neck	IJV	
	Right flank/RUQ	Hepatorenal	Hemoperitoneum, hemothorax, ascites
	Left flank/LUQ	Splenorenal recess	
	Suprapubic	Pelvis [FAST]	
	Anterior chest	Lung/pleura	Pneumothorax and pulmonary edema
	Chest/abdomen	Aortic slide view	*Pipes*—ruptured aortic aneurysm
	Femoral, popliteal veins	Limited DVT study	DVT/PE
E FAST exam	Anterior chest	Lung/pleura	Pneumothorax, pulmonary edema
*E*xtended *F*ocused *A*ssessment of *s*onography in *t*rauma	Subxiphoid	SC cardiac	Pericardial tamponade
	Right flank/RUQ	Hepatorenal	Hemoperitoneum
	Left flank/LUQ	Splenorenal recess	Splenic rupture
		Pleural space	Hemothorax
	Suprapubic	Retrovesicular	Free fluid/pelvic hemorrhage
FALLS	PLAX/PSAX/ A4C/SC	Basic cardiac views	Rules out tamponade and PE
*F*luid *A*dministration *l*imited by *L*ung *S*onography	Lung US [BLUE protocol]	Lung/pleura	Rules out pneumothorax
			Determine A-line vs. B-line profile A-line profile → give fluids until improvement or B-line appear (points to septic or distributive shock) B-line profile → suggests cardiogenic shock

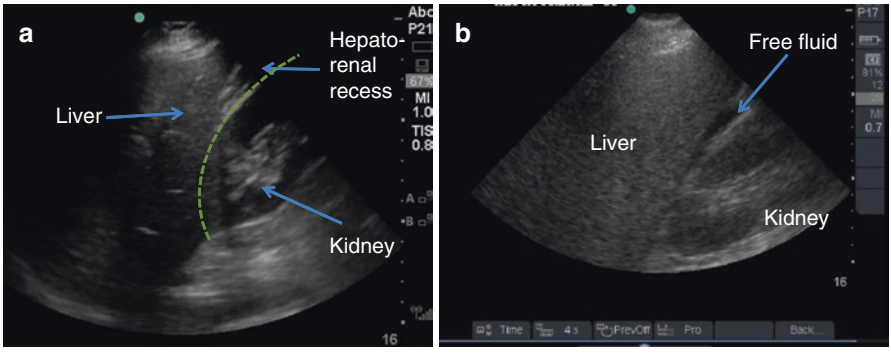

Fig. 10.24 (**a**) Hepatorenal recess. (**b**) Free fluid in hepatorenal recess

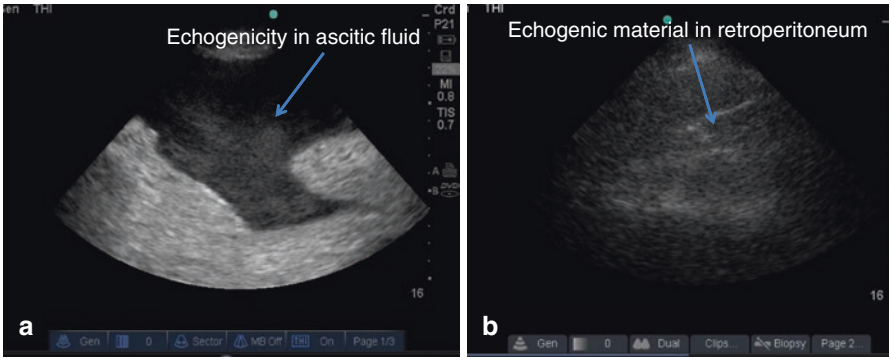

Fig. 10.25 (**a**) Hemoperitoneum, evidenced by layering of hyperechoic material. (**b**) Retroperitoneal hematoma

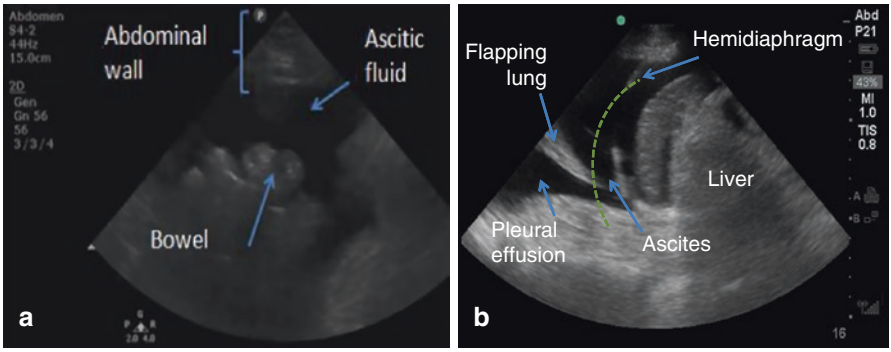

Fig. 10.26 (**a**) Ascites—simple anechoic fluid in pelvis. (**b**) Perihepatic ascites and pleural effusion in cirrhosis

Abdominal Aortic Ultrasonography

Aortic USG allows detection of aortic syndromes such as thrombosis, dissection, aneurysm, or rupture. Conventionally, an abdominal aortic aneurysm (AAA) is diagnosed when the diameter of aorta exceeds 4 cm. The risk of rupture at this level is <4% within a year, but it exponentially increases for AAA of larger diameter (>5 cm). The presence or absence of abdominal aortic aneurysm can be evaluated with POCUS with high sensitivity and specificity; however, it has poor sensitivity for extraluminal blood. Nevertheless, in one ED study, it was shown to improve diagnosis of ruptured AAA in the appropriate clinical setting and resulted in correct decision to perform surgery [48].

The proximal aorta can be visualized with a curvilinear transducer in the transverse view. Ideal conditions for scanning are a thin body habitus and a non-gas-filled transverse colon. The examiner should scan between the xiphoid process and the umbilicus, which generally correspond to the 12th thoracic and the 4th lumbar vertebral bodies, where the aorta enters the abdominal cavity and bifurcates to the

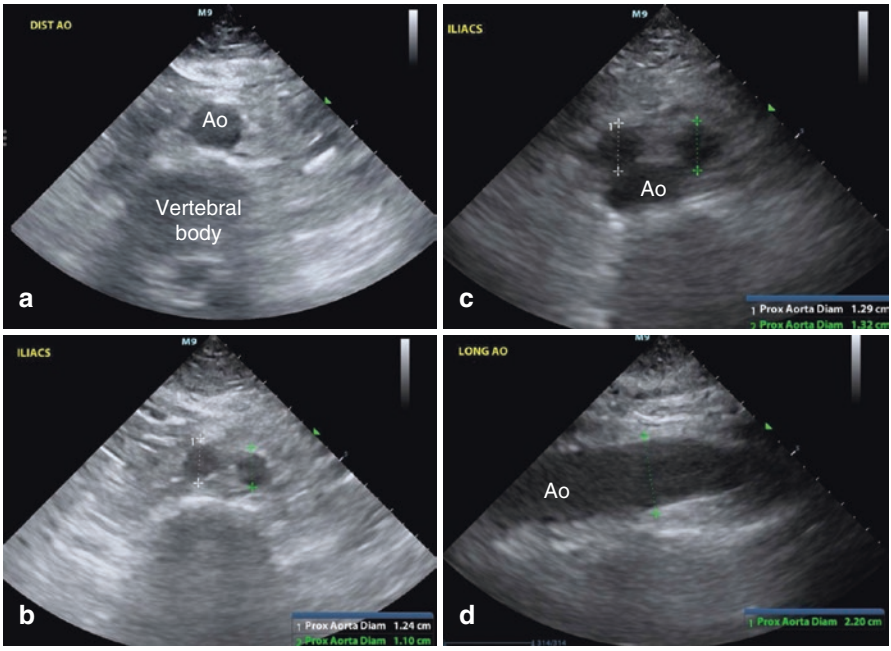

Fig. 10.27 (**a**) Distal aorta. (**b**) Aorta at the level of bifurcation to the common iliac arteries. (**c**) Aorta bifurcating in iliacs. (**d**) Proximal aorta—longitudinal view

iliac arteries, respectively. Approximately 1 cm below the diaphragm, the aorta gives rise to three major branches: the celiac trunk (immediately below the diaphragm) giving rise to the common hepatic artery and splenic artery (called *seagull sign*), the superior mesenteric artery (SMA), and the renal arteries. The vast majority of aortic aneurysms occur distal to the renal artery takeoffs. The various aortic branch points can be seen in Fig. 10.27. Obtaining a longitudinal view of the aorta can allow for further visualization of the aorta, especially when evaluating for dissection. Figure 10.28 demonstrates CXR, CT scan, and ultrasound correlations of a patient presenting with Type B aortic dissection.

Kidney and Bladder

Using POCUS to assess the kidneys and bladder can quickly add or eliminate etiologies from a differential. A normal kidney has a hyperechoic medulla with a hypoechoic cortex. As outflow obstruction causes urine accumulation in the collecting system, the center of the kidney will appear dilated with anechoic fluid (Fig. 10.29a). This hydronephrosis usually indicates a downstream obstruction, and the clinician should utilize US to evaluate for a large dilated anechoic bladder (Fig. 10.29b). It is not uncommon to see a Foley balloon in a dilated anechoic bladder, indicating the catheter itself is obstructed.

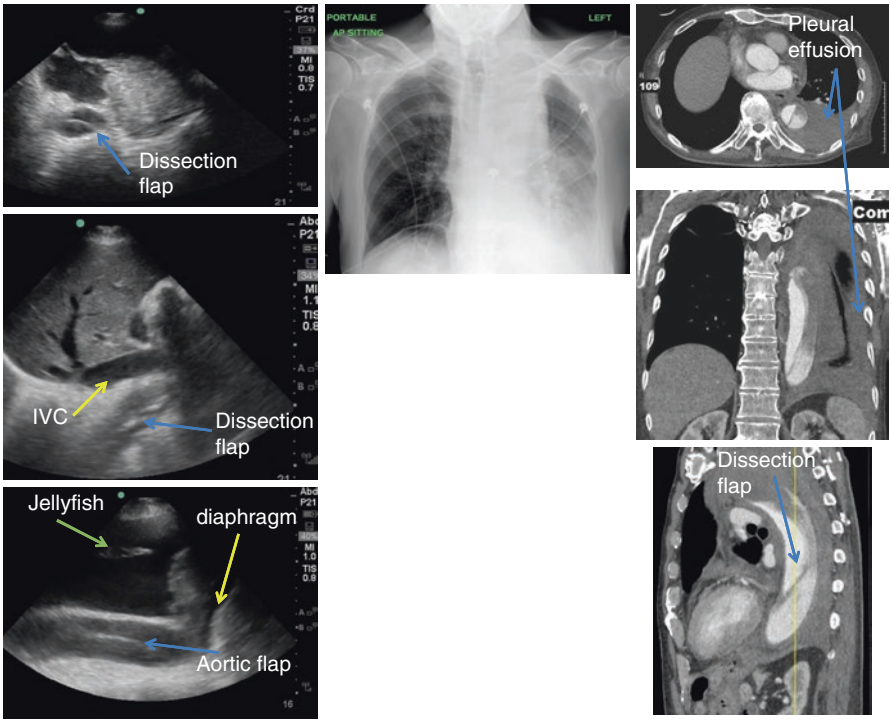

Fig. 10.28 CXR, CT, and ultrasound correlates for Type B dissection. Note the patient has a widened mediastinum and a new left pleural effusion

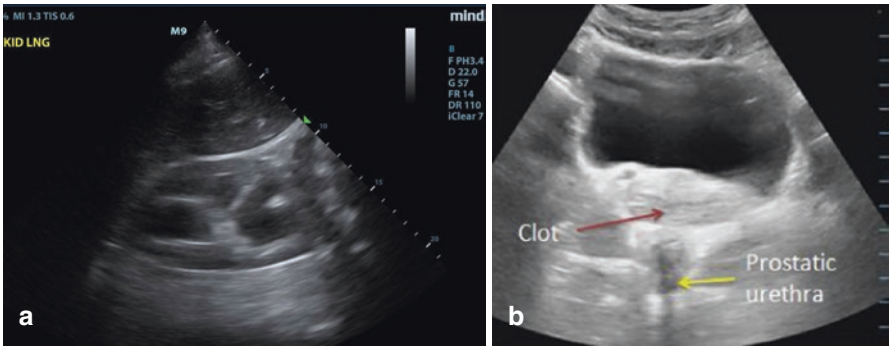

Fig. 10.29 (**a**) Hydronephrosis. (**b**) Full bladder with obstructing clot

Using a phased array or curvilinear transducer, the transverse and longitudinal views of the kidney can be obtained using the same anatomical landmarks as the FAST exam. By directing the probe marker cephalad and angling the probe anteriorly and posteriorly through each kidney, assessing for any dilation of the collecting system, one can rapidly evaluate for hydronephrosis. Color Doppler can be used to

ensure that an anechoic duct is not a blood vessel. At the same location, the transducer should be rotated 90° counterclockwise, tilting the probe superior to inferior to scan through the entire kidney. Once complete, the transducer can be placed superior to the pubic symphysis to evaluate the bladder in the transverse and longitudinal views [49].

Diagnostic Vascular Ultrasound

Deep Venous Thrombosis

Patients in the CCU have an increased risk of venous thromboembolism due to immobility, indwelling central venous catheters, multi-organ failure, and inflammatory states. The lower extremities are examined for DVT using a high-frequency linear array transducer. Compression ultrasound is performed to assess for venous collapse under pressure, with the lumen disappearing entirely under direct visualization. Visualization of echogenic thrombus in the vascular lumen or lack of collapsibility with compression maneuver is consistent with DVT.

Place the patient in supine position, with the knee slightly bent and the leg externally rotated. Identify the common femoral vein (CFV) and then perform compressions starting from above the inguinal ligament at the proximal portion of the external iliac vein (Fig. 10.30). Compress every 1–2 cm while moving dis-

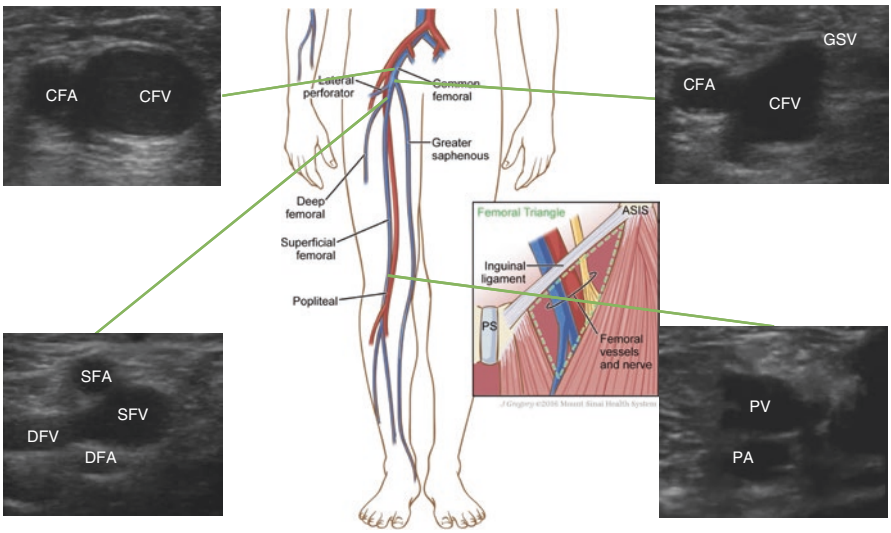

Fig. 10.30 Compression ultrasonography to assess for DVT

tally along the CFV, the greater saphenous vein, over the lateral perforator-CFV junction until the common femoral vein is seen branching into the superficial and deep branches. Apply downward pressure to the transducer until the vein collapses completely. Scan the popliteal region by flexing the knee 45° and externally rotated the leg. The popliteal vein overlies the popliteal artery. Perform sequential compression at approximately 1 cm intervals while moving distally to the trifurcation of the popliteal vein. Even minimal pressure can compress the popliteal vein. A minimum of three sites in the groin region and three sites in the popliteal fossa should be assessed for DVT. Figure 10.31 shows examples of venous thrombosis in the IJV and the common femoral vein. Blood flow augmentation maneuvers, color Doppler, and pulse-wave Doppler can be performed; however, compression US alone performed by non-radiologists has been shown to accurately diagnose DVT with 95% accuracy and reduce the time to diagnose DVT [50, 51].

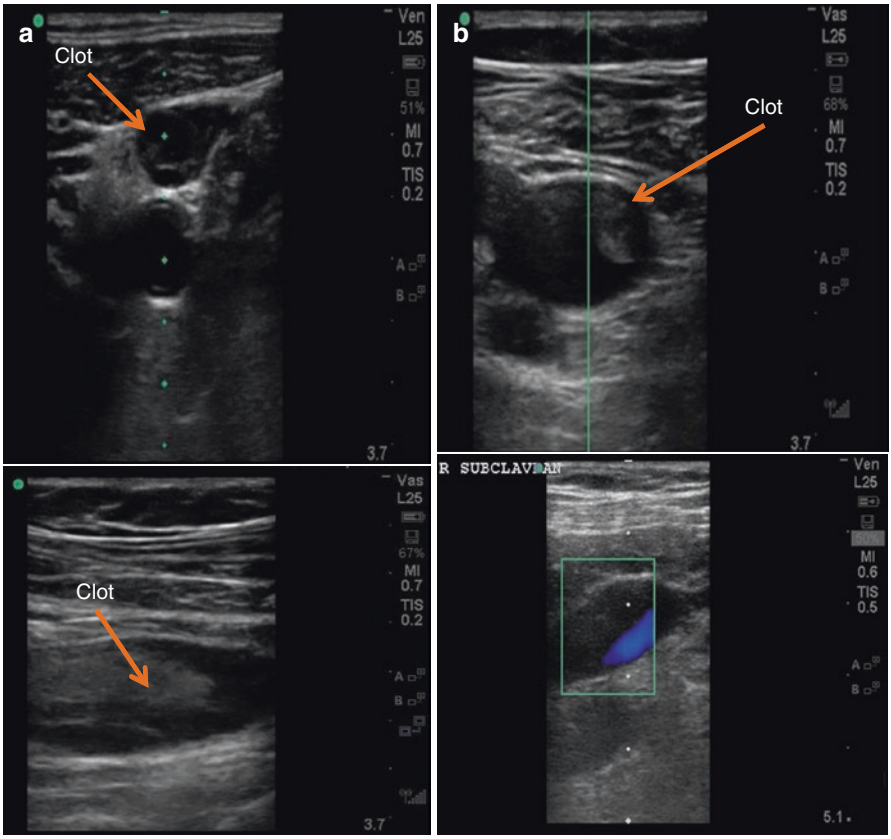

Fig. 10.31 Deep vein thrombosis with lack of compressibility and thrombus in vessel. (**a**) Right internal jugular clot. (**b**) Common femoral vein, visualized nonobstructing hyperechoic clot

Fundamentals of Ultrasonography in Undifferentiated Shock: Multi-organ POCUS

Shock is a commonly encountered condition in the CCU but is not always associated with cardiac causes. Physical examination and laboratory parameters along with multi-organ POCUS guide the evaluation and management. POCUS techniques involving the heart, lungs, abdomen, and vasculature are performed based on the appropriate clinical setting in an attempt to identify the cause of hypotension and optimize management. The goal-directed evaluation of a new, unexpected, or unexplained shock state in a CCU patient requires a structured approach that will diagnose or rule out reversible causes such as cardiac tamponade, tension pneumothorax, pulmonary embolus, ruptured aortic aneurysm, and intra-abdominal hemorrhage [16, 18].

Goal-directed echocardiography (GDE) allows the clinician to assess for right or left ventricular failure, pericardial effusion, major valvular failure, and fluid responsiveness. The statement on training in critical care ultrasonography makes the recommendation that training in critical care include training in basic critical care echocardiography [1–3]. GDE can be learned and performed well by non-cardiologists with adequate training [14, 52, 53]. Combining GDE with sonography of other organs (multi-organ or whole-body ultrasonography) adds to the diagnostic yield when evaluating the patient in shock [4, 16]. One can perform a goal-directed multi-organ POCUS exam in an efficient and systematic way to discern the etiology of shock:

1. Basic critical care echo to evaluate LV and RV function and rule out tamponade and valvular failure
   (a) Parasternal long-axis (PLAX), parasternal short-axis (PSAX), apical four-chamber (A4C), and subcostal views (SC)
2. IVC imaging to assess volume status in setting of hypovolemia or sepsis
3. Thoracic ultrasound to rule out pneumothorax and hemothorax
4. Limited abdominal exam
   (a) Right and left flank to rule out hemoperitoneum
   (b) Abdominal aorta to evaluate for dissection
   (c) The kidneys and bladder to rule out hydronephrosis in setting of sepsis or renal failure
5. Compression US of lower extremities to evaluate for DVT

A systematic approach to the CCU patient with shock also employs the following questions while performing POCUS [18]:

1. Is there an imminently life-threatening cause of shock?
2. Is there evidence of pump failure: LV or RV failure?
3. Is the shock state likely to be fluid responsive?
4. Is there more than one cause for the shock state?

5. Is it non-cardiac in origin?
6. Is there evidence of life-threatening hemorrhage?

Figure 10.32 illustrates an algorithmic approach to the CCU patient who is hypotensive. Many POCUS protocols exist for the evaluation of shock. Essentially, they all incorporate multi-organ POCUS to evaluate the etiology of shock. Table 10.9 summarizes a few of these protocols and the organs that are assessed [54–56]. Furthermore, Table 10.10 lists the whole-body US findings for the various organs in the setting of undifferentiated shock. Further discussions on cardiac etiologies of shock are found in other sections of this textbook.

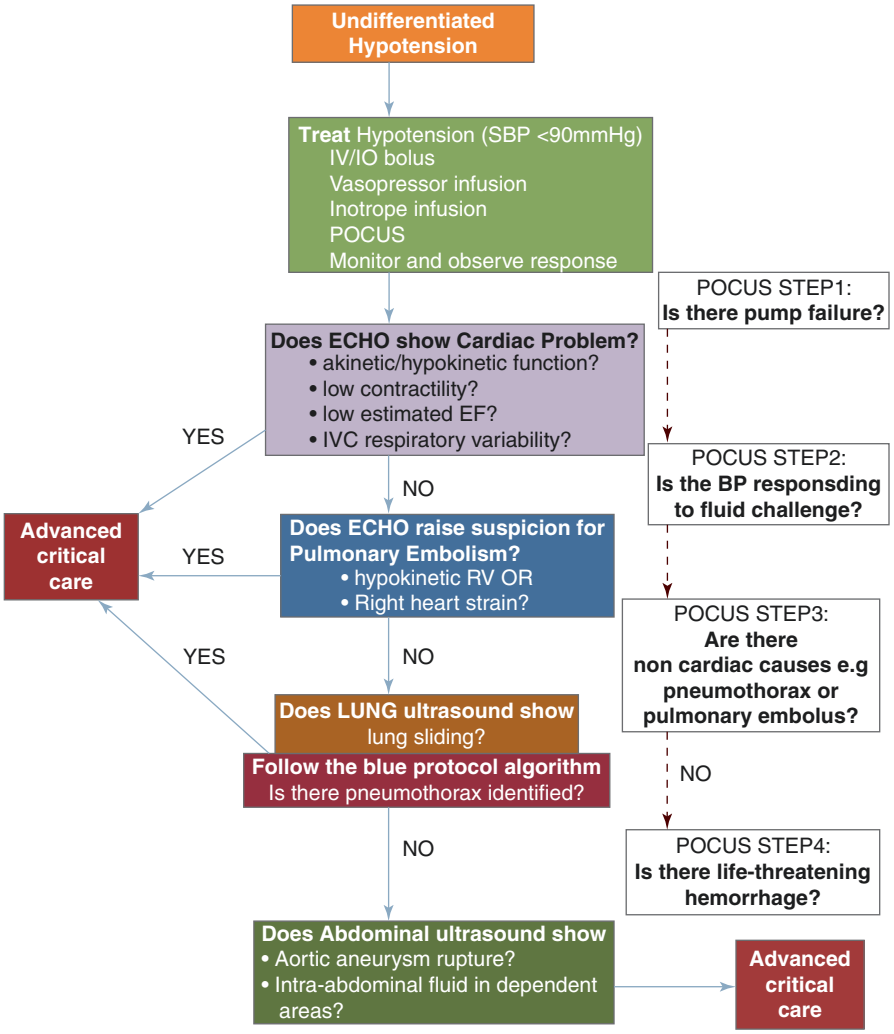

Fig. 10.32 Approach to undifferentiated shock

Table 10.10 Suspected US findings for undifferentiated shock

Ultrasound pattern	Organ evaluation	Corresponding signs
Hypovolemic	Heart	Hyperkinetic LV
	IVC	Diameter <2 cm + resp. collapse >50%
	Lungs	A-line pattern
	Abdomen	Free fluid/aortic aneurysm
Distributive	Heart	Hyperkinetic LV
	IVC	Diameter <2 cm + resp. collapse >50%
	Lungs	B-line pattern with consolidation/air bronchograms
Cardiac tamponade	Heart	Pericardial effusion with tamponade
Pulmonary embolism	Heart	Dilated and hypokinetic RV
	IVC	Diameter >2 cm without resp. collapse
Tension pneumothorax	Heart	Dilated and hypokinetic RV
	IVC	Diameter >2 cm without resp. collapse
	Lungs	No lung sliding/pulse, no B-lines or consolidation
Cardiogenic	Heart	Hypokinetic LV
	Lungs	B-Line pattern

Procedural Guidance for Vascular Access

Introduction

POCUS is invaluable for obtaining vascular access in the cardiac care unit (CCU) patient. Knowledge of vascular anatomy, familiarity with the equipment, and experience with the use of US are necessary prerequisites for the successful insertion of the catheter. The decision to place a line and the choice of site of insertion should be based on a thoughtful assessment by the operator and the CCU team of the patient's anatomy, clinical status, and coagulation profile. Real-time ultrasound guidance is recommended for CVC placement.

Ultrasound Guidance

Numerous studies have shown that US guidance increases the first-attempt success rates and decreases mechanical and infectious complications [5, 6, 57, 58]. The use of US for CVC placement is strongly advocated by various organizations such as the Agency for Healthcare Research and Quality (AHRQ), American Society of Anesthesiologists, American College of Surgeons, American Society of Echocardiography, and Society of Cardiovascular Anesthesiologists [59–62]. Studies have shown significant variation in the size of the vein and its position relative to the artery resulting in the possibility of an arterial puncture. Landmark methods lead to failure rates as high as 36%, even in experienced hands [6, 58]. Ultrasound

guidance allows the operator to identify the target vessel, ensure that there is no thrombus within the vessel, and allows for real-time visualization of the needle during the cannulation. Additionally, it allows confirmation of venous placement of the guidewire before dilation and placement of the catheter.

US guidance is most useful for cannulation of the internal jugular vein (IJV) and femoral vein (FV). Although US guidance can be used successfully for subclavian vein (SCV) access, it has a steeper learning curve and should only be performed by experienced operators, due to the risk of pneumothorax [5]. Prior to inserting a central line using US guidance, the operator should perform a pre-procedural scan. The portable US machine should be set to the "vascular" preset. A high-frequency linear array transducer should be used. It should be held like a pencil with the hypothenar eminence steady on the patient's body, allowing for a steady image during the actual procedure. The marker on the transducer should always be "operator left" to match the marker on the upper left corner of the screen. The left side of the US probe corresponds to the left side of the screen. With this setup, in order to aim the needle left, one would advance the needle to the left and vice versa. The depth and gain should be adjusted such that the vessel of interest is in the center of the screen and the image is not too bright or dark. Arteries have thick walls and are pulsatile, whereas veins are thin walled and are easily collapsible when pressure is applied over the vein. Color Doppler or pulsed Doppler can be used to further confirm arterial versus venous flow.

Transverse Approach

In the short axis or transverse plane, the vessels will appear as round circles (Fig. 10.33a) as the US beam intersects the vessel in a cross section at a perpendicular angle [63]. In the long-axis or longitudinal view, the US beam is parallel to the vessels, and the

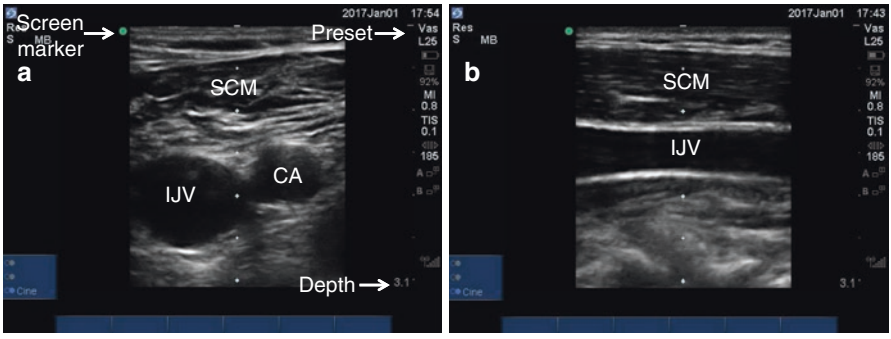

IJV - internal jugular vein
CA – carotid artery
SCM – sternocleidomastoid muscle

Fig. 10.33 (**a**) Short-axis view of IJV. (**b**) Longitudinal view of IJV

vessels will appear as long cylinders if the beams transect the vessel in the middle along its course (Fig. 10.33b). Ensure the vein and arteries are parallel to each other and not on top of each other. Figure 10.34a and b demonstrates examples of unsafe sites for cannulation as the carotid artery and IJV are not parallel to each other. Image the vein up and down in the transverse view to ensure patency. Do a compression maneuver by applying gentle pressure in at least three sites to ensure there is no thrombus (Fig. 10.35). Figure 10.36a and b shows examples of intraluminal thrombus detected prior to IJV CVC placement. Table 10.11 summarizes the steps for pre-procedural US scan, which should always be done prior to US-guided line placement.

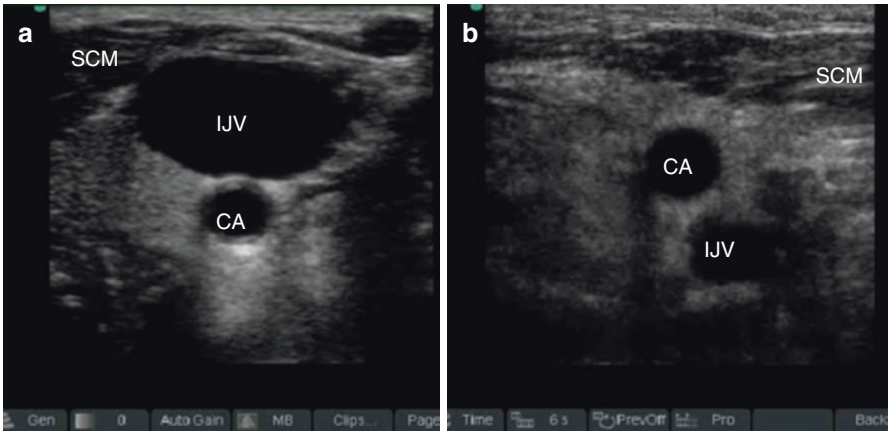

IJV - internal jugular vein
CA – carotid artery
SCM – sternocleidomastoid muscle

Fig. 10.34 (**a**) Unsafe site with carotid artery immediately beneath IJV. (**b**) Unsafe site with carotid artery above IJV

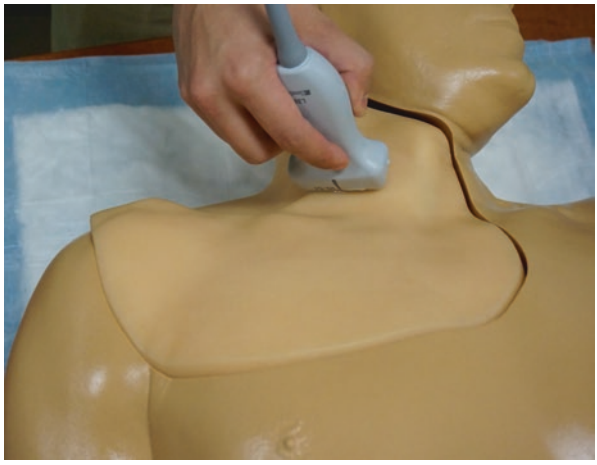

Fig. 10.35 Image the entire length of the IJV and do a compression maneuver

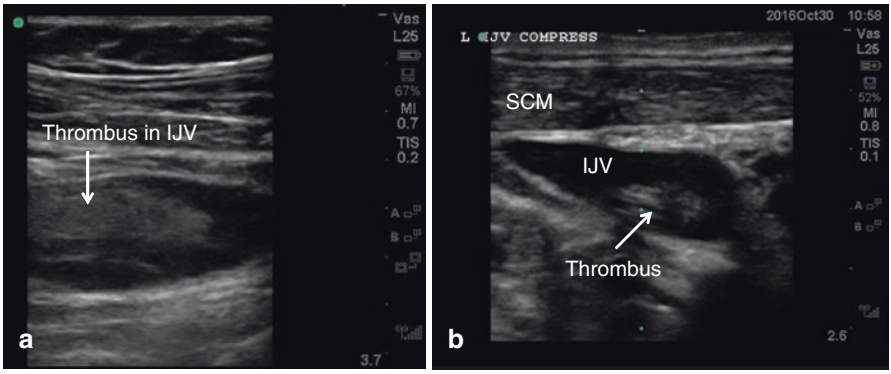

Fig. 10.36 (**a**) IJV intraluminal thrombus transverse view. (**b**) IJV compression maneuver shows intraluminal thrombus with lack of compressibility

Table 10.11 Steps for line placement: pre-procedural ultrasound scan

Step	Description
1	Set US machine in "vascular" preset mode
2	Hold vascular probe like a pencil with hand resting on patient
3	Ensure probe marker is "operator left"
4	Identify vein and artery
5	Optimize gain and depth, ensuring vein is in center of screen
6	Scan up and down the vessel to ensure patency
7	Do a compression maneuver at three sites along the vessel to ensure no thrombus
8	Ensure vein and artery are parallel to each other
9	Image both sides for optimal site selection
10	Identify safest site for cannulation

Once a safe site is identified, cannulation should be performed with the thin-walled introducer needle with the needle inserted at a steep angle (70°–90°) and directly beneath the center marker of the probe. A sterile probe cover should always be used, ensuring adequate sterile gel both inside and outside the probe cover. The US probe is held steadily with the non-dominant hand and the needle advanced with the dominant hand. During advancement to the vessel, the visualization of the needle may be limited to deformation of the soft tissue and the central vein prior to penetration of the vessel. The needle and syringe apparatus may have to be jiggled gently in order to appreciate the needle on the screen. It is imperative to maintain visualization of the needle tip by keeping the needle tip within the plane of the US beam. Once there is good blood flow, the angle should be decreased prior to inserting the guidewire. Alternatively, a lower angle (30°–60°) can be used with the ultrasound probe being advanced forward as the needle is being advanced, with gentle back-and-forth tilting of the probe to identify and follow the tip of the intro-

ducer needle directly into the vein (Fig. 10.37). Be careful not to confuse the shaft of the needle with the needle tip. Subtle tilting of the transducer at the point where the needle tip disappears on the monitor confirms location of the tip.

Once the needle is in the vein and there is good blood flow into the syringe, the operator must release the transducer and steady the needle with the non-dominant hand prior to advancing the guidewire with the dominant hand. The needle should now be removed and the vein imaged with US in both the transverse and longitudinal planes to confirm that the guidewire is in the vein. The guidewire should be visualized within the thin-walled vein, which will be compressible with gentle pressure (Fig. 10.38). This step must be performed prior to dilation and placement of the central venous catheter.

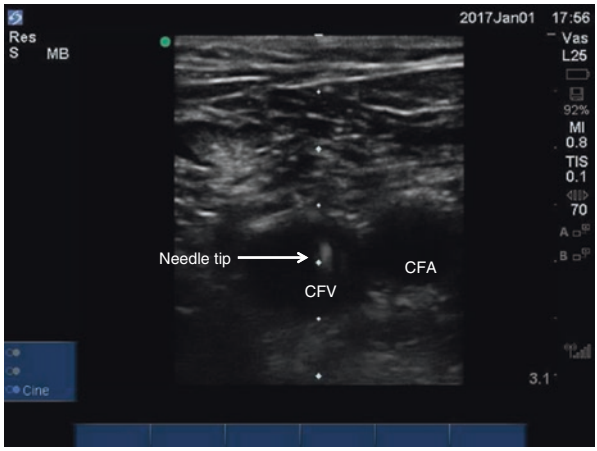

Fig. 10.37 Echogenic needle tip visualized within common femoral vein

CFV – common femoral vein
CFA – common femoral artery

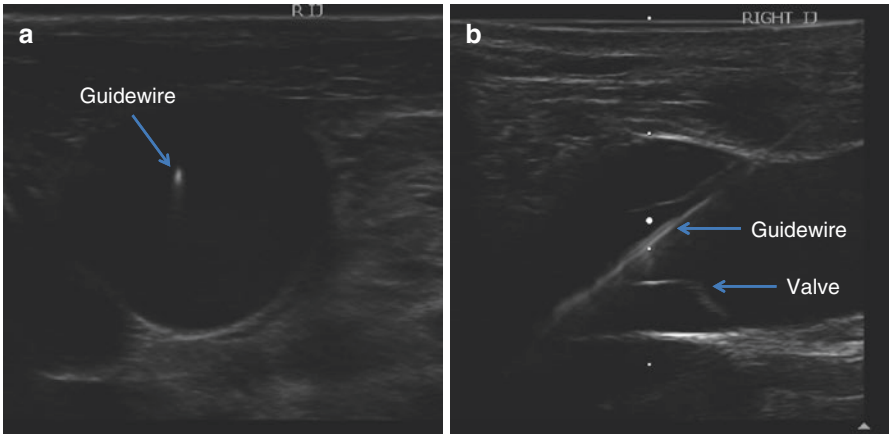

Fig. 10.38 (**a**) Guidewire in IJV. (**b**) Longitudinal view of guidewire in IJV

Longitudinal Approach

A longitudinal or in-plane approach can be utilized for CVC placement; however, this is not recommended for the beginner as there is increased risk of puncturing the adjacent artery. From a transverse view, the transducer is rotated counterclockwise such that the marker is facing the operator and the US beam is along the long axis of the target vein. The needle is inserted at a shallow angle (45°–60^0) at the transducer marker with the needle and syringe apparatus aligned with the long axis of the transducer. The needle insertion angle and the distance from the transducer should be appropriate for the depth of the target vessel. Identify the needle tip and shaft on the screen and adjust the needle trajectory as the needle is advanced into the central vein (Fig. 10.39).

Site-Specific Considerations Using Ultrasound-Guided Approach

Internal Jugular Vein

The IJV is a common site for central venous catheterization as it is easily accessed with ultrasonography [6]. The IJV jugular vein is located under the sternocleidomastoid muscle on either side of the neck. The right side of the neck is preferred

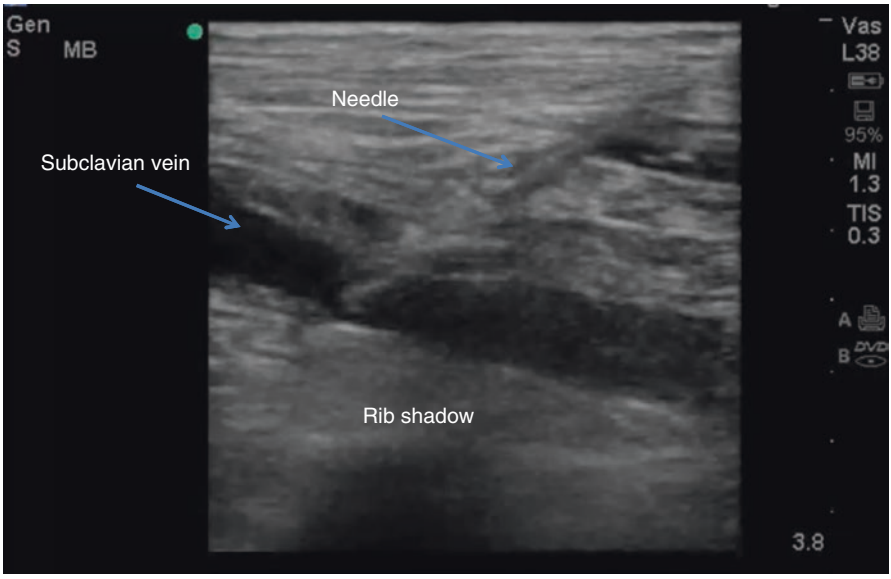

Fig. 10.39 US-guided subclavian vein cannulation using longitudinal approach

because the vessels run a straight course to the right atrium. IJV cannulation may be difficult in patients with tracheostomies as the tracheostomy holder often overlies the site.

Ensure the patient is in Trendelenburg position with the head slightly turned 45° to the contralateral side from the intended insertion side. Anatomical landmarks for the IJV begin at the triangle formed by the heads of the sternocleidomastoid muscles and the clavicle (Fig. 10.40). The IJV is easily collapsible and can often not be visualized due to excessive pressure by the US probe or the operator's finger.

A pre-procedural scan of the left and right IJV is done to select the best site. Place the US probe parallel and cephalad to the clavicle, at the apex of the triangle, with the transducer marker "operator left." Visualize the IJV and carotid artery in the transverse view. The carotid artery will be thick walled and pulsatile, while the IJV will be thin walled and easily compressible (Fig. 10.40). Identify a safe site for cannulation where the IJV is away from the carotid artery and not overlying it (Fig. 10.34). Position the transducer and optimize the depth such that the vein is centered on the screen. Stay in the mid-neck and avoid the lower neck region above the clavicle, as there is a risk of puncturing the apex of the lung, even with US guidance. Performing a quick lung ultrasound before and after the procedure to check for lung sliding is an efficient way to rule out pneumothorax.

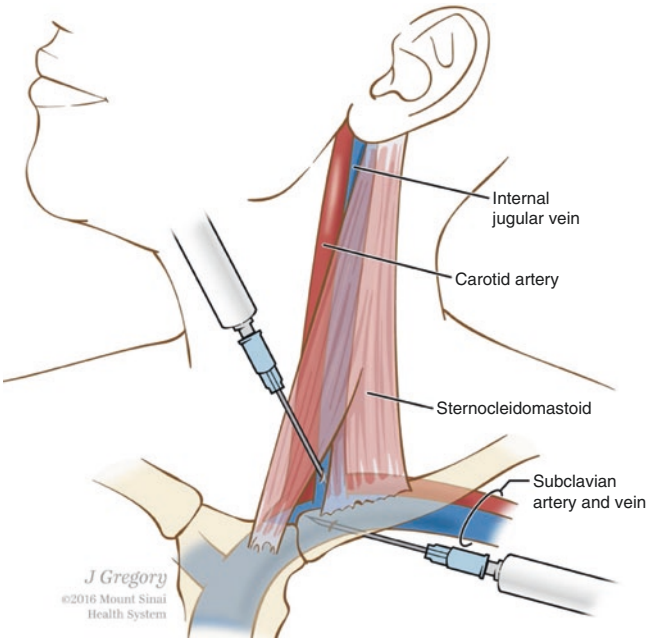

Fig. 10.40 Internal jugular vein and subclavian vein anatomy

Femoral Vein

The femoral vein site is associated with the fewest vascular and pulmonary complications; however, it carries a higher infection rate; hence it is discouraged by the Centers for Disease Control and Prevention (CDC) [64]. Femoral vein is the site of choice for central venous catheterization during emergencies such as cardiac arrest, respiratory distress, or in an agitated patient.

Place the patient in supine position, externally rotate and abduct the patient's leg away from midline [65]. The CFV lies medial to the common femoral artery as it runs distal to the inguinal ligament (Fig. 10.41). The mnemonic "VAN" illustrates

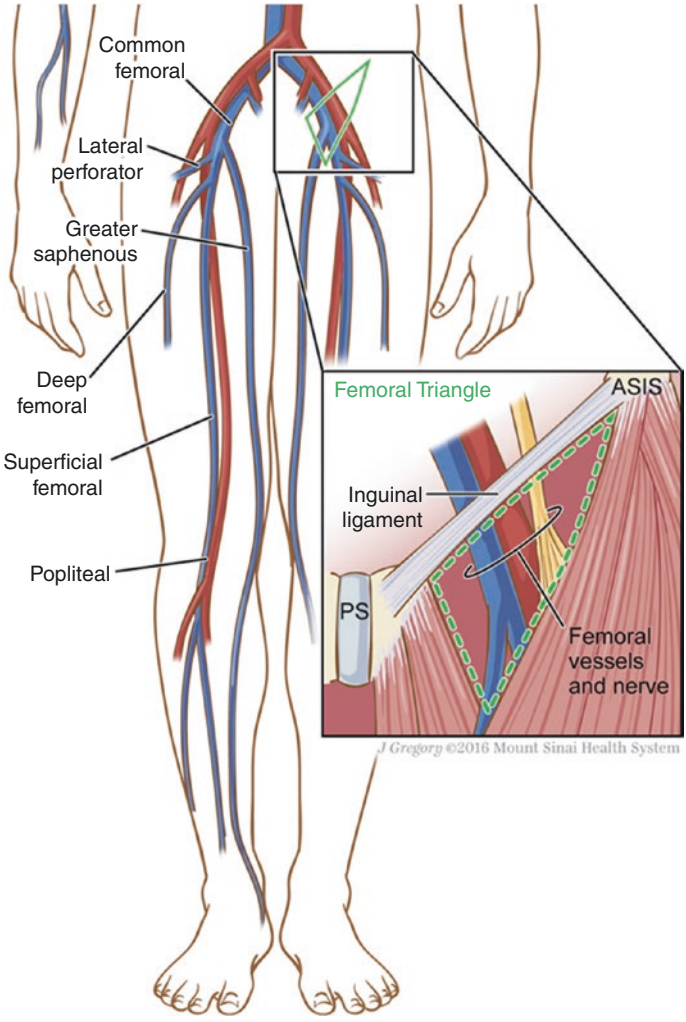

Fig. 10.41 Venous anatomy of femoral triangle and lower extremities

the contents of the femoral sheath (Fig. 10.41) from medial to lateral: femoral *V*ein, femoral *A*rtery, and femoral *N*erve. The femoral artery lies at the midpoint of a line connecting the pubic symphysis (PS) to the anterior superior iliac spine (ASIS). The FV lies 1 cm medial to the femoral artery. Localize the FV by palpating the artery or with ultrasonography. The cannulation site must be inferior to the inguinal ligament

Using a linear array transducer with the marker "operator left," identify the common femoral vein and artery (Fig. 10.42). Identify the safest site for cannulation, and holding the probe steady, insert the needle at a 45°–70° angle into the vein. Once there is venous blood return, hold the needle steady, detach the syringe, and thread the guidewire. Remove the needle and confirm venous placement of the guidewire in both the transverse and longitudinal view prior to dilation and insertion of the catheter.

Subclavian Vein

The subclavian site is the most preferable site for CVC placement as it carries the lowest risk of central line-associated blood stream infections (CLABSI) and thrombosis as compared to IJV or FV cannulation; however, it has a higher risk of pneumothorax [66]. Accessing the subclavian vein requires placement of the cannulation needle under the clavicle and near the apex of the lung so it is not surprising that pneumothorax is a potential complication. Subclavian vein catheterization should be avoided in patients with lung hyperinflation due to severe COPD or asthma, patients on high FiO_2 and PEEP while on mechanical ventilation, and patients with parenchymal lung disease and limited pulmonary reserve. The insertion point using a landmark approach is normally 2 cm caudal to the point where the clavicle takes the turn superiorly. The introducer needle is inserted at the defined landmark till the clavicle is felt and then advanced under and along the inferior border of the clavicle in the direction of the suprasternal notch until the vein is entered.

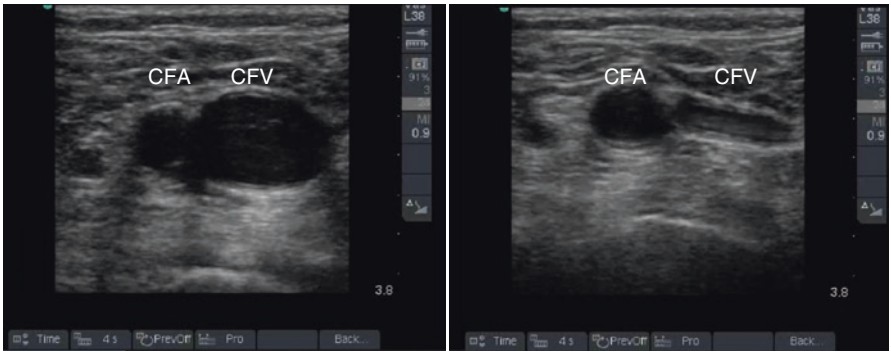

Fig. 10.42 Common femoral vein with compression maneuver

Although the traditional landmark approach is preferred by many, several articles suggest that US can increase the likelihood of success [5, 67]. With the short-axis approach, using the linear array probe with the orientation marker left scan along the inferior margin of the midclavicular region in a sagittal plane such that the transducer is almost perpendicular to the clavicle. Visualize the subclavian artery and vein and the pleural line below the vessel. Identify the vein where it is most superficial and separate from the artery. Insert the needle at 45°–70° angle relative to the skin surface and look for deformation of the soft tissue and vessel as the needle courses through and penetrates the SCV.

For the long-axis approach, find the SCV and artery in the short axis. Holding the transducer steady with the non-dominant hand, turn the probe counterclockwise with the dominant hand such that the marker faces the operator and obtain a longitudinal view of the SCV. Maintain the vessel in the middle of the screen while going from short to long axis. Insert the needle at the midpoint of the transducer at a 45°–70° and follow the needle as it punctures the midpoint of the SCV (Fig. 10.39). Although the long-axis approach appears to be a safer method as the needle is better visualized, a recent study showed that the short-axis method led to higher first pass and overall success rates, and fewer needle redirections, punctures, and complications [68].

Arterial Line Placement

Ultrasound use is often helpful in arterial catheterization of the critically ill CCU patient. The insertion of the catheter by blind palpation can sometimes require multiple attempts and thus can cause patient discomfort and arterial vasospasm. The radial artery is the most common site for arterial cannulation because it is thought to have a low rate of associated complications. This low rate occurs as a result of extensive collateral circulation involving the ulnar artery and palmar arches with flow to the distal limb. US guidance can be helpful with radial, axillary, and femoral artery catheterization. The use of ultrasound guidance has been shown to increase first-pass success rate and reduce number of attempts [69, 70].

Identify the artery that will be cannulated and adjust the gain and depth to optimize the image such that the vessel of interest appears in the center of the screen. Scan up and down in the transverse view to ensure there is no tortuosity or calcification. Locate a section with the largest diameter. The radial artery will be located adjacent to the styloid process of the radial bone. The femoral artery is the pulsatile vessel located in the femoral triangle. (Fig. 10.41) For axillary artery cannulation, have the patient place their arm under their head and scan the axillary region until the vessels are identified. Table 10.11 lists general anatomic landmarks and considerations for each potential site.

Arterial catheterization can be performed in either the transverse view or longitudinal view (Fig. 10.43a and b) [71]. With the transverse view, after locating the artery, optimize the image and center the artery in the transverse view. Anesthetize

the skin and insert the catheter-covered needle at the midpoint of the transducer at a 45°–60° angle. Slide or tilt the probe up and down until the needle tip is visualized. As the needle is advanced toward the artery, follow the tip of the needle. Adjust the position of the needle until it is directly over the artery and then puncture through the vessel wall into the lumen.

For the longitudinal view approach, first obtain a transverse view with the vessel in the center of the screen. Hold the base of the transducer steady and turn the transducer counterclockwise with the dominant hand and obtain a longitudinal view (Fig. 10.43b). While holding the transducer steady with the non-dominant hand resting on the body, insert the needle at the midpoint of the transducer at a 30°–45° angle (Fig. 10.44) and follow the needle as it punctures the midpoint of the artery. The longitudinal approach can be useful for radial artery cannulation, whereas the transverse approach is preferable for femoral artery and axillary artery catheterization (Table 10.12).

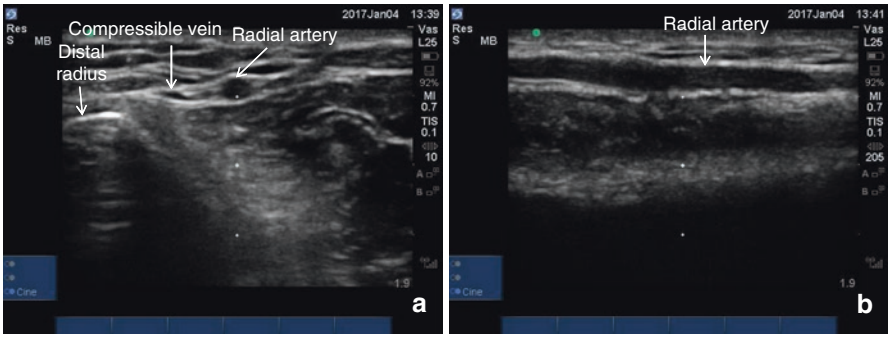

Fig. 10.43 (**a**) Radial artery in transverse view. (**b**) Radial artery in longitudinal view

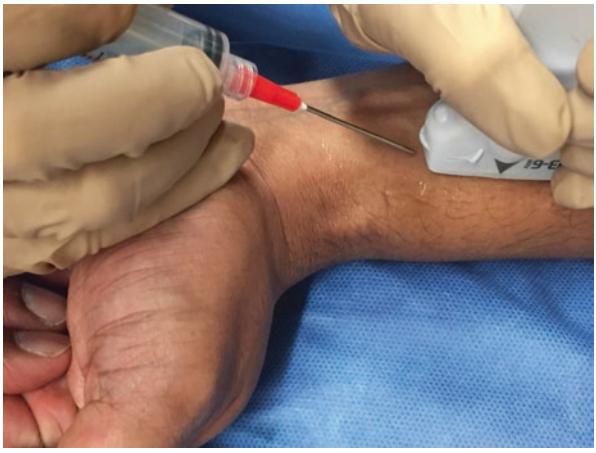

Fig. 10.44 Transducer holds for longitudinal approach for cannulation

Table 10.12 Site-specific characteristics of arterial line placement

Site	Landmarks	Advantages	Disadvantages	Complications
Radial	Distal end of radius between tendons of brachioradialis and flexor carpi radialis	Easy to locate Ease of placement Most common site of cannulation Presence of collateral flow (ulnar artery and palmar arch) Easily maintained	Easily collapsible Easily vasoconstricting Difficult in profound shock High thrombosis risk Lower accuracy due to distal position Frequent accidental removal	Thrombosis risk Limb ischemia
Femoral artery	Below the inguinal ligament Palpated midway between pubic symphysis and anterior iliac crest	Easy cannulation especially with US guidance Lower thrombosis risk Easily maintained Comfortable Largest accessible arterial access	Highest infection rate Compressible for bleeding control Avoid in peripheral arterial disease	Retroperitoneal hemorrhage
Axillary artery	Palpated in the intramuscular groove between the coracobrachial and triceps muscles Deep to pectoralis minor muscle	Lower infection and thrombosis risk Maintains pulsation in profound shock due to proximity to aorta Second largest after femoral artery Preferred in obese it radial access difficult	US guidance often needed High failure rate Proximity to pleural space: brachial plexus Right axillary line in continuity with right carotid ⇒ risk for cerebral thromboembolism	Brachial plexus compressive injury from hematoma Paresthesia Cannulation of left axillary is preferred compared to the right
Brachial artery	Medial side of antecubital fossa Lateral border of brachial muscle	Easily accessed but lacks the anatomic benefit of collateral circulation	Highest likelihood for thrombosis and loss of radial pulsations	Do not use Any cannulation may lead to upper limb ischemia Median nerve injury

Limitations of POCUS

Ultrasonography has developed as an irreplaceable tool in for the critical care physician in the management of a critically ill patient. Patient factors such as obesity, body habitus, rib shadows, artifacts, the presence of edema, subcutaneous

emphysema, or suboptimal patient position can be a limitation. It is also operator dependent, so adequate training and a proper certification process are required.

Conclusions

Point-of-care ultrasonography has evolved into an invaluable tool in facilitating the diagnosis and treatment of acutely ill patients. With the advent of portable US machines, POCUS has revolutionized the way that patients are managed and has drastically improved the safety of procedures. With the popularity of POCUS, medical schools are now adopting US education into undergraduate medical curriculum, and societies are offering courses to practicing clinicians. Goal-directed critical care ultrasonography readily answers clinical questions in the management of critically ill patients in the CCU with conditions such as shock, acute respiratory failure, and multi-organ failure.

References

1. Expert Round Table on Ultrasound in ICU. International expert statement on training standards for critical care ultrasonography. Intensive Care Med. 2011;37:1077–83.
2. Levitov A, Frankel HL, Blaivas M, et al. Guidelines for the appropriate use of bedside general and cardiac ultrasonography in the evaluation of critically ill patients—part II. Crit Care Med. 2016;44:1206–27.
3. Mayo PH, Beaulieu Y, Doelken P, et al. American College of Chest Physicians/La Société de Réanimation de Langue Française statement on competence in critical care ultrasonography. Chest. 2009;135:1050–60.
4. Narasimhan M, Koenig SJ, Mayo PH. A whole-body approach to point of care ultrasound. Chest. 2016;150:772–6.
5. Fragou M, Gravvanis A, Dimitriou V, et al. Real time ultrasound guided subclavian vein cannulation versus the landmark method in critical care patients: a prospective randomized study. Crit Care Med. 2011;39:1607–12.
6. Karakitsos D, Labropoulos N, De Groot E, et al. Real-time ultrasound-guided catheterisation of the internal jugular vein: a prospective comparison with the landmark technique in critical care patients. Crit Care. 2006;10:R162.
7. Mayo PH, Goltz HR, Tafreshi M, Doelken P. Safety of ultrasound-guided thoracentesis in patients receiving mechanical ventilation. Chest. 2004;125:1059–62.
8. McGee D, Gould M. Preventing complications of central venous catheterization. N Engl J Med. 2003;348:1123–33.
9. Greenstein YY, Littauer R, Narasimhan M, Mayo PH, Koenig SJ. Effectiveness of a critical care ultrasonography course. Chest. 2017;151:34–40.
10. Moore CL, Copel JA. Point-of-care ultrasonography. N Engl J Med. 2011;364:749–57.
11. Bakhru RN, Schweickert WD. Intensive care ultrasound: I. physics, equipment, and image quality. Ann Am Thorac Soc. 2013;10:540–8.
12. Scalea TM, Rodriguez A, Chiu WC, et al. Focused assessment with sonography for trauma (FAST). The Journal of Trauma: Injury, Infection, and Critical Care. 1999;46:466–72.
13. Feissel M, Fdr M, Faller J-P, Teboul J-L. The respiratory variation in inferior vena cava diameter as a guide to fluid therapy. Intensive Care Med. 2004;30:1834–7.

14. Manasia AR, Nagaraj HM, Kodali RB, et al. Feasibility and potential clinical utility of goal-directed transthoracic echocardiography performed by noncardiologist intensivists using a small hand-carried device (SonoHeart) in critically ill patients. J Cardiothorac Vasc Anesth. 2005;19:155–9.
15. Volpicelli G, Elbarbary M, Blaivas M, et al. International evidence-based recommendations for point-of-care lung ultrasound. Intensive Care Med. 2012;38:577–91.
16. Volpicelli G, Lamorte A, Tullio M, et al. Point-of-care multiorgan ultrasonography for the evaluation of undifferentiated hypotension in the emergency department. Intensive Care Med. 2013;39:1290–8.
17. Laursen CB, Sloth E, Lambrechtsen J, et al. Focused sonography of the heart, lungs, and deep veins identifies missed life-threatening conditions in admitted patients with acute respiratory symptoms. Chest. 2013;144:1868–75.
18. Schmidt GA, Koenig S, Mayo PH. Shock: ultrasound to guide diagnosis and therapy. Chest. 2012;142:1042–8.
19. Lichtenstein DA, Mezière GA. Relevance of lung ultrasound in the diagnosis of acute respiratory failure: the BLUE protocol. Chest. 2008;134:117–25.
20. Enghard P, Rademacher S, Nee J, Hasper D, Engert U, Jörres A, Kruse JM. Simplified lung ultrasound protocol shows excellent prediction of extravascular lung water in ventilated intensive care patients. Crit Care. 2015;19(36):1–8.
21. Doerschug KC, Schmidt GA. Intensive care ultrasound: III. Lung and pleural ultrasound for the intensivist. Ann Am Thorac Soc. 2013;10:708–12.
22. Lichtenstein DA, Menu Y. A bedside ultrasound sign ruling out pneumothorax in the critically ill. Lung sliding. Chest. 1995;108:1345–8.
23. Lichtenstein DA, Lascols N, Prin S, Mezière G. The "lung pulse": an early ultrasound sign of complete atelectasis. Intensive Care Med. 2003;29:2187–92.
24. Lichtenstein D, Mezière G. A lung ultrasound sign allowing bedside distinction between pulmonary edema and COPD: the comet-tail artifact. Intensive Care Med. 1998;24:1331–4.
25. Lichtenstein D, Mezière G, Biderman P, Gepner A. The comet-tail artifact: an ultrasound sign ruling out pneumothorax. Intensive Care Med. 1999;25:383–8.
26. Lichtenstein D, Mezière G, Seitz J. The dynamic air bronchogram. Chest. 2009;135:1421–5.
27. Kelbel C, Börner N, Schadmand S, et al. Diagnosis of pleural effusions and atelectases: sonography and radiology compared. Rofo. 1991;154:159–63.
28. Balik M, Plasil P, Waldauf P, et al. Ultrasound estimation of volume of pleural fluid in mechanically ventilated patients. Intensive Care Med. 2006;32:318.
29. Millington SJ, Koenig S. Better with ultrasound: pleural procedures in critically ill patients. Chest. 2018;153:224–32.
30. Mayo PH, Doelken P. Pleural ultrasonography. Clin Chest Med. 2006;27:215–27.
31. Lichtenstein DA, Mezière GA, Lagoueyte J-F, Biderman P, Goldstein I, Gepner A. A-lines and B-lines: lung ultrasound as a bedside tool for predicting pulmonary artery occlusion pressure in the crtically ill. Chest. 2009;136:1014–20.
32. Bouhemad B, Brisson H, Le-Guen M, Arbelot C, Lu Q, Rouby JJ. Bedside ultrasound assessment of positive end-expiratory pressure-induced lung recruitment. Am J Respir Crit Care Med. 2011;183:341–7.
33. Soummer A, Perbet S, Brisson H, Arbelot C, Constantin JM, Lu Q, Rouby JJ, Lung Ultrasound Study Group. Ultrasound assessment of lung aeration loss during a successful weaning trial predicts postextubation distress. Crit Care Med. 2012;40:2064–72.
34. Copetti R, Soldati G, Copetti P. Chest sonography: a useful tool to differentiate acute cardiogenic pulmonary edema from acute respiratory distress syndrome. Cardiovasc Ultrasound. 2008;6:16.
35. Sekiguchi H, Schenck L, Horie R, Suzuki J, Lee EH, McMenomy BP, Chen TE, Lekah A, Mankad SV, Gajic O. Critical care ultrasonography differentiates ARDS, pulmonary edema, and other causes in the early course of acute hypoxemic respiratory failure. Chest. 2015;148:912–8.
36. Lichtenstein DA, Mezière G, Lascols N, et al. Ultrasound diagnosis of occult pneumothorax. Crit Care Med. 2005;33:1231–8.

37. Lichtenstein D, Mezière G, Biderman P, Gepner A. The "lung point": an ultrasound sign specific to pneumothorax. Intensive Care Med. 2000;26:1434–40.
38. Galbois A, Ait-Oufella H, Baudel JL, Kofman T, Bottero J, Viennot S, Rabate C, Jabbouri S, Bouzeman A, Guidet B, Offenstadt G, Maury E. Pleural ultrasound compared with chest radiographic detection of pneumothorax resolution after drainage. Chest. 2010;138:648–55.
39. DiNino E, Gartman E, Sethi JM, McCool FD. Diaphragm ultrasound as a predictor of successful extubation from mechanical ventilation. Thorax. 2014;69:423–7.
40. Mathew JP, Kourouni I, Noronha S, Narayanswami G, Shapiro JM. A woman in her 70s with profound hypoxemia. Chest. 2016;150:e13–7.
41. Filopei J, Siedenburg H, Rattner P, Fukaya E, Kory P. Impact of pocket ultrasound use by internal medicine housestaff in the diagnosis of Dyspnea. J Hosp Med. 2014;9:594–7.
42. Rudski LG, Lai WW, Afilalo J, et al. Guidelines for the echocardiographic assessment of the right heart in adults: a report from the American Society of Echocardiography. J Am Soc Echocardiogr. 2010;23:685–713.
43. Marik PE, Baram M, Vahid B. Does central venous pressure predict fluid responsiveness?: A systematic review of the literature and the tale of seven mares. Chest. 2008;134:172–8.
44. Barbier C, Loubières Y, Schmit C, et al. Respiratory changes in inferior vena cava diameter are helpful in predicting fluid responsiveness in ventilated septic patients. Intensive Care Med. 2004;30:1740–6.
45. Lingawi SS, Buckley AR. Focused abdominal US in patients with trauma. Radiology. 2000;217:426–9.
46. Nazeer SR, Dewbre H, Miller AH. Ultrasound-assisted paracentesis performed by emergency physicians vs the traditional technique: a prospective, randomized study. Am J Emerg Med. 2005;23:363–7.
47. Barsuk JH, Cohen ER, Vozenilek JA, O'Connor LM, McGaghie WC, Wayne DB. Simulation-based education with mastery learning improves paracentesis skills. J Grad Med Educ. 2012;4:23–7.
48. Shuman WP, Hastrup W, Kohler TR, et al. Suspected leaking abdominal aortic aneurysm: use of sonography in the emergency room. Radiology. 1988;168:117–9.
49. Boniface KS, Calabrese KY. Intensive care ultrasound: IV. abdominal ultrasound in critical care. Ann Am Thorac Soc. 2013;10:713–24.
50. Blaivas M, Lambert MJ, Harwood RA, Wood JP, Konicki J. Lower-extremity Doppler for deep venous thrombosis—can emergency physicians be accurate and fast? Acad Emerg Med. 2000;7:120–6.
51. Kory PD, Pellecchia CM, Shiloh AL, Mayo PH, DiBello C, Koenig S. Accuracy of ultrasonography performed by critical care physicians for the diagnosis of DVT. Chest. 2011;139:538–42.
52. Melamed R, Sprenkle MD, Ulstad VK, Herzog CA, Leatherman JW. Assessment of left ventricular function by intensivists using hand-held echocardiography. Chest. 2009;135:1416–20.
53. Vignon P, Mücke F, Bellec F, et al. Basic critical care echocardiography: Validation of a curriculum dedicated to noncardiologist residents. Crit Care Med. 2011;39:636–42.
54. Kirkpatrick AW, Sirois M, Laupland KB, et al. Hand-held thoracic sonography for detecting post-traumatic pneumothoraces: the extended focused assessment with sonography for trauma (EFAST). The Journal of Trauma: Injury, Infection, and Critical Care. 2004;57:288–95.
55. Lichtenstein DA. BLUE-protocol and FALLS-protocol. Chest. 2015;147:1659–70.
56. Perera P, Mailhot T, Riley D, Mandavia D. The RUSH exam: Rapid Ultrasound in SHock in the evaluation of the critically ill. Emerg Med Clin North Am. 2010;28:29–56.
57. Sekiguchi H, Tokita JE, Minami T, Eisen LA, Mayo PH, Narasimhan M. A prerotational, simulation-based workshop improves the safety of central venous catheter insertion: results of a successful internal medicine house staff training program. Chest. 2011;140:652–8.
58. Milling TJ, Rose J, Briggs WM, et al. Randomized, controlled clinical trial of point-of-care limited ultrasonography assistance of central venous cannulation: the third Sonography Outcomes Assessment Program (SOAP-3) trial. Crit Care Med. 2005;33:1764–9.
59. Rupp SM, Apfelbaum JL, Blitt C, et al. American Society of Anesthesiologists Task Force on Central Venous Access. Practice guidelines for central venous access: a report by the

American Society of Anesthesiologists Task Force on Central Venous Access. Anesthesiology. 2012;116:539–73.
60. Troianos CA, Hartman GS, Glas KE, et al. Guidelines for performing ultrasound guided vascular cannulation: recommendations of the American Society of Echocardiography and the Society of Cardiovascular Anesthesiologists. J Am Soc Echocardiogr. 2011;24:1291–318.
61. Shekelle PG, Wachter RM, Pronovost PJ, et al. Making health care safer II: an updated critical analysis of the evidence for patient safety practices. Evid Rep Technol Assess. 2013:1–945. Chapters 18. Use of real time ultrasound for central line insertion brief update.
62. Pittirut M, Hamilton H, Biffi R, Mac Fie J, Pertkiewicz M. Espen. on parenteral nutrition: central venous catheters (access, care, diagnosis and therapy of complications). Clin Nutr. 2009;28:365–77.
63. Ortega R, Song M, Hanset CJ, Barash P. Ultrasound-guided internal jugular cannulation. N Engl J Med. 2010;362:e57.
64. O'Grady NP, Alexander M, Burns LA, Dellinger EP, Garland J, Heard SO, Lipsett PA, Masur H, Mermel LA, Pearson ML, Raad II, Randolph AG, Rupp ME, Saint S, Healthcare Infection Control Practices Advisory Committee. Guidelines for the prevention of intravascular catheter related infections. Am J Infect Control. 2011;39:S1–34.
65. Tsui JY, Collins AB, White DW, et al. Placement of a femoral venous catheter. N Engl J Med. 2008;358:e30.
66. Parienti JJ, Mongardon N, Megarbane B, et al. Intravascular complications of central venous catheterization by insertion site. N Engl J Med. 2015;373:1220–9.
67. Shiloh A, Eisen L, Yee M, Karakitsos D. Ultrasound-guided subclavian and axillary vein cannulation via an infraclavicular approach: in the tradition of Robert Aubaniac. Crit Care Med. 2012;40:2922–3.
68. Vezzani A, Manca T, Brusasco C, Santori G, Cantadori L, Ramelli A, Gonzi G, Nicolini F, Gherli T, Corradi F. A randomized clinical trial of ultrasound-guided infra-clavicular cannulation of the subclavian vein in cardiac surgical patients: short-axis versus long-axis approach. Intensive Care Med. 2017;43:1594–601.
69. Levin PD, Sheinin O, Gozal Y. Use of ultrasound guidance in the insertion of radial artery catheters. Crit Care Med. 2003;31:481–4.
70. Shiloh AL, Savel RH, Paulin LM, Eisen LA. Ultrasound-guided catheterization of the radial artery: a systematic review and meta-analysis of randomized controlled trials. Chest. 2011;139:524–9.
71. Ailon J, Mourad O, Chien V, et al. Ultrasound-guided insertion of a radial arterial catheter. N Engl J Med. 2014;371:e21.

Chapter 11
Contrast Echocardiography in the Cardiac Care Unit

Eyal Herzog, Seyed Hamed Hosseini Dehkordi, and Edgar Argulian

Abstract Suboptimal echocardiograms are common in critically ill patients. The obstacles that interfere with optimal echocardiographic imaging in cardiac care unit patients include suboptimal positioning, obesity, hyperinflated lungs due to mechanical ventilation, lung disease, subcutaneous emphysema, surgical incisions, chest tubes, bandages, and crowded quarters. It is well known that use of contrast in echocardiography significantly improves the image quality, but despite that, contrast echocardiography is widely underused. The current chapter outlines the basics of contrast echocardiography as it applies to critical care.

Keywords Contrast echocardiography · Myocardial infarction · Thrombus

Introduction

Cardiovascular disease is the foremost cause of death worldwide and is a major indication for diagnostic imaging [1]. More than 5.7 million patients are admitted annually to intensive care units in the United States for intensive and/or invasive monitoring. Approximately 20% of acute care admissions are to an intensive care setting [2].

Management of patients in the cardiac care unit (CCU) with acute symptoms and potentially life-threatening clinical conditions is a multifaceted task. Detailed history and comprehensive physical examination are the first steps. Laboratory and imaging diagnostic modalities are also crucially important steps in order to obtain a timely and accurate diagnosis and to stratify the risk to the patient's life in a timely and efficient manner. Echocardiography is a versatile, noninvasive, and easily available tool which can be performed at the bedside. It provides rapid results and avoids exposure to ionizing radiation. In addition, contemporary bedside echocardiography often renders invasive monitoring unnecessary in critically ill patients [3].

E. Herzog (✉) · S. H. H. Dehkordi · E. Argulian
Mount Sinai St. Luke's Hospital, New York, NY, USA
e-mail: Eyal.Herzog@mountsinai.org

E. Herzog, E. Argulian (eds.), *Echocardiography in the CCU*,
https://doi.org/10.1007/978-3-319-90278-4_11

Echocardiography is a common imaging procedure: approximately 32 million echocardiograms were done in the United States in 2016. The American Society of Echocardiography and other societies estimate that up to 20% of the echocardiograms are suboptimal which translate into approximately 6.4 million procedures a year. Suboptimal echocardiographic image is defined as an image in which two or more consecutive myocardial segments are not visualized well. Suboptimal echocardiograms are more common in critically ill patients accounting for up to 40–50% of all examinations in this patient population. It is well known that use of contrast in echocardiography significantly improves the image quality, but despite that, contrast echocardiography is widely underused.

The areas where use of contrast has the greatest impact include quantification of chamber dimensions, volumes, and ejection fraction (EF); assessment of regional wall motion abnormalities; documentation or exclusion of LV structural abnormalities; and documentation or exclusion of left ventricular or left atrial thrombus [4–7]. Contrast can also be used to enhance spectral Doppler signals.

Leading cardiovascular disease societies including the American Society of Echocardiography (ASE), International Academy of Cardiology (IAC), the International Contrast Ultrasound Society (ICUS), American College of Cardiology Foundation (ACCF), American Society of Nuclear Cardiology (ASNC), Heart Failure Society of America (HFSA), American Heart Association (AHA), Heart Rhythm Society (HRS), Society for Cardiovascular Angiography and Interventions (SCAI), Society of Critical Care Medicine (SCCM), Society of Cardiovascular Computed Tomography (SCCT), and Society for Cardiovascular Magnetic Resonance (SCMR) agree that contrast should be used when a suboptimal echocardiogram is acquired.

Ultrasound Contrast Agents

Contrast agents used in echocardiography are gas-filled microbubbles that are administered intravenously into the systemic circulation. There are currently three commercially available second-generation contrast agents in the United States: Optison™ (perflutren protein-type A microspheres; GE Healthcare, Buckinghamshire, UK), Definity® (perflutren lipid microsphere; Lantheus Medical Imaging, Billerica, MA), and Lumason® (sulfur hexafluoride lipid-type A microspheres; Bracco Diagnostics Inc., Monroe Township, NJ). The ultrasound properties of contrast agents are determined by the size of the microbubbles, the composition of the shell, and the encapsulated gas. Since the purpose of the contrast-enhanced imaging is typically opacification of the left-sided cardiac chambers, the microbubbles need to be small to be able to pass through the pulmonary capillaries into the systemic circulation in the absence of a shunt. At the same time, the echogenicity of microbubbles is directly proportional to their size; thus the largest microbubbles able to pass through the lung circulation have the strongest acoustic properties. The composition of the shell of microbubbles varies among the manufacturers and may include lipids

(Definity®, Lumason®) or human albumin (Optison™). The shell should provide elasticity for the microbubbles to resonate upon the application of ultrasound. Rigid and inelastic surface coating would get destroyed easily in the ultrasound field and may not provide effective continuous imaging. Finally, microbubbles are filled with high-molecular-weight gases which have poor blood solubility. As a result, they make microbubbles more stable and ensure high concentration of microbubbles in the left-sided chambers for real-time imaging.

The microbubbles in the commercially available contrast agents do not aggregate and are biologically inert. They remain entirely within the vascular space, have an intravascular rheology that is very similar to that of erythrocytes, and are eliminated from the body via the reticuloendothelial system.

Interaction of Contrast Agents with Ultrasound

The clinical application of contrast echocardiography relies on unique acoustic interaction of the microbubbles with the ultrasound. The microbubbles oscillate by asymmetrically changing their radius in response to compression and expansion in the ultrasound beam. As a result, they exhibit a nonlinear behavior generating strong harmonic signals at the multiples of the fundamental frequency. The strength of the harmonic signal is strongly dependent on the acoustic intensity of the ultrasound beam which is reported as mechanical index (MI). High MI imaging used for conventional echocardiography provides high-intensity contrast signal but results in rapid destruction of microbubbles. Therefore, it cannot be used for the purpose of continuous real-time imaging due to poor left ventricular opacification and swirling. Low and very low MI imaging allows detection of the microbubbles without destroying them, and it is well suited for continuous imaging such as assessment of left ventricular wall motion and ejection fraction. In low MI modes, the image quality may be degraded by tissue harmonic signal. Therefore, many manufacturers combine low-MI continuous imaging with tissue signal suppression techniques: these techniques enhance the signal from nonlinear scatterers (microbubbles) and cancel out signals from linear scatterers (tissue). All current cardiac ultrasound platforms use harmonic imaging for contrast echocardiography and conveniently provide presets to achieve optimal contrast imaging.

Safety of Contrast Echocardiography in the Critically Ill Patients

Despite the proven utility of contrast agents in the diagnosis and management of critically ill patients, concerns initially existed regarding the safety of these compounds. In a meta-analysis of 110,500 patients, the incidence of serious allergic and anaphylactoid reactions immediately after contrast administration was estimated at

0.009% and 0.004%, respectively. Anaphylactoid reactions are also known as complement activation-related pseudo-allergy (CARPA). CARPA reactions are not IgE mediated, do not necessarily need previous exposure, are generally milder or absent on repeated exposure, spontaneously resolve, and are more common among women and atopic patients [8]. Despite these reactions being extremely rare, busy echocardiography laboratories will likely eventually witness a severe allergic reaction; therefore staff education and provision of resuscitation medications and equipment are important.

Despite initial concerns, many safety studies have been published and led to a better understanding of contrast agents' safety in critically ill patients. For example, Main et al. [9] published a propensity-matched outcome study in critically ill patients undergoing echocardiography with and without a contrast agent. In this study, 1,006,381 critically ill patients were identified who underwent echocardiography. A propensity scoring algorithm was used to create matched cohorts of 16,217 patients who underwent echocardiography with or without contrast agents. At 48 h, mortality was lower in the cohort in which contrast agents were used (1.70% vs. 2.5%; odds ratio, 0.66; 95% confidence interval, 0.54–0.80); this difference persisted throughout the hospital stay (14.85% vs. 15.66%; odds ratio, 0.89; confidence interval, 0.84–0.96). Other studies in different subsets of patients with critical illness undergoing contrast echocardiography similarly demonstrated safety of ultrasound contrast agents. In addition, large studies have not confirmed the concerns raised by regulatory agencies regarding the use of contrast agents in patients with pulmonary hypertension or known intracardiac right-to-left shunts. Therefore in most of these circumstances, the benefit of ultrasound contrast agents outweighs their risks.

Echocardiography in Critical Care Settings

The primary importance for critical care delivery focuses on minimizing mortality and optimizing efficiency while preserving dignity and compassion for these patients with complex comorbidities and life-threatening conditions. Outcomes in critical care are mainly measured by reduced mortality, improved efficacy, decreased length of stay, and decreased cost of care. This is why performing the right tests at the right time and obtaining accurate diagnosis to initiate appropriate medical therapy are important factors in delivering quality patient care [10]. Echocardiography is one of the most powerful diagnostic and monitoring tools available to the modern critical care medicine. TTE has become the primary imaging tool for beside diagnosis and monitoring of patients with acute conditions. It is noninvasive, provides rapid and accurate assessment of cardiac morphology and hemodynamics, is useful in assisting therapeutic procedures, and provides quick results for rapid patient management decisions. The fact that echo can be easily repeated when required makes it highly valuable in emergency/critical care circumstances.

Due to the complex problems of patients in critical care, they have the most gain from accurate and reliable assessment of cardiac structure and function. However they can also present the greatest challenge in obtaining diagnostic studies.

The information echo provides has a significant impact on treatment strategies, but suboptimal image quality can often limit the accuracy or confidence in the data obtained.

Up to 50% of critically ill patients have nondiagnostic images which can have a significant impact on diagnosis and patient management.

The feasibility of TTE imaging can be limited because of the complex and dynamic profile of patients in the CCU, many of whom cannot assume an optimal position for imaging. Other obstacles that interfere with optimal echocardiographic imaging in CCU patients include obesity, hyperinflated lungs due to mechanical ventilation, lung disease, subcutaneous emphysema, surgical incisions, chest tubes, bandages, and crowded quarters. As a result, endocardial resolution is frequently suboptimal, preventing the accurate assessment of regional and global wall motion [4, 5].

Studies have shown that the use of contrast agents has a significant impact on outcomes and patient management decisions [4].

Kurt and colleagues [4] showed that there is a significant difference between the LV segments visualized using transthoracic echocardiography (TTE) between patients with and without the use of intravenous contrast agents (10.75 segments vs. 16.75 segments). This produced a significant change in the ability of the TTE to adequately evaluate LV function compared to unenhanced studies. In the subgroup analysis, this study also showed that use of contrast to enhance TTE images significantly improved visualization of abnormal LV segments in patients in surgical and medical ICUs (59% and 70% respectively). Also, when the cohorts of patients in both surgical and medical ICUs were combined, use of contrast enhancement significantly reduced the need for additional diagnostic procedures in 88% of patients. The combination of these effects resulted in altered medical management in 34.4% of patients in this study and resulted in 28% lower mortality at 48hours in critically ill patients. Other studies also supported this finding [9].

A major advantage of echocardiography is that both global and regional cardiac function can be evaluated early in the triage of patients with chest pain presenting to the cardiac care unit. The presence of regional wall motion abnormalities on a resting echo has a high sensitivity for detecting cardiac ischemia in these patients. Patients with regional wall motion abnormalities are six times more likely to have cardiac death, acute myocardial infarction, unstable angina, and congestive heart failure or need revascularization within 48 h of presentation ($p < 0.001$), and abnormal echocardiographic results are a more independent and incrementally useful prognostic indicator than clinical evaluation and ECG findings [5].

With improved visualization of the endocardial borders through the use of contrast, regional wall motion abnormalities can be identified that are otherwise not seen on the unenhanced images. The following cases exemplify real-life clinical scenarios in which use of contrast agents had an impact on patients' clinical course and management plan.

Examples of Clinical Applications of Contrast Echocardiography in the Cardiac Care Unit Which Changed Patient Management and Outcomes

Chest Pain Post Percutaneous Coronary Intervention

A 61-year-old man presented to the emergency department with right-sided chest pain. He recently underwent percutaneous coronary intervention (PCI) following an anterior ST elevation myocardial infarction. The TTE showed decreased LV EF (35%) and poorly visualized endocardial borders of the mid- and apical LV segments (Fig. 11.1).

A contrast agent was subsequently used which clearly demonstrated apical akinesis, mid- to distal septal akinesis, decreased LV systolic function, as well as existence of a protruding apical thrombus (Fig. 11.2).

Based on these findings, the patient management was changed, and he was started on anticoagulation therapy in addition to his dual antiplatelet therapy which eventually led to resolution of the clot on the follow-up echocardiogram.

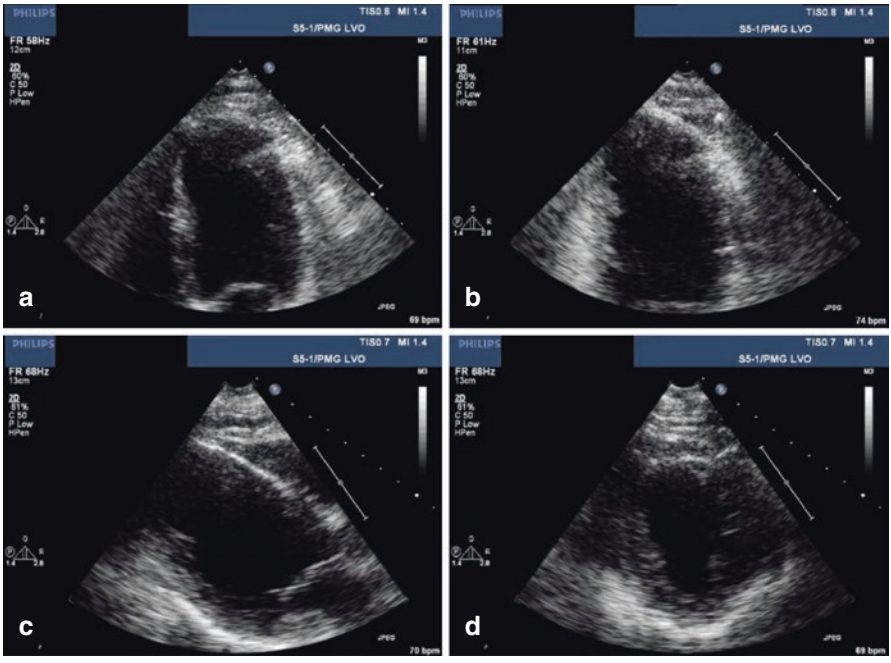

Fig. 11.1 Unenhanced apical four-chamber (**a**), apical two-chamber (**b**), parasternal long-axis (**c**), and parasternal short-axis (**d**) views

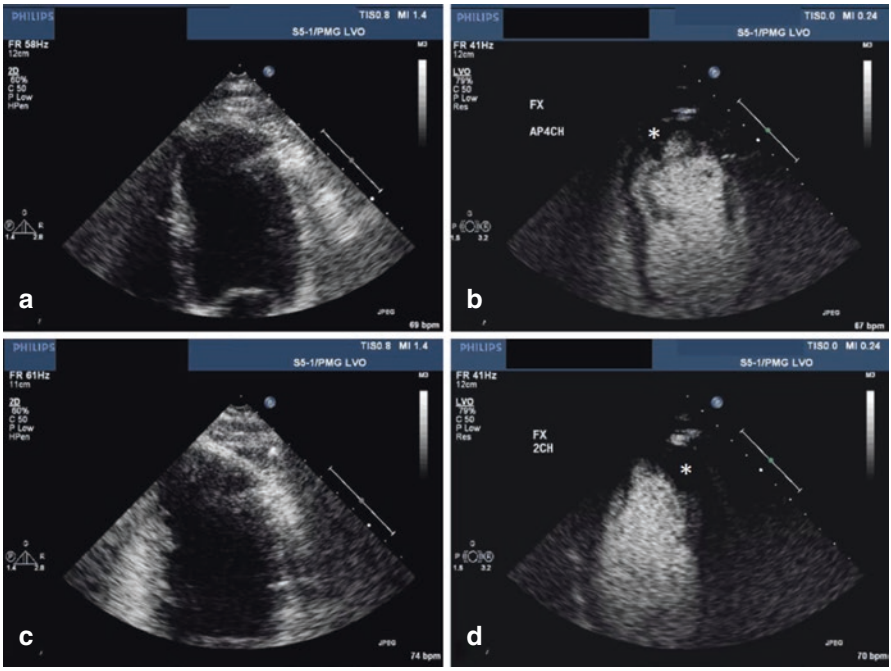

Fig. 11.2 Comparison between unenhanced (**a**) and contrast-enhanced (**b**) apical four-chamber views as well as unenhanced (**c**) and contrast-enhanced (**d**) apical two-chamber views demonstrating apical LV thrombus (asterisk)

Modern Management of Anterior Wall Myocardial Infarction

A 60-year-old man presented to the emergency department (ED) with new-onset severe substernal chest pain. His vital signs and physical examination were within normal limits. An electrocardiogram (ECG) was performed in the ED and showed concave ST segment elevation in the anterior precordial leads. He was immediately transferred to the cardiac catheterization laboratory where a diagnostic left heart catheterization showed complete occlusion of the mid-left anterior descending (LAD) coronary artery. He was treated with a drug-eluting stent to his mid-LAD, and he was started on eptifibatide, dual oral antiplatelets, atorvastatin, and metoprolol. The patient was subsequently transferred to CCU where a blood pressure of 90/60 mmHg was recorded, but his chest pain eventually resolved. His troponin I levels increased from 0.02 to 23 ng/mL. The patient developed gingival bleeding, so the eptifibatide was discontinued, and he was continued on aspirin, ticagrelor, atorvastatin, and metoprolol.

Due to hypotension a TTE was performed (Fig. 11.3) using an ultrasound contrast agent which helped rule out an apical thrombus. The patient did not require addition of an anticoagulant to his dual antiplatelet therapy; he improved clinically and was discharged home directly from CCU with a total hospital stay of 72 h.

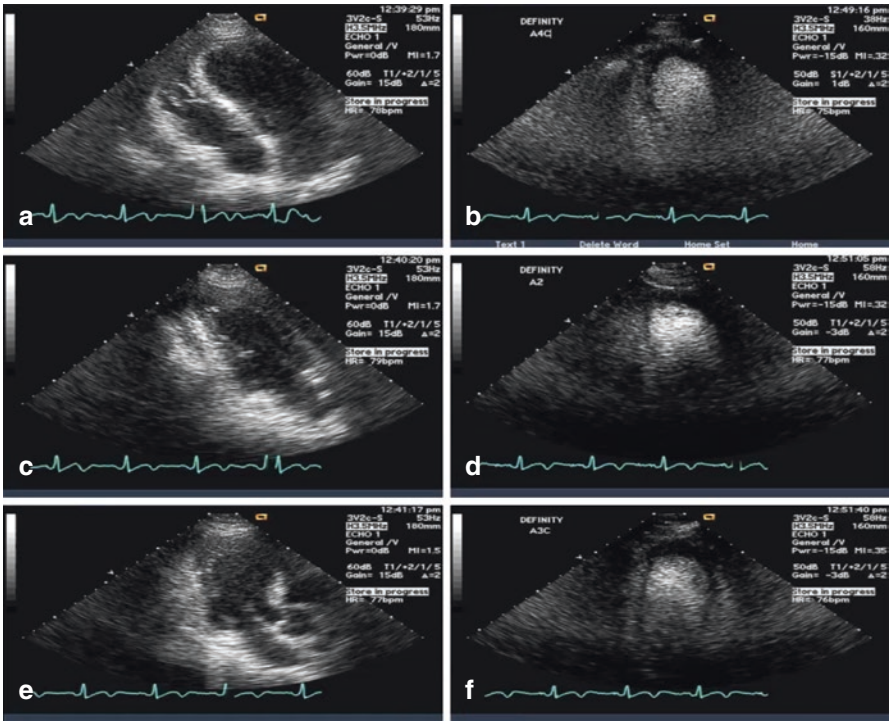

Fig. 11.3 Comparison between unenhanced (**a**) and contrast-enhanced (**b**) apical four-chamber views as well as unenhanced (**c**) and contrast-enhanced (**d**) apical two-chamber views and unenhanced (**e**) and contrast-enhanced (**f**) apical long-axis view

Shock in the Setting of Hypertrophic Cardiomyopathy

A 75-year-old woman arrived by ambulance to the ED after surviving an acute respiratory arrest which required intubation in the field. In the emergency department, her blood pressure was 212/98 mmHg with a heart rate (HR) of 56 bpm. Physical examination was remarkable for bibasilar rales and a 3/6 systolic murmur, best heard along the left sternal border. ECG showed sinus bradycardia with diffuse T wave inversion in the precordial leads.

Due to severe hypertension and bradycardia, the patient was treated with intravenous nitroglycerine and furosemide with initial BP improvement to 130/70 mmHg, but within 10 min, rapid response team was activated as her BP dropped to 66/30 mmHg with a pulse rate of 54 bpm. The patient's clinical condition changed dramatically from severe hypertension and bradycardia to shock with bradycardia. The patient was stabilized with normal saline and a transthoracic followed by transesophageal echocardiogram (TEE) was planned to both assess cardiac structure and function and rule out aortic dissection.

Figure 11.4 shows the bedside, unenhanced parasternal long-axis view with small pericardial effusion.

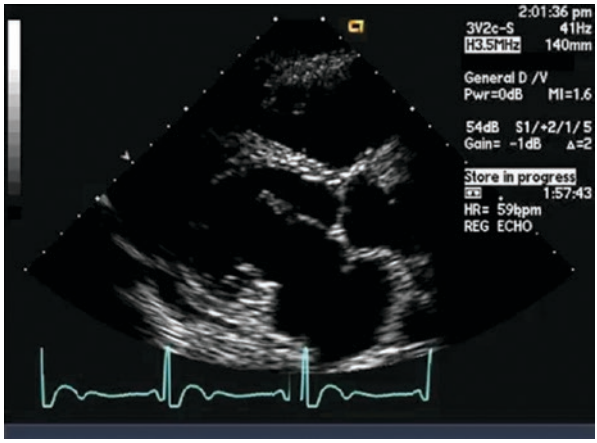

Fig. 11.4 Parasternal long-axis view showing small amount of pericardial effusion. LA is enlarged and the LVOT shows normal contractility. (*LA* left atrium, *LVOT* left ventricular outflow tract)

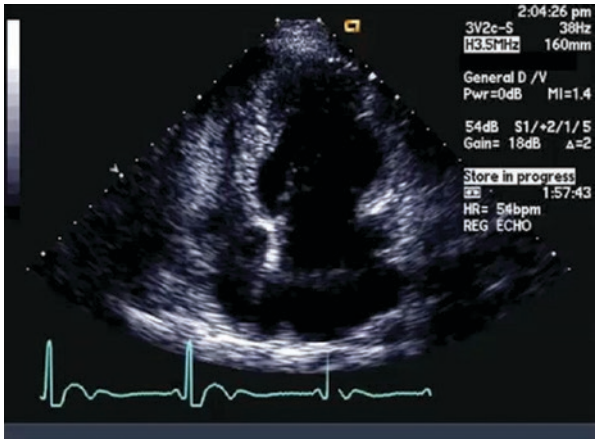

Fig. 11.5 Apical four-chamber view showing an enlarged LA and normal-sized RA and RV with normal RV contractility. (*LA* left atrium, *RA* right atrium, *RV* right atrium)

Figure 11.5 shows an unenhanced apical four-chamber view demonstrating an enlarged LA and normal-sized right atrium (RA) and right ventricle (RV) with normal RV contractility. Only the basal segments of the LV were seen, and they appeared to have normal contractility; however the apical segments were not well visualized.

Figure 11.6a, b demonstrate apical two-chamber views showing an enlarged LA with normal contractility of the base of the inferior and the anterior walls. In this view, it appeared that the apical and mid-inferior and apical and the mid-anterior segments are hypokinetic with a probable apical akinesis, but this was unclear due to poor quality of the images.

Figure 11.6c, d demonstrate apical long-axis views with good contractility of the base of the antero-septum and the basal inferolateral wall; however, the rest of the segments were not well seen.

Because of the suboptimal images, an echocardiographic contrast agent was used by the sonographer.

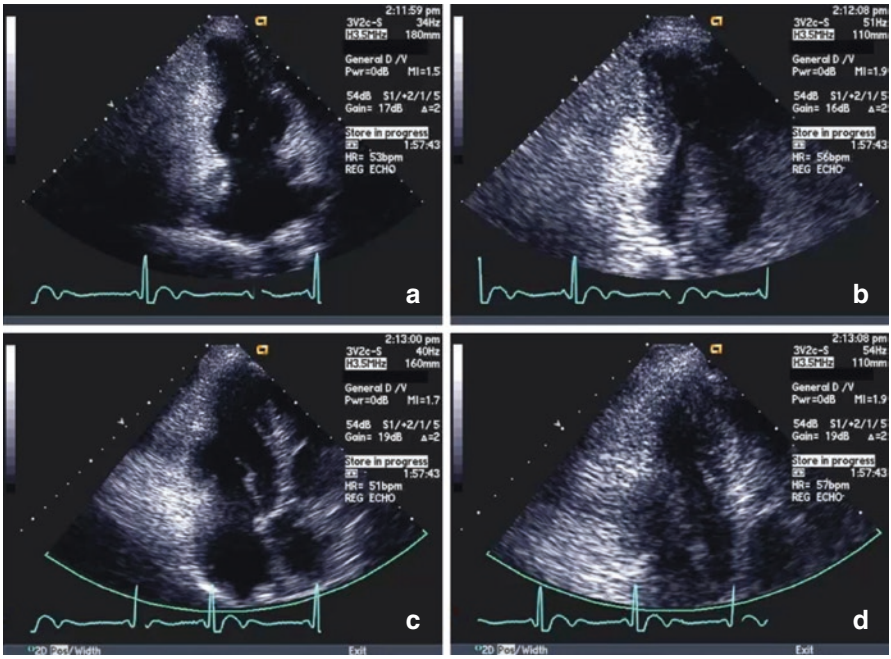

Fig. 11.6 Apical two-chamber (**a** and **b**) view showing enlarged LA but poor visualization of wall motion of the apical, mid-inferior and apical, mid-anterior segments. Apical long-axis view (**c** and **d**) with poor visualization of the apical lateral segment and the mid-antero-septum and the true apex. (*LA* left atrium)

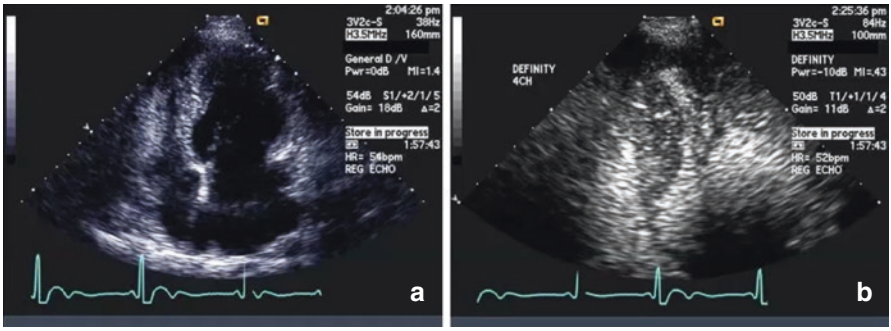

Fig. 11.7 Side-by-side comparison of the unenhanced (**a**) and contrast-enhanced (**b**) apical four-chamber view. Improved delineation of the endocardium helps demonstrate mid-cavitary obliteration from touching of the anterolateral and the infero-septal walls

Figure 11.7 shows side-by-side comparison of the unenhanced and enhanced apical four-chamber view. With improved delineation of the endocardium, it appeared as the anterolateral and infero-septal walls are touching each other causing mid-cavitary obliteration. In addition, there is trapping of contrast within the apex which is truly akinetic, consistent with subapical obstruction and apical akinetic chamber.

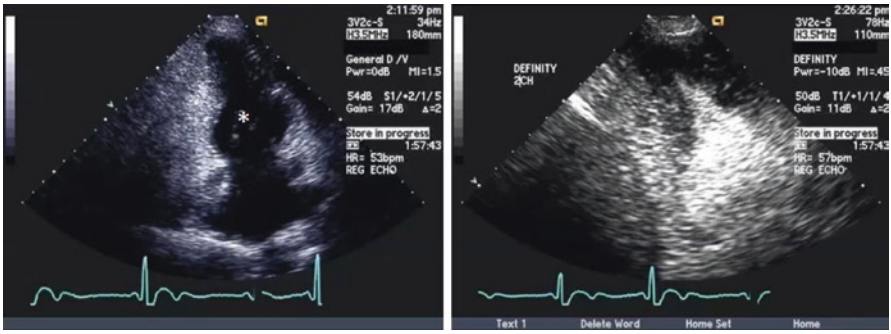

Fig. 11.8 Apical two-chamber view. Asterisk shows the typical "spade" shape ventricular cavity characteristic of apical hypertrophic cardiomyopathy

Figure 11.8 shows the apical two-chamber view with the typical "spade" shape ventricular cavity which is characteristic for apical hypertrophic cardiomyopathy.

Based on the new diagnosis, the patient was immediately treated with an intravenous beta-blocker, and the blood pressure improved to 120/80 mmHg. No additional testing was required, and the initially planned TEE was cancelled. The patient was discharged home 3 days later on a combination of a beta-blocker and a calcium channel blocker.

Conclusions

TTE is an invaluable tool in diagnosis and management of acutely ill patients seen in CCU or ED, but unfortunately, the image quality is often suboptimal. The use of ultrasound contrast agents to enhance the acquired images improves the diagnostic yield of echocardiography by rendering examination interpretable. Consequently, this may have implications in patient management. Studies have shown that these agents are not only safe but are associated with improved survival in critically ill patients.

References

1. Shaw LJ. Impact of contrast echocardiography on diagnostic algorithms: pharmacoeconomic implications. Clin Cardiol. 1997;20(suppl 1):I-39–48.
2. Critical Care Statics. http://www.sccm.org/Communications/Pages/CriticalCareStats.aspx. Accessed Jan 2018.
3. Orde S, Slama M, Hilton A, Yastrebov K, Mclean A. Pearls and pitfalls in comprehensive critical care echocardiography. Crit Care. 2017;21(1):279.
4. Kurt M, Shaikh KA, Peterson L, et al. Impact of contrast echocardiography on evaluation of ventricular function and clinical management in a large prospective cohort. J Am Coll Cardiol. 2009;53(9):802–10.

5. Mulvagh SL, Rakowski H, Vannan MA, Abdelmoneim SS, Becher H, Bierig SM, et al. American Society of Echocardiography Consensus Statement on the clinical applications of ultrasonic contrast agents in echocardiography. J Am Soc Echocardiogr. 2008;21(11):1179–201.
6. IAC Standards and Guidelines for Adult Echocardiography Accreditation. https://www.intersocietal.org. Accessed on Jan 2018.
7. The EFSUMB Guidelines and Recommendations on the Clinical Practice of Contrast Enhanced Ultrasound (CEUS): update 2011 on non-hepatic applications. Http://www.icus-society.org/ceus-guidelines. Accessed Jan 2018.
8. Szebeni J. Complement activation-related pseudoallergy: a new class of drug-induced acute immune toxicity. Toxicology. 2005;216:106–21. https://doi.org/10.1016/j.tox.2005.07.023.
9. Main ML, Hibberd MG, Ryan A, Lowe TJ, Miller P, Bhat G. Acute mortality in critically ill patients undergoing echocardiography with or without an ultrasound contrast agent. JACC Cardiovasc Imaging. 2014;7(1):40–8.
10. Weled BJ, Adzhigirey LA, Hodgman TM, et al. Critical care delivery: the importance of process of care and ICU structure to improved outcomes: an update from the American College of Critical Care Medicine Task Force on Models of Critical Care. Crit Care Med. 2015;43(7):1520–5.

Chapter 12
Use of Echocardiography in Patients with Intracardiac Devices

Edward Chu, Karthik Seetharam, Brandon W. Calenda, and Farooq A. Chaudhry[†]

Abstract Intracardiac ventricular assist devices (VADs) are increasingly being used in the management of patients with severe heart failure refractory to medical therapy. In the CCU, echocardiography is utilized to confirm appropriate position and function of intracardiac VAD components as part of routine surveillance or in response to concerning signs and symptoms. This chapter will focus on the use of echocardiography in adult patients with durable continuous-flow left ventricular assist devices (LVADs) as well as short-term, percutaneous left- and right-sided Impella VADs.

Keywords Impella · Assist devices · Heart failure

Introduction

Intracardiac ventricular assist devices (VADs) are increasingly being used in the management of patients with severe heart failure refractory to medical therapy. In the CCU, echocardiography is utilized to confirm appropriate position and function of intracardiac VAD components as part of routine surveillance or in response to concerning signs and symptoms. This chapter will focus on the use of echocardiography in adult patients with durable continuous-flow left ventricular assist devices (LVADs) as well as short-term, percutaneous left- and right-sided Impella VADs. First-generation, pulsatile-flow surgical LVADs are no longer implanted and will not be discussed. Durable right ventricular assist devices do not contain intracardiac components and will also not be discussed.

[†]Deceased

Dedication: This chapter is dedicated to the memory of Dr. Farooq Chaudhry who was a cherished colleague in the Division of Cardiology at Mount Sinai hospital. His untimely passing in 2017 has left a void in our hearts and minds.

E. Chu · K. Seetharam · B. W. Calenda (✉) · F. A. Chaudhry
Mount Sinai School of Medicine, New York, NY, USA
e-mail: brandon.calenda@mountsinai.org

E. Herzog, E. Argulian (eds.), *Echocardiography in the CCU*,
https://doi.org/10.1007/978-3-319-90278-4_12

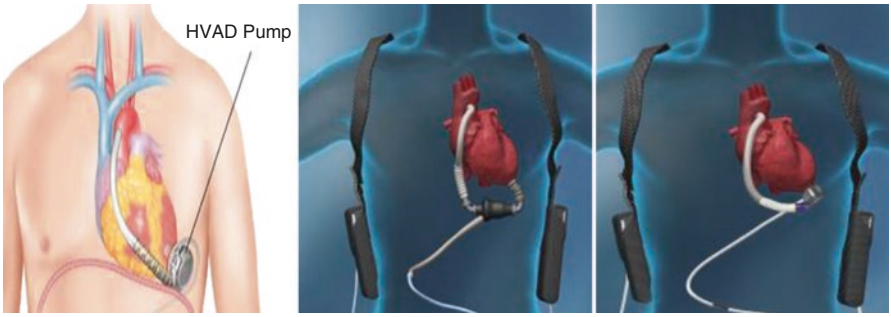

Fig. 12.1 FDA-approved CF LVADs: the HVAD, HeartMate II, and HeartMate III (far right)

Echocardiography in Continuous-Flow Left Ventricular Assist Devices

LVADs are indicated for use in patients with severe heart failure as a bridge to native heart recovery, a bridge to eventual heart transplant, or a destination therapy in those who are not heart transplant candidates. The LVADs currently approved by the FDA are the HeartWare HVAD and the Thoratec HeartMate II and III (Fig. 12.1).

The notable components of a continuous-flow LVAD include an inflow cannula that is inserted into the left ventricular apex, an outflow cannula that is inserted into the ascending aorta, an extracardiac pump that receives blood from the inflow cannula and delivers blood through the outflow cannula, and a driveline that runs from the pump to a wearable controller.

When to Consider Echocardiography

After LVAD implantation, echocardiographic examination can be performed for routine surveillance, in response to concerning signs, symptoms, or device alarms, or to optimize LVAD settings as part of a ramp study. During each echocardiographic examination, the LVAD speed (in rotations per minute, rpm) and blood pressure should be recorded as these conditions can alter the degree of unloading of the left ventricle. Comparisons of serial echocardiograms should also be made in the context of the LVAD speed and blood pressure. Echocardiographic examination of patients with LVADs includes the standard views as well as LVAD-specific views that interrogate the inflow cannula and outflow cannula, assess the impact and sequelae of left ventricular unloading by the LVAD, and evaluate for potential LVAD-related complications such as suction, aortic regurgitation, and thrombus formation.

Echocardiography for Routine Surveillance

The purpose of a surveillance echocardiogram is to trend baseline LVAD and native heart anatomy and function over time to ensure appropriate response to LVAD therapy and to detect subclinical LVAD or native heart abnormalities. After LVAD implantation, surveillance transthoracic echocardiograms should be performed prior to discharge from index hospitalization, 1 month after initial implant, every 3 months after initial implant in the first year, and every 6–12 months after the first year [1].

Echocardiography in Response to Signs, Symptoms, or Device Alarms

There should be a low threshold to perform echocardiographic examination in response to a deterioration in clinical status and/or new controller alarms as LVAD malfunction or inappropriate patient response to LVAD therapy can be fatal if not addressed. Common LVAD alarms include notifications related to changes in pulsatility index, changes to flow, suction triggers, and high-power consumption. LVAD-related complications detectable by echocardiography include intracardiac thrombus formation, intravascular hemolysis from motor-related shear stress, suction events, new or worsening aortic regurgitation, and inappropriate unloading conditions. These conditions will be further discussed in the section titled "Abnormal Findings on Echocardiogram."

Echocardiogram to Optimize LVAD Speed

An echocardiogram to optimize LVAD speed and its immediate effect on left heart function, known as unloading conditions, relative to baseline conditions is known as a ramp study. Ramp studies are often performed as part of routine surveillance or in response to concerning clinical features. Poor response to specific ramp study protocols can be suggestive of LVAD pump thrombosis [2].

During a ramp study, the unloading conditions as determined by the LV internal diastolic dimension (LVIDd), interventricular septum (IVS) orientation, aortic valve opening frequency/duration, and MR severity are tracked as the LVAD speed is incrementally increased to establish a LVAD minimum speed, maximum speed, and optimal speed. Relative to baseline measurements, the minimum speed is defined as the speed below which the LVIDd is increased and the IVS becomes shifted more rightward, aortic valve opening becomes more frequent, and the MR becomes more severe. Relative to baseline measurements, the maximum speed is defined as the speed above which the LVIDd is reduced and IVS shifts leftward leading to inflow cannula turbulence, obstruction or suction events, and the aortic valve ceases to open. The optimal speed occurs below the maximum speed when the aortic valve opening occurs with a frequency determined by the LVAD medical team (e.g., every third cardiac cycle).

Normal Findings on Echocardiogram

LVAD-specific transthoracic echocardiographic views are used to assess the inflow cannula, outflow cannula, and left heart unloading conditions. Standard views of native heart structures can be used to evaluate for LVAD-related complications such as aortic regurgitation, vegetations, and intracardiac thrombus.

Inflow Cannula

The inflow cannula, typically implanted at or near the cardiac apex, is best visualized on transthoracic echocardiogram in the parasternal long-axis or apical views. Although direct visualization may be challenging due to image quality or device material artifact, several parameters should be identified.

On direct visualization, the inflow cannula should be free of any adherent masses. Color Doppler assessment should demonstrate laminar flow from the left ventricle to the outflow cannula. Inflow should not be impeded by the interventricular septum. Pulsed and CW Doppler should demonstrate low-velocity, continuous flow throughout the cardiac cycle. Due to intrinsic left ventricle contractility, the waveform will always be somewhat pulsatile, even when the ventricle is appropriately off-loaded and the aortic valve does not open. In a normally functioning device, peak systolic velocity should be less than 1.5 m/s [1]. Accurate Doppler interrogation of the inflow cannula frequently requires off-axis, individualized views to ensure an angle of interrogation parallel to flow.

Of note, in the HVAD, and at times the HeartMate III, color and spectral Doppler may be severely limited or unavailable due to Doppler artifact caused by the proximity of the impeller to the inflow cannula [1].

Outflow Cannula

Unlike the inflow cannula, which can be seen on standard TTE views, the outflow cannula requires atypical views. The aortic anastomosis is best visualized on transthoracic echocardiogram in a high left parasternal long-axis view. In some patients, this can also be seen in a supraclavicular or suprasternal view. Similar to the inflow cannula, pulsed and CW Doppler profiles should be obtained. The waveform will again show mild pulsatility with continuous flow throughout diastole. Although there are no clear benchmarks for abnormal peak systolic velocity at the outflow cannula, normal velocities should generally be less than 2 m/sec[1].

Unloading Conditions

Left heart unloading conditions are a means of assessing the extent to which the failing, dilated left ventricle has been decompressed and bypassed by the LVAD. This is largely modulated by the speed of the LVAD. Loading conditions are best appreciated in the parasternal long-axis and the apical four-chamber views. An optimally unloaded left ventricle should display the following characteristics:

- The LV internal diastolic dimension (LVIDd) should be significantly reduced compared with the preimplantation echo.
- The interventricular septum should be midline or shifted toward the left ventricle as compared with the preimplantation echo. The septum should not be bowing toward or obstructing the inflow cannula.
- The aortic valve should not open with every cardiac cycle (although the ideal frequency of aortic valve opening is often patient and physician dependent).
- Mitral regurgitation should be less than that seen on the preimplantation echo.
- Tricuspid regurgitation and RVSP should be less than that seen on the preimplantation echo.

Abnormal Findings on Echocardiogram

There are a number of key, pathologic echocardiographic findings which are important to recognize, whether the echo is performed for routine follow-up or to investigate concerning signs or symptoms. These findings must be integrated with the clinical situation and device alarms to arrive at an appropriate diagnostic plan.

Excessive Unloading and Suction Events

As discussed above, when the LV is appropriately unloaded, the LVIDd decreases and the IVS shifts leftward, and the aortic valve opens infrequently or not at all. Taken to extremes, the LV cavity can become small and underfilled, leading to significant leftward shift of the interventricular septum. This can lead to "suction events," in which nearby endocardium (typically septum) is transiently pulled into the path of the inflow cannula, leading to impaired flow through the inflow cannula and ventricular arrhythmias due to local irritation of the "sucked in" endocardium. Intermittent high velocities at the inflow cannula can be seen. Suction events can result from inappropriately high LVAD speeds and may be exacerbated by conditions of decreased LV preload, as may be seen in hypovolemia, RV failure, or cardiac tamponade. This typically manifests as low-flow alarms on the VAD.

Excessive unloading, with its leftward shift of the septum, alters RV geometry with multiple potential downstream effects. Progressive RV dysfunction can result from increased RV end-diastolic volume, impaired RV systolic function, and increased tricuspid regurgitation.

Inadequate Unloading

The characteristics of an inadequately unloaded LV include a minimal or absent decrease in LVIDd, rightward-shifted IVS, increased mitral regurgitation, increased right-sided pressures, and aortic valve opening with every cardiac cycle. This can result from inappropriately low LVAD speeds or pump malfunction. This frequently manifests as high-flow alarms on the VAD.

Thrombosis

LVAD thrombosis is a feared complication in the care of patients with durable LVADs. Pump thrombosis is usually not directly visualized on echocardiography, and its presence must be inferred from the available data. Pump thrombosis usually manifests with signs of inadequate unloading, along with increased speed and power requirements, as may be demonstrated during a ramp study [2]. Other supportive signs include reduced inflow or outflow cannula Doppler velocities. If thrombosis or obstruction is localized to the outflow graft, increased peak systolic velocities may be seen on Doppler interrogation of the outflow tract. This is associated with high-flow alarms on the VAD.

Cardiac Tamponade

Although the features of cardiac tamponade are well described elsewhere in this text, there are some unique features to tamponade in the presence of LVAD which bear mentioning. In the postoperative state, there may be pericardial hematoma rather than free-flowing effusion. Both the LV and RV may appear underfilled, and typical features of ventricular interdependence may not be seen. Valve inflow velocities, specifically mitral inflow velocities, often do not have excessive respiratory variation due to the presence of the LVAD. Thus, in the presence of low-flow alarms and significant clinical suspicion, one should not depend upon "classic" features of tamponade to make the diagnosis.

Echocardiography in Impella Ventricular Assist Devices

The Abiomed portfolio of Impella heart pumps, including the left heart systems Impella 2.5, 5.0, CP, and LD, as well as the right heart Impella RP, are short-term ventricular assist devices used to augment cardiac output in critically ill patients

with advanced heart failure or undergoing complex cardiac intervention. Correct positioning of the Impella catheter in the ventricular outflow tract and associated great vessel is critical for proper device functioning. During initial implantation, fluoroscopy is necessary to guide placement of the Impella catheter. After implantation, catheter-related complications can develop, leading to hemodynamic instability and activation of device alarms. In these acute situations, echocardiography is commonly used to reassess catheter position and function.

Impella 2.5, 5.0, CP, and LD [3, 4]

The left heart Impella catheter systems, including the Impella 2.5, 5.0, CP, and LD, are indicated for use in patients with ongoing cardiogenic shock immediately after myocardial infarction or open-heart surgery. The Impella 2.5 and CP can be additionally used in patients with depressed left ventricular ejection fraction ≤35% without three-vessel disease or ≤30% with three-vessel disease and undergoing high-risk percutaneous coronary intervention. The Impella 2.5, 5.0, and CP catheter systems can be implanted percutaneously, whereas the Impella LD can only be implanted surgically (Fig. 12.2).

When to Consider Echocardiography

Transthoracic or transesophageal echocardiogram allows for simultaneous visualization of the inlet and outlet areas of the left heart Impella catheters and is the preferred imaging modality for routine position surveillance or in response to signs,

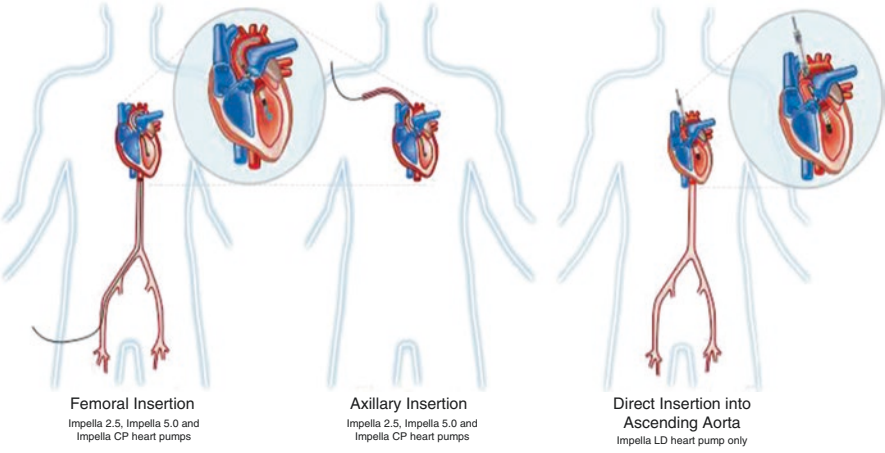

Fig. 12.2 Implantation techniques for left heart Impella pumps

Table 12.1 Concerning indicators of left heart Impella pump malfunction

Symptoms	Chest discomfort, shortness of breath, palpitations, light-headedness, and loss of consciousness
Vital signs	Hypotension, tachycardia, and hypoxemia
Physical exam	Features of left-sided heart failure (lung crackles, new S3 or S4 murmur, etc.)
ECG/telemetry	PVC, NSVT, VT/VF
Labwork	Markers of poor perfusion (increased lactate, decreased pH, etc.), markers of hemolytic anemia (decreased hemoglobin/hematocrit, increased LDH, decreased haptoglobin, etc.)
Cardiac imaging (CXR, CT, MRI, etc.)	Movement of Impella catheter on serial studies
Impella Controller display	Abrupt change in the placement signal (waveform or pressure reading) Abrupt change in motor current (waveform or current reading) Abrupt change in flow reading
Impella catheter position alarms	Including but not limited to: Impella position in the ventricle Impella position wrong Impella position unknown Impella outflow blocked Impella flow reduced Suction

symptoms, and device alarms concerning for Impella malfunction. Similar to intra-aortic balloon pumps and endotracheal tubes, the Impella catheter can migrate as a result of excess "slack" or patient movement or inadvertently from necessary medical care. Displacement and/or obstruction of the catheter inlet and outlet areas can lead to blood flow disturbances which may in turn cause electrical and mechanical cardiac dysfunction. The following signs, symptoms, and device features may be indicative of Impella catheter malfunction (Table 12.1):

Normal Position on Echocardiogram

The distal portion of the left heart Impella catheters is notable for the motor housing unit, blood outlet area, a 6–8 cm cannula, a blood inlet area, and a pigtail end in the Impella 2.5, 5.0, and CP or a straight end in the Impella LD. The cannula for the Impella 2.5, 5.0, and CP catheters is longer and contains a slight bend, whereas the cannula for the Impella LD catheter is shorter and straight (Fig. 12.3).

Visualization of both the distal catheter inlet and outlet orientation in the left ventricular outflow tract and ascending aorta is best achieved with parasternal long-axis transthoracic echocardiogram view or with long-axis transesophageal view. When properly positioned in the heart, the inlet area should be in the left ventricular outflow tract approximately 3.5 cm below the aortic valve, and the outlet area should be distal to the aortic valve in the ascending aorta. The catheter inlet area can be distinguished by faint railroad track markings, whereas the outlet area is hyperechoic in appearance relative to the adjacent cannula. Except for the cannula which

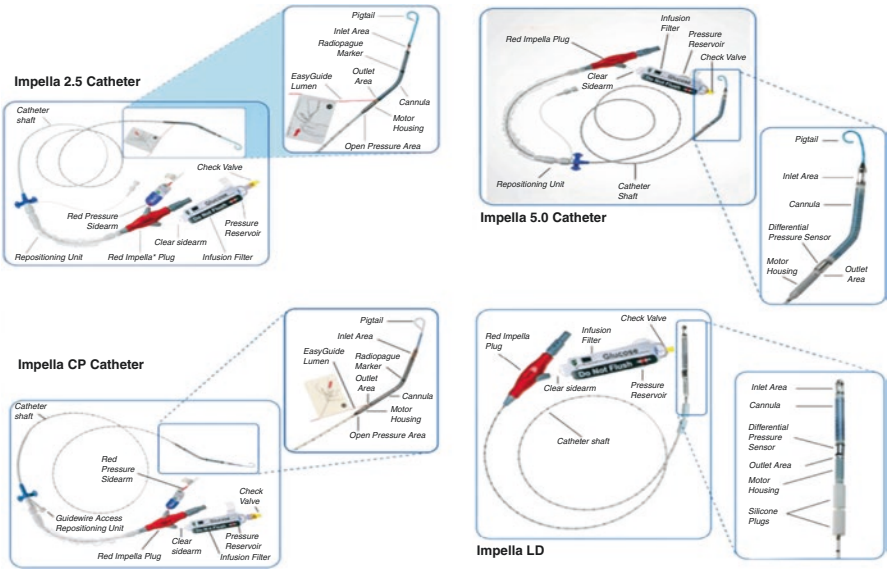

Fig. 12.3 Anatomy of left heart Impella catheters

is in contact with the aortic valve leaflets, no portion of the distal Impella catheter should be in contact with cardiac structures, including the left ventricular wall and mitral valve apparatus (Figs. 12.4 and 12.5).

Color Doppler analysis over the correctly positioned outlet area will show a dense mosaic pattern consistent with turbulent blood flow above the aortic valve in the ascending aorta (Fig. 12.6).

Abnormal Findings on Echocardiogram

The most common catheter-related abnormalities detected on echocardiogram are the presence of adherent masses and changes to catheter position. Masses adherent to the catheter surface are most concerning for thrombus or infected vegetation. By protocol, patients with an implanted left heart Impella catheter should be receiving anticoagulation with a goal ACT 160–180 s to prevent thrombus formation. Infected vegetation should be considered in individuals with signs and symptoms of endocarditis, including fever and positive blood cultures.

Minor position fluctuations of the left heart Impella catheter from the motion of nearby blood flow and surrounding cardiac structures are unlikely to have any functional consequence on device operation or patient hemodynamic parameters. Major position changes necessitating catheter adjustment occur when the catheter inlet area moves above the aortic valve, the catheter outlet area moves below the aortic valve, or a contact between the catheter and nearby cardiac structures leads to device or cardiac displacement. Echocardiography can be used to detect and guide repositioning of the Impella catheter in each of these three situations.

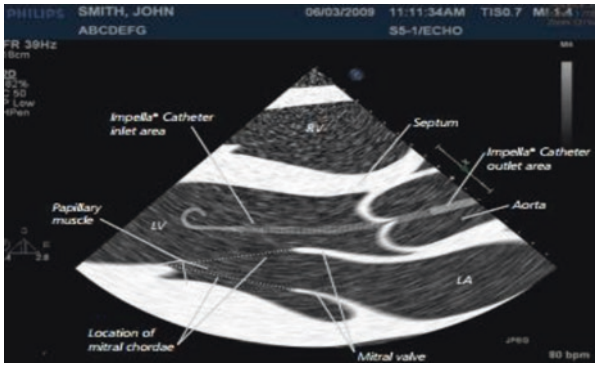

Fig. 12.4 Correct Impella catheter position on transthoracic echocardiogram parasternal long-axis view

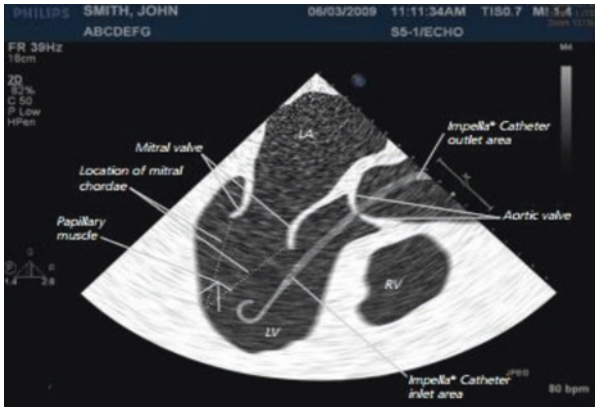

Fig. 12.5 Correct Impella catheter position on transesophageal echocardiogram long-axis view

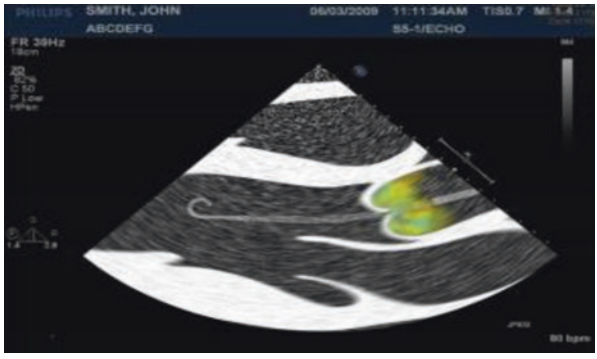

Fig. 12.6 Correct Impella catheter position on transthoracic echocardiogram parasternal long-axis view with color Doppler flow

Impella Catheter Moves Too Far into the Left Ventricle

If the Impella catheter has migrated too far into the left ventricle, the outlet area may be incorrectly positioned below the aortic valve. Blood flow from the catheter inlet area to the outlet area is recycled within the left ventricle, and there is no augmentation of cardiac output. On echocardiogram, the most distal end of the Impella catheter will appear below the midpoint of the left ventricular cavity and close to the LV apex. The radiopaque portion of the outlet area will appear within the left ventricular outflow tract (Fig. 12.7).

Impella Catheter Moves Too Far Out of the Left Ventricle

If the Impella catheter has migrated too far out of the left ventricle, the inlet area may be incorrectly positioned above the aortic valve. Blood flow from the catheter inlet area to the outlet area is recycled within the thoracic aorta, and there is no augmentation of cardiac output. On echocardiogram, the terminal portion of the Impella catheter will appear above the midpoint of the left ventricular cavity and in extreme cases entirely out of the left ventricle. The railroad track appearance of the inlet area will appear within the ascending aorta. If the Impella catheter is completely out of the left ventricle, it should not be repositioned into the left ventricle without the use of a guidewire under fluoroscopic guidance (Fig. 12.8).

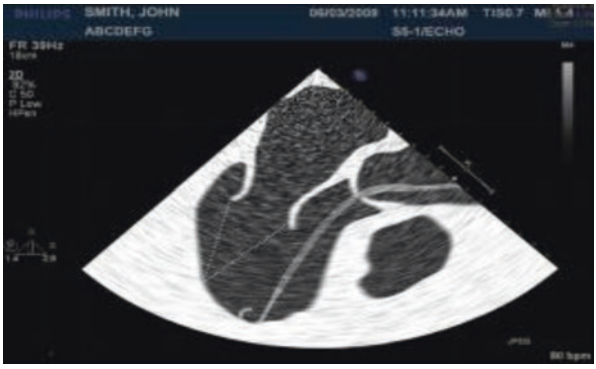

Fig. 12.7 Impella catheter too far into the left ventricle on transesophageal echocardiogram

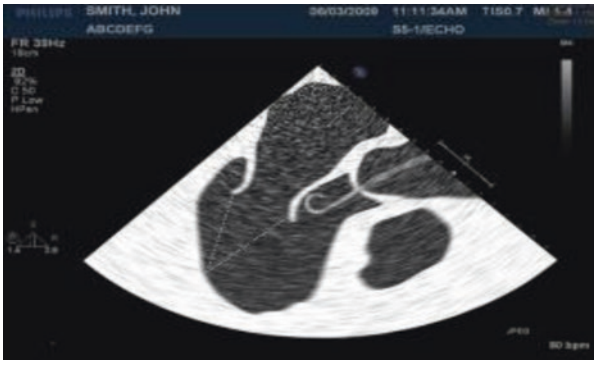

Fig. 12.8 Impella catheter too far out of the left ventricle on transesophageal echocardiogram

Impella Catheter in Contact with Cardiac Structures

If a portion of the Impella catheter is caught on or against a cardiac structure, it may lead to partial or complete obstruction of the catheter inlet and/or outlet causing hemolysis, low pump flow, and suction events. Irritation of the left ventricular wall by the catheter can lead to ventricular ectopy, NSVT, or VT/VF. Entanglement of the catheter in the chordae tendineae or papillary muscles can disrupt mitral valve function resulting in mitral regurgitation. Similar entanglement of the distal pigtail in the aortic leaflets can result in aortic regurgitation. On echocardiogram, the Impella catheter will be found against the endocardium and moving simultaneously with cardiac systole and diastole. In some cases, gentle manipulation of the proximal Impella catheter from the percutaneous access site may be sufficient in relieving contact of the distal catheter from adjacent cardiac structures. If there is risk of damaging adjacent cardiac structures or extensive entanglement, the use of a guidewire may be required (Fig. 12.9).

Impella RP [4, 5]

The right heart Impella RP is indicated for use in patients with acute right heart failure, defined by echocardiographic criteria global RV hypokinesis, TAPSE score ≤14 mm, RV base diameter >42 mm, or RV mid-cavity diameter >35 mm, after LVAD implant, MI, heart transplant, or open-heart surgery. The Impella RP is the first short-term percutaneous right ventricular assist device (Fig. 12.10).

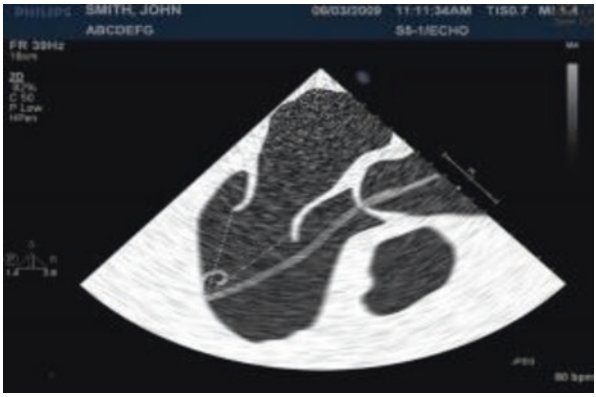

Fig. 12.9 Impella catheter in contact with the left ventricular wall on transesophageal echocardiogram

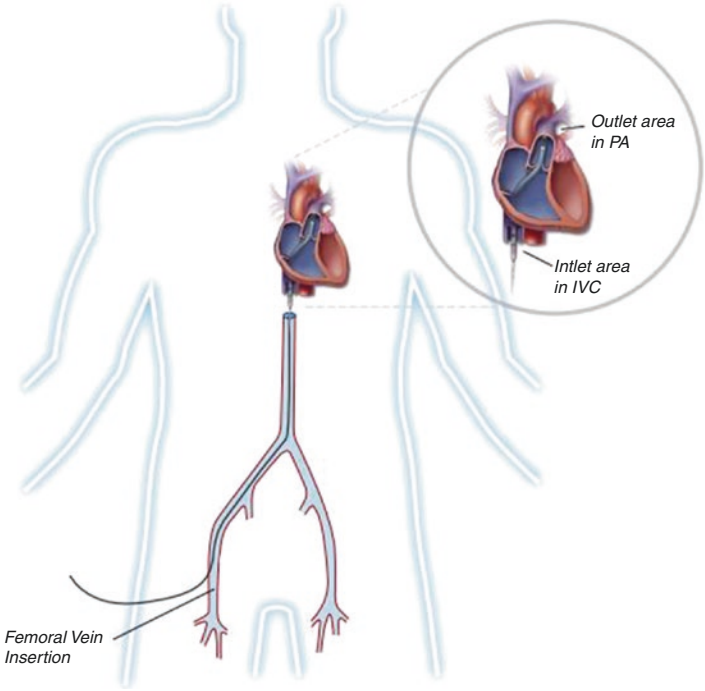

Fig. 12.10 Implantation techniques for Impella RP

When to Consider Echocardiography

Daily chest X-ray is the preferred imaging modality for position surveillance of the Impella RP catheter as echocardiogram is unable to simultaneously display both the inlet and outlet areas in the same view. However, the position of the inlet and outlet areas can be separately evaluated by echocardiogram in greater detail than can be provided by chest X-ray. Similar to the left heart Impella catheters, the Impella RP catheter can migrate as a result of excess "slack" and patient movement or inadvertently from necessary medical care. Displacement and/or obstruction of the catheter inlet and outlet areas can lead to blood flow disturbances which may in turn cause electrical and mechanical cardiac dysfunction. The following signs, symptoms, and device features may be indicative of Impella RP catheter malfunction (Table 12.2).

Normal Position on Echocardiogram

The distal Impella RP catheter is notable for the motor housing unit, blood inlet area, a 16 cm cannula, a blood outlet area, and a pigtail end (Fig. 12.11).

Table 12.2 Concerning indicators of Impella RP malfunction

Symptoms	Chest discomfort, shortness of breath, palpitations, light-headedness, loss of consciousness
Vital signs	Hypotension, tachycardia, hypoxemia
Physical exam	Features of right-sided heart failure (elevated JVD, hepatomegaly, LE edema, etc.)
ECG/telemetry	PVC, NSVT, VT/VF
Labwork	Markers of poor perfusion (increased lactate, decreased pH, etc.), markers of hemolytic anemia (decreased hemoglobin/hematocrit, increased LDH, decreased haptoglobin, etc.)
Cardiac imaging (CXR, CT, MRI, etc.)	Movement of Impella catheter on serial studies
Impella Controller display	Abrupt change in placement signal (waveform or pressure reading) Abrupt change in motor current (waveform or current reading) Abrupt change in flow reading
Impella catheter alarms Note: The Impella RP does *not* have specific position alarms	Alarms suggestive of position change may include: Impella failure Impella stopped Retrograde flow Placement signal not reliable Suction

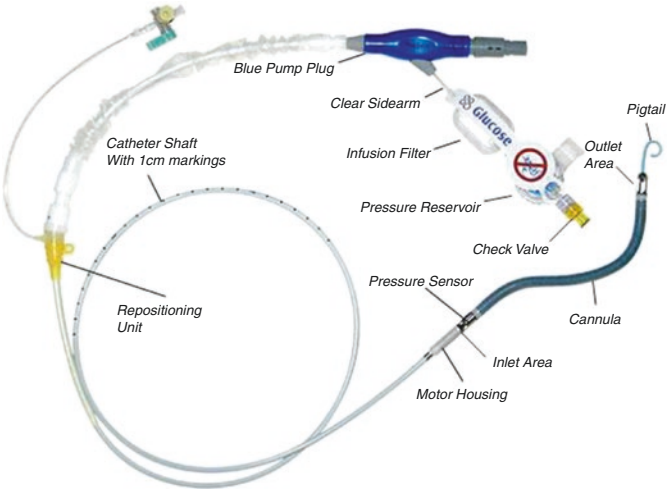

Fig. 12.11 Anatomy of Impella RP catheter

When properly positioned in the heart, there are three bends in the cannula corresponding to the presence of the IVC/RA junction, tricuspid valve, and pulmonic valve. Based on this configuration, the inlet area should rest in the IVC at the level of the diaphragm, and the outlet area should be 2–4 cm distal to the pulmonic valve typically in the pulmonary trunk or left pulmonary artery. This positioning is most readily seen on chest X-ray, as shown below (Fig. 12.12).

On echocardiogram, the Impella RP catheter inlet area can be best seen in the IVC/RA junction from the transthoracic subcostal view or from the trans-

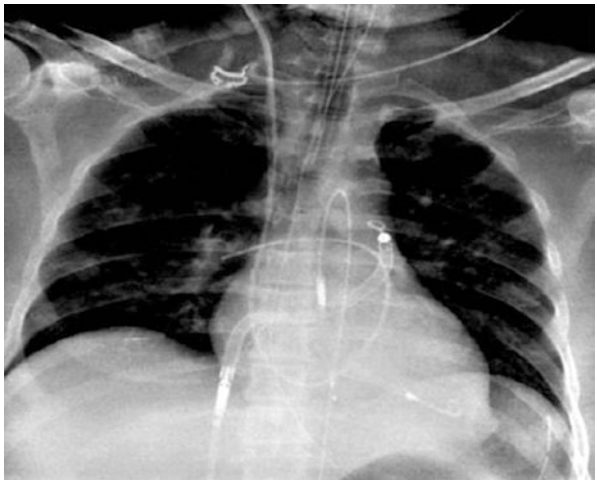

Fig. 12.12 Chest X-ray of correct Impella RP position

esophageal bicaval view. The inlet area can be identified by its faint railroad tracking markings. The Impella RP outlet area can be best seen just beyond the pulmonic valve in the pulmonary trunk from the transthoracic parasternal short-axis view or from the transesophageal mid-esophageal long-axis view. The outlet area can be identified by its hyperechoic appearance and should be 2–4 cm beyond the pulmonic valve. Color Doppler over the inlet and outlet area will reveal mosaic pattern of blood flow turbulence. Except for the cannula which is in contact with the tricuspid and pulmonic valve leaflets, no portion of the terminal Impella catheter should be in contact with cardiac structures, including the right ventricular wall and tricuspid valve apparatus. Representative images of the Impella RP catheter in proper positioning are shown below (Figs. 12.13 and 12.14).

Abnormal Findings on Echocardiogram

The most common catheter-related abnormalities detected on echocardiogram are the presence of adherent masses and changes to catheter position. Masses adherent to the catheter surface are most concerning for thrombus or infected vegetation. By protocol, patients with an implanted Impella RP catheter should be receiving anticoagulation with a goal ACT 160–180 s to prevent thrombus formation. Infected vegetation should be considered in individuals with signs and symptoms of endocarditis, including fever and positive blood cultures.

Minor position fluctuations of the Impella RP catheter from the motion of nearby blood flow and surrounding cardiac structures are unlikely to have any functional consequence on device operation or patient hemodynamic parameters. In addition, migration of the catheter inlet area further into or out of right atrium is also unlikely to cause any significant device or hemodynamic dysfunction as long as the outlet area remains above the pulmonic valve. Major position changes

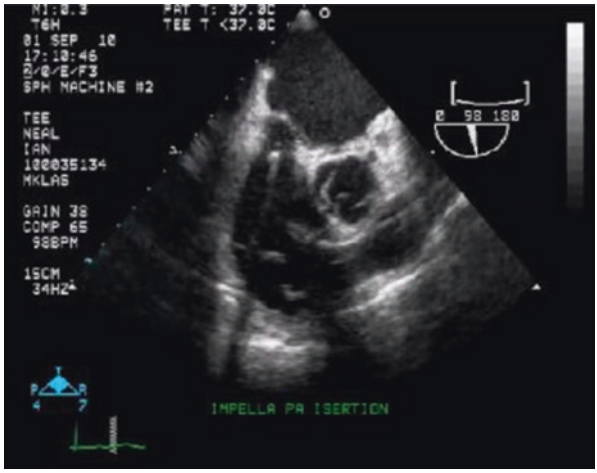

Fig. 12.13 Correct Impella RP catheter position on transesophageal echocardiogram, mid-esophageal long-axis view optimized for right ventricular outflow tract

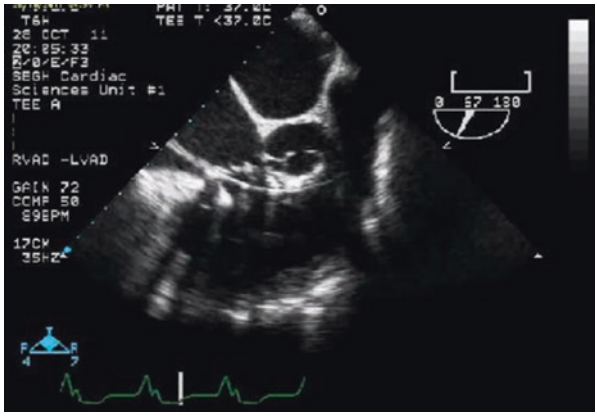

Fig. 12.14 Correct Impella RP catheter position on transesophageal echocardiogram, mid-esophageal long-axis view optimized for tricuspid valve

necessitating catheter adjustment occur when the catheter outlet area moves below the pulmonic valve or contact between the catheter and nearby cardiac structures leads to device or cardiac dysfunction. Echocardiography can be used to detect and guide repositioning of the Impella catheter in each in both of these situations.

Impella Outlet Area Below Pulmonic Valve

If the pigtail of the Impella RP catheter has migrated back toward the right ventricle, the outlet area may become incorrectly positioned below the pulmonic valve. Blood flow from the catheter inlet area to the outlet area becomes recycled within the right ventricle and with no augmentation of cardiac output. On echocardiogram, the

"silver ball" outlet area of the Impella RP catheter will appear in the right ventricular cavity. Color Doppler analysis of the pulmonary trunk or left main pulmonary artery will show absence of the mosaic pattern of blood flow turbulence consistent with the presence of the outlet area. Similar to a Swan-Ganz catheter, the Impella RP catheter can be repositioned at beside with guidance from waveform tracings on the Impella Controller display. Echocardiography and/or CXR can be used to confirm correct placement.

Impella Catheter in Contact with Cardiac Structures

If a portion of the Impella RP catheter is caught on or against a cardiac structure, it may lead to partial or complete obstruction of the catheter inlet and/or outlet causing hemolysis, low pump flow, and suction events. Irritation of the right ventricular wall by the catheter can lead to ventricular arrhythmias. Entanglement of the catheter in the chordae tendineae can disrupt tricuspid valve function resulting in tricuspid regurgitation. Similar entanglement of the distal pigtail in the pulmonic leaflets can result in pulmonic regurgitation. On echocardiogram, the Impella catheter will be found against the endocardium and moving simultaneously with cardiac systole and diastole. Gentle manipulation of the proximal Impella catheter repositioning unit near the percutaneous access site may be sufficient in relieving contact of the distal catheter from adjacent cardiac structures. If there is risk of damaging adjacent cardiac structures or extensive entanglement, the use of a guidewire may be required.

References

1. Stainback RF, Estep JD, Agler DA, Birks EJ, Bremer M, Hung J, Kirkpatrick JN, Rogers JG, Shah NR, American Society of Echocardiography. Echocardiography in the management of patients with left ventricular assist devices: recommendations from the American Society of Echocardiography. J Am Soc Echocardiogr. 2015;28(8):853–909.
2. Uriel N, Morrison KA, Garan AR, Kato TS, Yuzefpolskaya M, Latif F, Restaino SW, Mancini DM, Flannery M, Takayama H, John R, Colombo PC, Naka Y, Jorde UP. Development of a novel echocardiography ramp test for speed optimization and diagnosis of device thrombosis in continuous-flow left ventricular assist devices: the Columbia ramp study. J Am Coll Cardiol. 2012;60(18):1764–75.
3. Abiomed, Inc. (2017). Impella ventricular support systems for use during cardiogenic shock and high-risk PCI: instructions for use and clinical reference manual. Retrieved from http://abiomed-private.s3.amazonaws.com/assets/files/15039258016c46c7de0add7d0ed814691eec8376c8.pdf.
4. Burzotta F, Trani C, Doshi SN, Townend J, van Geuns RJ, Hunziker P, Schieffer B, Karatolios K, Møller JE, Ribichini FL, Schäfer A, Henriques JP. Impella ventricular support in clinical practice: Collaborative viewpoint from a European expert user group. Int J Cardiol. 2015;201:684–91.
5. Abiomed, Inc. (2017). Impella RP with the Automated Impella Controller: instructions for use & clinical reference manual. Retrieved from http://abiomed-private.s3.amazonaws.com/assets/files/1503926088a9505afa2213ed05af2f8c9b37a35ff9.pdf.

Chapter 13
Echocardiography in Structural Cardiac Interventions

Gnalini Sathananthan, Gila Perk, and Amir Ahmadi

Abstract Echocardiography plays an important role in the assessment of structural heart disease. The work-up for the assessment for structural interventions often requires a combination of both transthoracic (TTE) and transoesophageal (TEE) imaging. Three-dimensional (3D) echocardiography provides added value to traditional two-dimensional (2D) echocardiography, allowing for definition of anatomical and spatial relationships. Echocardiography is portable and easily accessible, whilst avoiding the need for radiation and contrast making it the preferred mode of imaging in the cardiac catheterisation lab.

Keywords Aortic stenosis · Mitral regurgitation · Closure devices

Echocardiography plays an important role in the assessment of structural heart disease. The work-up for the assessment for structural interventions often requires a combination of both transthoracic (TTE) and transoesophageal (TEE) imaging. Three-dimensional (3D) echocardiography provides added value to traditional two-dimensional (2D) echocardiography, allowing for definition of anatomical and spatial relationships.

With the evolution of less invasive transcatheter structural cardiac interventions, there is an increasing need for echocardiographic planning and intraprocedural guidance. As the number and complexity of the devices and therapeutic strategies increase, the role of transoesophageal echocardiography in this setting is becoming ever important. Live 3D imaging intraprocedurally has dramatically transformed the efficiency with which some of these procedures can be performed.

Echocardiography is portable and easily accessible whilst avoiding the need for radiation and contrast, making it the preferred mode of imaging in the cardiac catheter lab.

G. Sathananthan · G. Perk · A. Ahmadi (✉)
Division of Cardiology, University of British Columbia, St Paul's Hospital, Vancouver, Canada

Icahn School of Medicine at Mount Sinai Hospital, Mount Sinai Heart, New York, NY, USA
e-mail: amirali.ahmadi@mountsinai.org

E. Herzog, E. Argulian (eds.), *Echocardiography in the CCU*,
https://doi.org/10.1007/978-3-319-90278-4_13

Transcatheter Aortic Valve Replacement

Transcatheter aortic valve replacement (TAVR) was first performed in France in 2002 for severe aortic stenosis [1]. The PARTNER trial published in 2010 was a game changer showing superiority of TAVR to standard medical therapy for individuals who were not suitable candidates for surgical aortic valve replacement [2]. The AHA/ACC guidelines give a Class I indication for the use of TAVR in individuals who are considered high risk for surgical aortic valve replacement. More recently in 2016, the PARTNER II trial showed non-inferiority of TAVR to surgical aortic valve replacement in intermediate-risk patients [3]. The updated 2017 AHA/ACC guidelines give this a Class IIa recommendation, thus expanding the role of this novel technology [4].

To date, TAVR includes the three generations of balloon-expandable valves, namely, the Edward Sapien, the Edward Sapien XT and the Edward Sapien 3. These are tri-leaflet pericardial bovine valves, mounted within a balloon-expandable cobalt-chromium frame. The Edward Sapien XT is available as a 23, 26 and a 29 mm device, whilst the Edward Sapien 3 is available as a 20, 23, 26 mm and a 29 mm device. The Medtronic CoreValve is a pericardial valve in a self-expanding nitinol frame. The Medtronic CoreValve anchors within the LVOT and ascending aorta. This is available in 23, 26, 29 and 31 mm. This device requires a well-sized ascending aorta to accommodate the broad distal portion of the valve. This device is limited to implantation via a retrograde approach [5]. The Evolut R is the next-generation self-expandable TAVR valve which was first introduced in 2014. It was designed to overcome some of the issues faced with the CoreValve. It has a lower delivery profile and an extended sealing skirt to reduce the incidence of paravalvular leaks. Despite no long-term data, this device appears to show good promise [6].

Echocardiography is the gold standard in the assessment of aortic stenosis (AS). It allows assessment of morphology and severity of disease. The AHA/ACC guidelines classify aortic stenosis as severe when peak velocity is $\geq$4.0 m/s, mean gradient is $\geq$40 mmHg and valve area is <1.0 cm^2. These parameters are however flow dependent, and thus grading the severity of AS should also take into account left ventricular function, coexistence of regurgitant valvular disease and clinical symptoms [7].

Echocardiography can also be helpful in determining anatomical suitability for TAVR by providing information regarding the extent and distribution of calcification, as well as aortic annular dimensions. The aortic annular dimension and area determine prosthesis size, which is ultimately the key to procedural success. The aortic annulus, which was once thought to be circular, has now been well described as more oval shaped from both 3D TEE and CT. As a result, 2D TEE can underestimate the annular dimension. On TEE, the annular dimension is measured in early to mid-systole at the level of the basal attachments of the aortic cusps. It is measured from the trailing edge to leading edge, from the three-chamber view which is often between 110° and 140°. Areas of calcification can often result in overestimation of the annular diameter. 3D TEE can be used to calculate the annular area from the 2D

image. The transverse, sagittal and coronal views are all oriented along the aortic root. The transverse plane is then placed at the level of the hinge points. The orthogonal views are then repeatedly rotated (the turnaround rule) ensuring the hinge points have been transacted accurately. The maximum dimension is often seen in the coronal view with the minimum dimension in the sagittal view (Fig. 13.1 [8]).

More recently however multi-detector CT imaging (MDCT) has become an integral part of the work-up for TAVR. In addition to providing accurate assessment of annular area and perimeter, it also allows visualisation of coronary artery origins and iliofemoral anatomy. A gated cardiac CT is required for imaging of the aortic root, and with an adequately low heart rate, excellent spatial resolution can be achieved with minimal radiation exposure. Although cardiac CT has largely taken over the role of the work-up for sizing of the prosthetic valve, TEE still plays an important role in those in whom adequate CT imaging cannot be obtained such as due to arrhythmia, or in whom cardiac CT cannot be performed due to the risk of contrast-induced nephropathy. 3D TEE annular sizing has been found to correlate well with MDCT sizing [9].

Choosing prosthesis size is dependent on the annular area and perimeter, the extent of calcification around the annulus and the type of valve that is to be used. Marked calcification increases the inherent risk of root rupture, and thus it is prudent that the valve is not significantly oversized. Sizing charts are available for each prosthesis to determine the correct valve size [10]. Undersizing a valve can result in paravalvular aortic regurgitation or embolisation of the valve, whilst oversizing can result in valvar aortic regurgitation or aortic root rupture.

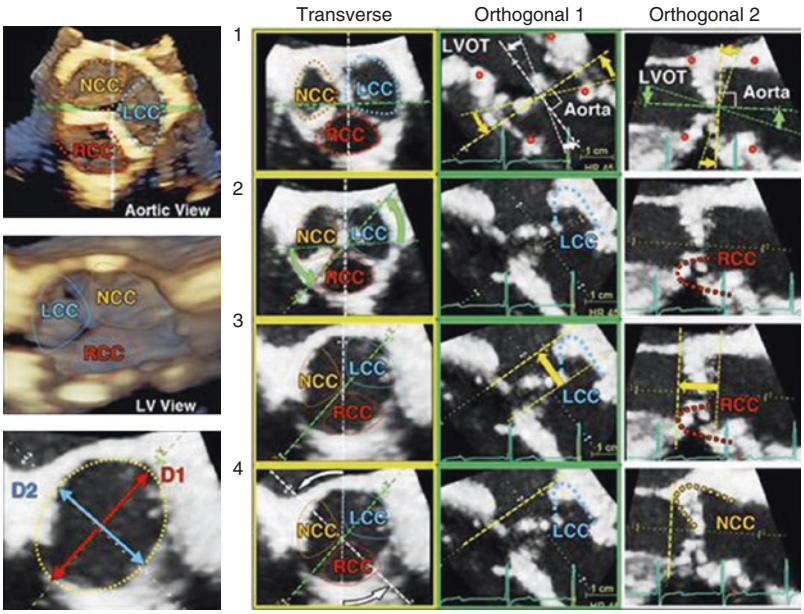

Fig. 13.1 Measuring aortic valve area using 3D multiplanar reconstruction

TAVRs are performed either transaortically or transapically. The transapical approach, which requires a mini thoracotomy, is opted for in patients who have difficult peripheral vascular access and are not amenable to the transaortic technique.

The use of periprocedural TEE can be extremely helpful; however a general anaesthetic is then required for the procedure. Periprocedural TEE has the advantage of providing assistance with balloon dilatation, valve positioning and assessment of valve function immediately after valve deployment and for the early detection of periprocedural complications [11, 12].

The standard TEE working view for guidance during TAVR is generally the three-chamber view for both transfemoral and transapical cases. This view provides the best visualisation of the LVOT, with a clear view of surrounding structures that need to be accounted for during valve deployment, such as the anterior leaflet of the mitral valve. This view is also used to guide the transapical puncture when required as it also provides a view of the true apex and the trajectory needed to reach the aortic valve. TEE can confirm position of the guidewire in the ascending aorta. 3D TEE provides better spatial resolution and allows for optimal balloon positioning. Imaging during balloon inflation ensures that the balloon does not migrate, and in the absence of TEE, this is often done with fluoroscopy. The balloon is prone to migrating in the absence of an adequate landing zone, such as with extensive subaortic septal hypertrophy or a small sinotubular junction. Real-time echocardiography can also be useful when marked areas of ectopic calcification are present to guide safe balloon dilatation (Fig. 13.2).

When assessing valve function following TAVR, imaging of the prosthesis should be performed in multiple views. Mid-oesophageal short- and long-axis views of the aortic valve help confirm valve seating and normal leaflet function. The site and severity of aortic regurgitation should be assessed. Differentiating valvular and paravalvular aortic regurgitation is important. Some degree of aortic regurgitation is not uncommon after TAVR and is often paravalvular. The presence of significant paravalvular aortic regurgitation immediately post valve deployment is due to

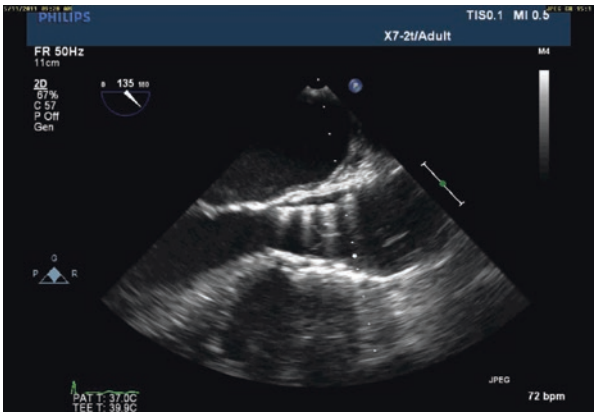

Fig. 13.2 Core valve post deployment

incorrect valve position, suboptimal balloon expansion or an undersized valve. Being aware of this immediately post valve deployment gives the interventionalist the opportunity to further dilate the balloon or deploy a second prosthesis if needed. Oversizing of the prosthesis can result in suboptimal stent expansion, impaired cusp mobility and central aortic regurgitation. There is also a risk of aortic root rupture.

Transgastric view of the aortic valve is useful as it allows Doppler alignment of the aortic valve to determine the gradient across the valve post TAVR. This view can also help identify paravalvular regurgitant jets that may not be well appreciated in the mid-oesophageal view.

3D TEE is useful to help evaluate prosthetic valve function. It can also be a helpful tool to determine the site and severity of aortic regurgitation, especially if the distinction between transvalvular and paravalvular is not clear on 2D.

Early periprocedural complications include aortic rupture and cardiac tamponade. Acute coronary obstruction is exceedingly rare as pre-procedural imaging helps avoid this complication. This can however be a complication if the valve migrates during balloon inflation or deployment. The most commonly described cause for coronary obstruction during TAVI is however displacement of the calcified valve cusp towards the coronary ostia. This can occur in the setting of low coronary height or a small aortic root [13]. The ostia of the coronary arteries can sometimes be appreciated on TEE, though this is not always the case. More commonly left ventricular dysfunction will be seen, and it is important to consider coronary artery occlusion as a possible cause if this is seen. The landing zone of the valve should be at least 10 mm from the coronary ostia [14].

A follow-up echocardiogram is often done prior to hospital discharge. A successful result post TAVR includes a well-positioned prosthesis with a valve area of >1.2 cm^2, a mean gradient of <20 mmHg, a peak velocity of <3 m/s and the absence of moderate or severe aortic regurgitation as moderate or severe aortic regurgitation post TAVR is associated with a twofold increase in all-cause mortality at 1 year [14, 15]. The frequency of follow-up echocardiograms thereafter varies from centre to centre. It is generally recommended that a TTE be performed at 1-, 6- and 12-month follow-up, with an annual TTE thereafter.

Mitral Interventions

Transcatheter mitral valve intervention is an expanding field that has great potential for the future of mitral valve disease. MitraClip technology was approved for use in humans in 2004, for the treatment of mitral regurgitation (MR). The MitraClip device is a 5-mm-wide cobalt-chromium implant with two arms which can be opened and closed using the delivery system handle. The maximal dimension of the device, when the arms are open to 180°, is 20 mm. This technology is designed to create a double-orifice repair, with reestablishment of leaflet coaptation.

The EVEREST II trial published in 2011 found that although percutaneous repair was less effective at reducing mitral regurgitation when compared with

conventional surgery, it was associated with superior safety and similar improvements in clinical outcomes [16]. A sub-study of the EVEREST trial published in 2014 however found that it reduced MR, improved clinical outcomes and decreased LV dimensions at 12 months in an elderly high-risk surgical cohort. Seventy percent of this cohort had functional MR [17].

TTE can be used to determine the severity and the mechanism of the MR. It can also determine suitability of the valve for the MitraClip. TEE can be a useful adjunct when the mechanism of the MR is not clear on TTE; however it is almost always performed for screening purposes when determining anatomical suitability. The severity should be based on a combination of traditional qualitative and quantitative measures. 3D TEE can provide excellent spatial resolution to help determine the mechanism and site of origin of the MR. The MR jet should originate from the central two-thirds of the line of coaptation. As the device creates a double orifice, it is important that there is no pre-existing mitral stenosis. A valve orifice area of >4 cm^2 is ideal. A flail segment width of <1.5 cm and a flail gap of <10 mm are recommended in those with degenerative mitral valve disease. A cleft in the mitral valve or calcified leaflets is a relative contraindication for MitraClip. The MitraClip is not indicated for use in patients with rheumatic heart disease or active infective endocarditis [18] (Fig. 13.3).

TEE guidance is an essential part of this procedure which cannot be performed under fluoroscopy alone. A transseptal puncture is first performed. The site of the

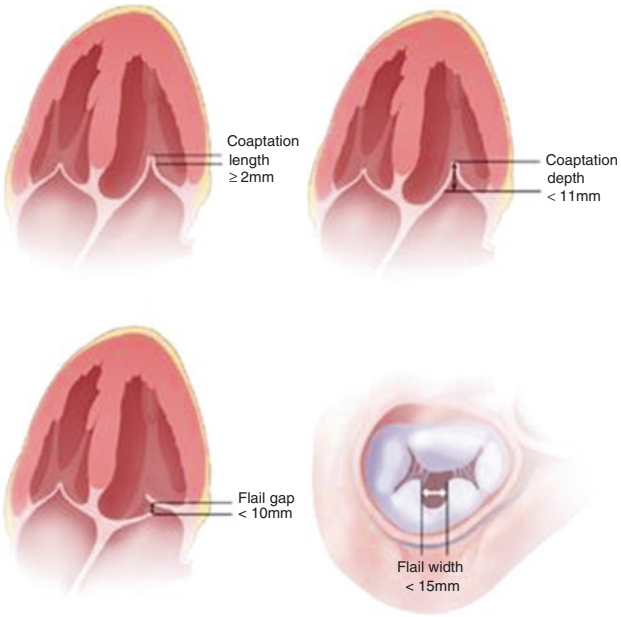

Fig. 13.3 Coaptation length and depth as measured in functional mitral regurgitation. Flail gap and width as measured in degenerative mitral regurgitation

puncture is a crucial step in the procedure. A more supero-posteriorly located puncture is ideal, as it provides adequate space for manipulation of the delivery system within the left atrium to direct it towards the mitral valve. The transseptal puncture should be made approximately 35–40 mm from the level of the mitral valve (Fig. 13.4).

A guidewire is then placed in the left upper pulmonary vein, and the steerable guide catheter advanced over the guidewire. The steerable guide catheter has an echo-bright double ring which can be well appreciated on both 2D and 3D echo. This should lie 2–3 cm within the left atrium. The clip delivery system (CDS) is then advanced through the steerable guide catheter into the left atrium. The arms of the clip are directed perpendicular to the coaptation line of the mitral valve. 3D TEE can be extremely useful in this setting, helping to guide and position the CDS using a bird's-eye view from the left atrial roof (Fig. 13.5).

The device should also be aligned with the origin of the MR jet. It is then advanced approximately 2 cm into the left ventricle. This is usually performed when

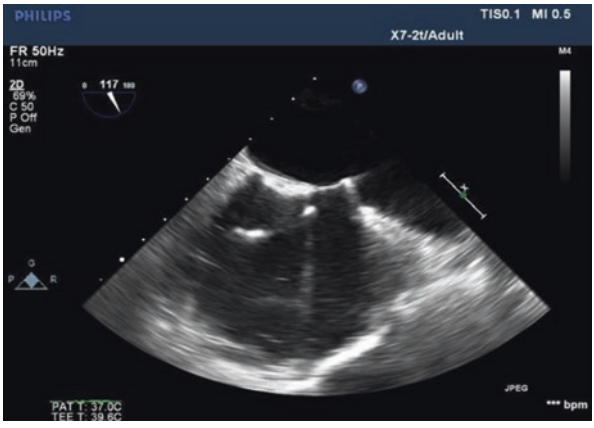

Fig. 13.4 Bicaval view demonstrating tenting of the interatrial septum immediately prior to a transseptal puncture

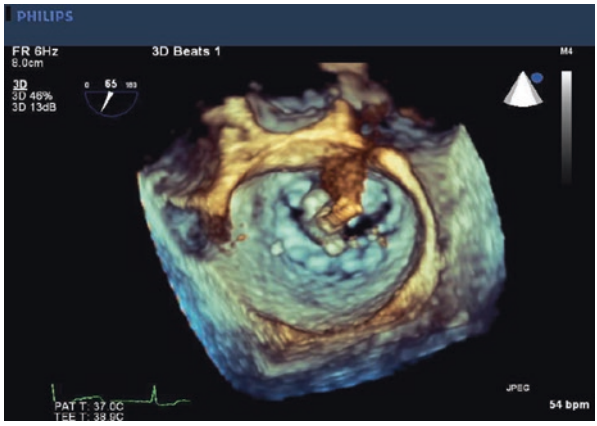

Fig. 13.5 Surgical en face view from the left atrium, look straight down on the mitral valve. The arms of the clip are above the mitral valve and need to be rotated clockwise another 60°, such that they are directly perpendicular to the coaptation line

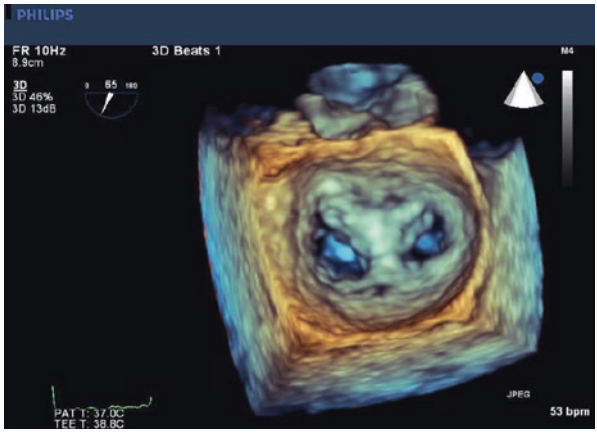

Fig. 13.6 Post MitraClip deployment demonstrating the final result

the device is completely open at 180°. The clip arms are then placed into a grasping position at 120° and pulled back in systole to capture the leaflets. The latter part of this procedure should be done using X-plane, with a bicommissural and LVOT view. This helps to identify the position of the clip from a medial-lateral and anterior-posterior perspective, respectively. It is important there is no tension in the leaflets and that the leaflets move freely above the arms. The MitraClip is then slowly closed and released. Colour Doppler is in fact placed over the mitral valve at various stages of device positioning to gauge the ideal position in which the MR reduction is greatest (Fig. 13.6).

Following the release of the MitraClip, valve function needs to be assessed. The degree of mitral regurgitation should be qualitatively and quantitatively assessed. A reduction in the grade of MR to 2+ or less is the aim of this procedure. A second device may be used to help achieve this. The degree of mitral stenosis (MS) however needs to be assessed prior to this. Quantitative assessment using the mean gradient is a quick and informative means of assessing this. The role of pressure half-time for the assessment of mitral valve area in this scenario is unknown. Planimetry of the mitral valve orifices using 3D MPR can also be very helpful. The degree of mitral stenosis should be taken into account when considering a second clip, as the MR could be reduced at the risk of worsening MS.

An iatrogenic atrial septal defect (IASD) is created following the transseptal puncture. This should be assessed at the end of the study using an X-plane image of the bicaval view, which is at approximately 110°. The size and direction of the shunt should be determined. The persistence of an ASD following a MitraClip procedure is reported in up to 50% of cases. It was associated with a worse clinical outcome and increased mortality [19]. Although there are no clear guidelines as to how to manage iatrogenic ASD's following a MitraClip, closure at the time of index procedure can be considered in the setting of a large right to left shunt associated with pulmonary hypertension or if there are any concerns about systemic embolisation [20].

Transcatheter Paravalvular Leak Closures

Paravalvular leaks are a well-recognised complication following surgical valve replacement, occurring in 5–17% of cases. They are generally more frequently associated with the mitral valve than the aortic valve in this setting [21]. In the era of TAVR, however, the aortic valve too is frequently prone to paravalvular leaks. Postsurgical paravalvular leaks often occur in the setting of significant annular calcification, infection or technical errors that result in incomplete apposition of the sewing ring to the native valve tissue. Paravalvular AR following TAVR was discussed in the earlier segment.

Paravalvular leaks can range from trivial to severe. It is important to distinguish a paravalvular leak from a washing jet, which is a normal finding with mechanical valves. A washing jet is a small jet that arises from between the sewing ring and disc or leaflet. These jets are in theory meant to prevent blood stasis and thrombus formation [22]. Most patients with a paravalvular leak are asymptomatic. Those that are symptomatic, however, often present with congestive heart failure, haemolysis or both. This can sometimes be managed conservatively with medical therapy. Those that are refractory to such therapy however require correction of this leak. Surgical correction requires a repeat sternotomy which carries a significant morbidity and mortality risk. Transcatheter device closure of these leaks has therefore revolutionised the management of these patients. There is a wide range of devices that are used in this setting and are used off-label. The device chosen often depends on the size and shape of the defect. The devices used include Amplatzer and Occlutech. Depending on the leak, more than one device can also be used [23].

The approach to closure of these leaks depends on the valve affected. A mitral paravalvular leak will be antegradely approached via a transseptal puncture in the cardiac catheter lab. Alternative approaches include a retrograde transapical and retrograde transaortic. Aortic paravalvular leaks can be readily approached retrogradely.

Pre-procedural planning is crucial. An initial TTE to identify the severity and origin of the jet is required. A negative TTE however does not exclude a significant paravalvular leak. Acoustic shadowing from calcification and from the mechanical prosthesis can make identification and quantification of the regurgitant jet difficult. Multiple views and off-axis views are recommended to ensure the jet is not being missed.

In those with a high index of suspicion, a TEE is recommended to clarify this. 2D in conjunction with 3D TEE can help quantify and determine the site of regurgitation. Quantification of paravalvular regurgitation is the same as for native valve regurgitation, though this is not well validated. Quantification of paravalvular leaks is difficult even when detected as they are often eccentric, and there are often multiple jets. It is therefore recommended that a combination of multiple qualitative, semi-quantitative and quantitative findings be used to assess the severity of the regurgitation. An additional measurement that is recommended for paravalvular leaks is imaging of the neck of the jet in the short-axis view at the level of the

sewing ring and expressing it as a percentage of the total sewing ring circumference. Thirty percent or greater is considered severe. Greater than 40% valve dehiscence results in rocking of the prosthesis and is therefore associated with severe paravalvular regurgitation [24].

3D TEE can be extremely useful in identifying the exact position and size of the leak. Most mitral paravalvular leaks are crescentic or oblong in shape, rather than being circular. 3D TEE can therefore in this setting provide an accurate measure of the size and shape of the defect. 3D TEE can also provide details of the position of the defect in relation to other anatomical structures. Acoustic shadowing can also occur with TEE, however, and this needs to be taken into consideration. Anterior aortic paravalvular jets are often underdetected or underestimated as a result [25] (Figs. 13.7, 13.8 and 13.9).

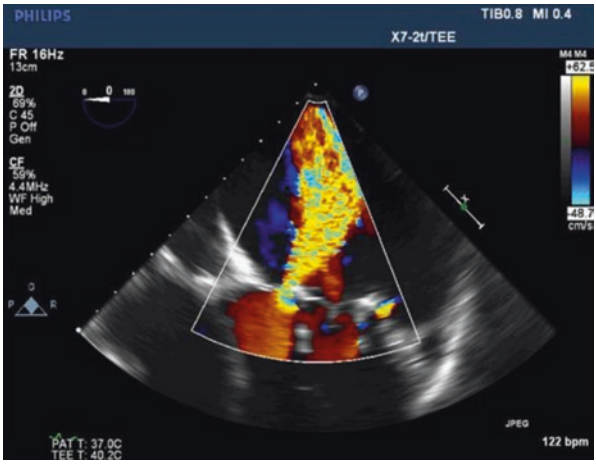

Fig. 13.7 Severe mitral paravalvular leak originating from the medial aspect of the valve

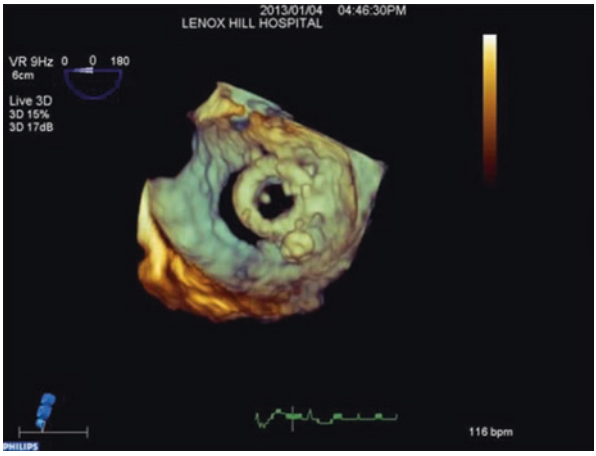

Fig. 13.8 A large defect is seen on 3D at the medial aspect of the sewing ring, extending from 7 o'clock to 11 o'clock

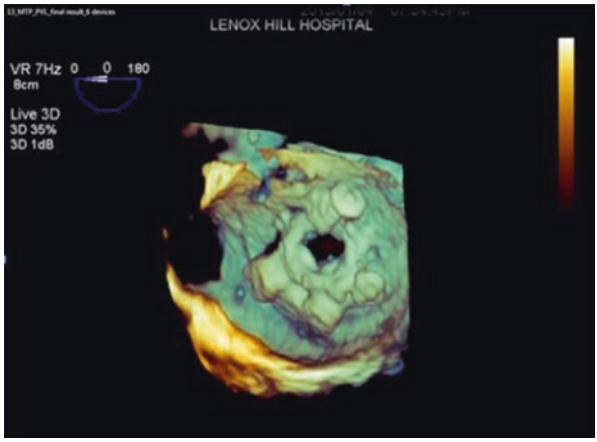

Fig. 13.9 The final result with three new closure devices inserted into the defect

In the setting of a mitral paravalvular leak, the site of transseptal puncture is a crucial aspect of the procedure. An appropriate transseptal puncture site ensures an adequate trajectory directed towards the defect. A medially located paravalvular leak requires a higher puncture on the interatrial septum compared to a laterally located paravalvular leak. Once the left atrium has been accessed, the guide wire is directed towards the defect. The wire can be seen on 2D TEE, but live 3D is extremely useful when it comes to actually directing the wire towards the defect. The en face surgical view from the left atrium visualises the defect from the position of the wire itself, thus enabling the interventionalist to see each incremental movement of the wire. 3D TEE has improved the ease with which these procedures can be performed. Once the wire is passed through the defect, the device is then deployed. It is important to ensure the device is aligned along the correct axis, especially in an irregularly shaped defect. 3D TEE is very useful in this scenario and can confirm appropriate positioning of the device. Colour Doppler can be performed prior to device deployment to confirm the defect is adequately sealed. Once the device is deployed, the device should be interrogated to confirm adequate seating of the device. Colour Doppler should be applied again across the device to assess for residual leak. If a significant residual leak exists, a second device can be considered if it can be safely positioned alongside the first. In some cases, more than one device placement can help stabilise the devices, by anchoring onto each other.

Left Atrial Appendage Device Closures

The left atrial appendage (LAA) is the most common site of thrombus in patients with atrial fibrillation or atrial flutter. Certain LAA morphologies have been shown to have different levels of thromboembolic risk [26]. The LAA can occasionally be seen on TTE, but largely TEE is required for visualisation.

Patients with these arrhythmias who are at a significant risk of cardioembolic stroke are advised to be on an anticoagulant. However, anticoagulants are not without risk, and there remains a small proportion of patient in whom the risk of bleeding outweighs the benefit of anticoagulation. It is in these individuals in whom closure of the left atrial appendage can be a useful alternative to anticoagulation. Surgical closure of the LAA has mostly been unsuccessful [27]. LAA device closure on the other hand was shown to be non-inferior to warfarin therapy [28].

Three devices are currently designed for this procedure, namely, the Watchman, the Amplatzer Cardiac Plug and the WaveCrest.

TEE imaging of the LAA should be performed from multiple views, namely, 0°, 30°, 45°, 90° and 135°. This enables measurement of the short and long axis. The 135° view often captures the widest diameter, which is deemed the landing zone. The landing zone is measured from the area of the left circumflex coronary artery across the LAA to approximately 1 cm inward from the tip of the ridge separating the LAA and left upper pulmonary vein. The depth of the LAA is measured from the ostium line to the apex. For this procedure, a low transseptal puncture is preferred to allow coaxial alignment with the LAA. Thrombus in the LAA is a contraindication to device closure, as it can be dislodged during device positioning. The device chosen is generally 10–20% larger than the diameter of the landing zone. Ideally the device should not protrude more than 4–7 mm beyond the LAA. No or minimal residual flow should be seen following device deployment. However residual peri-device flow is a common finding on TEE following the use of the Watchman device. The PROTECT AF study however found no difference in thromboembolic risk with the presence of a peri-device leak using the Watchman device [29]. The Amplatzer device tends to have less residual flow (Figs. 13.10 and 13.11).

The Watchman device is made of a nitinol cage with a polyethylene terephthalate membrane covering the surface that faces the left atrium. Fixation barbs are available to attach to the neck of the appendage, to minimise the risk of embolisation. This can be used for a LAA with a landing zone between 17 and 31 mm.

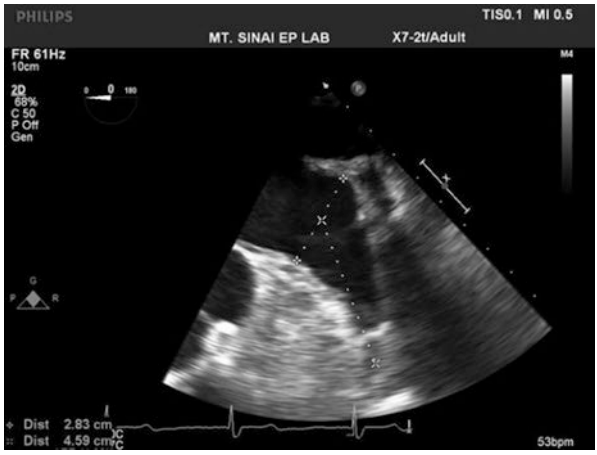

Fig. 13.10 Measurements of the os and height of the left atrial appendage

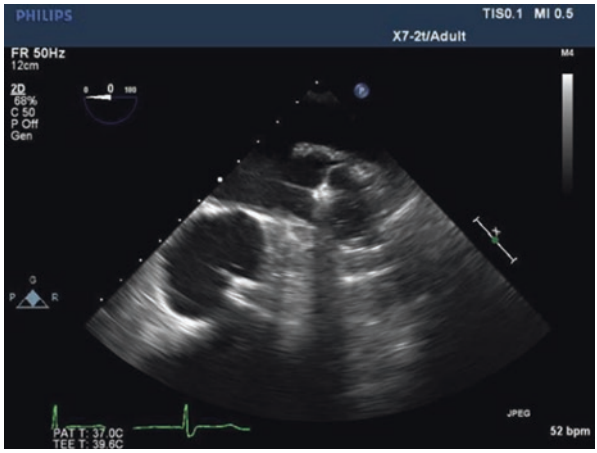

Fig. 13.11 Left atrial appendage device post deployment

The Amplatzer Cardiac Plug (APC) consists of a cylindrical nitinol cage connected by a short flexible waist to a nitinol plate covering the appendage ostium. This device has two discs. This device is shorter than its diameter and is therefore suited for wider appendages. The landing zone should be less than 28 mm for use of the APC. Post deployment, the lobe should be compressed, with an adequate distance to the disc. The disc will develop a slightly concave shape and cover most if not all of the LAA ostium.

The WaveCrest device is made of a nitinol structure with a foam layer that sits within the LAA to promote rapid organisation. The PTFE layer facing the left atrium is designed to reduce thrombus formation. This device sits more proximally within the LAA and is designed for short appendages [30].

Atrial Septal Device Closure

The large majority of secundum atrial septal defects (ASD) can now be closed with a transcatheter device, rather than requiring surgery. The defects however need sufficient rims to be suitable for device closure. TTE can most often help identify the presence of an atrial septal defect, though generally cannot help further delineate the defect. On TTE, the ASD is generally best seen on the subcostal view as the Doppler beam is parallel to flow across the defect. In other views in which the atrial septum is seen on TTE, the interatrial flow is perpendicular to the beam and the septum is subject to artefactual dropout which can falsely give the illusion of a defect. A modified apical view can be used for those with suboptimal subcostal imaging. An agitated saline study is recommended if there is a suspicion of interatrial communication without clear visualisation of the defect itself. The appearance of microbubbles in the left atrium within 3–6 cardiac beats after opacification of the RA confirms the presence of an intracardiac shunt. Provocation manoeuvres such as

the Valsalva are sometimes required to transiently increase right atrial pressure and encourage right atrial opacification [31].

A TEE is recommended for any patient with a secundum ASD who is being considered for device closure. TEE enables assessment of the anteroposterior and superoinferior rims. The interatrial septum should be viewed at multiple angles, starting at 0° to determine the size and location of the defect. It is important to assess the number of defects, as it is not uncommon for more than one defect to be present. The anteroposterior rim refers to the relationship of the defect with the aortic valve and posterior wall, respectively. The superoinferior rim refers to the defects relationship with the SVC and IVC, respectively. 3D TEE can provide a comprehensive assessment of the ASD whilst allowing for measurement of the dimensions and area [32].

The most commonly used device is the Amplatzer septal occluder. This is a double-disc device made from nitinol mesh and polyester fabric. The aortic rim is not uncommonly deficient in secundum ASDs, though it is not an absolute contraindication for device closure. The device can often sit nicely splayed on the aortic valve. There is a risk of erosion in this scenario though it is unlikely especially if the device appears seated well at the conclusion of the procedure. Device closure is contraindicated in the setting of a deficient rim, which is defined as a rim less than 5 mm [28]. Surgical closure is also recommended in the setting of very large defects.

Balloon sizing is generally always recommended. When flow across the defect has completely disappeared, the diameter of the balloon is measured. This is best performed using orthogonal planes on X-plane. This ensures there are no residual defects that have been missed. The device is sized approximately 2 mm larger than the size determined on balloon sizing. 3D TEE however allows for accurate dimensions without the need for balloon sizing. 3D TEE is also very useful during device placement for guiding the delivery system and to ensure appropriate seating of both discs on either side of the septum. At the conclusion of the study, no flow should be seen across the defect. Follow-up can be done with a TTE, which can clearly display the device and confirm appropriate seating [33] (Figs. 13.12 and 13.13).

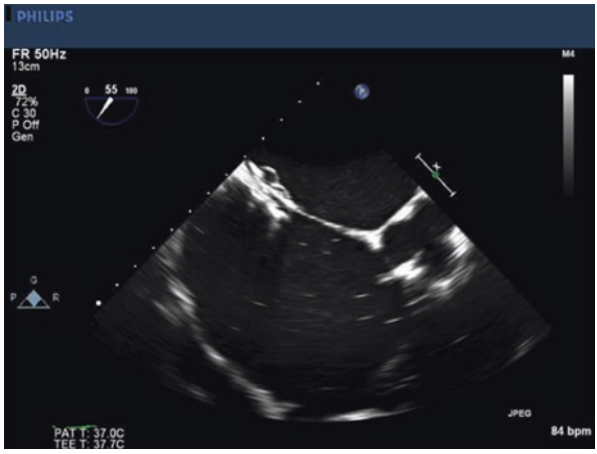

Fig. 13.12 An ASD device is seen well seated on the interatrial septum

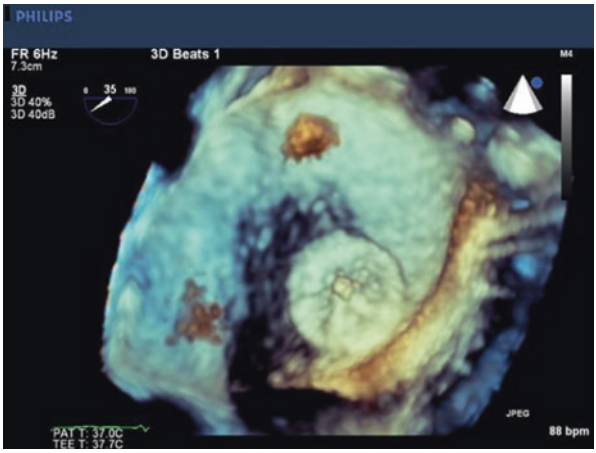

Fig. 13.13 The ASD device as seen on 3D

References

1. Dvir D, Barbash IM, Ben-Dor I, Okubagzi P, Satler LF, Waksman R, Pichard AD. The development of transcatheter aortic valve replacement in the USA. Arch Cardiovasc Dis. 2012;105:160–4.
2. Leon MB, Smith CR, Mack M, Miller DC, Moses JW, Svensson LG, Tuzcu EM, Webb JG, Fontana GP, Makkar RR, Brown DL, Block PC, Guyton RA, Pichard AD, Bavaria JE, Herrmann HC, Douglas PS, Petersen JL, Akin JJ, Anderson WN, Wang D, Pocock S, PARTNER Trial Investigators. Transcatheter aortic-valve implantation for aortic stenosis in patients who cannot undergo surgery. N Engl J Med. 2010;363(17):1597–607.
3. Leon MB, Smith CR, Mack MJ, Makkar RR, Svensson LG, Kodali SK, Thourani VH, Tuzcu EM, Miller DC, Herrmann HC, Doshi D, Cohen DJ, Pichard AD, Kapadia S, Dewey T, Babaliaros V, Szeto WY, Williams MR, Kereiakes D, Zajarias A, Greason KL, Whisenant BK, Hodson RW, Moses JW, Trento A, Brown DL, Fearon WF, Pibarot P, Hahn RT, Jaber WA, Anderson WN, Alu MC, Webb JG, PARTNER 2 Investigators. Transcatheter or surgical aortic-valve replacement in intermediate-risk patients. N Engl J Med. 2016;374(17):1609–20.
4. Nishimura RA, et al. AHA/ACC focused update of the 2014 AHA/ACC guideline for the management of patients with valvular heart disease. Circulation. 2017;135:e1159–95.
5. Hahn RT, Little SH, Monaghan MJ, Kodali SK, Williams M, Leon MB, Gillam LD. Recommendations for comprehensive intraprocedural echocardiographic imaging during TAVR. J Am Coll Cardiol Img. 2015;8:261–87.
6. Schulz E, Jabs A, Gori T, von Bardeleben S, Hink U, Kasper-König W, Vahl CF, Münzel T. Transcatheter aortic valve implantation with the new-generation Evolut R™: Comparison with CoreValve® in a single center cohort. Int J Cardiol Heart Vasc. 2016;12:52–6.
7. Baumgartner H, Hung J, Bermejo J, Chambers JB, Edvardsen T, Goldstein S, Lancellotti P, LeFevre M, Miller F Jr, Otto CM. Recommendations on the echocardiographic assessment of aortic valve stenosis: a focused update from the European Association of Cardiovascular Imaging and the American Society of Echocardiography. J Am Soc Echocardiogr. 2017;30:372–92.
8. Kasel AM, Cassese S, Bleiziffer S, Amaki M, Hahn RT, Kastrati A, Sengupta PP. Standardized imaging for aortic annular sizing implications for transcatheter valve selection. J Am Coll Cardiol Img. 2013;6:249–62.
9. Blanke P, Schoepf UJ, Leipsic JA. CT in transcatheter aortic valve replacement. Radiology. 2013;269(3):650–9.

10. Binder RK, Webb JG, Willson AB, et al. The impact of integration of a multidetector computed tomography annulus area sizing algorithm on outcomes of transcatheter aortic valve replacement: a prospective, multicenter, controlled trial. J Am Coll Cardiol. 2013;62(5):431–8. https://doi.org/10.1016/j.jacc.2013.04.036. Epub 2013 May 15.
11. Silvestry FE, Kerber RE, Brook MK, Carroll JD, Eberman KM, Goldstein SA, Herrmann HC, Homma S, Mehran R, Packer DL, Parisi AF, Pulerwitz T, Seward JB, Tsang TSM, Wood MA. Echocardiography-guided interventions. JASE. 2009;22:213–31. https://doi.org/10.1016/j.echo.2008.12.013.
12. Kronzon I, Jelnin V, Ruiz CE, Saric M, Williams MR, Kasel AM, Shivaraju A, Colombo A, Kastrati A. Optimal imaging for guiding TAVR: transesophageal or transthoracic echocardiography, or just fluoroscopy? JACC Cardiovasc Imaging. 2015;8(3):361–70.
13. Ribeiro HB, Sarmento-Leite R, Siqueira DAA, Carvalho LA, Mangione JA, Rodés-Cabau J, Perin MA, Sandoli de Brito F Jr. Coronary obstruction following transcatheter aortic valve implantation. Arq Bras Cardiol. 2014;102(1):93–6.
14. Young MN, Inglessis I. Transcatheter aortic valve replacement: outcomes, indications, complications, and innovations. Curr Treat Options Cardiovasc Med. 2017;19(10):81.
15. Takagi H, Umemoto T, ALICE (All-Literature Investigation of Cardiovascular Evidence) Group. Impact of paravalvular aortic regurgitation after transcatheter aortic valve implantation on survival. Int J Cardiol. 2016;221:46–51.
16. Feldman T, Foster E, Glower DD, Kar S, Rinaldi MJ, Fail PS, Smalling RW, Siegel R, Rose GA, Engeron E, Loghin C, Trento A, Skipper ER, Fudge T, Letsou GV, Massaro JM, Mauri L. Percutaneous repair or surgery for mitral regurgitation. N Engl J Med. 2011;364:15.
17. Glower DD, Kar S, Trento A, Lim DS, Bajwa T, Quesada R, Whitlow PL, Rinaldi MJ, Grayburn P, Mack MJ, Mauri L, McCarthy PM, Feldman T. Percutaneous mitral valve repair for mitral regurgitation in high-risk patients: results of the EVEREST II study. J Am Coll Cardiol. 2014;64(2):172–81.
18. Feldman T, Wasserman HS, Herrmann HC, Gray W, Block PC, Whitlow P, St Goar F, Rodriguez L, Silvestry F, Schwartz A, Sanborn TA, Condado JA, Foster E. Percutaneous mitral valve repair using the edge-to-edge technique: six-month results of the EVEREST Phase I Clinical Trial. J Am Coll Cardiol. 2005;46(11):2134–40.
19. Schueler R, Öztürk C, Wedekind JA, Werner N, Stöckigt F, Mellert F, Nickenig G, Hammerstingl C. Persistence of iatrogenic atrialseptal defect after interventional mitral valve repair with the MitraClip system: a note of caution. JACC Cardiovasc Interv. 2015;8(3):450–9.
20. Alkhouli M, Sarraf M, Holmes DR. Iatrogenic atrial septal defect. Circ Cardiovasc Interv. 2016;9(4):e003545.
21. Binder RK, Webb JG. Percutaneous mitral and aortic paravalvular leak repair: indications, current application, and future directions. Curr Cardiol Rep. 2013;15(3):342. https://doi.org/10.1007/s11886-012-0342-2.
22. Kumar D, Nareppa U, Shetty SP, Wali M. Transvalvular mitral regurgitation following mitral valve replacement a diagnostic dilemma. Ann Card Anaesth. 2015;18(4):584–6.
23. Rodríguez Muñoz D, Lázaro Rivera C, Zamorano Gómez JL. Guidance of treatment of perivalvular prosthetic leaks. Curr Cardiol Rep. 2014;16(1):430. https://doi.org/10.1007/s11886-013-0430-y.
24. Lancellotti P, Pibarot P, Chambers J, Edvardsen T, Delgado V, Dulgheru R, Pepi M, Cosyns B, Dweck MR, Garbi M, Magne J, Nieman K, Rosenhek R, Bernard A, Lowenstein J, Vieira ML, Rabischoffsky A, Vyhmeister RH, Zhou X, Zhang Y, Zamorano JL, Habib G. Recommendations for the imaging assessment of prostheticheart valves: a report from the European Association of Cardiovascular Imagingendorsed by the Chinese Society of Echocardiography, the Inter-American Societyof Echocardiography, and the Brazilian Department of Cardiovascular Imaging. Eur Heart J Cardiovasc Imaging. 2016;17(6):589–90.
25. Pate GE, Al Zubaidi A, Chandavimol M, Thompson CR, Munt BI, Webb JG. Percutaneous closure of prosthetic paravalvular leaks: case series and review. Catheter Cardiovasc Interv. 2006;68(4):528–33.

26. Di Biase L, Santangeli P, Anselmino M, Mohanty P, Salvetti I, Gili S, Horton R, Sanchez JE, Bai R, Mohanty S, Pump A, Cereceda Brantes M, Gallinghouse GJ, Burkhardt JD, Cesarani F, Scaglione M, Natale A, Gaita F. Does the left atrial appendage morphology correlate with the risk of stroke in patients with atrial fibrillation? Results from a multicenter study. J Am Coll Cardiol. 2012;60(6):531–8.
27. Kanderian AS, Gillinov AM, Pettersson GB, Blackstone E, Klein AL. Success of surgical left atrial appendage closure: assessment by transesophageal echocardiography. J Am Coll Cardiol. 2008;52(11):924–9.
28. Holmes DR, Reddy VY, Turi ZG, Doshi SK, Sievert H, Buchbinder M, Mullin CM, Sick P, Investigators PROTECTAF. Percutaneous closure of the left atrial appendage versus warfarin therapy for prevention of stroke in patients with atrial fibrillation: a randomised non-inferiority trial. Lancet. 2009;374(9689):534–42.
29. Viles-Gonzalez JF, Kar S, Douglas P, Dukkipati S, Feldman T, Horton R, Holmes D, Reddy VY. The clinical impact of incomplete left atrial appendage closure with the Watchman Device in patients with atrial fibrillation: a PROTECT AF (Percutaneous Closure of the Left Atrial Appendage Versus Warfarin Therapy for Prevention of Stroke in Patients With Atrial Fibrillation) substudy. J Am Coll Cardiol. 2012;59(10):923–9.
30. Meier B, Blaauw Y, Khattab AA, Lewalter T, Sievert H, Tondo C, Glikson M, Reviewers D. EHRA/EAPCI expert consensus statement on catheter-based left atrial appendage occlusion. Europace. 2014;16(10):1397–416.
31. Silvestry FE, Cohen MS, Armsby LB, Burkule NJ, Fleishman CE, Hijazi ZM, Lang RM, Rome JJ, Wang Y, American Society of Echocardiography, Society for Cardiac Angiography and Interventions. Guidelines for the echocardiographic assessment of atrial septal defect and patent foramen ovale: from the American Society of Echocardiography and Society for Cardiac Angiography and Interventions. J Am Soc Echocardiogr. 2015;28(8):910–58.
32. Cao Q, Radtke W, Berger F, Zhu W, Hijazi ZM. Transcatheter closure of multipleatrialseptaldefects. Initial results and value of two- and three-dimensionaltransoesophaglechocardiography. Eur Heart J. 2000;21(11):941–7.
33. Lodato JA, Cao QL, Weinert L, Sugeng L, Lopez J, Lang RM, Hijazi ZM. Feasibility of real-time three-dimensional transoesophageal echocardiography for guidance of percutaneousatrialseptal defect closure. Eur J Echocardiogr. 2009;10(4):543–8.

Index

A
Acoustic shadowing, 253, 254
ACS, *see* Acute coronary syndrome
Acute aortic syndrome (AAS)
  CAAD, 22–25
  DeBakey system, 21
  diagnosis, 21
  incidence, 21
  intersocietal guidelines, 21
  intramural hematoma, 21–22
  penetrating aortic ulcer, 25
  Stanford classification, 21
Acute chest pain, 5, 12, 20
  AAS (*see* Acute aortic syndrome (AAS))
  ACS (*see* Acute coronary syndrome (ACS))
  AHA/ACC guidelines, 10
  AMI (*see* Acute myocardial infarction (AMI))
  TTE, 10
  ultrasound modalities, 4
Acute coronary syndrome (ACS)
  echocardiographic contrast microbubbles, 6
  ischemic cascade, 9
  LVEF, 6
  regional systolic function assessment, 5
  TTE, 10, 11
  wall motion scoring, 5, 6
Acute mitral regurgitation, 16, 17
  acute vs. chronic on spectral Doppler, 99
  clinical presentation, 97, 98
  mitral valve apparatus, 98
  papillary muscle blood supply, 99
  pathophysiology, 98
  ruptured anterior papillary muscle, 99
Acute myocardial infarction (AMI)
  acute mitral regurgitation, 16, 17
  acute-phase complications, 12
  chronic-phase complications, 12
  left ventricular free wall rupture, 12, 13
  left ventricular pseudoaneurysm, 17, 19
  LVA, 16–18
  LV thrombus, 20
  right ventricular infarction, 14–16
  ventricular septal rupture, 12–15
Acute neurologic syndrome, *see* Stroke
Acute respiratory failure, lung ultrasound profiles and algorithm, 185
Advanced Cardiac Life Support Algorithms (ACLS), 50
Advance life support (ALS) guidelines, 77
Alveolar-interstitial syndromes, 171, 180
American Society of echocardiography (ASE), 6, 78
Amplatzer Cardiac Plug (APC), 257
Amplatzer device, 253, 256
Amplatzer septal occluder, 258
Antiarrhythmic drug selection, 49
Aortic atheroma
  anatomic features, 126
  CT and CMR, 129
  differential diagnosis, 128
  dissection, 128
  hemodynamic features, 127
  intramural hematoma, 127
  neurologic symptoms, 126
  penetrating ulcer, 127
Aortic regurgitation (AR) gradient, 143
Aortic stenosis, 142
Aortic thromboembolism syndrome (ATS), 126

E. Herzog, E. Argulian (eds.), *Echocardiography in the CCU*,
https://doi.org/10.1007/978-3-319-90278-4

Arrhythmia, 53
atrial fibrillation
anticoagulation, 50
echocardiographic features, 46
etiology, 46–48
management, 48, 49
rate control, 48
rhythm control, 48, 49
TOE, 46
TTE, 46
bradyarrhythmias, 61, 62
ICD shocks, 61
post-cardiac catheter ablation, 62
syncope, 70
ventricular tachycardia (*see* Ventricular tachycardia (VT))
Atheroma triad, 127
Atherosclerotic plaque, 126, 127, 129
Atrial arrhythmias, 116–117
Atrial fibrillation, 116, 117
anticoagulation, 50
echocardiographic features, 46
etiology, 46–48
management, 48, 49
rate control, 48
rhythm control, 48, 49
TOE, 46
TTE, 46
Atrial septal aneurysm (ASA), 129, 130
Atrial septal defects (ASD) closure, 257
Amplatzer septal occluder, 258
anteroposterior and superoinferior rims, 258
balloon sizing, 258
device on 3D, 258, 259
interatrial septum, 258

B

Bernoulli equation, 135
BLUE protocol, 172, 184
Bradyarrhythmias, 61, 62, 70

C

Canadian Cardiology Society (CCS), 74
Cardiac arrest
ALS, 77, 81–82
echocardiography
accurate assessment, 78
cardiac ischemia, 52
cardiac output detection, 86
cardiac rhythm identification, 87, 89
challenges, 78–79
coronary artery disease, 86–88
emergency echocardiography, 82
hypovolemia, 53, 82–83
International Liaison Committee on Resuscitation guidelines, 78
pericardial tamponade, 84–86
post-arrest, 53, 54
pulmonary embolism, 52, 53, 83, 84
tamponade, 52
TEE, 78, 89
TTE, 79–81
environment, 77
etiologies, 51
prognosis, 77
10-s pulse check, 51
spontaneous cardiac movement (SCM) detection, 51
team leader, 77
treatment, 77
Cardiac auscultation areas, 95
Cardiac cycle, 158
Cardiac etiology, 131
Cardiac output (CO) calculation, 145
Cardiac tamponade, 52, 232
Cardiogenic syncope, 69–70
Carney complex, 124
Central venous catheters (CVCs), 61
CHA_2DS_2-VASc score, 50
Chest pain, 149
Cholesterol emboli syndrome (CES), 126
Cinefluoroscopy, 123
Classic acute aortic dissection (CAAD), 22–25
Clip delivery system (CDS), 251
Contrast echocardiography, 222, 224, 225
anterior wall myocardial infarction, 221, 222
chest pain post percutaneous coronary intervention, 220, 221
hypertrophic cardiomyopathy
mid-cavitary obliteration, 224
pericardial effusion, 222
physical examination, 222
spade shape ventricular cavity, 225
TEE, 222
treatment, 222, 225
safety, 217, 218
ultrasound contrast agents, 216, 217
Core valve post deployment, 248
Critical care ultrasonography (CCUS), *see* Point-of-care ultrasonography (POCUS)
Curvilinear transducers, 168
Cushing syndrome, 124

D
DeBakey and Stanford classification schemes, 21, 126
Deep vein thrombosis (DVT), 168, 196, 198
Diaphragmatic excursion, M-mode, 183
Diastolic heart failure, 41–43
Dilated cardiomyopathy, 152
Dyspnea
  cardiac causes, 27
  diastolic heart failure, 41–43
  differential diagnosis, 27
  left ventricular systolic function, 32–35
  pericardial effusion, 28, 30, 31
  right ventricular dysfunction, 35–37
  ultrasound modalities, 27–28
  valvular abnormalities, 37–41

E
Edward Sapien, 246
Edward Sapien 3, 246
Edward Sapien XT, 246
Endocarditis
  anatomic features, 120
  diagnosis, 120
  differential diagnosis, 121
  echocardiography findings, 120, 121
  hemodynamic features, 120
E-point septal separation (EPSS), 151
European Society of Cardiology (ESC) guidelines, 10, 74
EVEREST II trial, 249
Evolut R, 246

F
Flat mural thrombus, 118
Fluid responsiveness, 159
Focused echocardiographic evaluation in life support (FEEL), 82

G
Gallop, 94

H
Handheld devices, 150
Heart murmurs, *see* Murmurs
HeartWare HVAD, 228
Hemodynamic assessment
  right atrial pressures, 135, 136
  tricuspid valve during systole, 136
Hemorrhagic stroke, 114
Hepatorenal recess, 191
Hydronephrosis, 194
Hypertrophic cardiomyopathy
  mid-cavitary obliteration, 224
  physical examination, 222
  spade shape ventricular cavity, 225
  TEE, 222
  treatment, 222, 225
Hypovolemia, 53, 82–83, 159

I
Iatrogenic atrial septal defect (IASD), 252
Impella VADs, 238
  catheter malfunction, 234
  implantation techniques, 233
  left ventricle (*see* Left heart Impella catheters)
  right ventricle (*see* Right heart Impella RP catheter)
Implantable cardioverter defibrillator ICD shocks, 61
Infective endocarditis (IE), 120, 124
  clinical presentation, 104
  murmur in, 104
  vegetation, ECG, 104–106
Inferior vena cava (IVC)
  collapsibility index, 160
  size and respiratory variation, 136
Inflow cannula, 230
Internal jugular vein aspect ratio, 160
International Liaison Committee on Resuscitation (ILCOR) guidelines, 78
International Registry of Acute Aortic Dissection (IRAD), 21
Interstitial syndrome, differentiating causes, 181
Intracardiac devices, 227
  Impella VADs (*see* Impella VADs)
  LVADs (*see* Left ventricular assist devices (LVADs))
Intracardiac pressures, 147
Intracardiac shunt, 129, 130
Intracardiac tumors
  anatomic features, 124
  differential diagnosis, 126
  echocardiography findings, 124, 125
  embolic events, 124
  hemodynamic features, 124
  magnetic resonance imaging, 126
Intramural hematoma (IMH), 21, 22, 127
Ischemic cascade, 9
Ischemic stroke, 114, 115

K
Kentucky gallop, 94

L
Left atrial appendage (LAA)
  Amplatzer Cardiac Plug, 257
  anatomic features, 117
  anticoagulation, 256
  echocardiography findings, 117, 118
  vs. left atrium, 116, 117
  post deployment, 257
  Watchman device, 256
  WaveCrest device, 257
Left atrial enlargement (LAE) on POCUS, 151
Left atrial pressure, 144, 145
Left heart Impella catheters
  anatomy, 234, 235
  cardiac structure contact, 238
  catheter malfunction, 233–234
  normal position, 235, 236
  too far into left ventricle, 237
  too far out of left ventricle, 237
Left ventricular aneurysm (LVA), 16–18
Left ventricular assist devices (LVADs)
  cardiac tamponade, 232
  excessive unloading, 231, 232
  HeartWare HVAD, 228
  inadequate unloading, 232
  inflow cannula, 230
  outflow cannula, 230
  routine surveillance, 229
  signs, symptoms/device alarms, 229
  speed optimization, 229
  suction events, 231
  therapy, 60
  Thoratec HeartMate II and III, 228
  thrombosis, 232
  unloading conditions, 231
Left ventricular diastolic pressure (LVDP), 138, 143
Left ventricular ejection fraction (LVEF), 6
Left ventricular end-diastolic pressure (LVEDP), 143, 145
Left ventricular filling pressures, 144
Left ventricular free wall rupture (LVFWR), 12, 13
Left ventricular (LV) function, 151–153
Left ventricular internal diastolic dimension (LVIDd), 229, 231, 232
Left ventricular outflow tract (LVOT) obstruction, 37
  clinical presentation, 107
  echocardiographic findings, 107, 108
  murmur of, 107
Left ventricular pseudoaneurysm (LVPA), 17, 19
Left ventricular systolic pressure (LVSP), 141, 142
Left ventricular thrombus, 20, 116, 118
  anatomic features, 118
  cardiac magnetic resonance imaging, 119
  echocardiography findings, 119
  incidence, 117
Left ventricular wall motion scoring, 5
Linear array transducers, 166, 184
Lung hepatization, 177
Lung sliding, 174, 175
Lung ultrasound, patterns, 174

M
Marantic endocarditis, *see* Noninfective endocarditis
Medtronic CoreValve, 246
MitraClip technology, 249
Mitral interventions
  coaptation length and depth, 250
  IASD, 252
  mechanism, 250
  MitraClip device dimension, 249
  mitral stenosis, 252
  post MitraClip deployment, 252
  surgical view from left atrium, 251
  transseptal puncture, 251
Mitral regurgitation (MR), 16, 17
Mitral stenosis, 47
Mitral valve apparatus, 98
Mobile thrombus, 118
Moderator band ventricular tachycardia, 56, 57
Monomorphic ventricular tachycardia (MVT), 56–58
Murmurs, 102, 103
  acute mitral regurgitation
    acute vs. chronic on spectral Doppler, 99, 101
    clinical presentation, 97, 98
    mitral valve apparatus, 98
    papillary muscle blood supply, 99
    pathophysiology, 98
    ruptured anterior papillary muscle, 99, 100
    ruptured posterior papillary muscle, 99, 101
  causes, 94

conditions, 95, 96
definition, 94
detection, 95
echocardiography after detection of, 96
infective endocarditis
aortic valve endocarditis, 105
clinical presentation, 104
new regurgitant murmur, 104
vegetation, ECG, 104–106
intensity and grades, 94, 95
myocardial infarction, 97
prosthetic valve thrombosis
clinical presentation, 110
echocardiographic findings, 110, 111
prosthetic valve stenosis, 110
shock, 106, 108
aortic dissection (*see* Type A Aortic dissection)
LVOT (*see* Left ventricular outflow tract (LVOT) obstruction)
types, 94–96
ventricular septal rupture
acute VSR, 102
clinical presentation, 100
echo findings, 103
pathophysiology, 102
Myocardial infarction (MI), 97
See also Left ventricular thrombus
Myxoma, 124–126

N
Neurally mediated/reflex syncope, 68
Noncardiac syncope, 72
Noninfective endocarditis, 120

O
Occlutech, 253
Orthostatic hypotension, 69
Outflow cannula, 230
Outflow tract/idiopathic VT (OT-VT), 54–56

P
Papillary fibroelastoma (PFE), 124–126
Papillary muscle blood supply, 99
Paravalvular aortic regurgitation, 247, 248
Paravalvular leaks
closure devices into defect, 255
colour Doppler, 255
medial aspect of valve, 254
position and size of leak, 254
quantitative findings, 253
sewing ring, medial aspect, 254
transcatheter devices, 253
transseptal puncture, 255
vs. washing jet, 253
PARTNER trial, 246
Patent foramen ovale (PFO)
anatomic features, 129
echocardiography findings, 130, 131
hemodynamic features, 129
transcranial Doppler, 131
Penetrating aortic ulcer (PAU), 25, 127, 128
Pericardial effusion, 28, 30, 31
on handheld echo, 158
hypotension, 157, 159
and IVC size assessment, 149–150
measurements and quantification, 158
Pericardial tamponade, 29, 31, 84–86
Phased array transducers, 168, 170
Pneumothorax mimickers on ultrasonography, 183
Pocket-sized imaging devices, 4
Point-of-care cardiac ultrasound (POCUS), 165, 199–200, 202–204
advantages, 149
applications, 169, 170
battery-powered devices, 149
diagnostic accuracy, 149
in hypotensive patients, 149
indications, 149
limitations, 161, 210
management errors, 161
medical management, 149, 160
non-cardiac ultrasound (*see* Non-cardiac POCUS)
physical examination, 149, 150, 165
pleural effusion, 179
pleural line, 175
quality of care, critically ill patients, 165
shock evaluation, 191, 197, 198
in structural abnormalities, 161
undifferentiated shock, 197, 199
vascular access, cardiac care unit
clinical status, 199
coagulation profile, 199
patient's anatomy, 199
ultrasound guidance, 199–200, 202–204
Polymorphic VT (PVT), 59–60
Post-cardiac catheter ablation, 62–63
Post MitraClip deployment, 252
Pre-procedural ultrasound scan, line placement, 202

Prosthetic valve stenosis
echocardiographic findings, 110, 111
murmur, 110
Prosthetic valve thrombosis, 41, 110
anatomic features, 122
cinefluoroscopy, 123
clinical presentation, 110
differential diagnosis, 123
echocardiography findings, 122, 123
hemodynamic features, 122
incidence, 122
PROTECT AF study, 256
Protruding thrombus, 118
Pulmonary artery diastolic pressure (PADP), 139, 140
Pulmonary artery (PA) pressures, 140, 141
Pulmonary artery systolic pressure (PASP), 138, 139
Pulmonary hypertension, 157
Pulmonary vascular resistance (PVR), 146, 147
Pump thrombosis, 229, 232

R
Right atrial pressure (RAP), 136, 138
Right heart Impella RP catheter
anatomy, 240
cardiac structure contact, 243
implantation technique, 238, 239
normal position
chest X-ray, 240, 241
right ventricular outflow tract, 241, 242
tricuspid valve, 241, 242
outlet area below pulmonic valve, 242, 243
Right ventricular diastolic pressure (RVDP), 138, 139
Right ventricular (RV) function, 155–157
Right ventricular infarction (RVI), 14–16
Right ventricular systolic pressure (RVSP), 136–139

S
Severe mitral regurgitation, 155
Shock
murmur, 106, 108
aortic dissection (*see* Type A Aortic dissection)
LVOT (*see* Left ventricular outflow tract (LVOT) obstruction)
Shunt flow calculation, 146
Sound waves, 166
Speckle-tracking echocardiography, 32, 42
Stanford classification, 21
ST-elevation myocardial infarction (STEMI), 5
Stroke, 120, 122, 124, 126, 129
aorta (*see* Aortic atheroma)
atrial septal aneurysm, 129, 130
cardiac sources, 115, 116
cardiac tumors (*see* Intracardiac tumors)
cardioembolic etiology, 114
cardioembolic stroke, 115
high embolic risk cardiovascular conditions, 115
left atrial appendage
anatomic features, 117
computed tomography scan, 117
echocardiography findings, 117, 118
vs. left atrium, 116, 117
myocardial infarction (*see* Left ventricular thrombus)
PFO (*see* Patent foramen ovale (PFO))
prevalence, 113
prosthetic valve (*see* Prosthetic valve thrombosis)
subtypes, 113–115
thrombus, 116
vegetations (*see* Vegetations)
Structural cardiac interventions, 246, 249, 253
TAVR (*see* Transcatheter aortic valve replacement (TAVR))
transcatheter mitral valve intervention (*see* Mitral interventions)
transcatheter paravalvular leak closures (*see* Paravalvular leaks)
Suboptimal echocardiograms, 216
Syncope
blood flow obstruction, 70
cardiogenic syncope, 69–70
definition, 67
diagnostic approach, 73
ECG, 72
European Society of Cardiology guidelines, 74
history, 71
mechanisms of, 68, 69
neurally mediated/reflex syncope, 68
vs. noncardiac syncope, 72
orthostatic hypotension, 69
physical examination, 71
risk stratification, 73
TEE, 75
TTE, 68, 72

Systemic embolism, 117, 120, 124, 132
Systolic anterior motion of the mitral valve (SAM), 107, 108
Systolic blood pressure (SBP), 137, 141
Systolic ventricular septal defect (SVSD) gradient, 137

T
Tachyarrhythmias, 70
Tennessee gallop, 94
Thoracic ultrasonography
  abdominal ultrasonography
    abdominal aortic aneurysm, 192, 193
    applications, 188
    ascites, cirrhosis/right heart failure, 190, 192
    dual antiplatelet therapy and anticoagulation, 188
    focused assessment with sonography in trauma, 189, 190
    kidneys and bladder, 193–195
    US-assisted paracentesis, 190
  A-lines, 174
  alveolar consolidation, 176
  B-lines, 176
  cardinal signs, 172
  clinical applications
    alveolar-interstitial process, 178, 180
    bilateral A-line pattern, 184
    CCU patient with acute respiratory distress, 184
    diaphragmatic function, 181, 184
    phrenic nerve injury/paralysis, 181
    pleural drainage procedures, 185, 186
    pneumothorax detection, 180, 181
  comet tails/lung rockets, 176
  deep venous thrombosis, 195, 196
  IVC imaging, fluid status and responsiveness, shock, 186–189
  lung and pleural ultrasonography, 172–174
  lung examination, 171
  lung sliding, 174
  lung ultrasound patterns, 174
  lung zones, 171
  pleural effusion, 177, 178
  pleural examination, 172
  principles, 170
Thoratec HeartMate II and III, 228
To-and-fro murmur of acute AR, 109
Transcatheter aortic valve replacement (TAVR)
  AHA/ACC guidelines, 246
  annular area, 3D TEE, 246, 247
  aortic stenosis, 246
  balloon-expandable valves, 246
  CT imaging, 247
  follow-up echocardiogram, 249
  paravalvular aortic regurgitation, 248
  periprocedural complications, 249
  periprocedural TEE, 248
  prosthesis size, 247
  transapical approach, 248
Transcatheter mitral valve intervention, *see* Mitral interventions
Transcatheter paravalvular leak closures, *see* Paravalvular leaks
Transesophageal echocardiography (TEE), 4, 21, 117, 119
  cardiac arrest, 78, 89
  syncope, 75
Transmitral pulsed-wave Doppler spectral tracing, 47, 48
Transseptal puncture, 251
Transthoracic echocardiography (TTE), 4, 10, 218, 219
  cardiac arrest, 79–81
  syncope, 68, 72
Trial of Org 10,172 in Acute Stroke Treatment (TOAST) criteria, 113
Type A aortic dissection
  aortic regurgitation, 109
  clinical presentation, 108
  echocardiographic findings, 109
  pathophysiology, 109

U
Ultrasonography (USG)
  anechoic region, 166
  contrast agents, 216, 217
  Doppler, 169
  equipment and modalities, 166
  hyperechoic region, 166
  M-mode, 169
  normal and abnormal signs, 173
  principles of, 166
  probes, 166
  procedural guidance, vascular access, 168
  tissue echogenicity, 166, 167
  transducers, 166, 168
  waves, 166
US transducers, 166, 168

V
Valve thrombosis, *see* Prosthetic valve thrombosis
Valvular abnormalities, 37–41
Valvular disease assessment, 153–155
Vascular access, cardiac care unit
  site-specific considerations
    arterial catheterization, 208
    arterial line placement, 208–210
    femoral vein site, 206, 207
    internal jugular vein, 200–205
    longitudinal view approach, 209
    subclavian site, 207, 208
  US guidance
    longitudinal/in-plane approach, 204
    mechanical and infectious complications, 199
    pneumothorax, 200
    transverse approach, 200, 201, 203
Vegetations, endocarditis
  anatomic features, 120
  diagnosis, 120
  differential diagnosis, 121
  echocardiography findings, 120, 121
  hemodynamic features, 120
Ventricular septal defect (VSD), 137, 138
Ventricular septal rupture (VSR), 12–15
  clinical presentation, 100
  echo findings, 103
  murmur of, 102
  pathophysiology, 102
Ventricular tachycardia (VT)
  central venous catheters, 61
  LVAD therapy, 60
  management strategies, 58, 59
  moderator band VT, 56, 57
  monomorphic VT, 56–58
  OT-VT, 54–56
  polymorphic VT, 59–60
  premature ventricular contractions, 60
Volume resuscitation/diuresis, 159, 160

W
Wall motion score index (WMSI), 6
Washing jet, 253
Watchman device, 256
WaveCrest device, 257
Whole-body ultrasound (WBU), *see* Point-of-care ultrasonography (POCUS)